

Sara García Salinas

Smart dressings based on  
nanostructured fibers containing  
natural origin antimicrobial and  
anti-inflammatory compounds

Director/es

Irusta Alderete, Silvia  
Mendoza Cantos, Gracia

<http://zaguan.unizar.es/collection/Tesis>

© Universidad de Zaragoza  
Servicio de Publicaciones

ISSN 2254-7606

Tesis Doctoral

SMART DRESSINGS BASED ON  
NANOSTRUCTURED FIBERS CONTAINING  
NATURAL ORIGIN ANTIMICROBIAL AND ANTI-  
INFLAMMATORY COMPOUNDS

Autor

Sara García Salinas

Director/es

Irusta Alderete, Silvia  
Mendoza Cantos, Gracia

**UNIVERSIDAD DE ZARAGOZA**  
**Escuela de Doctorado**

Programa de Doctorado en Ingeniería Química y del Medio Ambiente

2020





*“Smart dressings based on nanostructured fibers containing natural origin antimicrobial and anti-inflammatory compounds”*

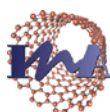
This thesis dissertation is submitted to the Department of Chemical Engineering and Environmental Technologies at the University of Zaragoza (Spain) in partial fulfillment of the requirements for the degree of Doctor

**Sara García Salinas**

**Zaragoza, 2020**



Departamento de Ingeniería  
Química y Tecnologías  
del Medio Ambiente  
**Universidad Zaragoza**



Instituto Universitario de Investigación  
en Nanociencia de Aragón  
**Universidad Zaragoza**







*“Smart dressings based on nanostructured fibers containing natural origin antimicrobial and anti-inflammatory compounds”*

A thesis prepared in the framework of a national research project funded by the Spanish Ministry of Economy and Competitiveness under the FPI predoctoral contract (grant number CTQ2014-52384-R) and carried out at

University of Zaragoza, Department of Chemical Engineering and Environmental Technology



**Departamento de Ingeniería  
Química y Tecnologías  
del Medio Ambiente**  
**Universidad Zaragoza**

Houston Methodist Research Institute, Center for Musculoskeletal Regeneration



Supervisors

**Dr. Silvia Irusta Alderete**, Associate Research Professor, Department of Chemical Engineering and Environmental Technology, University of Zaragoza, Spain.

**Dr. Gracia Mendoza Cantos**, Miguel Servet Researcher, Aragon Institute of Health Research (IIS Aragon), Zaragoza, Spain.





**Dr. Silvia Irusta Alderete,**

Professor at the University of Zaragoza in the Department of Chemical Engineering and Environmental Technologies and member of the Institute of Nanoscience of Aragon.

and **Dr. Gracia Mendoza Cantos,**

Miguel Servet Researcher and member of the Aragon Institute of Health Research (IIS Aragon).

Inform that,

The Doctoral thesis entitled:

**“Smart dressings based on nanostructured fibers containing natural origin antimicrobial and anti-inflammatory compounds.”**

has been written by Ms. **Sara García Salinas** under our supervision and has not been submitted in support of an application for another degree at this or any other University. This thesis has been carried out at the laboratories of the Institute of Nanoscience of Aragon and the Biomedical Research Institute of Aragon with the economic support of the research national project: “Smart dressings based on nanostructured fibers containing natural origin biocides with pharmacokinetic controlled release” (CTQ2014-52384-R) funded by the Spanish Ministry of Economy and Competitiveness under the FPI predoctoral contract (grant number CTQ2014-52384-R) in the call of 2014.

We authorize and approve the presentation of this dissertation, in Zaragoza on May 06, 2020

**Dr. Silvia Irusta**

**Dr. Gracia Mendoza**



La Dra. **Silvia Irusta Alderete**, Profesora Titular perteneciente al Departamento de Ingeniería Química y Tecnologías del Medio Ambiente de la Universidad de Zaragoza y miembro del Instituto Universitario de Nanociencia de Aragón,

y **Dra. Gracia Mendoza Cantos**,

Investigadora Miguel Servet y miembro del Instituto de Investigación Sanitaria Aragón (IIS Aragón).

CERTIFICAN

Que la presente memoria titulada:

**“Smart dressings based on nanostructured fibers containing natural origin antimicrobial and anti-inflammatory compounds.”**

Se ha realizado bajo su dirección y supervisión por Dña. **Sara García Salinas**, en los laboratorios del Instituto Universitario de Nanociencia de Aragón y en el Centro de Investigación Biomédica de Aragón gracias a la ayuda del proyecto nacional de investigación: “Apósitos inteligentes basados en fibras nanoestructuradas conteniendo biocidas naturales con control farmacocinético de su liberación” (CTQ2014-52384-R) financiado por el Ministerio de Economía y Competitividad bajo el contrato predoctoral FPI (número de referencia CTQ2014-52384-R) en la convocatoria del 2014.

Y para que así conste, firmamos este certificado en Zaragoza a 06 de mayo de 2020.

**Silvia Irusta**

**Gracia Mendoza**



## Acknowledgements

When I was studying my master's degree in Madrid, some researchers from Zaragoza came to show their line of research. In that moment, I realized that I had to leave the chaotic city and came to my homeland. 5 years later... and here I am, writing my dissertation and at that point, I am completely sure that these years turned out to be not only in a professional but a personal development.

First, I would like to thank to Victor Sebastian and Pilar Martin, they believed in me as future scientific in the first place. I acknowledge NFP group for the scientific support during this time and the funny moments that we had in and out of laboratories. Nuria, a key piece in our lives. My biomedical background made me find difficult some chemical devices in INA, and you were there to solve my problems, always with a smile in your face. Thank you for your patience.

I spent most of my PhD time in CIBA, so I would like to acknowledge to all scientific-technical services and particularly Cesar and Maria for their scientific support and many hours in front of the microscopy. I should acknowledge animal facilities; their flexibility and advices made our work easier. Vanesa, thank you for your support and help, and more important, thank you for being a friend. BSICoS group, thank you for the entertainment and for feeding me with chocolate, it was a pleasure being with you. Ainhoa and Ernesto, I am so glad to share laboratory with you. I learnt a lot of tuberculosis and P3 bio-security in laboratories. Ale and Marce, you have been one of the best surprises in this thesis. Thank you for all these moments in and out the laboratory, this story will continue.

“La sala”... if the walls could talk... no one would believe the conversations that flow in that place. Seriously, no filter. Thank you, guys, for all these moments in which all of us escape from science. Marta, my co-leader in the nigga's small group. I am glad to have shared this period with you. Your sense of humor makes the work-time happier. Bea, you arrived in the middle of my thesis and I was barely at INA, but your personality made you be “one more” very soon, keep it up. Roberta, I can assure that you are my favorite Italian since I came back from my stay. Thank you for being you, the mix that you have of goodness and little malice, makes you unique. Cris, are we the people who love mice and rats the most? I am really happy to have shared this time with you, I do not lie if I say that I learnt a lot with you. Isa, the first time I saw you I felt a hunch and I was not wrong, you became to be part of my life and I am very grateful.

## Acknowledgements

As you said, I could not have asked for a better thesis-twin and friend. Fer, what an earthquake! I am really happy to have shared your madness and laugh until cry. Alberto, my thesis-confidant person. It was a surprise find a person as you and it is a pleasure to keep the friendship after you left. Thank you for your honesty. Martin, I wish I would have “discover” you earlier. Thank you for sharing your wisdom. Maria, another earthquake as Fer!! I am so happy to have shared the periods of time hand by hand in CIBA in which we were alone. Arturo, Ainhoa, Cristobal, Nacho, Javi, Laura, thank you for making the days happier! Enrique, thank you for your friendliness during all these years and your “quimica fina” knowledge, although it has taken a while for me understand what it is about. I am not sure if I know yet what is this. Hellen, I cannot describe the moments we shared, how in the little time you were here, you left a mark in all of us. You always will have a home in Spain and... Costa Rica is waiting for me, soon...

Thank you, Silvia, Gracia and Manuel. Thank you for your knowledge, patience and support. I really appreciate the trust placed in me from the first time and up to now. At first, I was not sure if wound healing and essential oils were the topic I wanted to develop, but now I can say that I love the work done and all the things we have learnt. Thank you for your effort, dedication, and teaching me to be a scientific.

Unbelievable where we were, and where we are. Setas, the way is easier beside you, thank you. Alba and Miri, thank you for always being there and more important, for your honesty. Love you all.

The perfect combination exists, and it is formed by Andre, Nat, Reich (and me). Only the fact of being with you let me take a deep breath in the moments I really needed it. Thank you and love you.

My family... if I am here, is mainly because of you, for your unconditional support. Thank you for teaching me that I can achieve all the things I propose, being just me (in spite of being part of the dark side of the family). You are incredible. Ah, by the way, I have the best aunts ever, love you.

*To my family*





## Table of contents

Abbreviations	1
Summary and objectives	3
Resumen y objetivos	9
I. Introduction	15
<b>I.1. Wound healing process</b>	<b>17</b>
I.1.1. Coagulation and hemostasis phase	18
I.1.2. Inflammatory phase	18
I.1.3. Proliferative phase	19
I.1.4. Remodeling phase	20
<b>I.2. Factors affecting wound healing</b>	<b>21</b>
I.2.1. Importance of infection	21
I.2.2. Biofilm formation	23
I.2.3. Bacteria resistance to antibiotics	25
I.2.4. Antiseptics	27
<b>I.3. Essential oils</b>	<b>27</b>
I.3.1. Activity of essential oils against bacteria	29
I.3.2. Anti-inflammatory activity of essential oils	30
I.3.3. Biomedical application of essential oils	33
<b>I.4. Wound dressings</b>	<b>33</b>
I.4.1. Advanced wound dressings	34
I.4.2. Bioactive wound dressings	34
<b>I.5. Electr spun nanofibers</b>	<b>35</b>
I.5.1. History of electrospinning	35
I.5.2. Principle of electrospinning	36
5.2.1. Formation of Taylor Cone	37
5.2.2. Thinning of the Jet	37
5.2.3. Solidification of the Jet	38
I.5.3. Materials of electrospinning	39
II. Antimicrobial and cytotoxicity evaluation of different free natural compounds	41
<b>II.1. Introduction</b>	<b>43</b>
<b>II.2. Objective</b>	<b>45</b>


<b>II.3. Experimental</b>	<b>45</b>
<b>II.4. Results and discussion</b>	<b>46</b>
II.4.1. Bactericidal activity against planktonic bacteria	46
4.1.1. MIC and MBC values	46
4.1.2. Bactericidal mechanism	47
4.1.3. Synergism	53
II.4.2. Antibiofilm activity	54
II.4.3. Cytotoxicity	56
<b>II.5. Conclusions</b>	<b>58</b>
<b>III. Antimicrobial wound dressing against fluorescent and methicillin-sensitive pathogenic bacteria</b>	<b>59</b>
<b>III.1. Introduction</b>	<b>61</b>
<b>III.2. Objective</b>	<b>63</b>
<b>III.3. Experimental</b>	<b>63</b>
<b>III.4. Results and discussion</b>	<b>64</b>
III.4.1. Physico-chemical characterization of the electrospun nanofibers	64
III.4.2. Bactericidal activity	66
III.4.3. Antibiofilm activity	68
III.4.4. Cytotoxicity assessment of the PCL-THY patches	70
III.4.5. <i>In vitro</i> model of infection of J774 macrophages	72
<b>III.5. Conclusions</b>	<b>75</b>
<b>IV. Electrospun anti-inflammatory patch loaded with essential oils for wound healing</b>	<b>77</b>
<b>IV.1. Introduction</b>	<b>79</b>
<b>IV.2. Objective</b>	<b>80</b>
<b>IV.3. Experimental</b>	<b>80</b>
<b>IV.4. Results and discussion</b>	<b>81</b>
IV.4.1. Cell viability, morphology and flow cytometry of free EOs	81
IV.4.2. Anti-inflammatory effects of the different free natural compounds	83
VI.4.3. Characterization of electrospun nanofibers	85
IV.4.4. Cell viability of natural compounds-loaded PCL patches	87
IV.4.5. Anti-inflammatory effects of the loaded patches	88
IV.4.6. Cell migration towards PCL-loaded nanofibers	90
IV.4.7. Immunofluorescence assay	91
<b>IV.5. Conclusions</b>	<b>93</b>

V. Efficiency of antimicrobial electrospun thymol-loaded polycaprolactone patches <i>in vivo</i>	95
V.1. <b>Introduction</b>	<b>97</b>
V.2. <b>Objective</b>	<b>98</b>
V.3. <b>Experimental</b>	<b>99</b>
V.4. <b>Results and discussion</b>	<b>100</b>
V.4.1. Electrospun PCL nanofibers characterization	100
V.4.2. Mechanical properties of PCL-THY patches	101
V.4.3. <i>In vivo</i> bactericidal activity	101
V.4.4. Histopathological and immunohistochemical studies	103
V.5. <b>Conclusions</b>	<b>108</b>
VI. General conclusions	111
VI. Conclusiones generales	115
Appendix I. Materials and methods	119
AI.1. <b>Materials</b>	<b>122</b>
AI.2. <b>Synthesis of loaded PCL nanofibers</b>	<b>123</b>
AI.2.1. Solutions preparation and characterization	123
AI.2.2. Electrospinning process	124
AI.3. <b>Characterization of electrospun nanofibers</b>	<b>124</b>
AI.3.1. Morphology	124
AI.3.2. Water uptake	125
AI.3.3. Patches porosity	125
AI.3.4. Mechanical properties	125
AI.3.5. Essential oils loading and encapsulation efficiency	125
AI.3.6. Release of natural compounds	126
AI.4. <b>Antimicrobial activity</b>	<b>126</b>
AI.4.1. Bacteria culture	126
AI.4.2. Preparation of essential oils	127
AI.4.3. MIC and MBC determination	127
AI.4.4. Bacteria morphology	128
AI.4.5. Bactericidal mechanism	128
AI.4.6. Confocal microscopy	128
AI.4.7. Synergi studies	129
AI.4.8. Biofilm formation and characterization	129
AI.4.9. Antibiofilm activity measurement	130

<b>AI.5. Cell assays</b>	<b>131</b>
AI.5.1. Cytotoxicity metabolism assays	131
AI.5.2. Flow cytotoxicity for apoptosis detection	133
AI.5.3. <i>In vitro</i> model infection of J774 macrophages	133
<b>AI.6. Anti-inflammatory studies</b>	<b>134</b>
AI.6.1. <i>In vitro</i> inflammation	134
AI 6.2. Gene expression analysis	135
AI.6.3. Cell colonization model	135
AI.6.4. Immunofluorescence assay	136
<b>AI.7. <i>In vivo</i> experiments</b>	<b>136</b>
AI.7.1. Mouse excisional wound splinting model infection	136
AI 7.2. Evaluation of infection wounds	138
AI.7.3. Histological studies	138
<b>AI.8. Statistical analysis</b>	<b>139</b>
<b>Appendix II. References</b>	<b>142</b>
<b>Appendix III. Published scientific papers &amp; participation in conferences</b>	<b>171</b>

## Abbreviations

B-CAR	$\beta$ -caryophyllene
CAR	Carvacrol
CFU	Colony Forming Units
CIN	Cinnamaldehyde
CUR	Curcumin
DAMP	Danger-associated molecular pattern
DCM	Dichloromethane
DL	Drug loading
DMEM	Dulbecco's Modified Eagle Medium
DMF	<i>N,N</i> -dimethylformamide
Dpi	days post-infection
EE	Encapsulation efficiency
EGF	Epidermal growth factor
EO	Essential oil
EUG	Eugenol
FBS	Fetal Bovine Serum
FICI	Fractional Inhibitory Concentration Index
HaCaT	Human epidermal keratinocytes
HE	Hematoxylin and eosin
iNOS	Inducible nitric oxide synthase
IL	Interleukin
LPS	Lipopolysaccharide
MBC	Minimal Bactericidal Concentration
MIC	Minimal Inhibitory Concentration
MIP	Maximum Intensity Projection
MW	Multiwell
NO	Nitric oxide
NOS	Nitric oxide synthase
PAMP	Pathogen-associated molecular pattern
PBS	Phosphate buffered saline
PCL	Polycaprolactone
PDGF	Platelet-derived growth factor
PIA	Polysaccharide Intracellular Adhesion
PMA	Phorbol 12-myristate 12-acetate
RPMI	Roswell Park Memorial Institute
SD	Standard Deviation
SEM	Scanning Electron Microscopy
SQU	Squalene
TGF	Transforming growth factor
THY	Thymol
TLR	Toll-like receptor TNF: Tumor necrosis factor
TSA	Tryptone soy agar



TSB	Tryptone soy broth
TYR	Tyrosol
VEGF	Vascular endothelial growth factor

## Summary and objectives

The current Doctoral Thesis, named “Smart dressings based on nanostructured fibers containing natural origin antimicrobial and anti-inflammatory compounds” has been developed at the Department of Chemical Engineering and Environmental Technology (University of Zaragoza, Spain) in the group of Nanostructured Films and Particles (NFP), which is a member of the Aragon Institute of Nanoscience (INA). This research has been developed in this institute and also in the Biomedical Research Center of Aragon (CIBA). A predoctoral stay of 6 months was performed at the Methodist Hospital Research Institute in Houston (Texas, US) supervised by Professor Ennio Tasciotti. This research was supported by a FPI predoctoral fellowship, funded by the Spanish Ministry of Economy and Competitiveness (CTQ2014-52384-R). The short stay was also funded by the Network of Biomedical Research Center in the field of Bioengineering, Biomaterials and Nanomedicine (CIBER-BBN).

Due to the development of bacterial resistances, the search of new compounds to treat infections is in the spotlight of researchers. In this scenario, this thesis is focused on the design of a bioactive dressing based on electrospun polycaprolactone (PCL) nanofibers loading natural compounds obtained from essential oils (EOs) acting as anti-inflammatory and antimicrobial compounds for wound healing treatment. For this aim, a deep research in bactericidal and anti-inflammatory EOs compounds properties was carried out.

The first purpose of the thesis was to tackle wound infection with plant-derived natural compounds. For this goal, the bactericidal properties and mechanisms of different free EOs in planktonic bacteria cultures using a Gram-positive strain, *Staphylococcus aureus* (ATCC 25923) and a Gram-negative strain, *Escherichia coli* S17 were studied. In addition, since biofilm formation is a challenge in wound infections, the effect of natural compounds was studied in *S. aureus* biofilm. The high volatility character of EOs and the fact that they can be oxidized in contact with air or ultraviolet light, make difficult their application. Encapsulation of EOs is a good technique to protect their properties. Thus, thymol (THY), the compound that demonstrated the best antimicrobial activity against planktonic bacteria and biofilm, was encapsulated into PCL nanofibers. Nanofibers synthesis and THY encapsulation were carried out using the electrospinning technique. This method allows the fabrication of patches with high load of volatile compounds as THY. The bactericidal properties of these patches were studied

using a cGFP-expressing *S. aureus* strain through quantitative assays and confocal microscopy. In order to use these natural compounds for wound healing applications, free-compound cytotoxicity assays were carried out in three different cell types: fibroblast, keratinocytes and macrophages. Moreover, a co-culture model using J774 macrophages and cGFP-expressing *S. aureus* was developed to study and to monitor the effect of THY loaded PCL patches in intracellular bacteria.

The second goal in the thesis was to find an anti-inflammatory natural compound effective for wound treatment. For these assays, an *in vitro* inflammatory model was optimized in lipopolysaccharide (LPS) -activated J774 macrophages. These experiments were developed in the Methodist Hospital Research Institute in Houston (Texas, US). The study of the increase or reduction levels of inflammatory cytokines allowed us to determine the best anti-inflammatory natural compounds evaluated in our studies. Among them, PCL-THY patches demonstrated to be the patches that better reduced inflammation in an *in vitro* inflammatory model.

After concluding that THY had antimicrobial and anti-inflammatory properties when loaded in PCL nanofibers, an *in vivo* experiment to determine the effectiveness of the designed patches in an infected skin wound model was developed. SKH1 hairless mice were used to analyze the *in vivo* bactericidal and anti-inflammatory properties of PCL-THY patches for their potential clinical application.

The document is structured in different chapters that address each of the goals of this doctoral thesis:

- **Chapter I** corresponds with the introductory part where general concepts are exposed. The chapter includes a description of wound healing processes, pointing the factors affecting the procedure such as infection and inflammation. Different types of wound healing treatments as antibiotics are described, highlighting antibiotic resistance as the reason to choose plant-derived compounds as wound healing treatment. Electrospinning technique is explained to understand the synthesis of PCL nanofibers and the encapsulation of the active principle.
- **Chapter II** focuses on antimicrobial activity of free EOs to tackle wound infection. Minimum Inhibitory Concentration (MIC) and Minimum Bactericidal Concentration



(MBC) were measured for different plant-derived natural compounds in *S. aureus* (ATCC 25923) and *E. coli* S17 strains. In addition, a biofilm *S. aureus* model was optimized to determine the effect of EOs in these bacterial formations. The mechanism of action of EOs in bacteria was studied by scanning electron microscopy (SEM) and flow cytometry. Cytotoxicity of EOs treatment was also evaluated in skin-related cell types such as fibroblasts, keratinocytes and macrophages. Carvacrol (CAR), cinnamaldehyde (CIN) and THY exhibit the highest *in vitro* antimicrobial activities against *E. coli* and *S. aureus* by disrupting bacteria membrane. These results are included in the published article entitled “*Evaluation of the antimicrobial activity and cytotoxicity of different components of natural origin present in essential oils*”. García-Salinas, S.; Elizondo-Castillo, H.; Arruebo, M.; Mendoza, G.; Irusta, S. *Molecules* 2018, 23 (6), 1–18. <https://doi.org/10.3390/molecules23061399>.

- **Chapter III** considering the results obtained in Chapter II, THY was chosen as the compound to be loaded into electrospun PCL nanofibers due to its antimicrobial activity and low cytotoxicity compared with the other EOs tested. PCL-THY patches were synthesized, and bactericidal properties were measured against both, planktonic culture and biofilm of cGFP-expressing *S. aureus*. A co-culture model using cGFP-expressing *S. aureus* and J774 macrophages was developed to study the effect of PCL-THY patches in infected cells. Compared to non-loaded dressings, PCL-THY dressings were able to eliminate the pathogenic bacteria in coculture models using infected murine macrophages. In addition, it was corroborated the successful ability of the patch in preventing biofilm formation. These results are included in the recently submitted article entitled “*Antimicrobial Wound Dressings Against Fluorescent and Methicillin-Sensitive Intracellular Pathogenic Bacteria*” Garcia-Salinas, S.; Gamez-Herrera, E.; Landa, G.; Arruebo, M.; Irusta, S.; Mendoza, G. ACS Applied Materials & Interfaces Manuscript ID: am-2020-05668q.
- **Chapter IV** describes the anti-inflammatory activity of EOs with the aim of reducing and controlling the inflammatory process during wound healing. Excessive inflammation can cause the activation of unnecessary cells or cytokines, generating deleterious effects, limiting healing. To develop this goal, an inflammatory model of J774 macrophages

activated with LPS was carried out. Different free natural compounds reported as anti-inflammatory were assessed. Thus, infected macrophages were treated and analyzed at the genetic level, measuring Il (interleukin) 1b, iNos (inducible Nitric oxide synthase) and Il10 cytokines by RT-PCR (Real Time-Polymerase Chain Reaction). PCL patches loaded with EOs were tested using the same *in vitro* model, confirming previous results. In addition, it was assessed cell morphology and average cell area comparing treated cells with positive (LPS-activated cells without treatment) and negative (non LPS-activated cells) controls. This experiment demonstrated the similarity among treated cells and non-activated cells, confirming the anti-inflammatory effect of THY loaded PCL patches. These results are included in the published article entitled “*Electrospun Anti-Inflammatory Patch Loaded with Essential Oils for Wound Healing*”. García-Salinas, S.; Evangelopoulos, M.; Gámez-Herrera, E.; Arruebo, M.; Irusta, S.; Taraballi, F.; Mendoza, G.; Tasciotti, E. *Int. J. Pharm.* **2020**, *577* (January), 119067. <https://doi.org/10.1016/j.ijpharm.2020.119067>.

- **Chapter V** joins all the research performed during the thesis in an *S. aureus* (ATCC 25923) infected wound *in vivo* model in SHK1 hairless mice. Thus, it was analyzed the *in vivo* bactericidal and inflammatory properties of the designed dressing. In addition, controls of free EO and a clinical compound (chlorhexidine) were added to assess the advantages of our patch against other treatments. Starting by infection, quantitative and qualitative measurements of bacteria present in the wound were collected at different dpi (days post infection). Moreover, the histological analysis of skin wounds was carried out to evaluate inflammatory reaction and new vessels formation. Studies demonstrated that PCL-THY can prevent infection, promote wound healing and prompt regeneration. These results are included in the recently accepted article entitled “*Efficiency of Antimicrobial Electrospun Thymol-Loaded Polycaprolactone Mats in vivo*” Garcia-Salinas, S.; Gamez-Herrera, E.; Asin, J.; de Miguel, R.; Andreu, V.; Sancho-Albero, M.; Mendoza, G.; Irusta, S.; Arruebo, M. *ACS Applied Biomaterials*. Manuscript ID: mt-2020-002706.
- **Chapter VI** summarizes the main conclusions obtained during this doctoral thesis.

- **Appendix I** describes the main characterization techniques and biological methods in order to evaluate the antimicrobial and anti-inflammatory ability of free and loaded compounds.
- **Appendix II** indicates the references used to write this work.
- **Appendix III** points the published scientific papers and participation in conferences during this thesis.



## Resumen y objetivos

La presente tesis doctoral denominada “Apósitos inteligentes basados en la encapsulación de compuestos antimicrobianos y anti-inflamatorios de origen natural en fibras nanoestructuradas” ha sido desarrollada en el Departamento de Ingeniería Química y Tecnologías del Medioambiente (Universidad de Zaragoza, España) en el Grupo de Películas y Partículas Nanoestructuradas (NFP), miembro del Instituto de Nanociencia de Aragón (INA). Parte de la investigación ha sido desarrollada en el Centro de Investigación Biomédica de Aragón (CIBA). Durante este periodo, se ha realizado una estancia de 6 meses en el Methodist Hospital Research Institute en Houston (Texas, US), supervisada por el Profesor Ennio Tasciotti. La tesis ha sido financiada por el Programa de Formación de Personal Investigador (FPI) proporcionado por el Ministerio de Economía y Competitividad de España (CTQ2014-52384-R). La estancia fue co-financiada por el Centro de Investigación Biomédica en Red en el campo de la Bioingeniería, Biomateriales y Nanomedicina (CIBER-BBN).

Debido al desarrollo de resistencias bacterianas, el interés en la búsqueda de nuevos compuestos para abordar infecciones ha crecido exponencialmente para los investigadores. Por este motivo, esta tesis doctoral está enfocada en el diseño de un apósito basado en nanofibras de policaprolactona (PCL) sintetizadas mediante electrospinning, que encapsulen compuestos naturales que actúen como anti-inflamatorios y antimicrobianos para el tratamiento de heridas. Con este objetivo, se ha llevado a cabo un profundo estudio de los aceites esenciales con propiedades bactericidas y anti-inflamatorias.

El primer objetivo de la tesis doctoral fue abordar la infección de heridas con compuestos naturales derivados de plantas. Para esto, se estudiaron las propiedades y los mecanismos de acción de diferentes compuestos en bacterias planctónicas utilizando dos modelos bacterianos, uno Gram-positivo, como *S. aureus* (ATCC 25923) y otro Gram-negativo, como *E. coli*-S17. Teniendo en cuenta que la formación de biofilm es un problema en las infecciones de heridas, se estudió el efecto de los compuestos naturales en un modelo de biofilm de *S. aureus*. El carácter volátil de los EOs y la posibilidad de oxidarse cuando están en contacto con luz ultravioleta o el aire, hacen difícil su aplicación. La encapsulación de estos compuestos ayuda a proteger sus propiedades y facilitar así su aplicación final. Así, el timol (THY) demostró ser el compuesto con mejor actividad antimicrobiana en ambos modelos bacterianos, de modo que fue encapsulado en nanofibras de PCL. La síntesis de nanofibras y la encapsulación del THY se

llevaron a cabo mediante la técnica de electrospinning. Este método permite la fabricación de nanofibras con encapsulación de compuestos volátiles, como el THY, gracias a la rápida formación de las fibras. Las propiedades bactericidas de los apósitos de PCL cargado con THY se estudiaron utilizando un modelo de *S. aureus* que expresaba GFP y así poder realizar ensayos cuantitativos y mediante microscopía confocal.

El segundo objetivo de la tesis ha sido encontrar un compuesto natural anti-inflamatorio para el tratamiento de heridas. Para ello, se ha optimizado un modelo inflamatorio *in vitro* en macrófagos J774 activados con lipopolisacárido (LPS). Estos experimentos se llevaron a cabo en el Methodist Hospital Research Institute en Houston (Texas, US), donde se determinaron los niveles de citoquinas inflamatorias lo que nos permitió determinar entre los testados los mejores compuestos naturales anti-inflamatorios. Además, las membranas de PCL-THY demostraron ser los mejores apósitos reduciendo la inflamación, entre los distintos tratamientos de estudio.

Tras concluir que el THY encapsulado en nanofibras de PCL mantiene las propiedades antimicrobianas y anti-inflamatorias, se desarrolló un modelo *in vivo* para determinar la efectividad de los apósitos en heridas de piel infectadas. Para ello, se utilizaron ratones sin pelo SKH1 para analizar las propiedades bactericidas e inflamatorias para su potencial aplicación clínica.

El documento está estructurado en diferentes capítulos que abordan cada uno de los objetivos de la tesis doctoral:

- El **Capítulo I** corresponde con la parte introductoria, donde se explican los conceptos generales. El capítulo incluye una descripción del proceso de curación de una herida, resaltando factores que afectan al mismo, como por ejemplo la infección e inflamación. Se explican también los diferentes tipos de tratamientos que existen, como los antibióticos, poniendo especial atención en el desarrollo de resistencias bacterianas a los mismos, como la razón principal de elección de compuestos naturales para el tratamiento de heridas. La técnica de electrospinning se detalla para entender la síntesis de fibras de PCL y la encapsulación de los principios activos.
- El **Capítulo II** se centra en la actividad antimicrobiana de los compuestos libres para abordar la infección de heridas. Se calculó la Concentración Mínima Inhibitoria (MIC) y la Concentración Mínima Bactericida (MBC) de diferentes compuestos derivados de

plantas en una cepa de *S. aureus* (ATCC 25923) y otra de *E. coli*-S17. Además, se desarrolló un modelo de biofilm en *S. aureus* para determinar el efecto de los compuestos libres en estas estructuras bacterianas. El mecanismo de acción de los aceites esenciales en las bacterias fue estudiado mediante microscopía electrónica de barrido (SEM) y citometría de flujo. Por último, se estudió la citotoxicidad de los compuestos en tres tipos celulares relacionados con la piel: fibroblastos, queratinocitos y macrófagos. Carvacrol (CAR), cinamaldehído (CIN) y THY demostraron tener la mayor actividad antimicrobiana en un modelo *in vitro* de *S. aureus* y *E. coli*. a través de la disrupción de la membrana bacteriana. Estos resultados están incluidos en el artículo publicado titulado “*Evaluation of the antimicrobial activity and cytotoxicity of different components of natural origin present in essential oils*”. García-Salinas, S.; Elizondo-Castillo, H.; Arruebo, M.; Mendoza, G.; Irusta, S. *Molecules* 2018, 23 (6), 1–18. <https://doi.org/10.3390/molecules23061399>.

- **Capítulo III:** Teniendo en cuenta los resultados obtenidos en el Capítulo II, el THY fue elegido para ser encapsulado en nanofibras de PCL, dada su capacidad antimicrobiana y su baja citotoxicidad comparada con el resto de los compuestos. Se midió el efecto del PCL-THY en contacto con cGFP-expressing *S. aureus* en suspensión y en forma de biofilm. Por último, se diseñó un modelo de co-cultivo con cGFP-expressing *S. aureus* y macrófagos J774 para estudiar el efecto del PCL-THY en células infectadas. Los apósitos de PCL-THY eliminaron el crecimiento bacteriano en un modelo de infección de macrófagos J774. Además, los estudios corroboraron la inhibición de la formación de biofilm. Los resultados están incluidos en el artículo titulado “*Antimicrobial Wound Dressings Against Fluorescent and Methicillin-Sensitive Intracellular Pathogenic Bacteria*” Garcia-Salinas, S.; Gamez-Herrera, E.; Landa, G.; Arruebo, M.; Irusta, S.; Mendoza, G. enviado para su publicación a ACS Applied Materials & Interfaces. Manuscript ID: am-2020-05668q.
- El **Capítulo IV** describe la actividad anti-inflamatoria de los aceites esenciales con el objetivo de reducir y controlar el proceso inflamatorio en la curación de heridas. La abundante inflamación puede causar la activación de células o citoquinas innecesarias que generan efectos deletéreos y retrasan el proceso de curación. Por esta razón, se optimizó

un modelo inflamatorio con macrófagos J774 activados con LPS y se estudió el efecto de diferentes compuestos naturales reportados como anti-inflamatorios. Los macrófagos infectados se trataron y se analizaron a nivel genético, midiendo los niveles de expresión de Il (Interleucina) 1b, iNos (óxido nítrico sintasa inducible) e Il10 por RT-PCR (Real Time-Polymerase Chain Reaction). Los aceites esenciales con mejor resultado se encapsularon en nanofibras de PCL y se estudió el efecto de los mismos, confirmando los resultados previamente obtenidos. Además, se realizaron experimentos en los que se evaluó la morfología celular, comparando las células tratadas con controles positivos (células activadas con LPS sin tratamiento) y negativos (células no activadas con LPS). Este experimento demostró la similitud entre las células tratadas y las no activadas, confirmando los efectos anti-inflamatorios del tratamiento. Los resultados están incluidos en el artículo publicado titulado “*Electrospun Anti-Inflammatory Patch Loaded with Essential Oils for Wound Healing*”. García-Salinas, S.; Evangelopoulos, M.; Gámez-Herrera, E.; Arruebo, M.; Irusta, S.; Taraballi, F.; Mendoza, G.; Tasciotti, E. *Int. J. Pharm.* **2020**, 577 (January), 119067. <https://doi.org/10.1016/j.ijpharm.2020.119067>

- El **Capítulo V** unifica toda la investigación realizada durante la tesis en un modelo *in vivo* de infección de heridas con *S. aureus* (ATCC 25923) en ratones sin pelo SKH1. Se analizaron las propiedades bactericidas y antiinflamatorias de los apósitos diseñados. Además, se realizaron controles del compuesto libre y de clorhexidina (compuesto utilizado en la clínica) para conocer las ventajas de nuestros apósitos frente a otros tratamientos. En cuanto al control de la infección, se realizaron medidas cuantitativas y cualitativas de las bacterias presentes en la herida a diferentes tiempos post-infección. En cuanto al control de la inflamación, se realizaron análisis histológicos de las heridas evaluando la reacción de células inflamatorias y la formación de nuevos vasos sanguíneos. Los estudios demostraron que los apósitos de PCL-THY pueden prevenir la infección, además de promover la regeneración en heridas. Los resultados están incluidos en el artículo titulado “*Efficiency of Antimicrobial Electrospun Thymol-Loaded Polycaprolactone Mats in vivo*” Garcia-Salinas, S.; Gamez-Herrera, E.; Asin, J.; de Miguel, R.; Andreu, V.; Sancho-Albero, M.; Mendoza, G.; Irusta, S.; Arruebo, M.: aceptado para su publicación en ACS Applied Biomaterials. Manuscript ID: mt-2020-002706.



- El **Capítulo VI** resume las principales conclusiones obtenidas en este trabajo.
- El **Apéndice I** describe las técnicas de caracterización y métodos biológicos utilizados para evaluar la actividad antimicrobiana y anti-inflamatoria de los compuestos libres y encapsulados.
- El **Apéndice II** indica las referencias utilizadas en este trabajo
- El **Apéndice III** señala los artículos publicados y la participación en congresos que se han llevado a cabo durante la tesis



# Chapter I

## INTRODUCTION

### **Summary**

This chapter provides a brief review of the literature and the state of the art about wound healing process and potential treatments. The chapter includes a description of factors that delay the procedure, such as infection and inflammation, and describes the emerging problem of antibiotic resistances. Abording the novel technology of nanoscience, electrospinning technique allows nanofibers synthesis encapsulating bioactive molecules. EOs demonstrated low levels of induction of antimicrobial resistance that make them interesting for bactericidal applications. This chapter describes electrospinning mechanism and the advantages that provides to encapsulate plant-derived natural compounds as bioactive molecules to deal with wound healing treatment.

## Table of contents

<b>I.1. Wound healing process</b>	<b>17</b>
I.1.1. Coagulation and hemostasis phase	18
I.1.2. Inflammatory phase	18
I.1.3. Proliferative phase	19
I.1.4. Remodeling phase	20
<b>I.2. Factors affecting wound healing</b>	<b>21</b>
I.2.1. Importance of infection	21
I.2.2. Biofilm formation	23
I.2.3. Bacteria resistance to antibiotics	25
I.2.4. Antiseptics	27
<b>I.3. Essential oils</b>	<b>27</b>
I.3.1. Activity of essential oils against bacteria	29
I.3.2. Anti-inflammatory activity of essential oils	30
I.3.3. Biomedical application of essential oils	33
<b>I.4. Wound dressings</b>	<b>33</b>
I.4.1. Advanced wound dressings	34
I.4.2. Bioactive wound dressings	34
<b>I.5. Electrospun nanofibers</b>	<b>35</b>
I.5.1. History of electrospinning	35
I.5.2. Principle of electrospinning	36
5.2.1. Formation of Taylor Cone	37
5.2.2. Thinning of the Jet	37
5.2.3. Solidification of the Jet	38
I.5.3. Materials of electrospinning	39

## I.1. Wound healing process

A cutaneous wound is defined as the disruption of the normal structure and function of the skin, in which many cell types collaborate to restore the tissue in a physiological process called wound healing.<sup>1,2</sup> A wound can range from a superficial damage in the epithelial integrity to the disruption of deeper subcutaneous tissues such as muscles and vessels.<sup>3</sup> There are different types of wounds:

- a. Acute wounds: These wounds imply both functional and anatomical restoration in 5-10 days or within 30 days. They can be acquired by traumatic loss of tissue or by a surgical procedure.<sup>1</sup>
- b. Chronic wounds: This type includes wounds that do not progress orderly and total healing may be delayed, incomplete and disturbed by many factors which prolong one or more physiological stages. These factors involve infection, hypoxia, necrosis, production of exudates and increased levels of cytokines or immune cells that perpetuate a non-healing state. These wounds can be caused by pressure, burns, vasculitis, etc.<sup>1,4</sup>
- c. Complicated wounds: These wounds are those that combine a cutaneous infection and a tissue defect. Bacteria colonization depends on the virulence, number and type of microorganism present and may perpetuate a non-healing state. In this type of wound, it becomes very relevant the tissue defect, including its traumatic or post-infectious aetiology.<sup>4</sup>

Wound healing is a complex and dynamic progression which involves four different steps represented in Figure I.1: 1) arrest the bleeding by blood coagulation and hemostasis; 2) initiation of an acute inflammatory response to the initial injury; 3) cell proliferation, migration and regeneration; 4) remodeling of connective tissue in which the aim is to restore the skin integrity and strength to culminate the repair of the tissue.<sup>5</sup> These events can occur together or independently depending on the cell type compromised by the injury.<sup>6</sup>

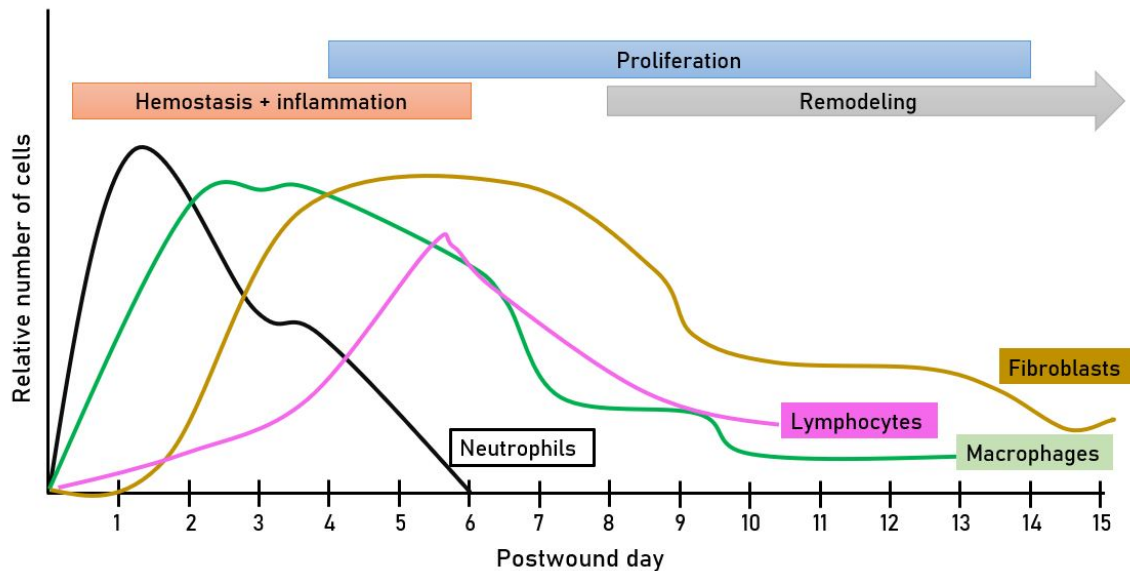


**Figure I.1:** Wound healing evolution and cell expression in each phase of the process. Adapted from *Plastic and Reconstructive Surgery*, 117/7, G. Broughton, J.E. Janis, C.E. Attinger, *The basic science of wound healing*, 12S-34S.

### I.1.1. Coagulation and hemostasis phase

Coagulation and hemostasis take place immediately after injury with two main goals; in a short term, to arrest bleeding. In a long-term, it provides an extracellular matrix needed during the wound healing process (monocytes, neutrophils, fibroblasts and endothelial cells) avoiding the colonization of external agents. Immediately upon injury, damaged blood vessels vasoconstrict and the coagulation cascade is initiated. The process results in a fibrin clot formation, which consists of an aggregation of collagen, platelets, thrombin, fibrinogen and fibronectin in a fibrin network, which stops bleeding and releases cytokines and growth factors that help to initiate the inflammatory response.<sup>7,8</sup> This phase needs special attention for infection. Microbes have free entrance to deeper tissues and thus, the possibility to colonize and contaminate them.

### I.1.2. Inflammatory phase

Inflammation is a localized and protective response to a tissue injury which can be aggravated under the presence of infection. Inflammatory cells play a key role in wound healing contributing to the clean-up of cell debris, as well as to the protection of the wound from microorganisms.<sup>9</sup> The inflammatory stage is divided in two different phases:

- a. Early inflammatory phase: The fibrin clot and damaged cells release intracellular contents such as danger-associated molecular patterns (DAMPs), which activate cytokines such as interleukin 1 (IL-1), tumor necrosis factor  $\alpha$  (TNF $\alpha$ ), transforming growth factor  $\beta$  (TGF $\beta$ ) or IL-18, among others. When they accumulate, the inflammatory phase is initiated.<sup>8,10</sup> In addition, pathogen-associated molecular patterns (PAMPs) join to their ligands in toll-like receptors (TLRs) leading the production of more growth factors and cytokines.<sup>11</sup> As response, prostaglandins manage the blood vessels vasodilation to allow the effective circulation of inflammatory cells.<sup>12,13</sup> As Figure I.1 shows, neutrophils take relevance in this phase by the expression of pro-inflammatory cytokines and the clearing of bacteria and debris by the release of proteolytic enzymes that will digest bacteria and damaged tissue.<sup>14</sup> This cell type is responsible for the transmigration through the endothelial layer to allow the expression of adhesion molecules, attracting more inflammatory cells.
- b. Late inflammatory phase: As part of the late inflammatory phase, more neutrophils and other immune and repairing cell types are attracted to the injury (Figure I.1).<sup>2</sup> For example, monocytes in the nearby tissue and blood are attracted to the injured area and transformed into macrophages, which are able to present antigens, call other inflammatory cells to the wound area, phagocyte the dead neutrophils, kill bacteria by phagocytosis and generate nitric monoxide (NO).<sup>2,15,16</sup> Two types of macrophages can be differentiated; i) classically activated M1 pro-inflammatory macrophages, present in a first stage of wound healing and ii) alternatively activated M2 anti-inflammatory and pro-angiogenic macrophages.<sup>17</sup>

This well-coordinated procedure is possible due to the production of arrest signals as checkpoint controllers of inflammation.<sup>18</sup>

### I.1.3. Proliferative phase: Epithelization, angiogenesis and provisional matrix formation

The closure of the injured tissue takes place during the proliferative phase, when angiogenesis, fibroplasia and re-epithelialization occur.<sup>19</sup> Macrophages are the link between the inflammatory and proliferative phases. M2 macrophages manage the transition into the proliferative phase acting as angiogenesis and fibroplasia mediators by the release of different factors such as the vascular endothelial growth factor (VEGF), TNF $\alpha$ , TGF $\beta$ , epidermal growth factor (EGF), platelet-derived growth factor (PDGF) and IL-1. It has been reported that animals showing macrophage depletion have a delayed epithelization.<sup>14,20</sup>

Chemotaxis is the ability of cells to move along a chemical gradient.<sup>21</sup> In response to EGF and TGF $\alpha$ , epithelial cells in the edge of the wound start proliferating and moving by chemotaxis to form a barrier against microorganisms and fluid losses.<sup>22</sup> Fibroblasts and endothelial cells are the most predominant cellular groups in this phase (Fig. I.1). Endothelial cells secrete VEGF, PDGF, TNF $\alpha$ , and TGF $\beta$  to promote vasodilation, neovascularization and vessel repair. In addition, NO released by endothelial cells in response to hypoxia, stimulates more VEGF production.<sup>15,16</sup> This chemotactic activity is necessary for angiogenesis, in order to supply nutrients and oxygen to tissues, and to promote immune cells migration.<sup>23-25</sup>

Fibroblasts migrate into the wound and secrete keratinocyte growth factor (KGF)-1 and IL-6 to stimulate keratinocytes migration, proliferation and differentiation to the injured area.<sup>15,16</sup> In addition, fibroblasts release PDGF and start synthesizing collagen to provide integrity and strength, and transform into myofibroblasts, which are important for wound contraction. Medrado *et al.*<sup>9</sup> demonstrated that myofibroblasts accumulated on the edges of the wound promote contractive activities, closing the wound's borders toward the center. Fibroblasts are also responsible for synthesizing a provisional matrix formed of collagen, glycosaminoclycans, hyaluronan and fibronectin. Abundant extracellular matrix (ECM) accumulates and promotes cell migration for tissue regeneration.<sup>26,27</sup>

#### I.1.4. Remodeling phase

Remodeling phase is characterized for forming new epithelium achieving the maximum tensile strength through degradation, reorganization and synthesis of ECM, to restructure normal tissue.<sup>6</sup> Three of the most remarkable processes during this phase are: a) maturing of the elements in tissue, b) resolution of the inflammation and c) changes in the composition of the ECM.<sup>28</sup> For example, the initial and disorganized matrix composed of fibrin and fibronectin is replaced;<sup>8</sup> collagen type III starts to degrade and hyaluronic and fibronectin acid levels are reduced, meanwhile the synthesis of type I collagen increases.<sup>29</sup> In the final step of wound healing, collagen fibers start to be thicker and to align in parallel in order to increase the tissue strength.<sup>30</sup> Depending on the injured area and healing duration, approximately 80% of collagen fibers recover the original strength, although it depends on the localization and duration of the repair. Nevertheless, the original strength can never be recovered.<sup>1,4</sup>

With the aim to form a scar with a reduced number of cells, inflammatory cells and fibroblasts disappear from the wounded area. The remaining fibroblasts change their phenotype



and transform into myofibroblasts with contraction properties to achieve an efficient tissue closure.<sup>9,31</sup> All the process is controlled by different growth factors such as PDGF, TFG- $\beta$  and FGF (Fibroblast Growth Factor).<sup>32,33</sup>

## **I.2. Factors affecting wound healing**

Wound healing is a complex process in which many factors can affect physiologic responses and cellular function. For example, hypoxia or decreased glucose levels can slow down the healing process due to the high requirement of an adequate supply of energy. Particularly, the proliferative phase is characterized by an enhanced metabolism that needs a rich blood supply to provide glucose and oxygen,<sup>34,35</sup> which may be impaired under hypoxic or hypoglycemic conditions. On the other hand, ischemia can be associated with edema or elevated tissue pressures, which compromises the inflammatory phase by affecting wound perfusion and thus, delaying the wound healing process.<sup>36</sup> Illnesses as diabetes mellitus or hypothyroidism can affect the proliferative and remodeling phases by decreasing collagen production and maturation. As consequence, wound tensile strength is reduced and wound healing delayed.<sup>37,38</sup> Some factors, such as age, hypothermia, nutrition, smoking or corticosteroids, can prolong the wound healing process at different phases.<sup>36</sup> For example, experimental studies have demonstrated a decreased healing in older animals in which inflammatory and proliferative phases are affected.<sup>39</sup> Hypothermia or nicotine induce vasoconstriction, reducing cellular response and, as consequence, the efficiency of healing.<sup>40,41</sup>

One important factor affecting healing is wound infection. Invasion and dissemination of microorganisms may affect the host natural immune system and delay wound healing.<sup>42,43</sup> The clinical significance of load infection in delaying wound healing was described back in 1964 by Bendy *et al.*<sup>44</sup> and until now, there have been multiple studies about effects, causes and treatments for wound infection.

### **I.2.1 Importance of infection**

When skin is damaged, bacteria can penetrate into the tissue causing infections.<sup>45</sup> In addition, the accumulation of cellular debris can promote bacterial colonization and infection, highlighting the importance of clearing the wound of microorganisms, dead tissue and foreign bodies.<sup>1,42</sup> The origin of wound contaminants are mainly three: a) the environment, b) the surrounding skin and c) endogenous sources involving mucosal membranes.<sup>46</sup> Aerobic or

facultative pathogens receive importance for being the main causes of delayed wound healing and infection. For example, the Center for Disease and Prevention guideline has recognized *Staphylococcus aureus*, *Escherichia coli*, *Pseudomonas aeruginosa* and coagulase-negative staphylococci, as the most frequent pathogens in surgical wound infections.<sup>47</sup> *S. aureus* takes relevance in cutaneous wounds, being the most common pathogen isolated from surgical site infections and cutaneous abscesses.<sup>48</sup> The most common wound infections depending on the origin are the following:

- a. Surgical site infection (SSI) has been described as the most typical type of hospital-acquired infection. SSI is defined as a postoperative infection that takes place within 30 days of a surgical practice.<sup>49,50</sup> Clean surgery implies 1-5% risk of post-operative infection, meanwhile the percentage rises to 27% in non-sterile procedures. SSI causes an increase in clinical and economical expenses not only due to prolonged hospitalization, diagnostic tests or additional treatments (direct costs), but also related to the patient's physical and mental health (indirect costs).<sup>51,52</sup> It has been reported that patients with SSI generate an economical burden double that patients who do not develop an infection.<sup>53</sup> In 2015, the Spanish healthcare costs related to SSI reached \$1.084.639, meanwhile when indirect costs were included, this number increased.<sup>54</sup>
- b. Soft tissue infections are defined as infections of any of the layers in the soft tissue (dermis, subcutaneous tissue, superficial or deep fascia and muscle). It has been demonstrated that *S. aureus* is the pathogen that infects 25-30% of this type of wounds, although infection can also have a polymicrobial origin.<sup>42,55</sup>
- c. Bite wound infections: Bacterial population of an animal bite depends on the oral flora of the animal and is often polymicrobial having a mixture of aerobic and anaerobic organisms. Most common bites are from dogs and cats.<sup>56</sup>
- d. Burn wound infections: Burns are a type of trauma related with thermal injury. The skin is a barrier to microbial invasion; when these wounds are moderate or severe, they need immediate specialized care to minimize morbidity and mortality. According to the National Center for Injury Prevention and Control in the United States, approximately 500,000 burn cases needed medical treatment in 2016 and about 5,000 patients died from burn related complications such as infections. *S. aureus* is the most common pathogen that colonize burns in a first instance.<sup>57,58</sup>

- e. Leg, foot and decubitus (pressure) ulcers are produced for the prolonged immobilization, causing skin breakdown due to pressure over a bony prominence. Bacterial infection is the most common complication associated with this trauma, specifically, with soft tissues and bones, resulting in both morbidity and mortality and increased costs for healthcare facilities.<sup>59,60</sup> There exist 4 different pressure injuries according to the severity and level of tissue damaged. Stage I corresponds with an erythema; Stages II and III are deep tissue injuries, and stage IV corresponds to a full thickness tissue loss.

Wounds heal quickly if the conditions in the injured site are optimal, in terms of maintaining blood perfusion to deliver oxygen, nutrients and immune cells and thus, providing a minimal chance for pathogenic microorganisms to colonize and proliferate.<sup>61</sup> However, there are predisposing factors for infection, including diseases, poor hygiene or low host immunity.<sup>62</sup> An infected wound progression includes a range of microbial and host factors such as type, size, site and depth of the wound, microbial load and level of virulence, the immune status of the host and level of blood perfusion.<sup>42</sup> Non-healing wounds are characterized by a prolonged inflammation, failure in re-epithelialization and remodeling. Signs of persistent infection can be pain, erythema, edema, heat and purulence, or in a more advanced wound, serous exudate, discoloration of granulation tissue and wound breakdown.<sup>63</sup>

### I.2.2 Biofilm formation

The existence of bacteria, particularly in chronic colonization, is not usually as a free-living planktonic state, but in clusters called biofilms. Biofilms are populations of bacteria aggregated and embedded in a self-secreted extracellular polymeric substance (EPS) which provides a protective environment to exogenous threats. Biofilm thickness can range from microns to millimeters and can be constituted of a single type of bacteria or polymicrobial. This matrix includes a complex structure of water channels to allow transfer of nutrients and waste products.<sup>64</sup>

Infected wounds can lead to severe conditions when biofilms are formed. It has been reported that biofilms can be many times more resistant than planktonic bacteria to antibiotic treatment.<sup>43</sup> Within biofilm, intercellular signaling molecules produced by bacteria are present; in response to factors secreted by other bacteria in the community, they can coordinate bacterial activities, control the biofilm growth pattern or change the phenotype and thus, its virulence factors. This phenomenon is called quorum sensing (cell-cell communication). In this regard,

two different groups of signaling molecules are released: Gram-negative bacteria release fatty acid derivatives, meanwhile Gram-positive bacteria use peptide derivatives for intercellular communication.<sup>65,66</sup>

Biofilm can grow in nature (plants, rocks, soil), medical devices (catheters, valves) and in the human body, in which biofilm helps bacteria to protect themselves of external agents, increasing the resistance to different therapies and host defenses. It has been reported that antibiotic concentration against biofilm should be many times higher than the dose used against planktonic bacteria.<sup>67</sup> As Figure I.2 shows, a biofilm cluster can detach from the original surface and move onto surrounding areas causing infection dissemination.<sup>64</sup>

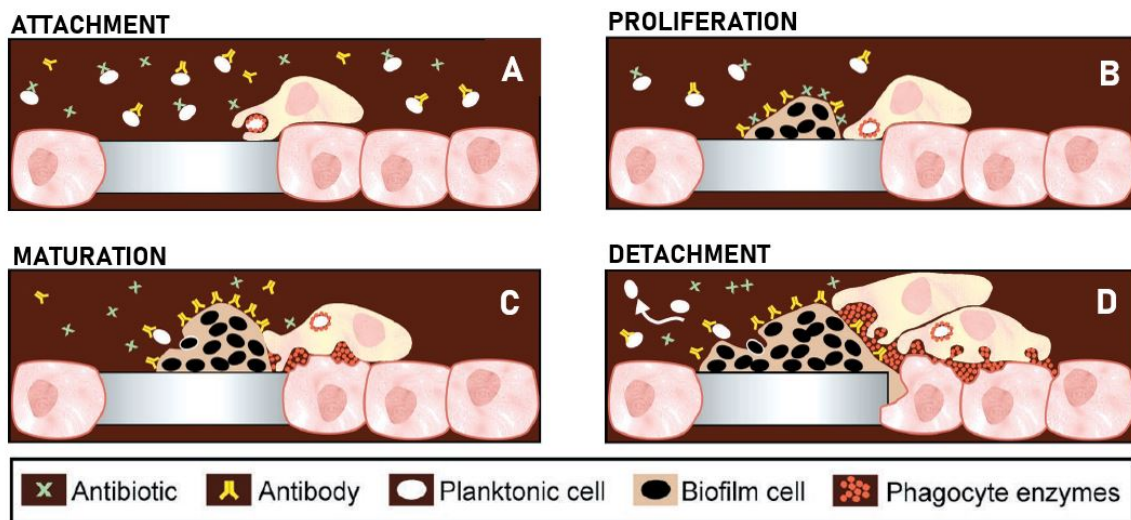


Figure I.2: Representation of biofilm formation. (A) Attachment: Bacteria in wounds can be cleared by antibodies and immune cells. (B) Proliferation: Bacteria can attach to the wound and start forming biofilm. (C) Maturing: Biofilm grows attracting more immune cells, which release phagocytic enzymes. (D) Bacteria can be released from biofilm and disseminate. Phagocytic enzymes can damage tissue in the edges of the wound. Adapted from Science, 284/5418, J. Costerton, P. Stewart, E. Greenberg, Bacterial biofilms: A common cause of persistent infections, 1318-1322.

Biofilm formation would allow bacteria to increase host inflammation, which alters the normal transition from inflammatory to proliferative phases and thus, delays wound healing process. Bacteria within biofilm can alter many inflammatory mediators such as cytokines and blood components, and change oxygen concentration and pH in the wound, affecting not only the inflammatory cellular response, but also the repair phase.<sup>68</sup> For example, prolonged presence of neutrophils in wounds, delay the healing process by the release of oxygen species and

inflammatory factors. Also, keratinocytes migration is inhibited by the presence of these cells.<sup>69</sup> Due to the expression of neutrophils and macrophages, pro-inflammatory cytokines secretion is increased, resulting in an impaired wound healing.<sup>70</sup>

### I.2.3 Bacteria resistance to antibiotics

How an infected wound should be treated is a widespread discussion that remarks the importance of clinical observations and microbiological care in wound healing. Advanced cutaneous infections or deep tissue affections are recommended to be treated with systemic antibiotics. However, if the infection is localized in an injured area, the treatment should be initiated with topical agents. Topical antimicrobial compounds include antiseptics and antibiotics. If these first topical treatments fail, an alternative topical therapy can be considered, unless clinical signs of infection are progressing. In that case, systemic antibiotic therapy should be prescribed with the narrowest spectrum of antimicrobial activity. With no signs of infection, systemic antibiotics should not be used.<sup>42</sup>

Antibiotics are substances that kill or inhibit the growth of bacteria in or on the body.<sup>71</sup> Although antibiotics have been one of the most important advances in research and medicine, the excessive use of these compounds, not only in human health, but also in agriculture and livestock, has helped bacteria to develop antibiotic resistance strategies, bringing today a global concern for human health. Antimicrobial resistance (AMR) development has been rated among one of the 10 urgent threats by the World Health Organization in 2019.<sup>72</sup> Antibiotic resistance is a mechanism of adaptation to antibiotic exposure in which microbes develop resistance against most used antibiotics.<sup>73,74</sup> The most common drug-resistant microorganisms are *Enterococcus faecium*, *S. aureus*, *Klebsiella pneumoniae*, *Acinetobacter baumannii*, *P. aeruginosa*, *Enterobacter spp.*, and *E. coli* pathogens, all of them belong to a group called ESKAPEE.<sup>75</sup> Some of them are considered as critical by the WHO.<sup>76</sup> Since 2000<sup>77</sup>, only 30 new antibiotics have been approved for clinical use, and around 40 are in different developmental phases.<sup>78</sup> AMR cause 50.000 deaths every year across the US and Europe, although it is expected to rise up to 10 million deaths in 2050.<sup>79</sup>

It is reported that changes that allow resistance to appear, are produced at the genetic level (Figure I.3). In particular, one of the mechanisms to develop AMR is that bacteria are capable to mutate or introduce new genetic information without disturbing their target function.<sup>80,81</sup> Another mechanism is that bacteria may block the target access by modifying membrane

permeability. In that case, Gram negative bacteria are less permeable than Gram positive bacteria due to the presence of outer membrane and thus, this type of bacteria have a higher possibility to develop AMR.<sup>82,83</sup> In addition, porins of the membrane (channels for diffusion of hydrophilic antibiotics) can mutate, reducing the diffusion of antibiotics inside the cell.<sup>84</sup> Another mechanism is through the use of active efflux pumps (EPs), which have the ability to reduce antibiotics concentration inside the bacterial cell by flushing them out.<sup>74</sup> Apart of all these mechanisms, bacteria have the ability to modify drug molecules inactivating the site of union to their target, for example, adding chemical groups such as phosphates or hydrolyzing antibiotics.<sup>85</sup>

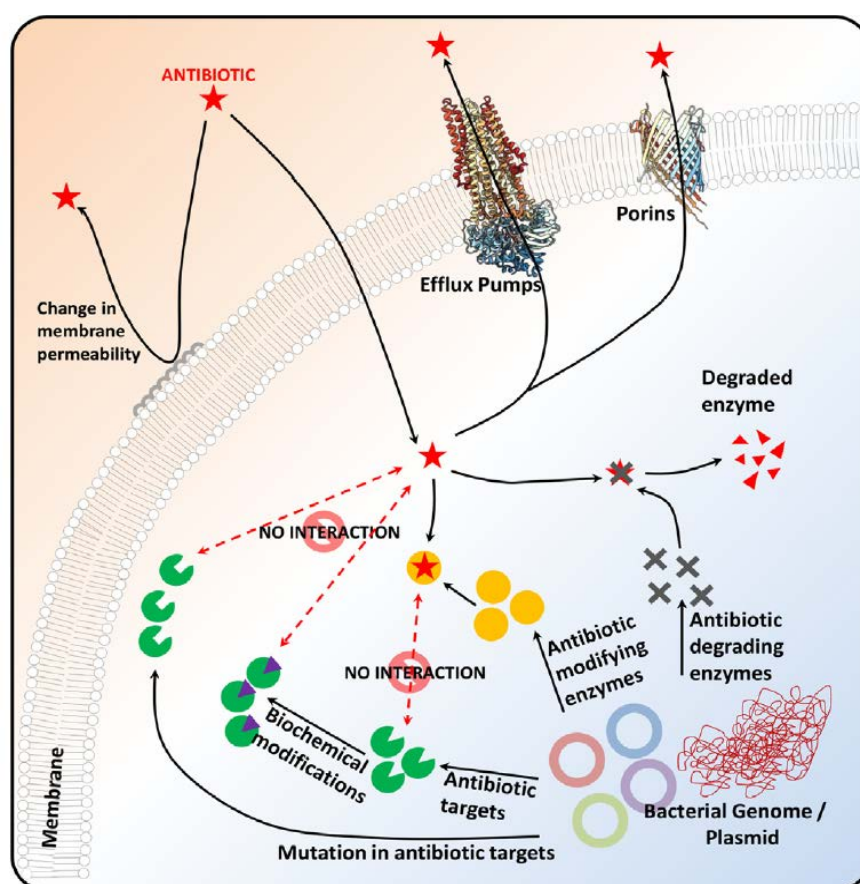


Figure I.3: Molecular mechanisms in bacteria to develop antimicrobial resistance. Reprinted from *Fitoterapia*, 140, Z. Yu, J. Tang, T. Khare *et al.*, The alarming antimicrobial resistance in ESKAPEE pathogens: Can essential oils come to the rescue? pages 1044-33., Copyright (2020), with permission from Elsevier.

Biofilm formation has an important role helping bacteria to develop antibiotic resistances.<sup>86</sup> It was thought that EPS matrix in biofilm did not allow antibiotics to penetrate and reach bacteria. However, it was demonstrated that antibiotic can diffuse through biofilms

and, as a consequence, the acquired resistance may be associated to intrinsic features of bacteria. It is known that antibiotic targets are related to bacterial metabolism. However, since bacteria within the biofilm are dormant, antibiotics have not an active effect on them. Related to the resistance acquisition, it has also been reported that oxidative stress, bacterial density and nutrition supply are factors that can help to develop mutation and specific gene expression.<sup>87,88</sup>

#### I.2.4 Antiseptics

Apart from antibiotics, there exist a wide range of antiseptics that have been used to control infections in wound healing. Antiseptics are chemical agents that are toxic to a wide range of microorganisms that inhibit their growth and development, in contrast to antibiotics, which selectively kill and inhibit the growth and development of bacteria.<sup>71,89</sup> Historically, the antiseptics most used have been hydrogen peroxide, iodine-based preparations, Dakin's solution (dilute hypochlorite), chlorhexidine and silver-releasing compounds. It has been reported that hydrogen peroxide, chlorhexidine and iodine-based preparations are toxic to tissues when they are applied chronically to wounds.<sup>89-91</sup> Silver ions have demonstrated efficacy against Gram-negative and antibiotic resistant microorganisms. Their mechanism of action consists on a sequence of events such as the disruption of bacterial cell walls, penetration into the cell and action at the target side, damaging intracellular and nuclear structures.<sup>92,93</sup> Silver ions should be used as a solution to produce bactericidal activity, being its effect not complete in a dry wound. In addition, this product can cause irritation and be toxic to keratinocytes and fibroblasts.<sup>89,94</sup> Other products described as antiseptics are natural compounds, which have been widely reported due to their antimicrobial activity.

### **I.3. Essential oils**

As previously commented, AMR is expected to cause 10 million deaths by 2050.<sup>79</sup> Since the development of resistance to antibiotics is increasing, there is a need for innovative approaches of new antimicrobials with reduced ability to generate resistances.<sup>73</sup> Even though essential oils (EOs) have been set aside by the antibiotic era, they possess different properties that make them potential compounds for clinical strategies in wound management.<sup>95</sup>

EOs are concentrated natural products formed by aromatic plants, among others, as secondary metabolites. In nature, these compounds are crucial in the protection of plants being antibacterial, antivirals, anti-fungal and insecticides. In addition, they play a key role reducing

the appetite of herbivores for such plants and attracting insects for pollen and seed dispersion. Historically, these compounds have been used in embalment, preservation of foods and for medical applications.<sup>95</sup> These compounds are volatile, rarely colored and soluble in lipids and in organic solvents, which are present, among others, in different plant organs such as buds, flowers, leaves, seed, fruits, roots, etc. There have been reported approximately 3,000 EOs, 300 of which are important for pharmaceutical, agronomic, food, sanitary, cosmetic and perfume industries due to their antioxidant, antibacterial, food preservation, anti-inflammatory and local anesthetic properties.<sup>95-97</sup> Each EO is a mixture of about 20 to 60 different components in different concentrations. Only 2 or 3 of these components are at high concentrations and determine the biological and chemical properties of the essential oil.<sup>98</sup> Next, most common used plant-derived natural compounds in medical applications are going to be here briefly described:

- a. Carvacrol: It is a volatile phenolic monoterpene present as active principle in essential oils in plants such as Lamiaceae (*Origanum* genera) and Verbenaceae (*Lippia* genera). This compound possesses different properties as antimicrobial, antioxidant, antifungal and anti-inflammatory.<sup>99-101</sup>
- b. Thymol: It is a phenolic monoterpene found in essential oils extracted from plants which belong to the Lamiaceae family, included in *Thymis*, *Lippia* and *Origanum* genera, among others. Different properties of this compound have been reported, as antimicrobial, antioxidant, antiseptic and anti-inflammatory.<sup>102-104</sup>
- c. Cinnamaldehyde: It is a phenylpropanoid present in *Cinnamomum cassia* (*Cinnamomum* genera), giving cinnamon its characteristic odor. It shows diverse pharmacological activities like antimicrobial, antioxidant and anti/pro-inflammatory.<sup>100,105,106</sup>
- d. Eugenol: Eugenol is the major component of clove, flower buds of the tree in the family Myrtaceae. This compound is an aromatic phenol that possesses antimicrobial, antioxidant, anti-inflammatory and cytotoxic properties.<sup>107</sup>
- e.  $\beta$ -caryophyllene: This compound is a bicyclic sesquiterpene derived from many plants such as basil (*Ocimum spp.*), black pepper (*Piper nigrum L.*), cinnamon (*Cinnamomum spp.*) or oregano (*Origanum vulgare L.*). Its biological effects are antimicrobial, antioxidant, anti-inflammatory and analgesic.<sup>108</sup>
- f. Rosmarinic acid: It is a phenolic acid present in several plants of the Lamiaceae family, including rosemary (*Rosmarinus officinalis*). The main properties of this compound are antioxidant, anti-inflammatory, antibacterial and adstringent.<sup>109,110</sup>



- g. Squalene: It is a triterpene compound present in a large amount of plants and other sources as shark liver oil. One species with high squalene content is *Polygonum chinense L.* The main properties of this compound are antioxidant, anti-inflammatory, antibacterial and antifungal.<sup>111,112</sup>
- h. Tyrosol: Tyrosol is a polyphenolic compound extract from *Olea europaea* that acts as antioxidant, anti-inflammatory and antimicrobial.<sup>113,114</sup>
- i. Curcumin: This compound is a polyphenolic present in the rhizome of turmeric of *Curcuma longa*. It possesses a wide range of biological actions as antiapoptotic, anti-inflammatory, antioxidant, anti-carcinogenic, among others.<sup>115,116</sup>

### I.3.1. Activity of essential oils against bacteria

To better understand the mechanisms of action of EOs against bacteria, it is necessary to know the different structures of the cell walls of Gram-positive and Gram-negative bacteria. Gram-positive bacteria wall consists of a 90-95% of peptidoglycans linked to other molecules and proteins. However, Gram-negative bacteria structure is more complicated due to the presence of an outer membrane (OM) that lies outside the inner peptidoglycan-based layer. Both layers are linked by Broun's lipoproteins, covalently connected to peptidoglycans and embedded in the OM. This layer allows hydrophilic solutes transport but it is almost impermeable to hydrophobic molecules.<sup>117</sup>

The activity of EOs against bacteria depends on their chemical composition and it is based on multiple mechanisms of action.<sup>118,119</sup> Commonly, EOs inhibit the growth of bacteria and the synthesis of toxic bacterial metabolites. For example, cell membrane is the first target of EOs. The integrity of this structure is crucial for bacteria survival because it is responsible for metabolites and ions transport, which are essential for all the activities occurring in the microbial cell. Also, the membrane represents an effective barrier from the external environment.<sup>120</sup> The hydrophobicity of EOs disrupts bacterial structures, resulting in an alteration of membrane permeability and thus, leading to the leakage of cell content, cytoplasm coagulation or proteins denaturation.<sup>119</sup>

The antimicrobial activity of terpenoids, such as thymol and carvacrol, is related to the hydroxyl group and the presence of delocalized electrons in their chemical structure.<sup>121</sup> It has been demonstrated that it is not as important the hydroxyl position as its presence.<sup>118,122</sup> Thymol can interact with the polar head-groups of lipids, damaging the outer and inner membranes. It

affects membrane permeability and thus, allows the release of  $K^+$  ions and Adenosine Triphosphate (ATP).<sup>121,123,124</sup> Carvacrol, an isomer of thymol, causes structural and functional damage to membranes, increasing fluidity and permeability and thus, releasing bacterial lipopolysaccharides (LPS). Moreover, carvacrol can alter ions transport, introducing  $H^+$  into the cytoplasm and exporting  $K^+$  outside the cell.<sup>122,123</sup> Regarding phenylpropenes molecules, such as eugenol and cinnamaldehyde, they can exhibit antimicrobial activity due to the methyl group and the presence of a double bond in the  $\alpha$ ,  $\beta$  positions of the side chain. Depending on the concentration, cinnamaldehyde can: a) inhibit enzymes involved in cytokine interactions at sub-lethal concentrations; b) inhibit ATPase at higher doses and c) modify membrane permeability, similar to thymol and carvacrol at lethal concentrations.<sup>125</sup> About eugenol, apart from affecting ATP transport, it can change the membrane fatty acid profile and target different enzymes as ATPase, histidine carboxylase, amylase and protease, affecting the membrane fluidity and thus acting as antimicrobial compound.<sup>125,126</sup>

To sum up, plant-derived natural compounds have not specific cellular targets but multiple ones. Owing their hydrophobicity, they can pass through the cell wall and the cytoplasmic membrane altering the cellular permeability, causing cellular destabilization by different mechanisms, what is known as “essential oils versatility”.<sup>119</sup> Only a few articles have described some bacterial mechanisms to counteract EOs damage, as for example, the effect on the fatty acids. Thus, bacteria would adapt the membrane to the damage trying to survive. When EOs modify membrane components and compromise fluidity, bacteria can increase the amount of unsaturated fatty acids, responsible for the fluidity of the membrane.<sup>127</sup> In spite of this mechanism, and due to the fact that EOs can act at different levels, there has not been described the development of EOs resistance.<sup>128</sup>

### I.3.2. Anti-inflammatory activity of EOs

Inflammation is a protective mechanism in response to injury or infection.<sup>9</sup> During this process, there is an influx of inflammatory cells to the damaged area, increased activity of different enzymes, expression of cellular adhesion molecules such as the intercellular adhesion molecule (ICAM), and release of cytokines.<sup>129</sup> With the aim to reduce excessive and prolonged inflammation, the anti-inflammatory activity of EOs has been studied. This EOs activity is attributed to their antioxidant properties and the interaction with signaling cascades related with cytokines and transcription factors. There are three typical targets for EOs:

- a. Effects on the arachidonic metabolism: Arachidonic acid is a polyunsaturated fatty acid present in cell membranes that can be released to the external medium when inflammation is activated. It is metabolized by two main pathways, the cyclooxygenase (COX) and lipoxygenase (LOX) pathways, in different eicosanoids such as prostaglandins and leukotrienes.<sup>129</sup> Both are responsible of amplifying and mediating inflammatory response, enhancing vascular permeability; in addition, leukotrienes mediate the contraction of muscle fibers in blood vessels.<sup>130</sup> It has been reported that some active principles of EOs, such as thymol and eugenol, can inhibit lipoxygenase effects and thus, acting as anti-inflammatory compounds.<sup>131</sup>
- b. Effects on cytokines production: The production of cytokines may be enhanced by the release of LPS and lipoteichoic acid (LTA). The first one is present in Gram-negative bacteria, meanwhile LTA is a molecule present in the cytoplasmic membrane of Gram-positive bacteria. Il-1 $\beta$  and TNF- $\alpha$  are two of the main cytokines which levels are increased in the inflammatory process. The major sources of Il-1 $\beta$  release are macrophages, neutrophils and T lymphocytes, whereas TNF- $\alpha$  is produced by macrophages, fibroblasts and endothelial cells.<sup>132</sup> It is known that active principles in EOs can reduce or even inhibit the production of these cytokines. For example, cinnamaldehyde can inhibit the secretion of Il-1 $\beta$  and TNF- $\alpha$  in J774 macrophages stimulated with LPS or LTA.<sup>133</sup> Furthermore, thymol reduces pro-inflammatory cytokines (Il-1 $\beta$  and iNOS) in J774 macrophages activated with LPS<sup>134</sup> and D-limonene suppresses Il-1 $\beta$ , Il6 and TNF- $\alpha$  in LPS-stimulated RAW 264.7 macrophages in a dose-dependent manner.<sup>135</sup>
- c. Modulation of pro-inflammatory genes expression: Nuclear factor-  $\kappa$ B (NF- $\kappa$ B) and mitogen-activated protein kinases (MAPK) are two of the most important signaling pathways activated during inflammation.<sup>136</sup> NF- $\kappa$ B is a transcriptional regulator linked to the inhibiting  $\kappa$ B molecule (I $\kappa$ B) in the cytoplasm of cells and thus, it is inactivated under homeostatic conditions. When an inflammatory signal arrives, I $\kappa$ B is degraded via proteasome, allowing NF- $\kappa$ B-p65 to translocate into the nucleus and bind to DNA, promoting the transcription of pro-inflammatory genes such as Il-1 $\beta$  and TNF- $\alpha$ , and enzymes such as inducible Nitric Oxide Synthase (iNOS) and COX-2.<sup>137</sup>

Apart from these signaling pathways, another molecule that plays an important role in inflammation is NO, which is catalyzed by NOS (Nitric Oxide Synthase) in different isoforms,

being iNOS the most important during inflammation. Inflammatory mediators, such as  $\text{IL-1}\beta$ ,  $\text{TNF-}\alpha$  and LPS, stimulate iNOS expression and thus, NO level increases and subsequently the inflammatory response. It has been demonstrated that some plant derived natural compounds can arrest signaling pathways and reduce the inflammatory response by inhibiting pro-inflammatory cytokines, and iNOS. Figure I.4 shows the NF- $\kappa\text{B}$  pathway interrupted at different levels by EOs. Thymol inhibits NO production and arrest NF- $\kappa\text{B}$  pathway at different levels via LPS-induced inflammation.<sup>132,138</sup> Furthermore, thymol, curcumin and squalene reduce phosphorylation of I $\kappa\text{B}$  decreasing NF- $\kappa\text{B}$  translocation.<sup>139,140</sup> Also, curcumin reduces NF- $\kappa\text{B}$  activation by inhibiting p65 translocation to the nucleus.<sup>140</sup> Cinnamaldehyde inhibits the TLR oligomerization, reducing NF- $\kappa\text{B}$  activation.<sup>141</sup> Eugenol blocks the release of  $\text{TNF-}\alpha$  and  $\text{IL-1}\beta$  and suppresses their mRNA expression in LPS-stimulated human macrophages.<sup>142</sup>

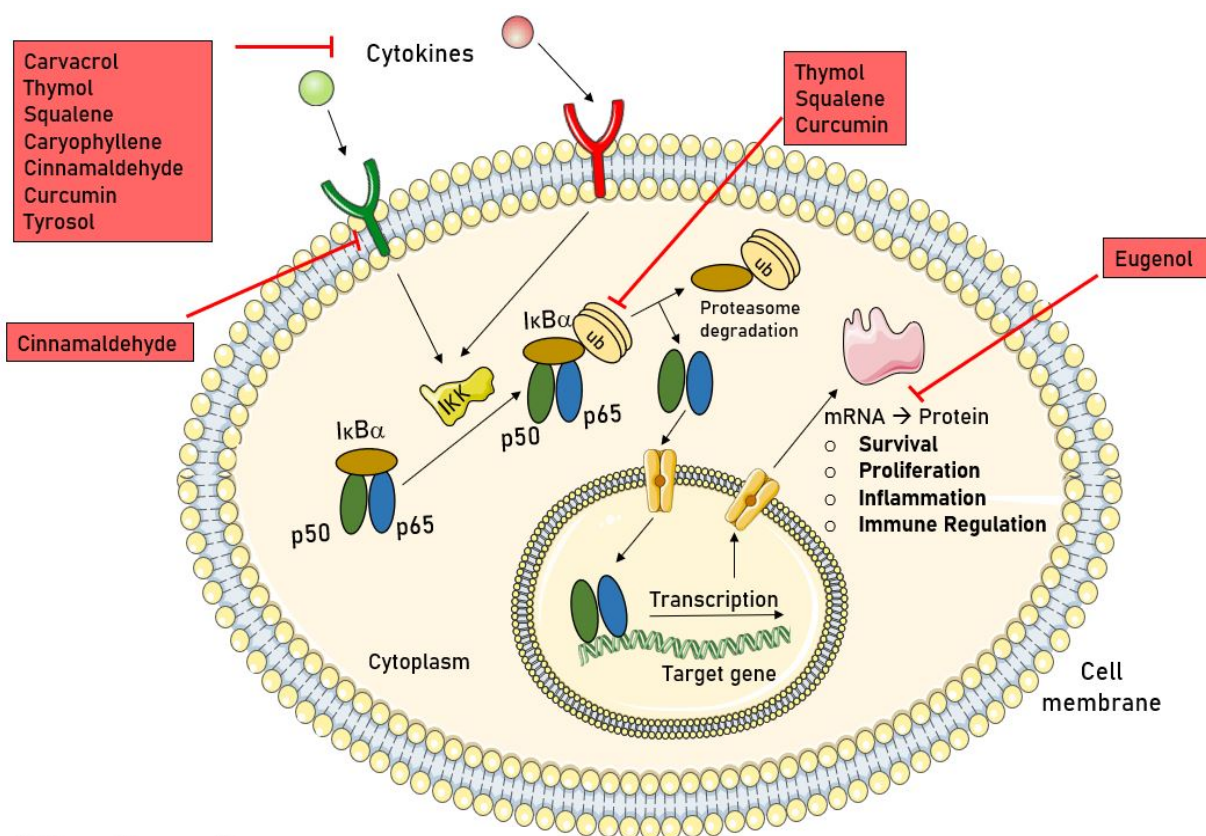


Figure I.4: Target sites of essential oils within NF- $\kappa\text{B}$  pathway.

### I.3.3. Biomedical applications of EOs

Some clinical trials have been developed in order to study the effectivity of EOs in different medical applications, especially, nasal and oral infections. For example, the accumulation and maturation of oral biofilm is common to be treated with chlorhexidine as oral antiseptic. However, secondary effects are well-known, increasing the interest for other alternative antiplaque agents such as thymol, menthol or eucalyptol. In this clinical trial, no significant differences were found between the 0.2% chlorhexidine and the essential oils (Listerine®) at reducing the bacterial vitality. However, chlorhexidine was more efficient reducing biofilm thickness.<sup>143</sup> Other application has been in vulvovaginal fungal infections.<sup>144</sup> In this clinical trial cumin seed extract cream was used to treat infections though no results have been published.

Despite EOs have been tested for infections, no clinical trials have been found related with wound healing process. Due to the demonstrated effectivity of EOs and the increasing problem with antibiotic resistances, EOs have been proposed as possible wound treatment in order to avoid or reduce infections and control inflammatory phase.

### **I.4. Wound dressings**

Traditionally, wet-to-dry dressings were used for wounds having debridement. It was in the late 20<sup>th</sup> century when occlusive dressings began to be produced to protect and provide an effective moist environment to wounds. Due to the hypoxia created by the dressing, processes such as angiogenesis, collagen synthesis and re-epithelialization were promoted.<sup>145,146</sup> In the mid 1980's a dressing which supplied moisture and absorbed fluids was produced, but it was in the mid 1990's when synthetic wound dressings such as hydrogels, alginates, tissue adhesives, etc. were designed to improve wound healing conditions.<sup>147</sup>

Nowadays, traditional wound dressings are used in the management of clean and dry wounds with mild exudate levels or applied as secondary dressings (used to keep the primary dressing securely in place). They consist on sterile gauzes that absorb exudates in an open wound. A frequent change of the dressing is necessary to avoid its adherence to the wound.<sup>148</sup> These dressings only cover the wound and reduce the possibility of infections. Because of this, the use of advanced dressings that promote healing and keep the wound hydration is necessary for complicated wounds.<sup>149,150</sup>

#### I.4.1. Advanced wound dressings

These dressings are usually based on synthetic polymers and are focused on healing promotion. There are different subtypes:

- a. Semi-permeable films: They are based on transparent and adherent polyurethane which allows the water vapor, O<sub>2</sub> and CO<sub>2</sub> transmission and provides a surface impermeable to bacteria. e.g.: Opsite™, Tegaderm™, Bioclusive™.<sup>147</sup>
- b. Semi-permeable foams: They consist of two parts, one hydrophilic foam, in contact with the wound, and another hydrophobic foam, exposed to the outdoor. The exposed surface protects the wound of liquid and the outside but allows gaseous and water vapor exchange. e.g.: Lyofoam™, Allevyn™ and Tielle™.<sup>151,152</sup>
- c. Hydrogels: They are based on insoluble hydrophilic polymers such as poly (methacrylates) and polyvinyl pyrrolidone. The high-water content promotes granulation and epithelization keeping an appropriate moist environment. e.g. Intrasite™, Nu-gel™, Aquaform™ polymers.<sup>152,153</sup>
- d. Hydrocolloids: They involve two different layers, an inner colloidal layer and a water-impermeable surface. The hydrocolloid is permeable to water vapor and impermeable to bacteria. When the dressing is in contact with the wound, it absorbs the exudate and creates a gel that provides moist environment that protects granulation tissue. e.g. Granuflex™, Comfeel™, Tegaserb™.<sup>148</sup>
- e. Alginate: They contain sodium and calcium salts with absorbent properties that allow wound exudates. Sorbsan™, Kaltostat™, Algisite™.<sup>148,154</sup>

#### I.4.2. Bioactive wound dressings

Advanced dressings can be improved by entrapping bioactive molecules to the wound bed. Sometimes they can encapsulate antimicrobials to avoid bacterial colonization and growth factors or bioactive particles to promote wound healing (proliferation, migration and vascularization of endothelial progenitor cells).<sup>147,155</sup> Bioactive molecules include natural molecules such as proteins, cytokines or lipids or other compounds that may modify signaling pathways or contribute to tissue repair. Bioactive molecules are usually cell-permeable and non-immunogenic and can modify intracellular processes in a reversible way.<sup>156</sup>

They are composed of biomaterials and widely recognized for their biocompatibility, biodegradability and lack of toxicity. They are made of materials previously described or

polymers such as chitosan, collagen, polycaprolactone (PCL) or poly lactic-co-glycolic acid (PLGA), among others.<sup>147,155,157,158</sup>

### **I.5. Electrospun nanofibers**

As it was mentioned before, in addition to other processes, the hydrophobicity of EOs can disrupt bacterial structures, leading to the membrane alteration and reduction of its viability.<sup>119</sup> However, this non-polar character and their high volatility character make difficult their application. In addition, some EOs can be oxidized in contact with air or ultraviolet light.<sup>159</sup> It becomes necessary to incorporate an emulsifier or appropriate solvent to guarantee their solubility in aqueous media when they are studied as free compounds. The agents most commonly used are Tween 80 (poly-sorbate 80), Tween 20 (polyoxyethylene (2) sorbitan mono-laurate) and dimethyl sulfoxide (DMSO). The use of these agents is reported to cause low stability and physicochemical changes in EOs, and thus, the active properties may be reduced. For this reason, numerous researchers have focused their studies on increasing EOs stability and bioactive function.<sup>160,161</sup>

Encapsulation of EOs is a good technique to protect their properties and to ensure an appropriate contact between natural compounds and their target.<sup>162</sup> There exist different methods to incorporate EOs to dressings. For example, immersing a gauze in an extract or mixing EOs with an alginate solution, letting the mixture dry until dressing formation.<sup>163,164</sup> However, the electrospinning method makes the encapsulation process easier for volatile materials due to the fast fibers' formation.<sup>165,166</sup>

#### **I.5.1. History of electrospinning**

This technique was first patented in 1902 by John Cooley and William.<sup>167</sup> In 1934 and 1944, Anton Formhals published two patents with improvements in the equipment that allowed its commercialization as a method for the processing of polymers producing materials with controlled size, porosity and morphology.<sup>168,169</sup> In the last years, researchers made electrospinning one of the most versatile methods to obtain materials with large surface area-to-volume ratio, high porosity and flexibility. Electrospinning is an adaptable technology used to produce ultrafine polymeric fibers on both nanometer and micrometer scales by applying an electrostatic field to the polymer solution, driven by the supply of a high voltage between a needle tip and a collector.<sup>168,170,171</sup> It is a versatile and viable method for the production of fibers

to target a large range of applications as for example, the use as wound dressing material, described by a patent filed in 1977.<sup>172</sup>

### I.5.2. Principle of electrospinning

Electrospinning is an electrohydrodynamic process in which a liquid drop is electrified to produce a jet that can be stretched and elongated to form fibers. During the process, the polymer solution is extruded through the spinneret to generate a liquid drop as a result of surface tension. Under the electric field, the drop becomes charged, generating an electrostatic repulsion among the surface and deforming the drop to a Taylor cone, from which a charged jet is ejected. The jet is then extended into a line and due to the electrostatic instabilities (also known as whipping instability), it is subjected to movements and the jet is split into thinner fibers. The small diameter allows solvent evaporation and the fibers to solidify quickly, leading to the deposition on the conductive collector.<sup>173–175</sup> The equipment consists of four main parts represented in Figure I.5:

- Syringe pump: The main function is to drive the polymer solution to the needle.
- Spinneret: It is usually a hypodermic needle with blunt tip connected to a positive pole. The polymer solution passes through the needle.
- High-voltage power supply: It handles the electric field between conductive collector and spinneret.
- Conductive collector: It could be connected to a negative pole.

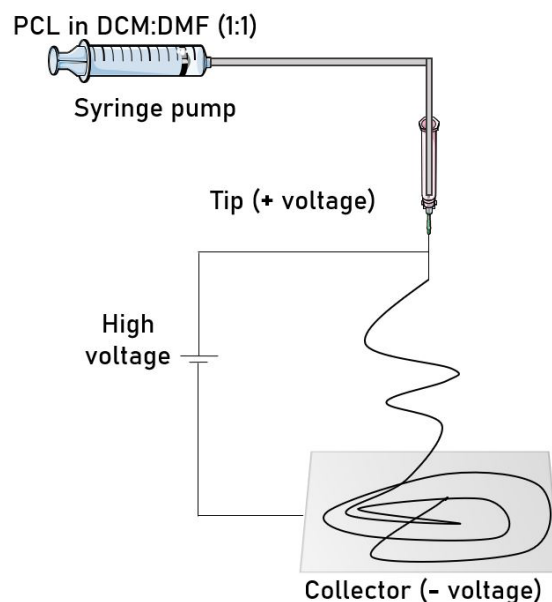


**Figure I.5:** Scheme of electrospinning



### I.5.2.1. Formation of Taylor Cone

In the presence of an electrical potential difference between the collector and the needle, the surface of the drop becomes positively charged. With the gradual increase of voltage, more charges are accumulated in the surface and higher is the repulsion. Meanwhile the surface tension of the drop favors a spherical shape to minimize the total surface free energy, the electrostatic repulsion tends to deform the drop increasing the surface to reduce the repulsion.<sup>176</sup> This phenomenon is exemplified in Figure I.6. When the electric forces overcome the surface tension, the Taylor cone is formed.

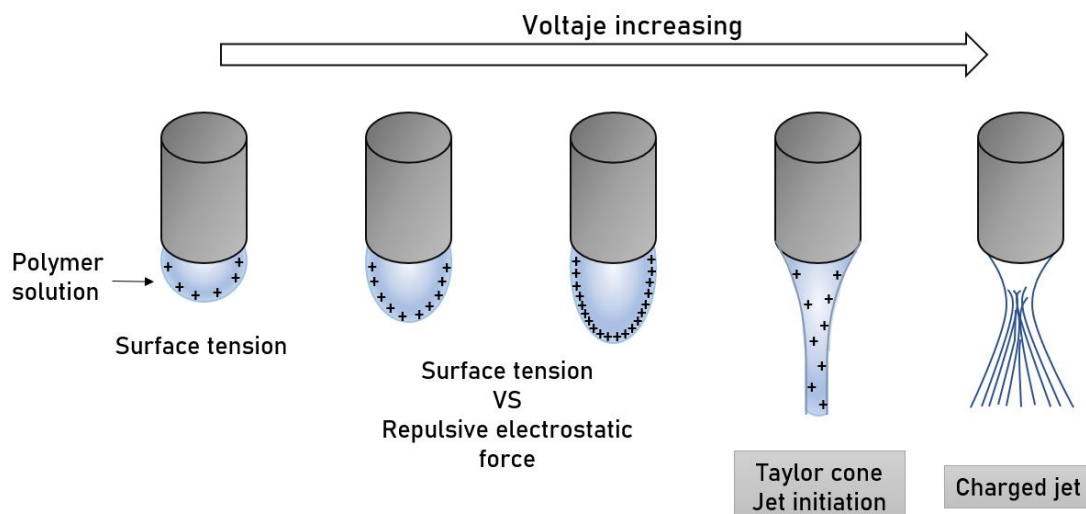


**Figure I.6:** Schematic figure of Taylor cone and jet formation varying the applied voltage. Adapted from Chemical Reviews, 119/8, Xue J. Wu T. Dai Y. Xia Y., Electrospinning and electrospun nanofibers: methods, materials, and applications, 5298-5415.

### I.5.2.2. Thinning of the Jet

Due to the repulsion between charges, an electrically charged jet is ejected and accelerated in the way of the electric field to the conductive collector.<sup>177</sup> The acceleration may be influenced by the surface tension and the viscoelastic force in the jet and thus progressively attenuated. The diameter decreases gradually with the distance between the needle and the collector. And thus, the jet is continuously stretched. If the acceleration is zero or constant, any small perturbation such as electrostatic repulsion among the surface charges, may destroy the straight movement.<sup>178-180</sup> There exist three types of instabilities:<sup>176</sup>

- a. Rayleigh instability is an axisymmetric instability and may promote the breakup of the jet into droplets, dominated by surface tension. It can be avoided with a strong electric field.

- b. The second one is also an axisymmetric instability and it happens at a stronger electric field than the previous one.
- c. The whipping or bending instability is non-axisymmetric. Due to the electrostatic repulsion among surface in a strong electric field, there are aerodynamic instabilities and “lateral electrostatic force” in a radial direction relative to the jet.

These instabilities depend on the interaction between the charges in the jet and the external electric field and appear at different rates controlled by physicochemical properties of the liquid and electrospinning parameters. For example, to obtain ultrathin nanofibers, it is necessary to get rapid growth of whipping instability to stretch the jet.<sup>178</sup>

#### I.5.2.3. Solidification of the jet

When the jet is elongated, the evaporation of solvent promotes the solidification into fibers. A thinner diameter of fibers causes a high evaporation rate. After solidification, the instabilities cease but charges may be trapped on the surface of the dry fibers due to the low conductivity of most materials.<sup>179</sup> Fibers morphology will depend on the instabilities that take part in the process. Figure I.7 represents the pathway followed by the jet.

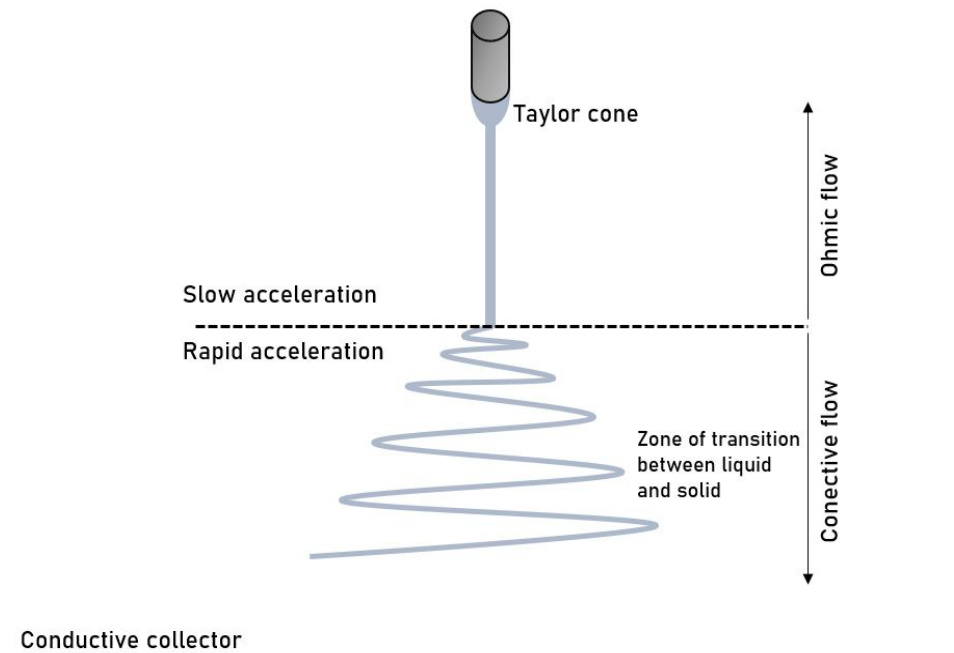


**Figure I.7:** Representation of the normal pathway followed by the jet in presence of an electric field.

The jet path from the needle to the collector can be divided in two parts; (a) An ohmic flux in which there is a slow acceleration characterized by surface tension and charges repulsion, and (b) a connective flux characterized by a fast acceleration where takes place the solidification of the jet. In the first phase, the jet follows a straight direction until an instability occurs. Then the jet enters in the second phase, where the jet is gradually thinner until total solidification.<sup>181</sup>

### I.5.3. Materials for electrospinning

Electrospinning technique has been used for the synthesis of nanofibers from different types of materials, for example, organic polymers including natural and synthetic and they have been used for multiple applications. For example, synthetic materials as polystyrene and poly (vinyl chloride) are used for environmental protection applications.<sup>176</sup> On the other hand, different materials have been described for their use in biomedical applications. Due to their biodegradability and biocompatibility, the most common polymers used are poly ( $\alpha$ -hydroxy acids), specifically, lactic and glycolic acids and their copolymers with  $\epsilon$ -caprolactone for their biodegradable character.<sup>165</sup> It is well reported that these materials hydrolyze and thus, degrade in nontoxic products in weeks or months depending on their molecular structure.<sup>182</sup> It is possible to electrospun into nanofibers other kind of materials as natural biopolymers (DNA, dextran, chitosan, collagen, etc.) and conductive polymers (polyaniline, polypyrrole).<sup>176</sup>

Different kinds of materials have been reported for EOs loading. For example, a composite of PVA-CHI-GT (polyvinyl alcohol-chitosan-gelatin) was electrospun with *Zataria multiflora* for wound healing applications<sup>183</sup> and polyethylene oxide nanofibers containing Tea tree oil has been used for antibacterial packaging.<sup>184</sup> Other materials such as cellulose acetate<sup>185</sup>, polyvinyl pyrrolidone, polylactide acid, polyurethane, polycaprolactone or silk fibroin have been loaded with EOs for biomedical applications.<sup>186</sup>

There are two conditions for a successful solution electrospinning: (a) enough high molecular weight for the polymer and (b) the polymer should be dissolved in appropriate solvents. Especially, polymers with low melting points, as for example PCL, have good stability in the electrospinning process. PCL is a synthetic bioresorbable material widely chosen for biomedical applications due to its biocompatibility and biodegradation rate. Besides, it degrades into not toxic fractions under physiological environment.<sup>187</sup> As it was mentioned before, the solvent used to dissolve PCL is very important. Most common solvents are chloroform, dichloromethane, dimethylformamide, methanol or a combination of them. It has been deeply

studied the electrospinning of PCL and it has been demonstrated that in medical applications, it is important to imitate the natural extracellular morphology to promote optimal cell growth. For this, it is essential that nanofibers synthesis may not produce beads.<sup>171,188</sup> Due to these properties, electrospun-PCL nanofibers have been widely used to encapsulate plant-derived natural compounds for medical applications. For example, Bui. *et al.*<sup>189</sup> synthesized curcumin-loaded PCL nanofibers, Tampau *et al.*<sup>190</sup> developed PCL nanofibers encapsulating carvacrol, and Martinez-Abad *et al.*<sup>191</sup> loaded cinammaldehyde and isothiocyanate in PCL films, all of them designed for antimicrobial properties.

# Chapter II

## ANTIMICROBIAL AND CYTOTOXICITY EVALUATION OF DIFFERENT FREE NATURAL COMPOUNDS

### Summary

This chapter studies the antimicrobial properties of different molecules present in EOs against planktonic and biofilm-forming Gram-positive (*Staphylococcus aureus*) and Gram-negative (*Escherichia coli*) bacteria. In addition, it was analyzed the bactericidal mechanisms of the different molecules and their cytocompatibility. Carvacrol, cinnamaldehyde, and thymol exhibit the highest *in vitro* antimicrobial activities against *E. coli* and *S. aureus*, with membrane disruption as bactericidal mechanism identified, fact that also hampers *S. aureus* biofilm formation and partially eliminates preformed biofilms. These three compounds also showed lower cell toxicity than the conventional widely used chlorhexidine.

The content of this chapter has been adapted from the following published work:

García-Salinas, S.; Elizondo-Castillo, H.; Arruebo, M.; Mendoza, G.; Irusta, S.

**Evaluation of the Antimicrobial Activity and Cytotoxicity of Different Components of Natural Origin Present in Essential Oils.**

*Molecules* **2018**, *23* (6), 1–18. <https://doi.org/10.3390/molecules23061399>.

## Table of contents

<b>II.1. Introduction</b>	<b>43</b>
<b>II.2. Objective</b>	<b>45</b>
<b>II.3. Experimental</b>	<b>45</b>
<b>II.4. Results and discussion</b>	<b>46</b>
II.4.1. Bactericidal activity against planktonic bacteria	46
4.1.1. MIC and MBC values	46
4.1.2. Bactericidal mechanism	47
4.1.3. Synergism	53
II.4.2. Antibiofilm activity	54
II.4.3. Cytotoxicity	56
<b>II.5. Conclusions</b>	<b>58</b>

## II.1. Introduction

As it was mentioned in Chapter I the use and misuse of antibiotics has led to the emergence of antibiotic resistance in human and animal pathogens, which is recognized as a serious and global concern.<sup>192</sup> The continued evolution of antimicrobial resistance (AMR) in hospitals is a growing concern because of its potential to endanger the future of antimicrobial drug therapy.<sup>193</sup> Even the new generation of antibiotics is becoming virtually ineffective, and it is predicted that AMR will cause more deaths than cancer-associated diseases by the middle of the century.<sup>194</sup> Sub-inhibitory antibiotic doses help stepwise selection of resistance, and the resulting resistant clones like methicillin-resistant *S. aureus*, *E. coli*, and *Klebsiella* are rapidly disseminated.<sup>195</sup> Multiple antimicrobial resistance determinants have been found in *E. coli* on the same plasmid, further facilitating their propagation and co-selection. For instance, the multidrug resistance plasmid IncA/C found in *E. coli*, often encodes for resistance to common antimicrobial agents such as tetracycline, chloramphenicol/florfenicol, streptomycin/spectinomycin, sulfonamides, and extended spectrum  $\beta$ -lactamases, and its spread to pathogenic bacteria may limit antibacterial means to fight infections caused by these bacteria.<sup>193</sup>

Because of the emergence of AMR, the Center for Disease Control (CDC) has endorsed the need for the research of new substances with the potential to combat resistant strains. In 2011, academics and industry collaborated on a priority list for approaches to resolve the “antimicrobial-resistance crisis.” Amongst the potential strategies suggested, the development of alternatives to antibiotics were proposed.<sup>196</sup> Compounds from natural sources such as animals, plants, and microorganisms have been highlighted as renewed potential antimicrobial alternatives.<sup>197</sup> Famous seafarers (e.g., Marco Polo) established routes for spice trade, and different compounds of natural origin present in spices are still being used today to prevent foodborne pathogens showing low levels of antimicrobial resistance.<sup>198</sup> Essential oils (EOs) are oily aromatic substances extracted from plants with antibacterial, antifungal, insecticidal, and antiviral properties. EOs have been distilled for more than 2,000 years, and there is now renewed interest in the antimicrobial properties of phytochemicals and EOs in particular. The demonstrated low levels of induction of antimicrobial resistance toward EOs could be related to the fact that these substances do not attack a single specific target but have multiple modes of antibacterial action.<sup>199</sup> Antibiotics, and antiseptics like chlorhexidine, have been shown to be

able to generate resistance in *Staphylococcus* by mechanisms (mutations in *qacA/B* gene) that may be common to other microorganisms.<sup>200</sup>

EOs are complex blends of a variety of molecules such as terpenoids, phenol-derived aromatic components, and aliphatic components. Their compositions depend on factors such as seasonal variation, climate, plant organ, age, subspecies, and even the oil extraction method. Consequently, the extracted product can fluctuate in quality, quantity, and composition.<sup>201</sup> Generally, EOs contain about 20–60 components, up to more than 100 single substances, at quite different concentrations; two or three are major components at fairly high concentrations (20–70%) compared to other components that are present only in trace amounts. Because of this, in order to have a systematic evaluation of EOs' antibacterial activity, it is necessary to focus on the study of their main components.

Different extracted components from EOs such as carvacrol, thymol, eugenol, perillaldehyde, and cinnamaldehyde have been reported as antibacterial agents.<sup>202</sup> However, the reported values for their minimum inhibitory (MICs) and bactericidal (MBCs) concentrations are extremely divergent. For example, the MIC of carvacrol toward *S. aureus* found in the literature ranges from approximately 0.15 mg/mL<sup>203</sup> to 15 mg/mL.<sup>204</sup> In some cases, the different MICs reported could be attributed to the bacteria strain used. Wang *et al.*<sup>205</sup> reported an MIC value for carvacrol of 0.31 mg/mL for *S. aureus* (ATCC 43300), while using *S. aureus* (ATCC 6538), Silva da Luz *et al.*<sup>206</sup> reported a MIC of 2.45 mg/mL for the same component. Even for the same bacteria strain (ATCC 6538), MIC values for carvacrol of 0.4 mg/mL<sup>207</sup> and 0.015% v/v (approximately 0.147 mg/mL)<sup>203</sup> can be found in the literature.

Beside the well-documented antibacterial action of EO components, there is some evidence corroborating the enhancement in the antimicrobial action of EO components used in combination with other antimicrobial agents, both synthetic and natural.<sup>208</sup> Thymol and carvacrol were found to have additive antibacterial effect against *S. aureus*, *E. coli*, *Salmonella*, and *Bacillus cereus*. Ye *et al.*<sup>209</sup> tested the synergy between cinnamaldehyde and carvacrol in *S. aureus* and *E. coli* among other bacteria and concluded that cinnamaldehyde and carvacrol exhibit high antibacterial activities and have synergistic antimicrobial action against these bacteria. Thymol and carvacrol were found to give an additive effect when tested against *S. aureus* and *Pseudomonas aeruginosa*.<sup>121</sup>



One interesting application of EO components with antimicrobial activity would be their incorporation into wound dressings since they can prevent or treat wound-associated infections and aid tissue regeneration.<sup>210</sup> Bacterial components have been highlighted as harmful factors during wound healing due to their interference with cell-matrix interactions and due a reduced inflammatory response they produce. In this regard, *S. aureus* colonize from 30% to 50% of healthy adults and is able to rapidly infect skin lesions with a consequential inflammatory process.<sup>211</sup> *E. coli* is also among the main bacterial species that commonly colonize skin wounds, and from this initial colonization, severe problems can occur such as topical infections or even sepsis.<sup>212</sup> Within the clinical settings, biofilm formation is a pressing challenge that leads to chronic infections. Biofilms are communities of microorganisms living at an interphase attached to each other through the extracellular polymeric substance, composed of extracellular DNA, proteins, and polysaccharides. Due to the protection of this matrix, bacteria show up to 1,000 times greater tolerance to antibiotics and biocides than their planktonic counterparts.<sup>213</sup> Prevention of biofilm formation is considered preferable to its removal, since the latter is a very difficult and demanding task, which can cause recontamination problems due to the uncontrolled release of bacterial cells and toxins after their disruption. One of the outstanding antimicrobial properties of many EOs is that they can also be effective even against microbial biofilms.<sup>214</sup>

## II.2. Objective

The aim of this work was to shed light on the evaluation of the bactericidal activity and mechanisms of action of EO-present molecules against *S. aureus* and *E. coli* in planktonic growth. The antibiofilm efficiency and the possibility of synergy between carvacrol (CAR), cinnamaldehyde (CIN) and thymol (THY) were also analyzed. The potential toxicity of those components was also investigated in different cell types, including human dermal fibroblasts, keratinocytes, and macrophages. The main goal of this work is to deepen our understanding of the effects and mechanisms of these purified molecules on bacteria, avoiding the intrinsic variability of their extraction from plants, and focusing on their own ability to hamper bacteria growth and colonization.<sup>215</sup>

## II.3. Experimental

First of all, a deep research in literature was done to know which EOs are reported as antimicrobial, and thus, some compounds were chosen to work with. The antimicrobial activity of these free EOs was studied following the broth microdilution method<sup>216</sup> in two different

bacteria, a Gram-positive model, *S. aureus* (ATCC 25923) and a Gram-negative model, *E. coli* S17. In addition, three techniques were performed to analyze the mechanism of action of selected compounds; Scanning Electron Microscopy (SEM), flow cytometry and Live/Dead®BacLight™ bacterial viability kit to be observed under confocal microscopy, that stains live and dead areas in bacteria membrane. Antimicrobial ability of free EOs was also studied in two different models of biofilm: effect of the compounds to eradicate preformed biofilms, and to prevent the formation of these structures. Moreover, a synergic study was carried out to know the effect of EOs when they interact. Finally, a metabolism cytotoxicity assay was done to study the effect of EOs treatment in three different cell lines related with skin: fibroblasts, keratinocytes and macrophages. The Blue Cell Viability assay was used for this goal.

The characterization techniques and different evaluation methods are described in detail in Appendix I.

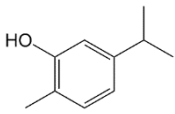
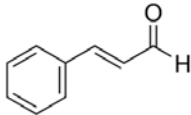
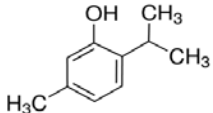
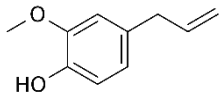
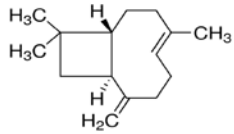
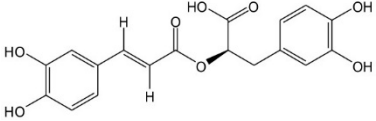
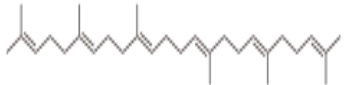
## **II.4. Results and discussion**

### **II.4.1. Bactericidal activity against planktonic bacteria**

#### **II.4.1.1. MIC and MBC values**

The antibacterial effect of several components present in different EOs reported as bactericidal, such as carvacrol,<sup>217</sup> thymol,<sup>215</sup> cinnamaldehyde,<sup>218</sup> eugenol,<sup>219</sup>  $\beta$ -caryophyllene,<sup>220</sup> rosmarinic acid,<sup>221</sup> and squalene<sup>222</sup> were studied. Table 1 shows the MIC and MBC results of these components against *E. coli* and *S. aureus*. The most active compounds were THY, CAR, CIN, showing the lowest concentrations to inhibit or hamper planktonic bacteria growth. EOs have been pointed out as a suitable strategy due to their bactericidal properties together with their inability to generate antimicrobial resistances.<sup>223–225</sup> According to our results, previous studies have highlighted the antimicrobial attribute though their complex composition.

**Table II.1:** Chemical structure, MIC and MBC values of different essential oils. Average of 12 replicas per compound.

Active compound	Structure	MIC (mg/mL)		MBC (mg/mL)	
		<i>E. coli</i>	<i>S. aureus</i>	<i>E. coli</i>	<i>S. aureus</i>
Carvacrol		0.2	0.2	0.4	0.3
Cinnamaldehyde		0.2	0.4	0.3	0.5
Thymol		0.2	0.2	0.3	0.3
Eugenol		0.4	1.3	0.5	1.5
$\beta$ -caryophyllene		>4.0	>4.0	>4.0	>4.0
Rosmarinic acid		>4.0	2.5	>4.0	4.0
Squalene		>4.0	>4.0	>4.0	>4.0

#### II.4.1.2. Bactericidal mechanism

*E. coli* and *S. aureus* exposed during 24 h to CAR, CIN, and THY at MIC and MBC concentrations were morphologically examined by scanning electron microscopy (SEM) (Figures II.1 and II.2). The morphology and microstructure of *S. aureus* before being exposed to any compound can be observed in Figure II.1.A, having a normal and spherical shape and a well-preserved cell membrane. However, after exposition to CAR, CIN and THY at MICs for 24 h (Figure II.1.B, D and F), the morphology of *S. aureus* was distorted. Part of the cell peptidoglycan structure appeared depressed, indicating an initial damage. Same pattern is

followed when *S. aureus* is exposed to MBC for 24 h (Figure II.1.C, E and G). Bacteria became deformed and wrinkled, indicating that the intracellular content had leaked out. There was a reduced number of bacteria in the samples, probably due to the severe damage to the bacterial peptidoglycan layer and cell membrane and subsequently cell death. The reduction in cell size, length, and diameter observed for *S. aureus* in response to the treatment with EOs could be reasonably attributed to the leakage of cytosolic fluids outside the cells.

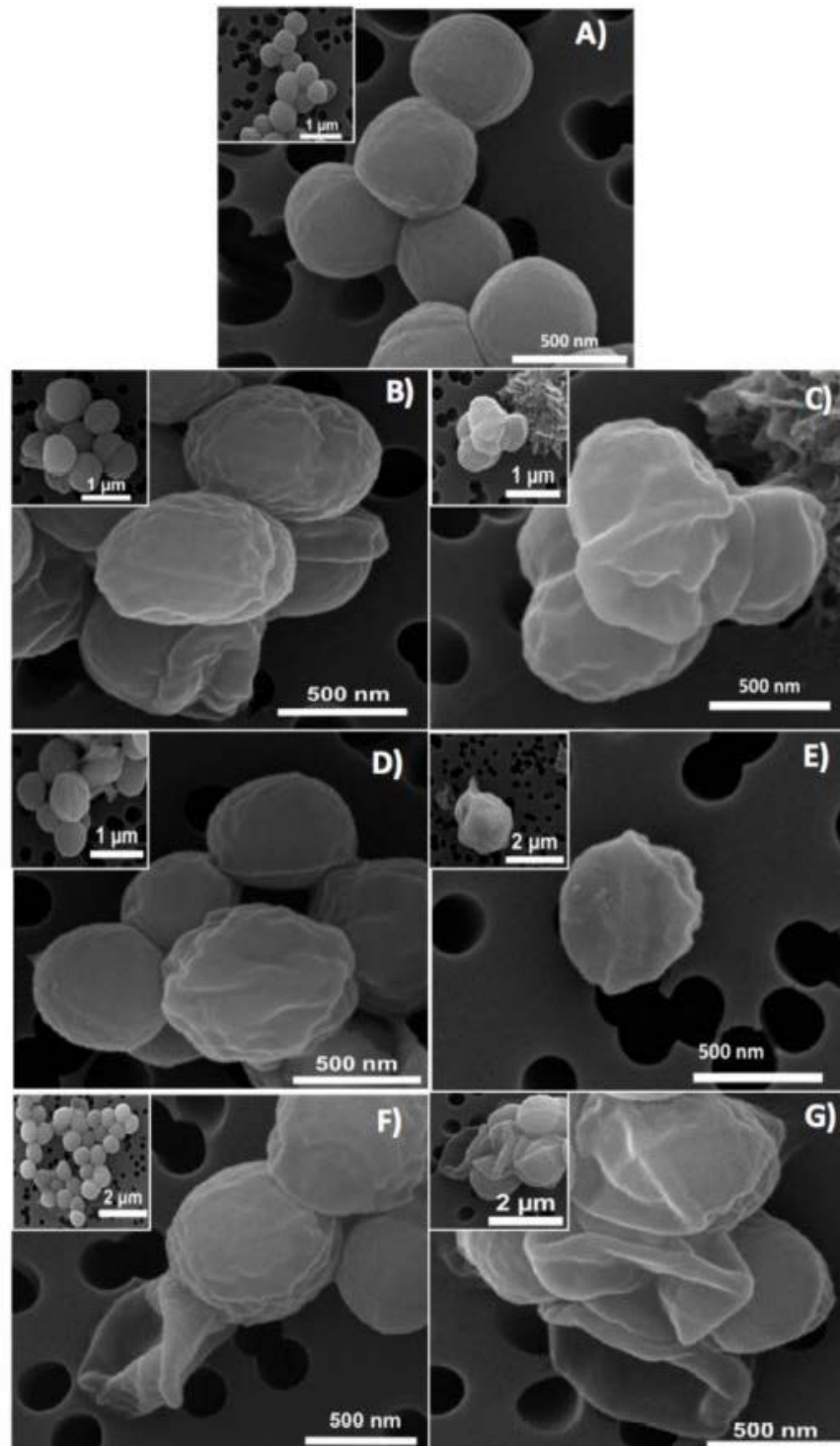


**Figure II.1:** SEM images of *S. aureus*: A) Untreated (control sample); Treatment with MIC of B) CAR; D) CIN; F) THY; and treatment with MBC of C) CAR; E) CIN; G) THY.

*E. coli* untreated cells were rod shaped, regular and kept intact morphology (Figure II.2.A) in contrast to MIC-treated cells (Figure II.2.B, D and F), which showed morphological alterations and lyses of the outer membrane integrity in cells. At MBC, a complete lysis or seriously damaged cells were observed.

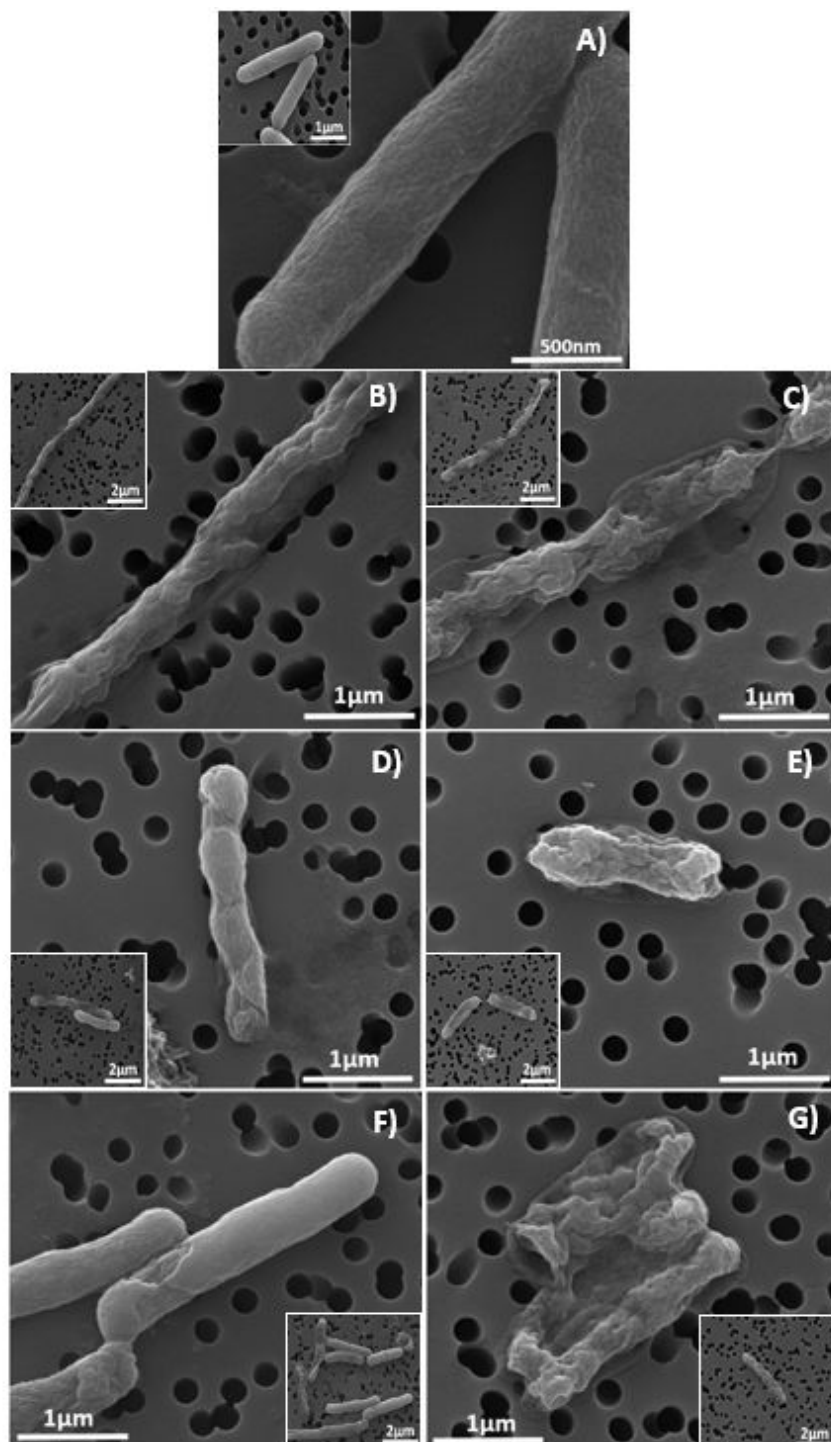


**Figure II.2:** SEM images of *S. aureus*: A) Untreated (control sample); Treatment with MIC of B) CAR; D) CIN; F) THY; and treatment with MBC of C) CAR; E) CIN; G) THY.

In order to confirm the bactericidal mechanism of the active compounds present in EOs, flow cytometry and confocal microscopy studies were developed. Flow cytometry histograms (Figure II.3) displayed peaks in the range of the negative control (damaged membrane caused by chlorhexidine<sup>226</sup>) when *S. aureus* and *E. coli* were treated with the tested compounds at MBC, which is consistent with cell membrane disruption as previously reported.<sup>227</sup> Only CIN-treated cells show peaks slightly displaced toward the positive control (undamaged membrane) for both microorganisms, suggesting that the involvement of cell membrane disruption in bacteria death was not as clear as the SEM images showed.

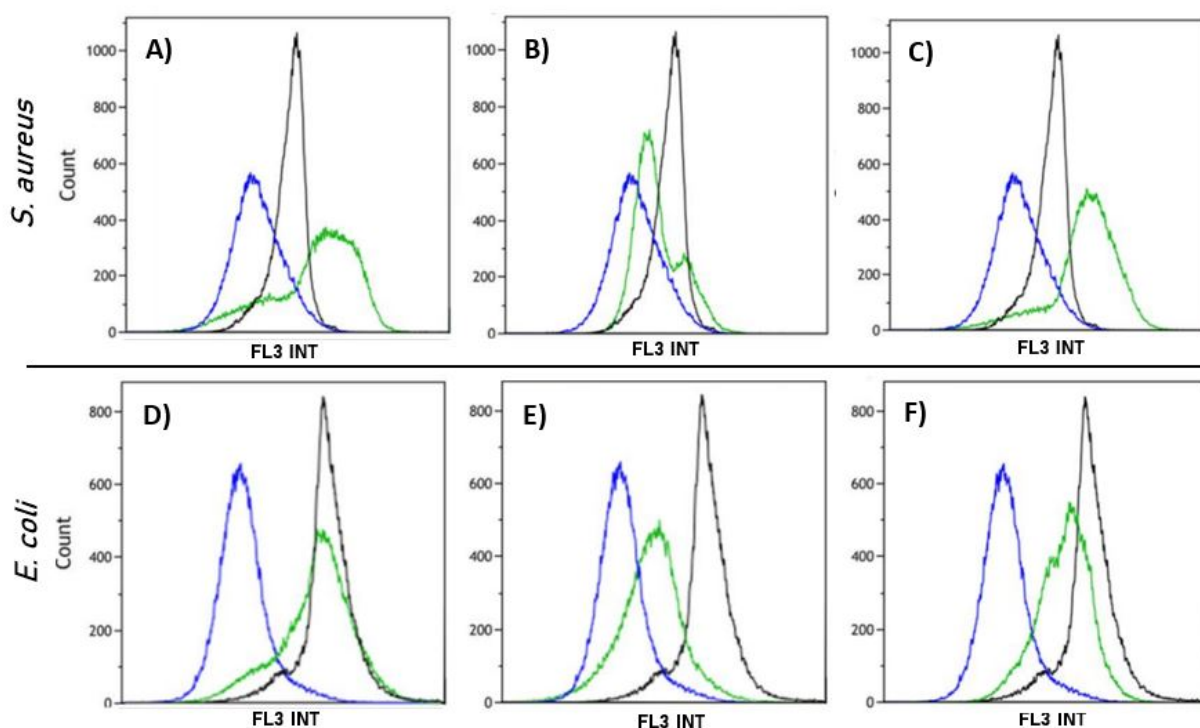


**Figure II.3:** Flow cytometry histograms at MBC of CAR (A, D), CIN (B, E) and THY (C, F) on *S. aureus* (A, B and C) and *E. coli* (D, E and F).

Confocal microscopy images (Figure II. 4) clearly confirmed membrane damage exerted by the compounds tested when bacteria were incubated with the MICs of the molecules, showing red staining related to membrane integrity compromise. Furthermore, for *E. coli*, the damaged membrane areas can be clearly distinguished (Figure II.4 D, E and F). All these results point out to the bacteria membrane disruption as the bactericidal mechanism exerted by the compounds present in the EOs.

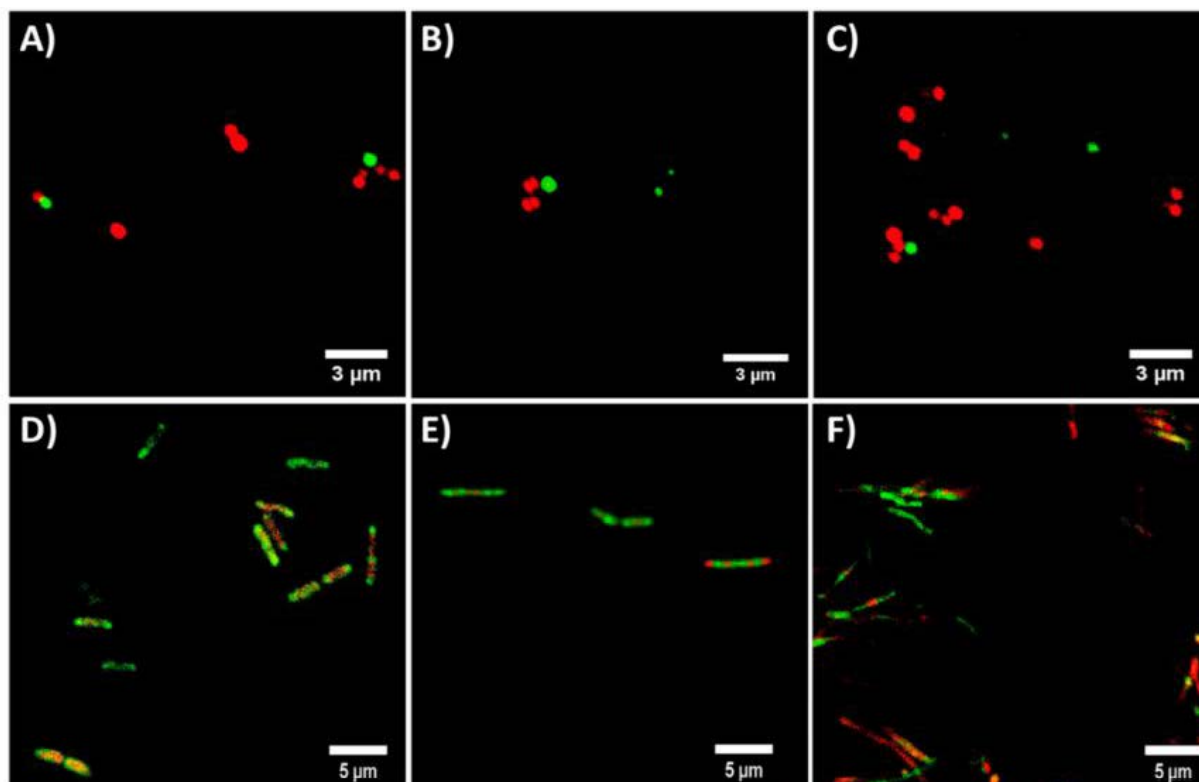


**Figure II.4:** Confocal microscopy images of *S. aureus* (A-C) and *E. coli* (D-F) treated with MIC of CAR (A, D), CIN (B, E) and THY (C, F), stained with the Live/Dead@BacLight™ bacterial viability kit. Red staining displays membrane damage.

Our work focuses on the bactericidal effects and the mechanisms of action of purified EOs (CAR, CIN, THY) against Gram positive (*S. aureus* ATCC 25923) and Gram negative (*E. coli*S17) bacteria in order to elucidate their own ability to kill bacteria. MIC and MBC studies (Table II.1) pointed to THY, CAR and CIN as the most effective studied molecules against *E. coli* and *S. aureus* showing the lowest concentrations to inhibit or hamper planktonic bacteria growth. The bactericidal mechanism of the most effective EOs (CAR, THY, CIN) was assessed by SEM, flow cytometry and confocal microscopy after treatment of *E. coli* and *S. aureus* planktonic cultures at MIC and MBC concentrations for 24 h (Figures II 1-4). These methodologies pointed to membrane disruption as the bactericidal mechanism exerted by these molecules. It is known that phenols, terpenes and aldehydes antibacterial effect is due to their action against the cell cytoplasmic membrane.<sup>125</sup> It has been reported that CAR and THY disturb the membrane integrity, increasing the membrane permeability and causing a leakage of protons and potassium finally leading to the loss of membrane potential.<sup>228</sup> Nazzaro *et al.*<sup>125</sup> suggested that the presence of the hydroxyl group in CAR and THY is related to the inactivation of the



microbial enzymes. This group would interact with the cell membrane causing leakage of cellular components, a change in fatty acids and phospholipids, and an impairment of the energy metabolism influencing genetic material synthesis. However, some authors have pointed out to different bactericidal mechanisms of action for both compounds due to the different location of the hydroxyl group in their structure affecting cell membrane permeability<sup>229</sup>, while others agree with our results, showing similar effects for both compounds on bacterial membrane structure.<sup>230</sup>

According to the literature, the antibacterial mechanism of CIN is not clear. On the one hand, its antimicrobial action was attributed to the inhibition of the amino acid decarboxylase activity to bind proteins and no disintegration of the membrane was observed.<sup>209</sup> However, Nazzaro *et al.*<sup>125</sup> sustained that like CAR, CIN inhibits the generation of adenosine triphosphate from dextrose and disrupts the cell membrane. In addition, the hydrophobicity of EOs enables their accumulation in cell membranes disturbing their structures and causing an increase in the permeability allowing intracellular constituents leakage.<sup>228</sup> Our studies would indicate similar trends in MIC and MBC values for CAR, THY, and CIN, as well as the disruption of the bacterial surface as target for their activity by three different experimental techniques analyzed.

#### II.4.1.3. Synergism

Synergistic interactions between EO active compounds may increase their efficacy as antibacterial agents. In our studies, the Fractional Inhibitory Concentration Index (FICI) values obtained against *S. aureus* (Table II.2) indicate that only the CAR-THY combination has an additive effect, while CIN has no interaction with the other compounds tested. These results may be related to their chemical structure as CAR and THY have almost the same molecular structure (Table II.1). It is worth noting that all the FICI values are smaller than 4.0 indicating that there is no antagonism between the tested active compounds.

**Table II.2:** Fractional Inhibitory Concentration (FIC) and Fractional Inhibitory Concentration Index (FICI) values for EOs combination.

CAR-CIN				CAR-THY				THY-CIN			
FIC <sub>CAR</sub>	FIC <sub>CIN</sub>	FICI	NI <sup>1</sup>	FIC <sub>CAR</sub>	FIC <sub>THY</sub>	FICI	ADD <sup>2</sup>	FIC <sub>THY</sub>	FIC <sub>CIN</sub>	FICI	NI <sup>1</sup>
0.7	1.0	1.7		0.4	0.5	0.9		0.8	0.4	1.2	
<sup>1</sup> NI: No interaction; <sup>2</sup> ADD: Additive											

On the other hand, it is reported that synergism between EOs is more efficient as bactericidal agents. For instance, polyethylene films containing a mixture of CAR and THY entrapped within halloysite nanotubes exhibited superior antimicrobial activity against *E. coli* than films containing the individual compounds alone.<sup>229</sup> The combination of CIN and CAR showed better bactericidal effect compared with the components alone against food-borne bacteria.<sup>209</sup> Zhou *et al.*<sup>231</sup> reported that CIN had a synergistic effect when combined with THY or CAR against *Salmonella typhimurium*. However, in our case, FICI data obtained against *S. aureus* (Table II.2) pointed to CAR-THY as the most efficient combination displaying an additive effect, while CIN did not exert any synergism. The synergistic mechanism between CIN with CAR or THY was proposed to be caused by the increase in the membrane permeability that enables CIN to be transported into the cell.<sup>209</sup> But according to the treated bacteria SEM micrographs (Figures II.1 and II.2), flow cytometry histograms (Figure II.3) and confocal microscopy images (Figure II. 4), the effect of the three compounds against *E. coli* is mainly outer membrane disintegration and the morphology of treated *S. aureus* was similar for the three active compounds. THY and CAR were previously found to give an additive antimicrobial effect on *S. aureus*<sup>121</sup>, which is in accordance with its similar chemical structure (Table I.1).

#### II.4.2. Antibiofilm activity

*S. aureus* biofilm formation was observed by calcofluor white staining and by SEM analysis after incubation for 16 h (Figure II.5 A, B, respectively). The quantification (colony forming units per milliliter = CFU/mL) of bacteria has been carried out following two methods, disrupting a preformed biofilm (Figure II.5.C) and interfering in biofilm formation (Figure II.5.D) with the antimicrobial compounds. The treatment with different concentrations (0.25-1 mg/mL) of EOs has shown a statistically significant decrease in bacteria growth compared to the untreated biofilms (Figure II.5.C). At 0.5 mg/mL of EOs, preformed biofilms showed a reduction in bacteria growth around 2 logs when biofilm was treated with CIN, while CAR and THY exerted a superior decrease (3 logs). The highest tested concentration (1 mg/mL) showed a reduction in CFU/mL higher than 5 logs. As expected, concentrations of the active molecules higher than MIC and even MBC values obtained for planktonic bacteria are needed for biofilm elimination. The addition of these compounds to the bacteria suspension before biofilm formation hindered this process since there was a significant decrease in the bacterial growth (Figure II.5.D). THY and CAR produced higher reductions of about 5 and 6 logs, respectively.

Again, the concentrations needed to retard biofilm growth and development were higher than the MIC values retrieved for planktonic bacteria (Table I.1).

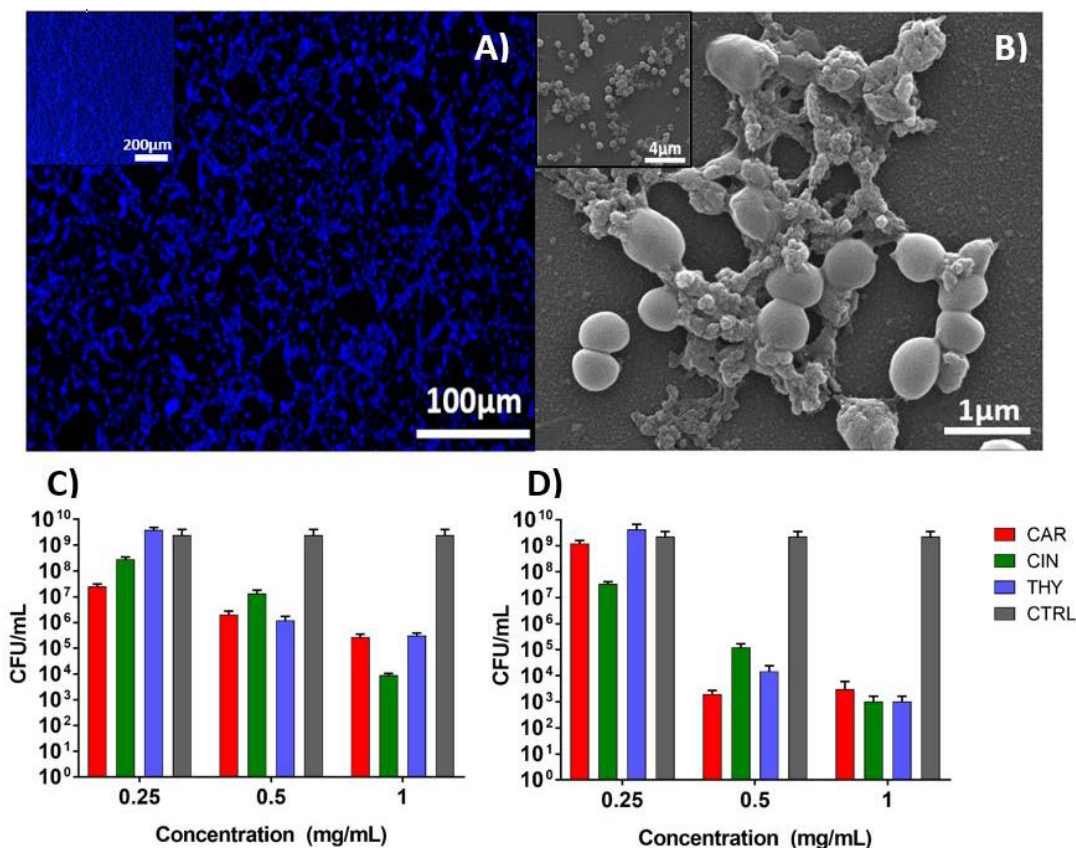


Figure II.5: Biofilm formation and eradication. A) calcofluor staining and B) SEM image of *S. aureus* biofilm formed after 16 h. Images C and D correspond with the effect of EOs at different concentrations (0.25-1 mg/mL) on *S. aureus* biofilm. C) Elimination of preformed biofilm and D) inhibition of biofilm formation. CAR: biofilm treated with carvacrol; CIN: biofilm treated with cinnamaldehyde; THY: biofilm treated with thymol; CTRL: not treated biofilm.

*S. aureus* is involved in a wide range of infections that are difficult to treat and it often resides within biofilms at the infection site.<sup>230</sup> Due to biofilm protection, bacteria show up more resistant to external threats than their planktonic counterparts.<sup>213</sup> Because of this, it is important to find compounds that interfere with the early steps of biofilm formation and slow down its formation rate. As expected, concentrations of the active molecules higher than MIC and even MBC values obtained for planktonic bacteria are needed for biofilm elimination. This study shows that concentrations higher than 1 mg/mL of any of the compounds tested would be necessary for the total elimination of preformed *S. aureus* (ATCC 25923) biofilms. Again, the concentrations needed to retard biofilm growth and development were higher than the MIC

values retrieved for planktonic bacteria (Table II.1), but they were in the same range than those reported in the literature.<sup>215</sup>

### II.4.3. Cytotoxicity

Cytocompatibility and not cytotoxicity is required for a wound-healing product since it would be in contact with the infected wound tissue and its neighboring eukaryotic cells. The cytotoxicity activities of these antimicrobial compounds were investigated using fibroblasts, macrophages, and keratinocytes cell lines (Figure II.6). Inflammatory cells such as macrophages are generated during wound healing,<sup>232</sup> whereas keratinocytes and fibroblasts are part of the epidermis and dermis, respectively. Due to the insolubility of those compounds in aqueous media, those were dissolved in Tween® 80 as described in the materials and methods section.

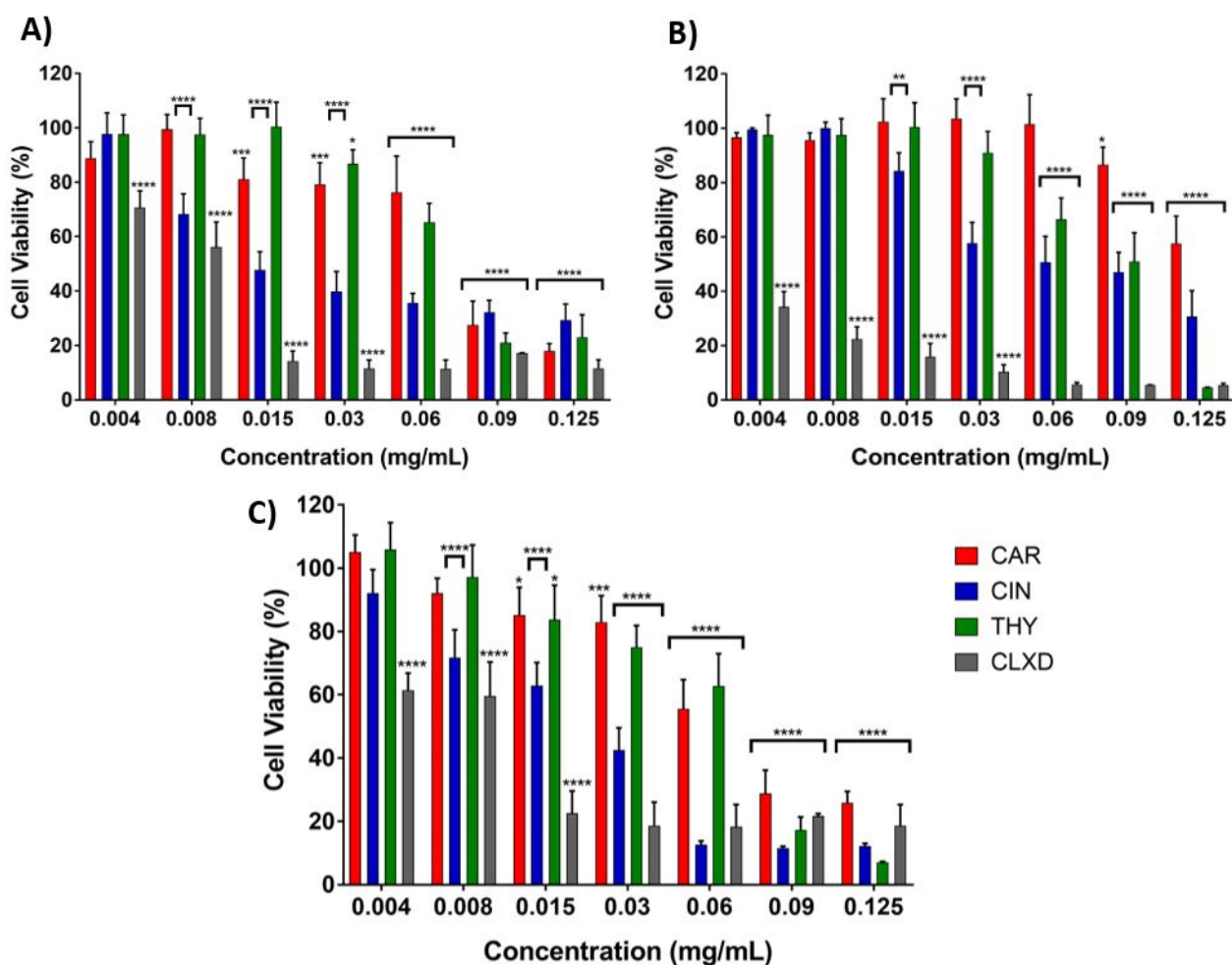


**Figure II.6:** Cell viability after treatment with carvacrol, cinnamaldehyde, thymol and chlorhexidine for 24 h on: A) human dermal fibroblasts; B) macrophages and C) keratinocytes. Samples are graphed considering untreated cells as 100% viability. \* $p < 0.05$ ; \*\* $p < 0.01$ ; \*\*\* $p < 0.001$ ; \*\*\*\* $p < 0.0001$ . Error bars represent mean  $\pm$  SD of three replicates.

CIN was the most cytotoxic chemical of the tested molecules; a dose of 0.03 mg/mL of this compound was enough to reduce the viability of the three cell types below 70% (lowest value established by the ISO 10993-5<sup>233</sup> to consider a material as non-cytotoxic). THY and CAR can be considered toxic to fibroblasts at concentrations equal or higher than 0.09 mg/mL, and the calculated subcytotoxic doses for keratinocytes were 0.06 mg/mL. There is also a difference between the effect of THY and CAR on macrophages, since subcytotoxic concentrations were 0.06 and 0.09 mg/mL, respectively. Chlorhexidine, a typical disinfectant and antiseptic drug used in skin disinfection, was tested for comparison. For the studied concentrations (0.004–0.125 mg/mL), chlorhexidine reduces the viability of the three cellular types to 70% or below. Only fibroblasts show viability higher than 70% in presence of chlorhexidine at 0.004 mg/mL. For keratinocytes and macrophages, the subcytotoxic concentration was lower than 0.004 mg/mL.

These subcytotoxic values of the tested compounds were lower than the MICs and MBCs retrieved for bacteria but higher than those obtained with chlorhexidine. In order to reduce bacterial burden in wounds, topical antiseptic agents, among them chlorhexidine gluconate, are usually applied as 2 and 4 v/v % topical solutions, concentrations five orders of magnitude higher than the subcytotoxic doses. Therefore, in this study, the presence of antibacterial compounds of natural origin in a wound dressing material at MBC concentrations would be only three orders of magnitude higher than the subcytotoxic dose in the worst case scenario demonstrating that those natural origin compounds are less harmful against eukaryotic cells than conventional antiseptics.

Previous studies have also evaluated the toxicity of different plant-derived natural compounds on different human cell types, such as fibroblasts<sup>234</sup>, intestinal cells<sup>235</sup> or different tumor cell lines<sup>236,237</sup>. Their results show subcytotoxic concentrations for CAR and THY in the same range as ours ( $\sim 500 \mu\text{M}$ )<sup>235</sup> or higher (50% viability at  $\sim 5 \mu\text{g/mL}$ )<sup>234</sup> and also very similar for CIN ( $\sim 10 \mu\text{g/mL}$ )<sup>237</sup> pointing to apoptosis and membrane damage as key cytotoxic mechanisms. Even though the studied molecules showed cytotoxic activity at doses above 0.06–0.09 mg/mL, it is important to point out that during the regenerative process in an infected wound the antimicrobial compound at those doses would eradicate both bacteria and eukaryotic cells, but while bacteria are removed from the injury, eukaryotic cells are continuously arriving

to the wound to participate in the regenerative process.<sup>210</sup> Hence, only a small fraction of eukaryotic cells would be damaged.

## II.5. Conclusions

Compounds present in EOs including CAR, CIN, and THY exhibit the highest *in vitro* antimicrobial activities against *E. coli* and *S. aureus* of all the antimicrobials tested. THY showed the lowest MBC values (0.3 mg/mL) among all of the compounds tested and was the most effective bactericide against the Gram-negative and Gram-positive strains evaluated. According to SEM images, flow cytometry and confocal microscopy bacteria membrane disruption is the bactericidal mechanism attributable to studied compounds. There was no antagonism between the tested active compounds, but no synergism was found either; only the CAR-THY combination showed an additive effect. The presence of those compounds at concentrations above 0.5 mg/mL hinders *S. aureus* biofilm formation and also partially eliminates preformed biofilms. Subcytotoxic values of the tested EOs (0.015–0.090 mg/mL) are much higher than chlorhexidine doses (0.004 mg/mL). All these studied properties make EOs optimal for biomedical applications such as wound healing treatment.

# Chapter III

## ANTIMICROBIAL WOUND DRESSING AGAINST FLUORESCENT AND METHICILLIN-SENSITIVE PATHOGENIC BACTERIA

### Summary

This chapter studies the antimicrobial action of thymol (THY) loaded in polycaprolactone (PCL) based electrospun dressings by measuring antibiofilm activity and the ability to eradicate intracellular and extracellular pathogenic bacteria. We have used *Staphylococcus aureus* Newman strain (methicillin-sensitive strain, MSSA) expressing the coral green fluorescent protein (cGFP) as a traceable model of pathogenic bacteria commonly infecting skin and soft tissue. Compared to non-loaded dressings, THY-loaded PCL was able to eliminate the pathogenic bacteria in a J774 macrophage coculture model. In addition, by using confocal microscopy and the conventional microdilution plating method, we corroborated the successful ability of THY in preventing also biofilm formation.

The content of this chapter has been adapted from the following submitted work:

Garcia-Salinas, S.; Gamez-Herrera, E.; Landa, G.; Arruebo, M.; Irusta, S.; Mendoza, G.

**Antimicrobial Wound Dressings Against Fluorescent and Methicillin-Sensitive Intracellular Pathogenic Bacteria.**

Submitted for publication: ACS Applied Materials & Interfaces Manuscript ID: am-2020-05668q.

## Table of contents

<b>III.1. Introduction</b>	<b>61</b>
<b>III.2. Objective</b>	<b>63</b>
<b>III.3. Experimental</b>	<b>63</b>
<b>III.4. Results and discussion</b>	<b>64</b>
III.4.1. Physico-chemical characterization of the electrospun nanofibers	64
III.4.2. Bactericidal activity	66
III.4.3. Antibiofilm activity	68
III.4.4. Cytotoxicity assessment of the PCL-THY patches	70
III.4.5. <i>In vitro</i> model of infection of J774 macrophages	72
<b>III.5. Conclusions</b>	<b>75</b>



### III.1. Introduction

The expansion of resistance to antibiotics is thwarting the search of new molecules due to the high investment that it implies for the pharmaceutical industry.<sup>196</sup> In addition, despite all the global efforts to control and reduce the use and misuse of antibiotics, the antibiotic use in 76 countries studied over 16 years (2000-2015) increased 65% (expressed as prescribed daily doses), and the antibiotic consumption rate increased 39%.<sup>238</sup> Thus, new alternatives have been developed to treat bacterial infections. As Chapter II shows, natural compounds have antimicrobial activity by damaging cell membrane, proposing this type of compounds as antibiotic substitutes. The probability to develop bacterial resistance towards essential oils (EOs) is low. This fact may fall on the multicomponent nature and varied composition of EOs and in their ability to target multiple bacterial pathways, meanwhile antibiotics normally focus on one single target.<sup>224</sup> However, it has been reported that bacteria can adapt its membrane composition and structure in response to subinhibitory concentrations of some antimicrobials present in EOs such as thymol (THY).<sup>128</sup> Therefore, sustained concentrations above minimal inhibitory concentrations should be maintained at all times to prevent resistances. THY, a monoterpenoid phenol compound present in different EOs as that obtained from *Thymus vulgaris*, have demonstrated its antimicrobial activity in different bacterial strains such as *Staphylococcus aureus*, a major human pathogen which causes substantial morbidity and mortality in skin and soft tissue associated infections as well as in implant-associated infections.<sup>239-241</sup>

To overcome EOs solubility limitations and provide with sustained release systems, new pharmaceutical formulations have been proposed.<sup>242</sup> Nanotechnology has contributed to the progress in different areas of medicine including diagnosis, therapy and in their combination (i.e., theragnostics).<sup>243</sup> Within the nanotechnology field, due to their large area per volume ratio, nanofibers outstand as ideal building blocks in different biomedical materials applied in drug delivery,<sup>244</sup> biomedical devices,<sup>245</sup> biosensing<sup>246</sup> or as dressings for wound healing.<sup>247</sup> Regarding this last application, the synthesis of polymeric electrospun nanofibers loading antimicrobial and anti-inflammatory drugs (including EOs), has been explored in the development of antimicrobial wound dressings.<sup>248</sup> Compared to conventional fibers, nanofibrous patches contain fibers ranging from nanometers to micrometers showing the great advantages of high porosity, narrow diameter distribution and high-specific surface area prone

for the release of loaded antimicrobial compounds. Some electrospun dressings are made of biomaterials recognized for their biocompatibility, biodegradability and lack of toxicity, such as natural or synthetic polymers (chitosan, collagen, polycaprolactone (PCL) or poly lactic-co-glycolic acid (PLGA)).<sup>249</sup> PCL is a biocompatible polymer approved by the FDA in many devices due to its high biocompatibility and controlled hydrolytic biodegradation.<sup>250</sup> Loaded with antimicrobial drugs, PCL nanofibers have demonstrated high efficiency not only preventing infection development, but also avoiding biofilm formation.<sup>251–253</sup>

As it was aforementioned, biofilms are populations of microorganisms aggregated and embedded in a polymeric matrix (EPS) which provides bacteria with a protector environment to medical treatments. It is well known that the existence of bacteria, particularly in chronic colonization, is commonly not as free-living planktonic state, but as organized clusters called biofilms.<sup>64</sup> Within the biofilm there are intercellular signaling molecules produced by bacteria that respond to cell population density by gene regulation. In response to factors secreted by other bacteria in the community, bacteria can coordinate their activities, control the biofilm growth pattern or change their phenotype and thus, their virulence factors.<sup>65</sup> Antibiotics can penetrate the extracellular surface of planktonic bacteria, but bacteria within the biofilm can be protected and the antibiotic diffusion impaired.<sup>254</sup> Against this fact, EOs have been studied for their biofilm disruption potential. It has been reported the ability of some EOs to inhibit biofilm formation or disrupt already formed biofilms, suggesting their potential use in food preservation and in antimicrobial therapies.<sup>255,256</sup> Their antibiofilm activity may be attributed to different mechanisms: inhibition of bacterial adhesion to surfaces at an initial stage, or inhibition of Quorum Sensing (cell to cell communication).<sup>256</sup> THY has been shown as an effective compound to inhibit biofilm formation, not only in monomicrobial cultures of *S. aureus*, but also with polymicrobial cultures of different bacteria (e.g., *S. aureus*, *Listeria monocytogenes*).<sup>240,255</sup> This effect may be attributed to the disruption of bacteria membranes permeability and thus, hindering surface adhesion.<sup>257</sup> Therefore, THY reduces bacterial growth, interferes with biofilm formation and promotes biofilm eradication.<sup>258</sup>

Exposed subcutaneous tissues have been shown as critical scenarios for potential infection development having the favorable microenvironment for bacteria colonization and contamination.<sup>46</sup> The risk of infection represents a general concern in skin and soft tissue open wounds, where each phase of wound healing is challenged by the possibility of microbial

infection.<sup>259,260</sup> Following postsurgical wound analysis, it has been demonstrated that the average hospitalization period rises from 14 to 24 days when wounds became infected.<sup>261</sup> Infected wounds are characterized by a failure in inflammation, re-epithelialization and remodeling phases. Signs of infection may be pain, erythema, edema, heat and purulence, exudate, discoloration or wound breakdown.<sup>63</sup>

For a complete tissue regeneration, the wound healing process requires the complete removal of any microbial exogenous contamination. Macrophages play an essential role in wound healing, not only eliminating pathogens or dead cells, but also releasing cytokines, growth and angiogenic factors that take part in the wound healing process.<sup>262</sup> In this regard, tissue-resident macrophages recognize pathogen-associated patterns, such as the presence of bacterial endotoxin lipopolysachharide (LPS) during infections, causing the enrollment of other cells which help to fight a potential infection.<sup>263</sup> *S. aureus* is a pathogen described to survive within phagocytic cells, such as macrophages, persisting in parts of their life-cycle intracellularly during infections.<sup>241,264,265</sup> Co-culture models of *S. aureus* infected macrophages have been developed to study the behavior of bacteria under the presence of different antimicrobial treatments.<sup>265–267</sup>

### III.2. Objective

This chapter develops the synthesis of electrospun THY-loaded PCL nanofibers and it is studied the effect of this drug-eluting wound dressing against cGFP-expressing antibiotic sensitive *S. aureus* (MSSA) growth. Three different infection models have been developed: (a) planktonic bacteria, (b) biofilm formation and (c) a co-culture model of J774 macrophages infected with cGFP-expressing *S. aureus*. Besides the development of quantitative methods, confocal microscopy was used to observe both biofilm formation and the co-culture model after the treatment with dressings based on THY-loaded PCL nanofibers.

### II.3. Experimental

Electrospun THY-loaded nanofibers were synthesized and characterized regarding morphology, drug loading and drug release after 24 h. Morphology was studied by Scanning Electron Microscopy (SEM), whereas drug loading and release were determined by GC-MS and UPLC liquid chromatography, respectively. Antimicrobial activity of free THY and PCL-THY patches was studied in a cGFP-expressing *S. aureus* strain following the broth microdilution

method<sup>216</sup> and agar broth (ASTME-2180-18) standard test<sup>268</sup>, respectively. The ability of PCL-THY patches to inhibit biofilm formation was measured quantitatively following the broth microdilution method and qualitatively by confocal microscopy. A co-culture model of J774 macrophages infected with cGFP-expressing *S. aureus* was developed to study the infective action of the pathogen in eukaryotic cells. These assays were analyzed by confocal microscopy.

The characterization techniques and different evaluation methods are described in Appendix I.

### III.4. Results and discussion

#### III.4.1. Physico-chemical characterization of the electrospun nanofibers

Figure III.1 shows the SEM micrographs of PCL and PCL-THY nanofibers. Both fibrous patches were homogeneous in their fiber diameter distribution having a bead-free surface. PCL patches showed mean diameter in their fibers of  $779 \pm 86$  nm, meanwhile THY-loaded PCL nanofibers mean diameter was  $794 \pm 96$  nm. Sadeghianmaryan *et al.*<sup>269</sup> also obtained PCL nanofibers with a small dispersity in size and random orientation following the same methodology.

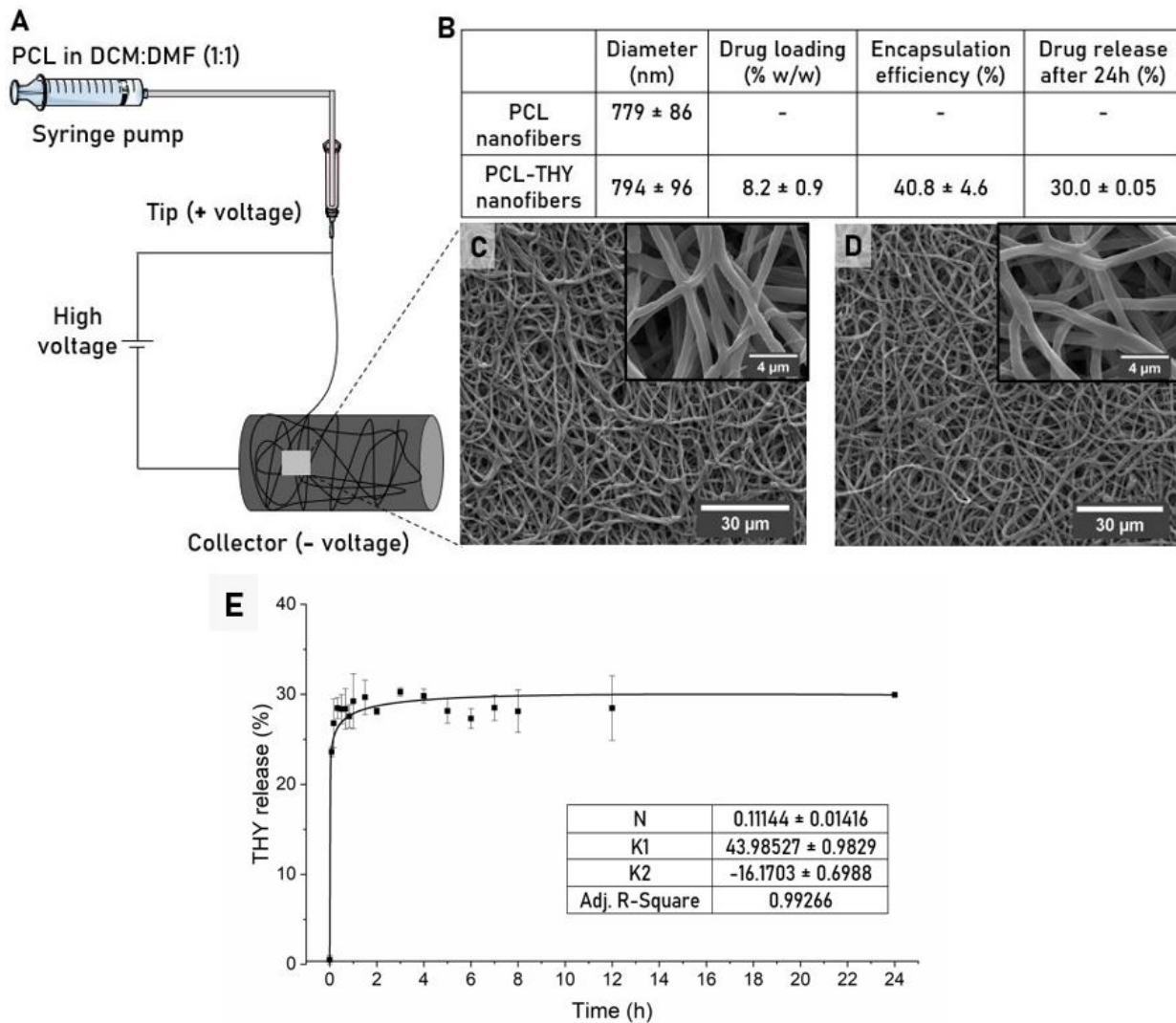


**Figure III.1:** Patches synthesis and characterization. A) Scheme depicting the PCL nanofibers synthesis by electrospinning. B) Table shows nanofiber diameters and PCL-THY drug loading (w/w %) and encapsulation efficiency (%). Mean ± SD (N=100). C) PCL morphological characterization by SEM. D) PCL-THY morphological characterization by SEM. E) THY release and Peppas and Sahlin equation parameters.

The morphology and dimensions of the electrospun fibers depend on processing and polymer solution parameters.<sup>270</sup> Syntheses parameters were the same for PCL or PCL-THY patches, using a polymer flow rate of 1 mL/h and a distance from tip to collector of 18 cm. The presence of THY in the synthesis solution did not change the ionic conductivity (22.2  $\mu\text{S}$  for PCL and 20.8  $\mu\text{S}$  for PCL-THY) and, despite of the increase in the solution viscosity (from 1.4 to 1.6 cP for PCL and for PCL-THY, respectively), it did not affect the resulting fibers

morphology.<sup>270</sup> Alfaro De Prá *et al.*<sup>271</sup> also demonstrated that PCL fibers with average diameters of  $663 \pm 334$  nm can be obtained using a rotatory drum collector.

THY loading in prepared fibers was  $8.2 \pm 0.9$  wt.% which renders an encapsulation efficiency of  $40.8 \pm 4.6$  wt.%. This low EE achieved could be related to the use of a rotating collector, since for carvacrol (isomer of THY) loaded polyvinyl acetate fibers prepared using this collection system, the EE was also low (43-55 %) attributed to the evaporation of the monoterpenoid phenol derivative.<sup>272</sup> The study of release kinetics demonstrated a fast burst THY release from the PCL-THY patches. Figure III.1.E shows that 28% of the encapsulated THY was released in the first hour. Peppas and Sahlin release kinetics model was the best mathematical fit for THY release with a  $R^2$  correlation coefficient of 0.993; results are shown in Figure III.1.E. This model explains a drug release occurring through the coupling of Fickian diffusion and polymer chains relaxation phenomena<sup>273</sup>. In our case the  $K_1 \gg K_2$  implies that the Fickian diffusion is the predominant mechanism in the THY release.

#### III.4.2. Bactericidal activity

Figure III.2 shows the antibacterial activity of free and THY encapsulated in PCL determined in cultures of cGFP-expressing *S. aureus*. A concentration of 0.05 mg/mL of free THY were enough to significantly inhibit bacteria growth (MIC), showing a reduction from  $10^9$  to  $10^7$  CFU/mL. When bacteria were treated with 0.15 mg/mL of free THY, no growth was found, meaning that MBC was reached. However, when bacteria were treated with PCL-THY, it was observed that 10 mg of PCL-THY reached the MIC inhibiting bacteria growth from  $10^9$  to  $10^6$  CFU/mL, whereas 12 mg of PCL-THY were enough to avoid cGFP-expressing *S. aureus* growth (MBC) in an agar culture of 3 mL of volume having  $10^5$  CFU of inoculum. Considering THY loading and release kinetics from the patches, a mat of 10 mg would provide with a THY concentration released of 0.08 mg/mL in the time analyzed, meanwhile 12 mg of PCL-THY would release THY to the medium reaching a THY concentration of 0.1 mg/mL in the same time. The slight MIC and MBC differences observed between free THY and THY released from the PCL-THY patches can be associated with the experimental method followed, since free THY is challenged against bacteria in a liquid culture medium (TSB), whereas THY-loaded patches are studied using solid agar (TSA).

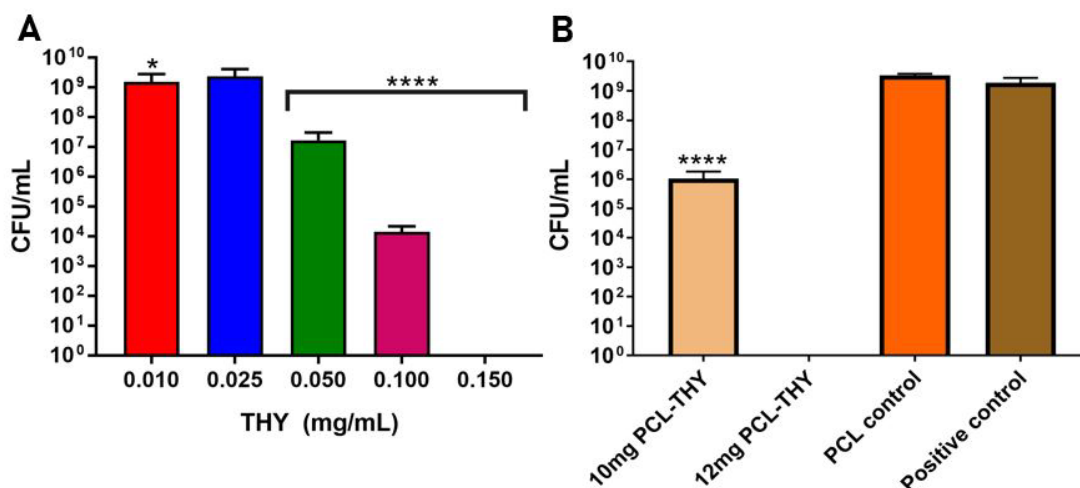


**Figure III.2:** Effect of THY treatment in cGFP-expressing *S. aureus* growth (CFU/mL) in contact during 24h. A) Free THY (0.01-0.15 mg/mL) and B) PCL-THY (10-12 mg). All samples are statistically compared with the positive control sample (non-treated bacteria). \* $p < 0.05$ ; \*\*\*\* $p < 0.0001$ . Mean  $\pm$  SD of three replicas are represented.

Wound healing may be impaired by wound infection mediated by different bacteria. The microorganisms closely related to the colonization of skin and soft tissue wounds are from the *Staphylococci* family (in particular, *S. epidermidis* and *S. aureus*).<sup>64</sup> As Chapter II demonstrates, THY is one of the best compounds inhibiting bactericidal growth of *S. aureus* strains, showing a MIC of 0.2 mg/mL and a MBC of 0.3 mg/mL against *S. aureus* (ATCC 25923).<sup>240</sup> In the treatment with THY, Badawy *et al.*<sup>274</sup> reported a MIC for *S. aureus* (ATCC 6538) of 0.13 mg/mL, meanwhile Rua *et al.*<sup>275</sup> identified a MIC in the range of 0.46-0.51 mg/mL for different *S. aureus* strains. These previous studies point out to the higher sensitivity of the cGFP-expressing *S. aureus* strain used in this work since a concentration of 0.05 mg/mL of free THY was enough to inhibit the bacteria growth (MIC), whereas the complete elimination of the bacteria was reached when free THY concentration was 0.15 mg/mL.

Superior sensitivity of this strain was also found for THY loaded PCL fibers. The comparison of these results with our previous studies<sup>247</sup> showed the same pattern. In the current study, 12 mg of THY-loaded PCL patches (corresponding with 0.1 mg/mL of THY released in 24h) were enough to achieve the MBC when working with cGFP-expressing *S. aureus*, meanwhile 30 mg of PCL-THY (0.38 mg/mL of THY released in 24 h) were needed to completely eradicate bacteria using a *S. aureus* (ATCC 25923) strain.<sup>247</sup> These differences in THY susceptibility may be attributed to phenotype differences among *S. aureus* strains as explained above.

## III.4.3. Antibiofilm activity

cGFP-expressing *S. aureus* biofilm formation was monitored by confocal microscopy by using the Calcofluor White stain (Figure III.3). As mentioned in the experimental section (Appendix I), two approaches were followed based on the incubation times and the amount of THY-loaded PCL patches used.

As it can be observed in Figure III.3, THY-free PCL patches (7 and 12 mg; left images) let the bacteria (stained in green) grow all over the well, forming a homogeneous layer of biofilm, which was clearly stained with Calcofluor White (in blue) on top of the bacteria settled underneath (green layer), as depicted in the bottom panels of both images. These results suggest that bacteria released the EPS typical of biofilm on the wells. However, PCL-THY patches clearly decreased the number of bacteria present in the wells being their numbers lower when the patch's weight was increased. The images on the right show that the presence of bacteria was almost totally reduced when the THY concentration was increased. In this case, although all treated samples were stained with Calcofluor White, none of them showed a top coating labelled in blue which would be characteristic of biofilm formation, demonstrating the lack of biofilm formation and highlighting the ability of the loaded patches to avoid or eradicate biofilms.

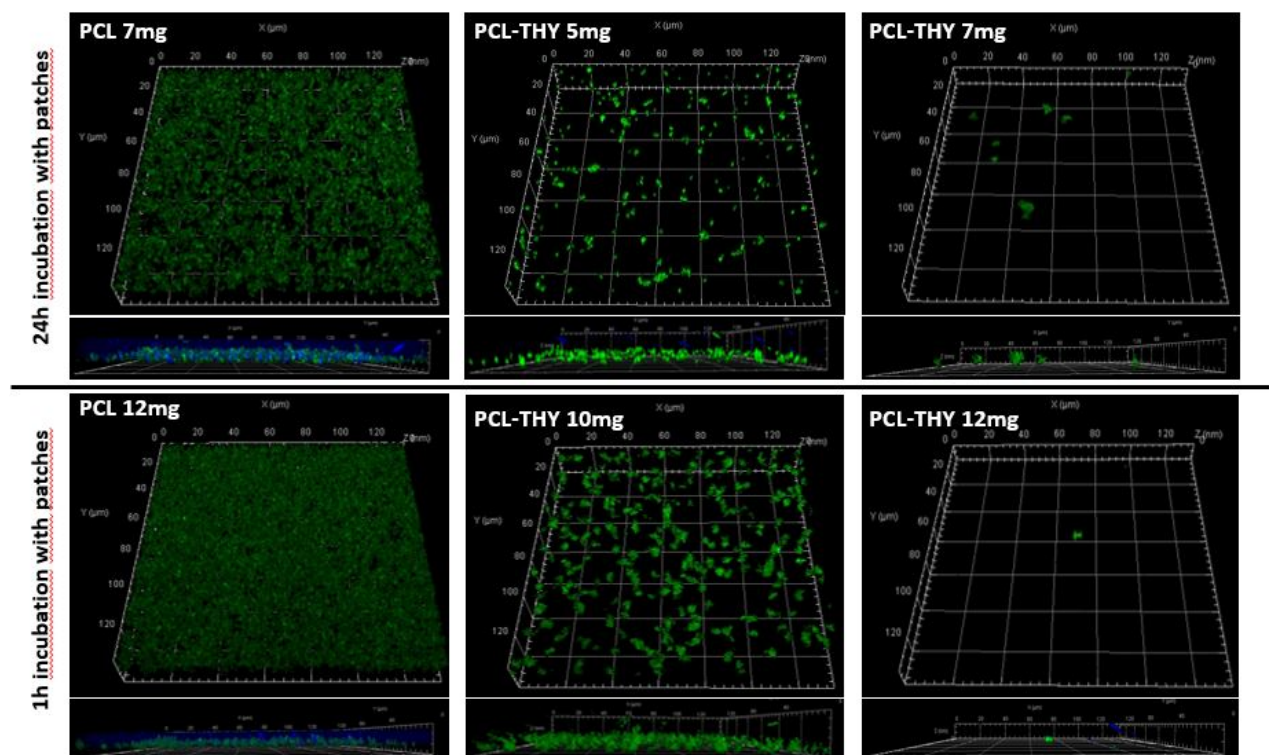




**Figure III.3:** Confocal laser scanning microscopy was performed to evaluate the effect of different THY-loaded patches having different weights (5-7 mg and 10-12 mg) and different incubation times (1 and 24h) compared with PCL control samples. For each incubation time, the three upper images correspond to cGFP-expressing *S. aureus* attached to the bottom of the well. Bottom images show the Calcofluor stain of biofilm formed. Bacteria is depicted in green whereas biofilm stains in blue.

These qualitative results were confirmed with a quantitative method. Attached bacteria were collected from the bottom of the wells and cultured in agar plates. Figure III.4 shows the bacteria growth quantification after treatment following both methodologies. Positive controls (7 and 12 mg of PCL patches) reached  $10^9$  CFU/mL of bacterial growth in 24h whereas the treatment with 5-7 mg of PCL-THY for 24h (Figure III.4.A) or with 10-12 mg of PCL-THY for 1h (Figure III.4.B) displayed a significant decrease in bacterial growth in the range of  $10^5$ - $10^6$  CFU/mL, confirming the qualitative results showed in Figure III.3.

Considering the release kinetics results, 5 and 7 mg of PCL-THY patches would release in 24h 0.06 and 0.09 mg/mL of THY, respectively. These concentrations in which we obtained MIC values, correlate with the inhibitory concentrations when using free THY in planktonic bacteria. Those results highlight the potential of these patches to provide with prophylaxis against biofilm formation and to reduce already formed biofilms.

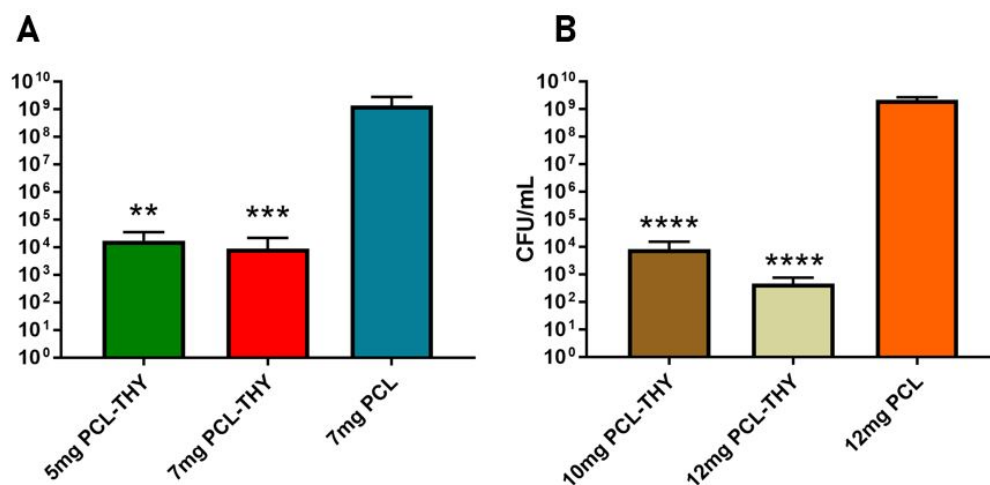


**Figure III.4:** Quantification of cGFP-expressing *S. aureus* to evaluate biofilm formation against different treatments with PCL-THY: A) 5-7 mg for 24h; B) 10-12 mg for 1h. Results derived from PCL-THY are statistically compared to those obtained from the PCL patches used as control. \*\* $p < 0.01$ ; \*\*\* $p < 0.001$ ; \*\*\*\* $p < 0.0001$ . Mean  $\pm$  SD of three replicas are represented.

A recent study states that 78% of non-healing chronic wounds contain biofilms.<sup>259</sup> The elimination of bacterial bioburden is essential to promote wound healing in chronic wounds.<sup>276</sup> Sharifi *et al.* demonstrated that sub-MIC concentrations (MIC/2 to MIC/16) of different EOs obtained from *Thymus daenensis* and *Satureja hortensis* in contact with *S. aureus* for 24h, significantly prevented biofilm formation.<sup>257</sup> Moreover, Cabarkapa *et al.*<sup>258</sup> treated bacteria (*Salmonella Enteritidis*) with sub-MIC (MIC/2-MIC/4) concentrations of *Origanum* and *Thymus* essential oils as well as their active components carvacrol and THY, and results showed that biofilm formation was inhibited. These studies corroborate our results, not only 7 mg of PCL-THY eliminate already formed biofilms, but also we demonstrate that the exposition to 5 mg PCL-THY for 24h, reduces bacterial attachment to the well. The obtained results may evidence that cell wall damage can negatively affect bacterial attachment as we previously described<sup>240</sup>, which, according to Kerekes *et al.*<sup>255</sup> represents the first step in biofilm formation, followed by formation of microcolonies, maturation and cell dispersal.<sup>256,275</sup> The effect of THY against bacterial adhesion has also been demonstrated by Yuan *et al.*<sup>278</sup> when they analyzed PIA (Polysaccharide Intracellular Adhesion), a component involved in adhesion and aggregation. This component was reduced under the presence of THY and thus, bacteria could adhere to materials at the initial stage, but they were unable to form biofilms due to a reduced cell-to-cell adhesion.<sup>278,279</sup> Therefore, THY reduces bacterial growth, interferes with biofilm formation and promotes biofilm eradication.<sup>258</sup>

#### III.4.4. Cytotoxicity assessment of PCL-THY patches

Cytotoxicity of PCL-THY was studied in J774 macrophages at cell metabolism level using the MTT reduction assay. This method depends on the cellular activity of viable cells by producing a colored solution. Cells were exposed to different amounts of PCL-THY following the two methodologies described in the experimental section (Appendix I). The results obtained from both approaches were compared with cells treated with PCL patches (control samples) and are represented in Figure III.5.

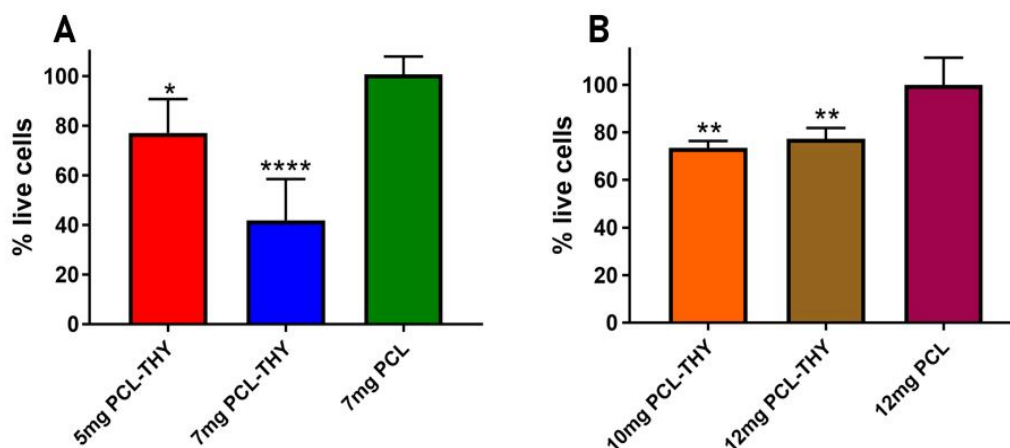


**Figure III.5:** J774 macrophages viability after treatment with PCL-THY following two different approaches regarding the patch weight: A) Treatment for 24h (5 and 7 mg of PCL-THY); B) Treatment for 1h and incubation for other 24h (10 and 12 mg PCL-THY). The results are graphed in basis to untreated cells which were assigned with a 100% viability. \* $p < 0.05$ ; \*\* $p < 0.01$ ; \*\*\*\* $p < 0.0001$ . Mean  $\pm$  SD of three replicas are represented.

In the first approach, cells were treated with 5 and 7 mg of PCL-THY for 24h. As depicted in Figure III.5, a 50% cell growth inhibition was attained with 7 mg of PCL-THY, which corresponds to 0.09 mg/mL of THY released. However, the treatment with 5 mg of PCL-THY (0.06 mg/mL of THY released in 24h) displayed a 80% cell viability after 24h incubation, classifying the material as non-cytotoxic (according to the value established by the ISO 10993-5).<sup>233</sup> Considering the direct relationship among increased concentration and cell toxicity, the treatment with more than 7 mg of PCL-THY for 24h would reduce significantly cell viability at levels below 70%. Due to that fact and keeping in mind that inhibitory and bactericidal concentrations were achieved with 10 and 12 mg PCL-THY, cells were treated with 10 and 12 mg PCL-THY but for a reduced incubation time (just 1h). Following this protocol, cell viability was quite similar for both amounts evaluated, obtaining  $>70\%$  of viability required to consider these concentrations as non-cytotoxic, which corresponds to 0.12 mg/mL using 10 mg PCL-THY and 0.14 mg/mL using 12 mg PCL-THY for 1h.

The cytotoxicity caused by THY against eukaryotic cells is related to its non-selective antiseptic character. During the regenerative process in an infected wound after adding an antiseptic, pathogenic prokaryotic cells are removed but also some somatic eukaryotic ones. However, due to the immune response, new regenerative cells are recruited to the wound area

compensating the initial loss owing to the antiseptic effect. In addition, short contact times would minimize this cytotoxic effect.

#### III.4.5. *In vitro* model of infection of J774 macrophages

In sections III.4 and III.5 it has been studied the effect of PCL-THY on bacteria growth and biofilm formation. As we mentioned before, macrophages play a crucial role in wound healing, managing pathogens, phagocytizing dead cells and recruiting other cells which help to fight infection, such as neutrophils, fibroblasts, keratinocytes or endothelial cells.<sup>262,263</sup> To investigate the impact of the treatment of PCL-THY on a *S. aureus* infected cell line, J774 macrophages were visualized in contact with cGFP-expressing *S. aureus*. Figures III.6 and III.7 represent the orthogonal projection using the maximum intensity projection (MIP), to visualize bacteria inside and outside cells, represented both in the same plane. Bacteria are shown in green while cell nuclei are stained with DAPI (blue) and cytoskeleton, with phalloidin 546 (red).

Figure III.6 depicts activated macrophages with LPS and treated with 5 and 7 mg of PCL-THY for 24h. Control samples (Figures III.6.A and III.6.B) showed cells totally filled with bacteria (green), indicating the successful infection of macrophages. However, the treatment with 5 mg of PCL-THY (Figures III.6.C and III.6.D) and 7 mg of PCL-THY (Figures III.6.E and III.6.F) for 24h clearly demonstrate the efficiency of the synthesized loaded antimicrobial patches showing a reduced number of bacteria in a dose-dependent manner. In the time span studied, 5 and 7 mg patches would release an amount of THY of 0.06 mg/mL and 0.09 mg/mL to the medium, respectively in 24h, concentration with which we obtained bacterial inhibition.

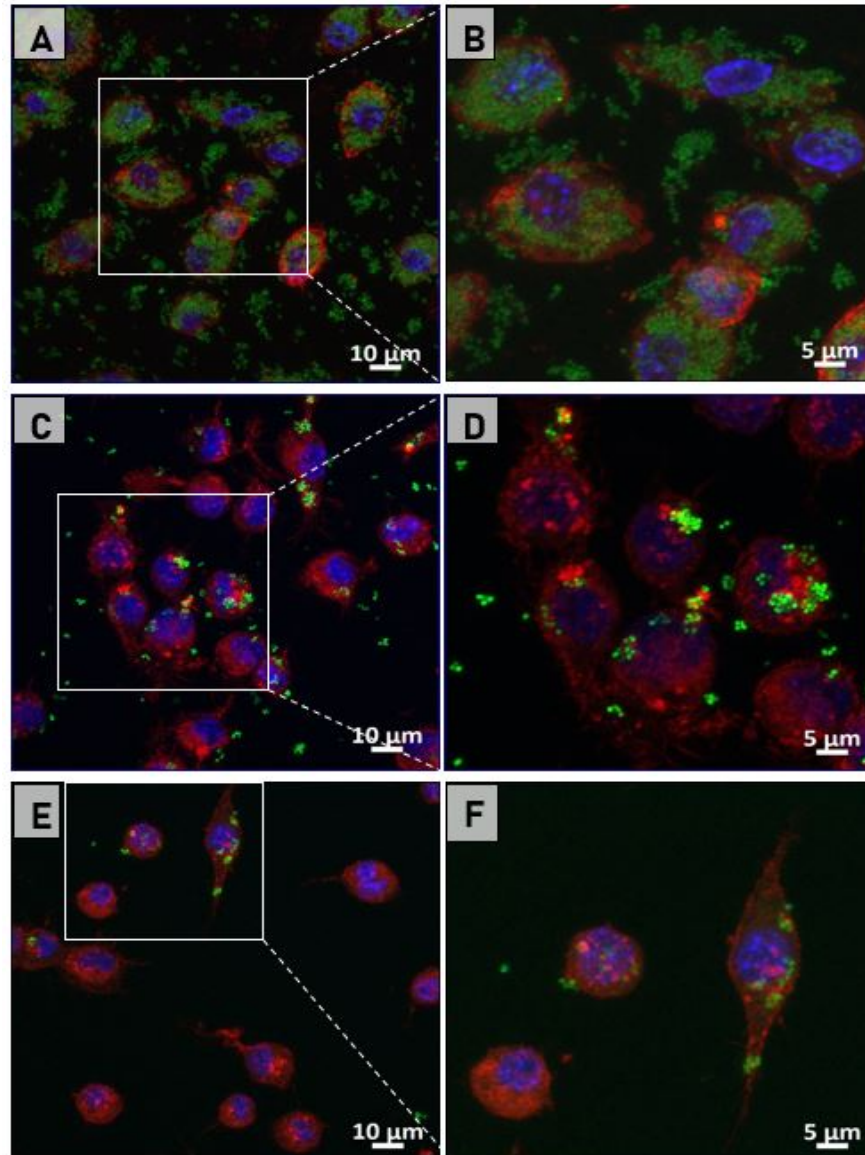


**Figure III.6:** *In vitro* co-culture model of cGFP-expressing *S. aureus* and J774 macrophages. Cells were treated for 24h with: (A, B) 7 mg of PCL patches (control samples); (C, D) 5 mg PCL-THY; (E, F) 7 mg PCL-THY. Left images were acquired with a 63x oil immersion objective. Right images correspond with a zoomed area of left images. Bacteria are stained in green while cell nuclei are stained with DAPI (blue) and cytoskeleton with phalloidin 546 (red).

Due to the results observed in the cell toxicity study, we treated infected macrophages also with 10 and 12 mg PCL-THY though reducing the time of incubation also to 1h (Figure III.7). These images demonstrate the same trend observed in the previous assay. When cells were treated with 12 mg of PCL (Figures III.7.A and III.7.B), bacteria were found throughout the plate. However, when cells were treated with 10 mg PCL-THY (0.12 mg/mL of THY released in 1h; Figures III.7.C and III.7.D) and 12 mg PCL-THY (0.14 mg/mL of THY released

in 1h; Figures III.7.E and III.7.F) for 1h, bacteria concentration was significantly reduced, even totally when using the highest amount, confirming the efficiency of the fabricated PCL-THY patches in an *in vitro* infection model, pointing to their potential antibacterial application.

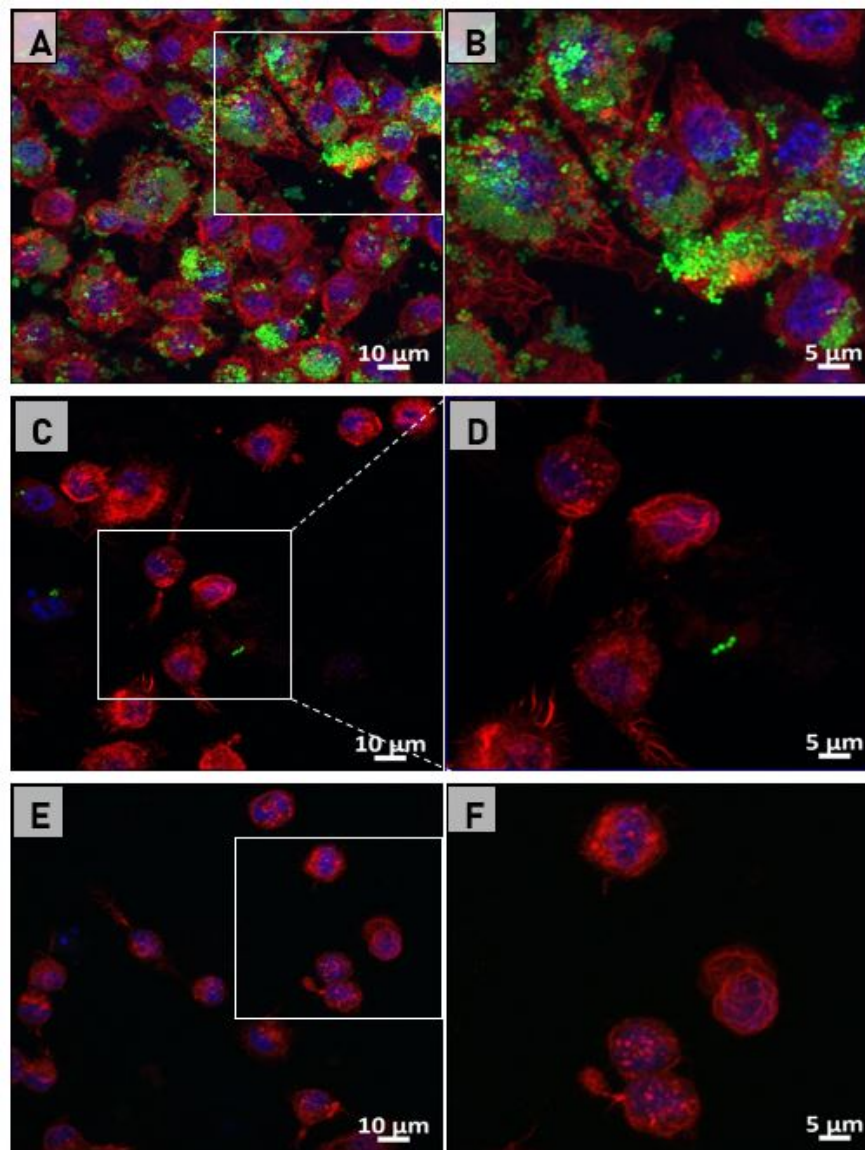


**Figure III.7:** *In vitro* co-culture model of cGFP-expressing *S. aureus* and J774 macrophages. Cells were treated for 24h with: (A, B) 12 mg of THY-free PCL; (C, D) 10 mg of PCL-THY; (E, F) 12 mg of PCL-THY. Left images were acquired with a 63x oil immersion objective. Right images correspond with a zoomed area of left images. Bacteria are stained in green while cell nuclei are stained with DAPI (blue) and cytoskeleton with phalloidin 546 (red).

Among other functions, biofilm allows bacteria to defend itself from external threats. Thus, immune cells are not able to reach and eliminate bacteria, and therefore a persistent inflammation and wound chronification occur.<sup>280</sup> *S. aureus* may survive within phagocytic cells including macrophages, even when host defense is activated.<sup>281</sup> Based on that, cGFP-expressing *S. aureus* was chosen as a model of a bacterial pathogen with part of its life cycle occurring intracellularly to study and visualize the effect of PCL-THY on J774 macrophages in a co-culture infection model. We observed that the treatment for 24h with a sub-inhibitory concentration (7 mg of PCL-THY, 0.09 mg/mL THY released) for cGFP-expressing *S. aureus*, was cytotoxic to macrophages. It is not the first time that a high toxicity of THY is reported in eukaryotic cell cultures. For example, Belato *et al.*<sup>282</sup> analyzed the cytotoxicity of free THY on murine macrophages (RAW 264.7) and showed that cell viability dropped from 75% to 5% at concentrations higher than 0.005 mg/mL. The toxicity mechanism of this compound is poorly understood. There are different hypothesis about this issue; Gutierrez *et al.*<sup>283</sup> reported that THY can affect the integrity of membranes in both prokaryotic and eukaryotic cells. However, Satooka *et al.*<sup>284</sup> proposed that THY is intracellularly transformed to a toxic radical and quinone, relating its toxicity to the oxidative-stress generated.

Compared with bactericidal planktonic studies, when J774 macrophages were infected with cGFP-expressing *S. aureus*, it has been shown that a lower dose of PCL-THY patches is able to fight cell infection. That is probably because THY may help macrophages in the control of the progression of the infection *in vitro*.<sup>285</sup> In summary, PCL-THY patches have demonstrated to induce a significant reduction of cGFP-expressing *S. aureus* into infected J774 macrophages, diminishing their intracellular colonization. In addition, the ability of THY to reduce biofilm formation, opens the possibility to fight bacterial infections and make the recovery of wound healing more efficient when using this locally delivery system of thymol.

### III.5. Conclusions

By comparing THY-free PCL electrospun patches as a model of a conventional wound dressing and THY-eluting PCL electrospun patches, the later stand out as efficient antimicrobial materials against a pathogenic Gram-positive bacteria sensitive to conventional antibiotics used as a model (methicillin-sensitive *S. aureus* Newman strain) expressing cGFP. The fluorescent bacteria were used to demonstrate the successful infective action of the pathogen in eukaryotic cells as a model of intracellular pathogen. Finally, it has been also demonstrated that the PCL-

THY patches are able to hinder biofilm formation by inhibiting the first stages of bacterial adhesion. The developed patches showed cytotoxicity against eukaryotic cells in a dose dependent manner, but at reduced doses and during short contact times, cell viability was similar to untreated controls. In this comparative study, research based on evidence demonstrates that THY-loaded electrospun PCL patches are more efficient than their THY-free counterparts against pathogenic *S. aureus*.



## Chapter IV

### ELECTROSPUN ANTI-INFLAMMATORY PATCH LOADED WITH ESSENTIAL OILS FOR WOUND HEALING

#### Summary

This chapter summarizes the wound healing process to highlight the importance of a bacterial infection as one of the main reasons to increase inflammation and delay the process. Thus, the possibility to find a strategy that combines antimicrobial and anti-inflammatory properties is particularly appealing for wound healing. The ability of essential oils reducing inflammation was studied as free compounds and loaded into electrospun-PCL nanofibers. Thus, the expression of Il1b, iNos and Il6 cytokines in J774 macrophages was analyzed by RT-PCR. Overall, results indicate that THY-loaded patches could serve as promising candidates for the fabrication of dressings that incorporate bactericidal and anti-inflammatory properties while simultaneously avoiding the limitations of traditional antibiotic-loaded devices.

The content of this chapter has been adapted from the following published work:

García-Salinas, S.; Evangelopoulos, M.; Gámez-Herrera, E.; Arruebo, M.; Irusta, S.; Taraballi, F.; Mendoza, G.; Tasciotti, E.

**Electrospun Anti-Inflammatory Patch Loaded with Essential Oils for Wound Healing.**

*Int. J. Pharm.* **2020**, *577* (January), 119067. <https://doi.org/10.1016/j.ijpharm.2020.119067>.

## Table of contents

<b>IV.1. Introduction</b>	<b>79</b>
<b>IV.2. Objective</b>	<b>80</b>
<b>IV.3. Experimental</b>	<b>80</b>
<b>IV.4. Results and discussion</b>	<b>81</b>
IV.4.1. Cell viability, morphology and flow cytometry of free essential oils	81
IV.4.2. Anti-inflammatory effects of the different free natural compounds	83
VI.4.3. Characterization of electrospun nanofibers	85
IV.4.4. Cell viability of natural compounds-loaded PCL patches	87
IV.4.5. Anti-inflammatory effects of the loaded patches	88
IV.4.6. Cell migration towards PCL-loaded nanofibers	90
IV.4.7. Immunofluorescence assay	91
<b>IV.5. Conclusions</b>	<b>93</b>

## IV.1. Introduction

Previous chapters in this thesis focused on the search of therapeutic or combinatory plant-derived natural compounds to fight infections. Recently, considerable interest has been shown in the use of strategies that combine antimicrobials with anti-inflammatory drugs.<sup>199</sup> Specifically, extracts derived from plants and animals were shown to effectively modulate inflammatory pathways.<sup>286,287</sup> The inflammatory response, led by macrophages, is the first line of defense against pathogens.<sup>288</sup> Toll-like receptors (TLRs), present on macrophages and dendritic cells, can be activated by lipopolysaccharide (LPS), an endotoxin from gram-negative bacteria which acts as a stimulator of inflammatory cytokines.<sup>289</sup> The stimulation of TLRs leads to the activation and nuclear translocation of nuclear factor kappa-light-chain-enhancer of activated B cells (NF- $\kappa$ B) and mitogen-activate protein kinase. Both signaling pathways involve stimulation of activating protein-1 (AP-1) and, consequently, the down-stream transcription of pro-inflammatory genes, such as interleukin (Il) 1b. This cytokine is synthesized in the early stages of inflammation, triggering subsequent signals which activate Il10, iNos, COX-2, Il6, and others.<sup>289,290</sup> When the inflammatory response is initiated, these paracrine signals recruit other effector cells to the wound area to advance the inflammation to tissue reparation and regeneration.<sup>286</sup>

Natural compounds may be used as anti-inflammatory substances because they could interfere in the NF- $\kappa$ B signaling pathway.<sup>291</sup> For example, squalene, a natural triterpene consumed as an integral part of the human diet, was found to reduce mRNA levels of NF- $\kappa$ B downstream genes such as Tnf-a or Il1b in LPS-treated murine peritoneal macrophages.<sup>139</sup> Curcumin modulates the inactivation of this signaling pathway, decreasing expression of pro-inflammatory genes.<sup>289</sup> THY and CAR, dietary monoterpenes found in certain plants, control the phosphorylation of multiple signaling molecules, inhibiting key mediators of inflammation in LPS-stimulated murine mammary epithelial cells.<sup>292</sup> However, natural compounds have shown several limitations in solubility and pharmaceutical formulations.

To overcome these pitfalls, various delivery systems have been developed to achieve increased solubility and efficacy while maintaining effective control and release.<sup>286</sup> More recently, electrospun patches loaded with antimicrobial and anti-inflammatory drugs have been explored as a promising platform to develop surgical dressings with enhanced wound repair. Additionally, with alternative antimicrobial therapeutics being sought to minimize AMR such

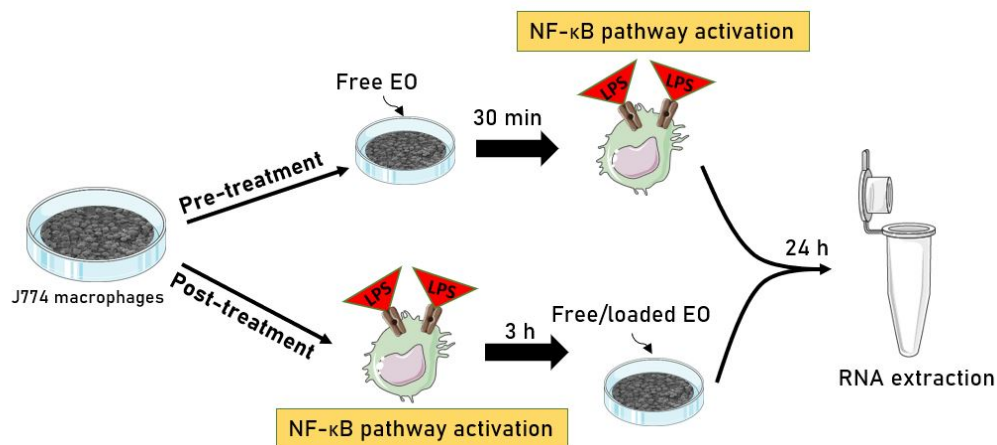
as natural compounds, electrospun patches have garnered significant support. As Chapter III shows, THY encapsulated in electrospun polycaprolactone (PCL) nanofibers keeps the efficient bactericidal properties against pathogenic *S. aureus*. PCL is a biocompatible and bioresorbable polymer that has been FDA-approved for use in several medical and drug delivery devices.<sup>99</sup>

## IV.2. Objective

Herein, PCL electrospun nanofibrous patches loaded with natural bactericidal compounds were prepared with the aim of reducing inflammation during wound healing. After the fabrication and characterization of the electrospun patches, the main goal was to study the ability of essential oils reducing inflammation by measuring the expression of Il1b, iNos and Il6 cytokines in J774 macrophages analyzed by RT-PCR. Genetical results were corroborated by carrying out an immunofluorescence assay. Furthermore, it was studied if PCL-loaded patches show affinity for cell attachment with the aim of understanding the feasibility of the fabricated patches as potential dressings for wound healing.

## IV.3. Experimental

With the aim of studying the effect of free essential oils (EOs) in an *in vitro* inflammatory model, J774 murine macrophages were used. EOs cytotoxicity was studied using the MTT viability assay, optical microscopy and flow cytometry. To develop the inflammatory model, J774 macrophages were activated using LPS and treated with optimal concentrations of free compounds following two procedures indicated in Scheme IV.1. The expression of pro- and anti-inflammatory cytokines was analyzed by RT-PCR. For this, RNA was obtained, and reverse transcribed to cDNA.



Scheme IV.1: *In vitro* inflammation experimental design for i) pre-treatment and ii) post-treatment.

The compounds displaying the best anti-inflammatory results were encapsulated into electrospun PCL nanofibers. Morphology was studied by Scanning Electron Microscopy (SEM), meanwhile drug loading and release were determined by GC-MS and UPLC liquid chromatography, respectively. Viscosity and conductivity of the polymer solution were studied both with and without natural compounds.

MTT viability assay was carried out with J774 macrophages in contact with different EOs-loaded PCL patches. The post-treatment approach (Scheme IV.1) was followed to determine the anti-inflammatory activity of these dressings analyzing Il1b, Nos2 and Il10 expression. Moreover, cells were stained with DAPI and Alexa Fluor 546™ and studied by confocal immunofluorescence. Finally, a cell colonization model was developed to study the cell migration and colonization of the patches by means of the MTT assay and SEM.

The characterization techniques, the inflammatory model and analysis are described in Appendix I.

#### **IV.4. Results and discussion**

##### **IV.4.1. Cell viability, morphology and flow cytometry of free EOs**

Macrophages play a key role during the inflammatory phase in wound healing.<sup>286</sup> As such, J774 murine macrophages were used to test the anti-inflammatory ability of our selected compounds. To assess the cytotoxicity of our EOs in macrophages, these were exposed to EO groups for 24 h and evaluated for metabolic activity (Figure IV.1.A). To ensure non-lethal treatment, cell viability of 70% or greater was considered acceptable as previously established.<sup>233</sup> Interestingly,  $\beta$ -caryophyllene (B-CAR) and curcumin (CUR) displayed the highest cytotoxicity, even at the lowest tested concentration (0.008 mg/mL). Similarly, CIN was also found to be cytotoxic, however, only at concentrations above 0.04 mg/mL. CAR and THY, which demonstrated strong bactericidal action (Chapter II), did not show differences in cytotoxicity; however, detrimental effects were observed at concentrations equal or > 0.12 mg/mL. Conversely, SQU and TYR displayed no indication of cytotoxicity at any of the tested doses.

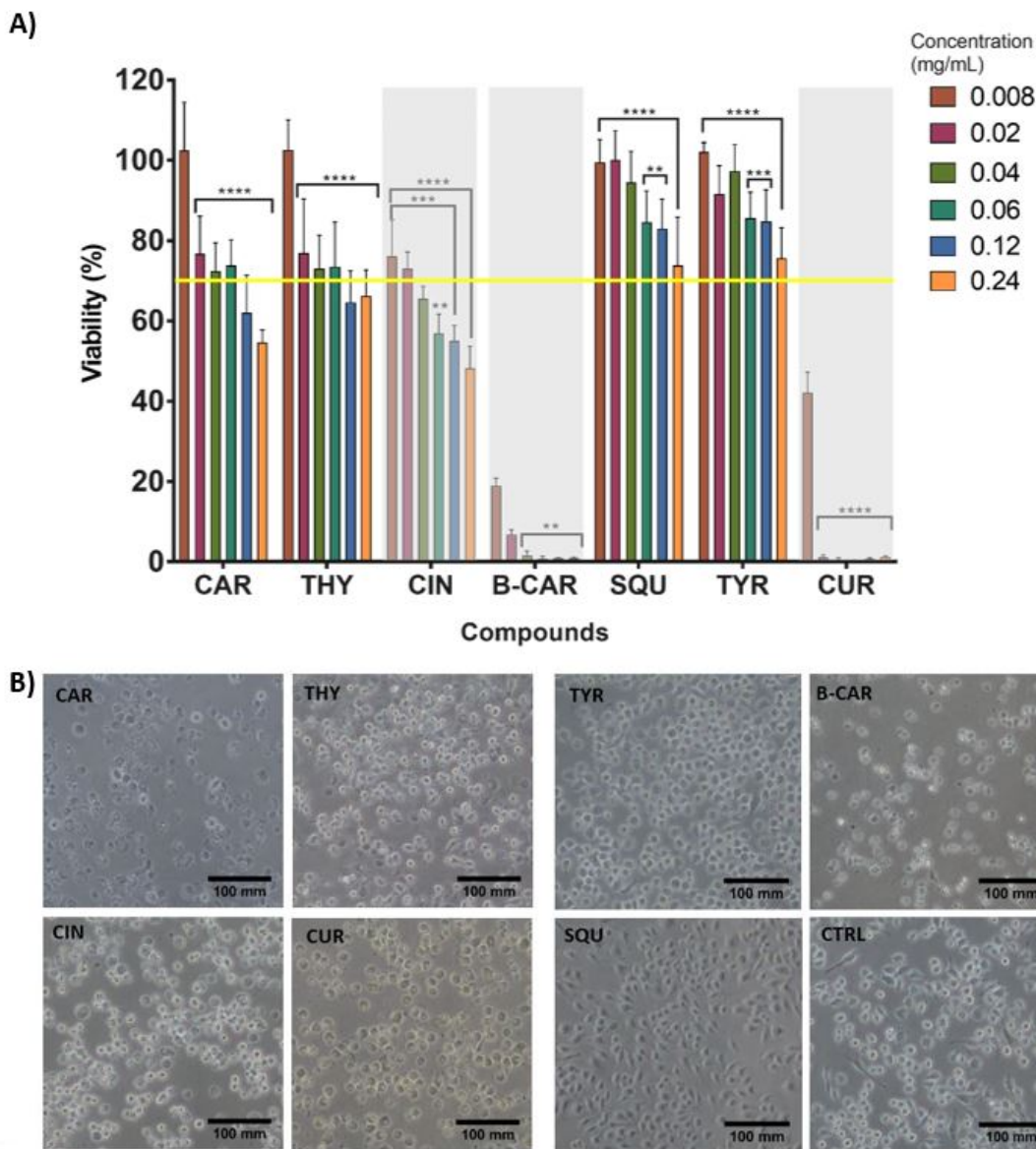
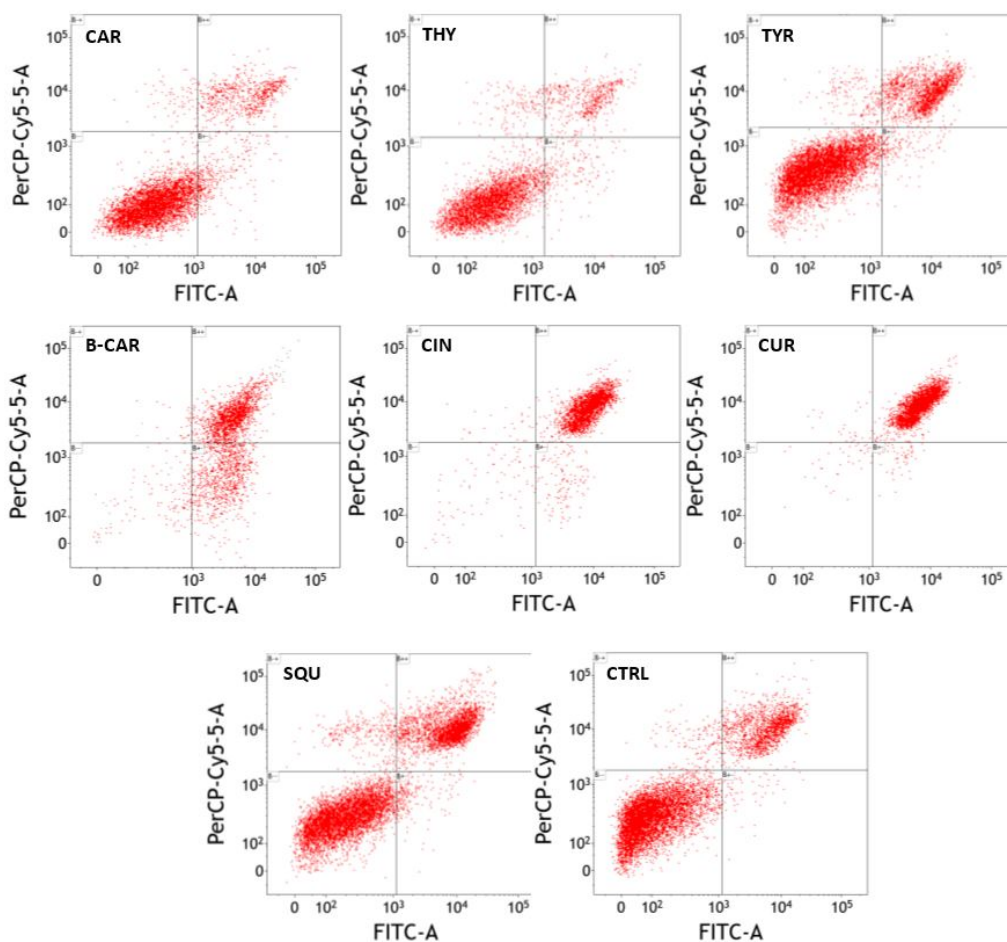


Figure IV.1: Cell viability of J774 macrophages in the presence of free EOs at concentrations ranging from 0.008 to 0.24 mg/mL after 24 h incubation. A) MTT cell viability assay; B) Optical microscope images showcasing cell morphology after 24 h of treatment. \* $p < 0.05$ ; \*\* $p < 0.01$ ; \*\*\* $p < 0.001$ ; \*\*\*\* $p < 0.0001$ . Error bars represent mean  $\pm$  SD of three replicas. Gray boxes highlight the EO compounds removed from additional testing during this chapter due to cytotoxicity.

These results were further confirmed using optical microscopy (Figure IV.1.B) and flow cytometry (Figure IV.2) following a 24 h treatment with the various EOs. B-CAR, CUR, and CIN showed the highest percentages of apoptotic/dead cells compared to untreated control cells. In addition, cell morphology and shape appeared round with heterogeneity in size, typical of dead or apoptotic cells.<sup>293</sup> Conversely, THY, SQU and TYR-treated samples demonstrated the

highest percentages of live cells compared to control samples. Both SQU and TYR-treated samples displayed an elongated cell morphology, while CAR demonstrated increased damage as depicted by Figure IV.1.B and IV.2. As such, despite their previously reported anti-inflammatory effects,<sup>142,294</sup> these compounds were eliminated from further evaluation due to the high toxicity exerted in our *in vitro* model.



**Figure IV.2:** Flow cytometry histograms of phospholipid redistribution in the apoptosis assay: Annexin V/Propidium iodide assay. X-axis corresponds with FITC fluorochrome and Y-axis shows the emission of PerCP-Cy5.5.

#### IV.4.2. Anti-inflammatory effects of the different free natural compounds

To maintain non-lethal working concentrations of EOs, CAR and THY were used at a concentration of 0.06 mg/mL while 0.12 mg/mL was used for SQU and TYR (results obtained in Section IV.4.1). Dexamethasone (DEX), a commercially available corticosteroid anti-inflammatory drug, was used as a negative control while untreated cells served as a positive control. The inflammatory effects of LPS and the effect of the natural compounds were studied

through the expression of the pro-inflammatory genes Il1b and iNos by RT-PCR (Figure IV.3). Results were statistically compared to a positive control.

Two experimental settings were performed (Scheme IV.1): pre-treatment<sup>289,295</sup> and post-treatment.<sup>199,290,296</sup> Interestingly, following pre-treatment, CAR and THY displayed a substantial decrease in pro-inflammatory gene expression following 24 h exposure, reaching levels similar to DEX-treated cells (Figure IV.3.A). On the other hand, mRNA expression levels of Il1b and iNos diminished in the presence of TYR ( $91.0 \pm 6.6$  and  $475.2 \pm 36.5$ , respectively), resulting in higher values when compared to CAR ( $34.1 \pm 5.3$  for Il1b and  $34.1 \pm 4.6$  for iNos) and THY, with expression levels of  $20.9 \pm 3.2$  for Il1b and  $49.8 \pm 9.8$  for iNos. Similarly, TYR expression showed lower values when compared to SQU ( $189.3 \pm 35.1$  for Il1b and  $1824.2 \pm 137.9$  for iNos). Furthermore, SQU was found to be the least effective in reducing pro-inflammatory gene expression, demonstrating comparable levels to LPS-treated cells whose expression levels were  $256.2 \pm 18.2$  for Il1b and  $2429.2 \pm 144.4$  for iNos.

Evaluation of post-treatment cells (Figure IV.3.B) revealed THY significantly reduced Il1b expression ( $51.4 \pm 8.4$ ) to levels comparable to DEX control samples ( $162.4 \pm 18.2$ ), whereas iNos levels displayed no difference. Similarly, iNos expression levels for THY were  $62.2 \pm 11.2$  and  $43.4 \pm 13.6$  for DEX samples. Furthermore, although TYR demonstrated a downregulation of Il1b and iNos ( $326.1 \pm 15.4$  and  $93.3 \pm 12.2$ , respectively), values were still higher when compared to THY-treated cells. This trend closely matched the pre-treatment observations (Figure IV.3.A). On the other hand, SQU did not reduce Il1b and iNos expression compared to the LPS-treated control cells, which was in accordance with the results obtained from the pre-treatment approach. Considering treatment concentrations for both CAR and THY were half of what was used for TYR and SQU (i.e., 0.06 vs 0.12 mg/mL), it can be concluded that the anti-inflammatory effect of CAR and THY was much higher than the other EOs. The differences between both compounds were highlighted in the post-treatment approach (Figure IV.3.B) in which CAR displayed lower inhibitory effects than THY in regulation of Il1b and iNos. These changes between both approaches may be related to increased levels of inducible p-NF- $\kappa$ B p65, which plays an inhibitory role and remained unchanged by THY.<sup>297</sup> Furthermore, of all tested EOs, THY consistently exhibited the highest anti-inflammatory effect. When compared to DEX, an anti-inflammatory drug known to inhibit NF- $\kappa$ B activation,<sup>298</sup> THY



showcased a similar ability to modulate the expression of Il1b and iNos, demonstrating its potential as a natural origin anti-inflammatory compound.

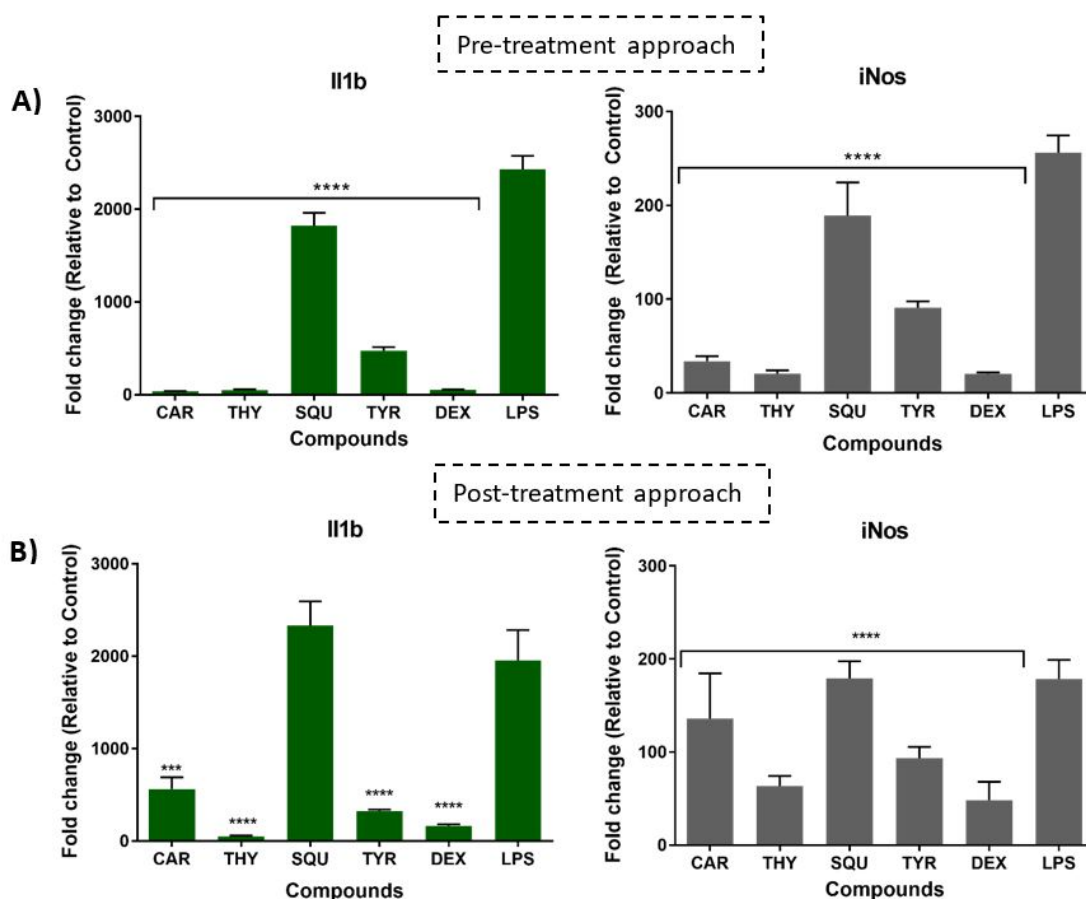


**Figure IV.3:** Comparison of pro-inflammatory markers (Il1b and iNos) in LPS -activated macrophages following A) pre-treatment and B) post-treatment with EOs. \*\*\* $p < 0.001$ ; \*\*\*\* $p < 0.0001$ . Mean  $\pm$  SD of three replicas are represented. Fold change relative to housekeeping gene ( $\beta$ -actin) and untreated cells.

#### IV.4.3. Characterization of electrospun nanofibers

The synthesis and characterization of electrospun nanofibers developed in this chapter were carried out by Enrique Gamez in a thesis collaboration.

The average diameters of the nanofibers were as follows: PCL nanofibers,  $480 \pm 109$  nm; PCL-THY,  $293 \pm 59$  nm; PCL-TYR,  $380 \pm 67$  nm; PCL-THY-TYR,  $948 \pm 277$  nm; PCL-CAR,  $258 \pm 47$  nm; PCL-SQU,  $493 \pm 106$  nm; and PCL-THY-SQU,  $752 \pm 257$  nm. Figure IV.4 shows SEM images and size distribution of PCL, PCL-THY, PCL-TYR and PCL-THY-TYR nanofibers.

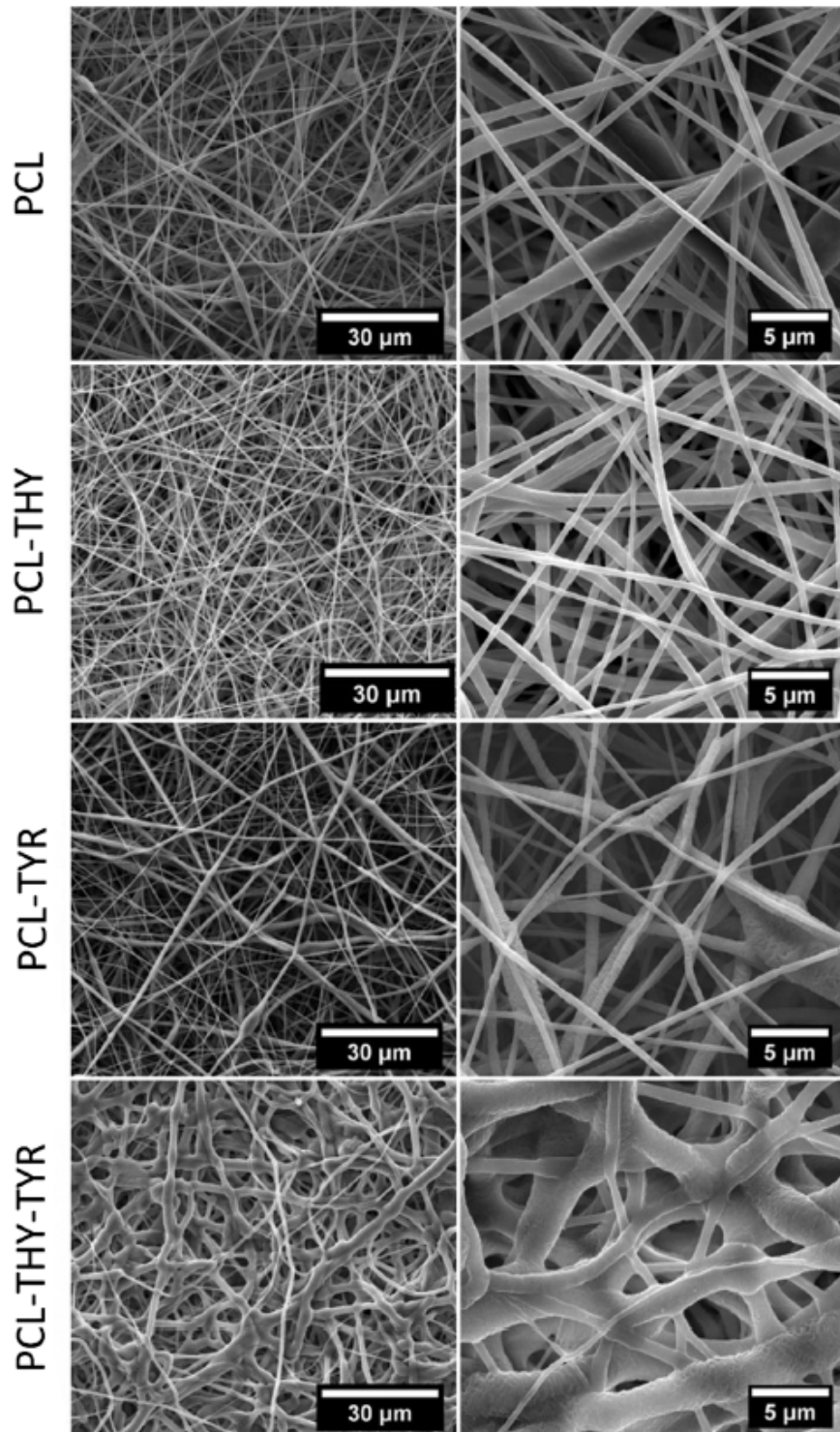


Figure IV.4: Characterization of electrospun PCL patches by SEM.

The drug loading and encapsulation efficiency of the PCL-patches are summarized in Table IV.1. In general, loading values for the PCL-EOs were found to be within range of

reported values.<sup>190,247</sup> PCL fibrous patches were found to possess a porosity of 78.8% with a pore diameter of 1.8  $\mu\text{m}$  and a density of 0.22 g/mL. Water uptake was in the range 52–66 %.

Evaluation of drug release kinetics demonstrated a burst release effect from the patch (Table IV.1). Specifically, PCL-THY showcased a 7.33% burst release of THY in the first 60 min while PCL-TYR resulted in release of 61.74% after 8 h. When co-loaded, PCL-THY-TYR displayed a release of 5.36% of THY and 41.38% of TYR. The difference observed between THY and TYR release may be explained by THY's lower solubility in water (0.9 mg/mL) compared to TYR (25.3 mg/mL), despite the use of a solubilizing agent.

Table IV.1: EOs compounds loading, encapsulation efficiency and release.

Sample	Drug loading (% w/w)	Encapsulation efficiency (%)	Drug release after 24 h (%)
PCL-THY	17.13 $\pm$ 1.61	85.65 $\pm$ 8.05	7.33 $\pm$ 0.85
PCL-TYR	17.72 $\pm$ 1.80	88.62 $\pm$ 8.99	61.74 $\pm$ 2.99
PCL-CAR	15.40 $\pm$ 1.44	77.00 $\pm$ 7.18	5.78 $\pm$ 0.93
PCL-SQU	16.32 $\pm$ 1.40	81.61 $\pm$ 7.01	0
PCL-THY-TYR	THY – 7.46 $\pm$ 1.35	74.62 $\pm$ 7.98	5.36 $\pm$ 0.12
	TYR – 7.17 $\pm$ 1.12	71.71 $\pm$ 11.19	41.38 $\pm$ 1.39
PCL-THY-SQU	THY – 7.75 $\pm$ 0.17	77.52 $\pm$ 7.16	8.92 $\pm$ 1.18
	TYR – 7.27 $\pm$ 0.73	72.73 $\pm$ 7.88	0

#### IV.4.4. Cell viability of natural compound loaded PCL patches

It is known that nanofibrous materials have several advantages as delivery systems due to their high surface to volume ratio and high favorable for wound dressing applications. Many bioactive substances can be loaded into polymeric nanofibers and maintain their function.<sup>294,299</sup> Although these compounds demonstrate effective anti-inflammatory effects, their low solubility makes them challenging to administer. As such, we investigated the use electrospun PCL as a delivery strategy for wound healing due to the large area per volume ratio of the nanofibers

To elucidate possible cytotoxic effects of the PCL patch, cell viability in macrophages was observed using an MTT assay. Instead, we evaluated the potential benefit associated with PCL patches developed in combination with CAR, THY, TYR, and SQU. In this case, all patches with the exception of PCL-CAR displayed cell viability > 70% (Figure IV.5).

Interestingly, macrophages treated with PCL-CAR exhibited cell viability below 50% with a dramatic reduction in viability observed at higher concentrations (i.e., 1.0 and 1.5 mg). Conversely, PCL-SQU was found to be the most biocompatible with cell viability consistently over 80%. As such, all subsequent studies maintained a patch mass of 0.75 mg while PCL-CAR was entirely removed from additional testing in this chapter. Moreover, in an effort to evaluate combinatory EO release from patches, PCL-THY-TYR and PCL-THY-SQU were tested and found to maintain viability >70% only at 0.75 mg. THY was specifically included in the combination patches due to its bactericidal properties demonstrated in Chapter II and Chapter III, therefore serving as a bactericidal and an anti-inflammatory therapeutic.

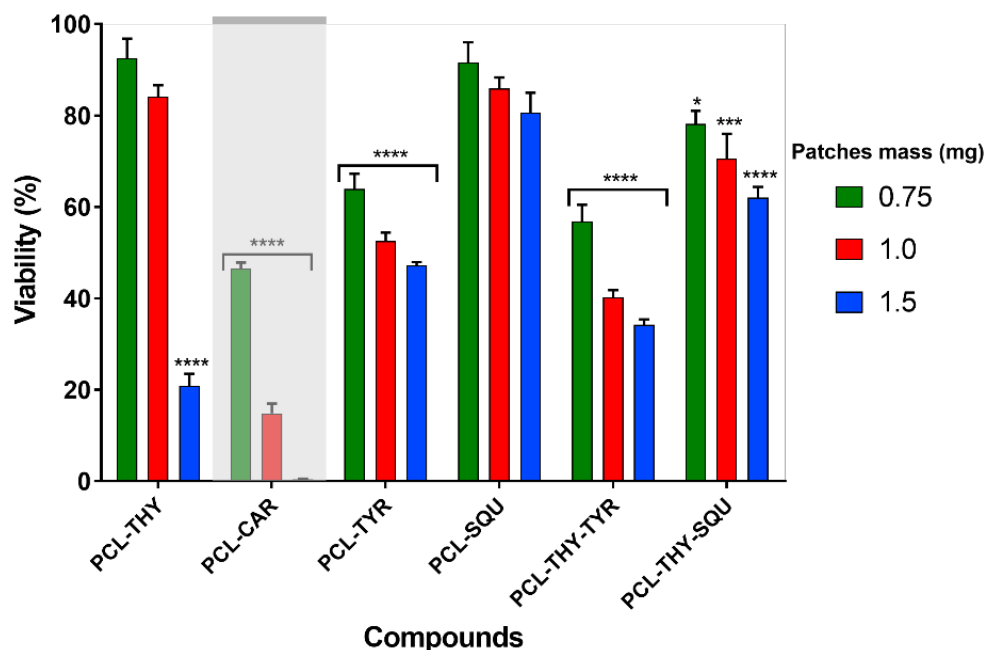


**Figure IV.5:** Cell viability of J774 macrophages after 24 h incubation in the presence of 0.75, 1.0, and 1.5 mg of patches loaded with various natural compounds. \* $p < 0.05$ ; \*\*\* $p < 0.001$ ; \*\*\*\* $p < 0.0001$ . Error bars represent the SD of three replicas. Gray boxes highlight the treatment group removed from additional testing due to cytotoxicity.

#### IV.4.5. Anti-inflammatory effects of the loaded patches

To evaluate anti-inflammatory properties, macrophages were exposed to loaded PCL patches using the post-treatment strategy above and evaluated for pro- and anti-inflammatory genes. Specifically, the expression of Il1b, iNos (i.e., pro-inflammatory) and Il10 (i.e., anti-inflammatory) were analyzed (Figure IV.6). When compared to an LPS treated control, PCL-THY demonstrated the highest anti-inflammatory effect for all genes tested. (i.e., lowest

expression). Conversely, TYR demonstrated higher levels of downregulation for Il1b when compared to SQU, although SQU displayed higher inhibition of Il10 and iNos. More so, when a combinatory treatment strategy was employed, THY-TYR loaded patches demonstrated a greater reduction in Il1b and Il10 cytokine levels when compared to THY-SQU although no difference was observed in iNos levels.

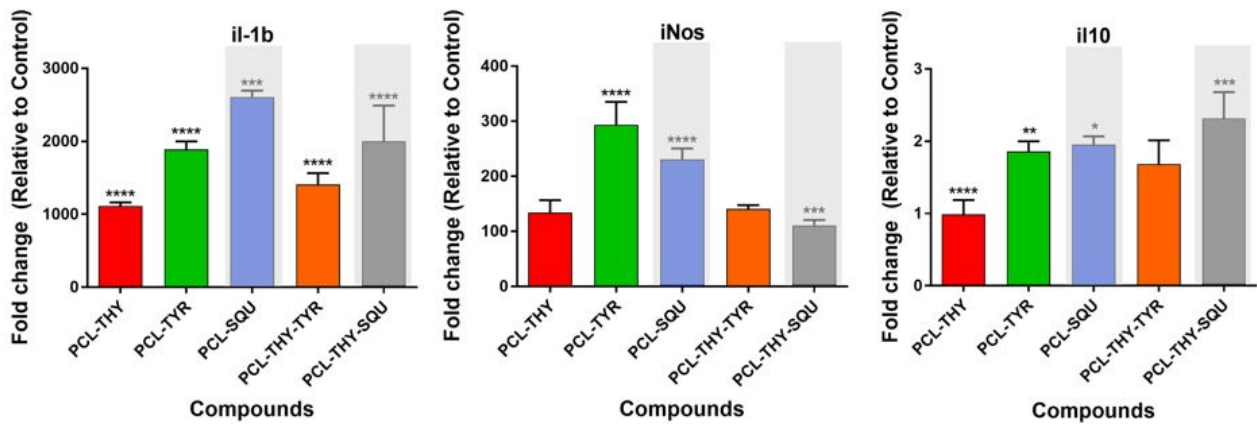


**Figure IV.6:** Expression of mRNA levels for pro-inflammatory (Il1b, iNos) and anti-inflammatory (Il10) genes following treatment with PCL-THY, PCL-TYR, PCL-SQU, PCL-THY-TYR and PCL-THY-SQU. Measurements were collected 24 h post-LPS activation. Post-treatment approach was followed to carry out this assay. \* $p < 0.05$ ; \*\* $p < 0.01$ ; \*\*\* $p < 0.001$ ; \*\*\*\* $p < 0.0001$ . Error bars represent the SD of three replicas. Fold change is relative to housekeeping gene and untreated control cells. Gray boxes highlight the treatment group removed from additional testing due to the low anti-inflammatory effect.

As THY and TYR displayed the highest levels of reduction in inflammatory markers, further analysis was performed to evaluate their therapeutic potential over 48 h (Figure. IV.7). Kinetic evaluation of mRNA levels revealed highest peaks of Il1b and iNos occurring at 24 h across all patch groups while Il10 expression remained consistently low for all time points. Furthermore, when compared with the LPS-treated cells, THY-loaded patches exhibited more efficient downregulation of anti-inflammatory genes than TYR- and THY-TYR-loaded patches. This data revealed a combinatory loading strategy does not offer increased anti-inflammatory potential likely due to the reduced loading of THY.

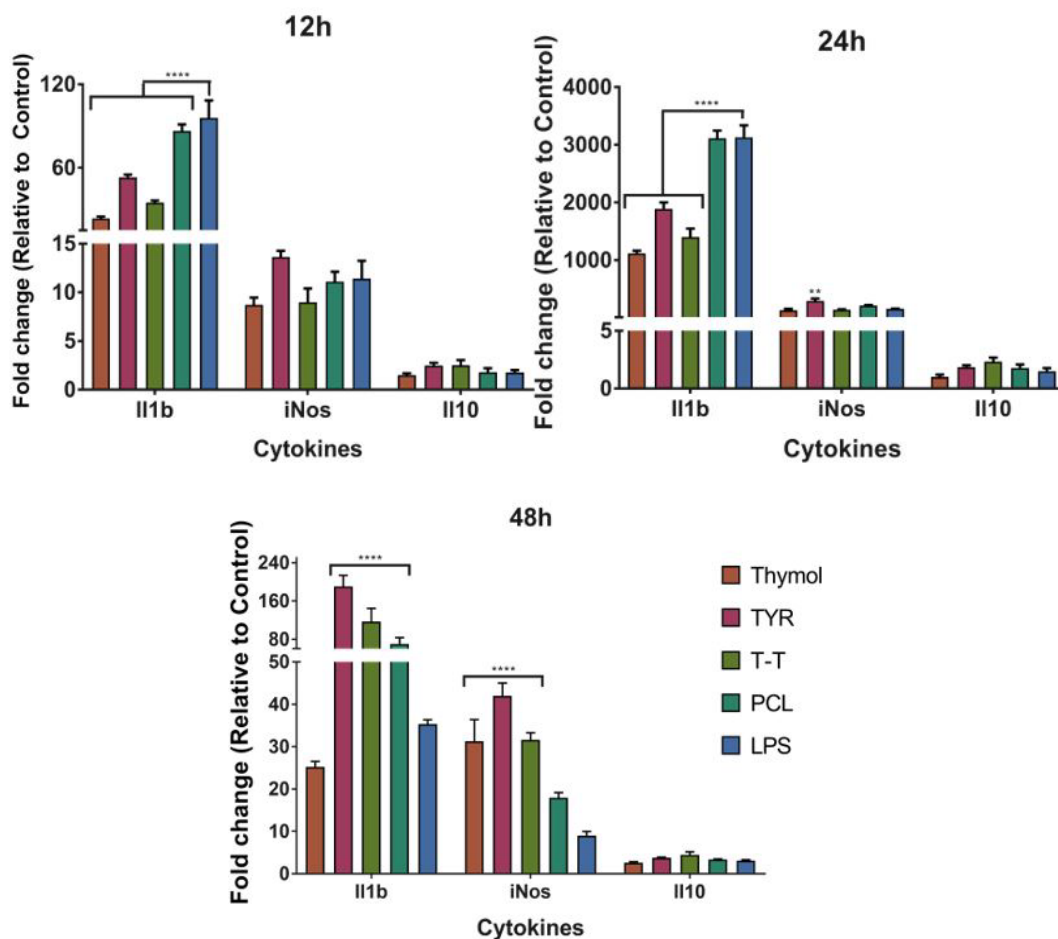


Figure IV.7: Expression of mRNA level for pro-inflammatory (II1b, iNos) and anti-inflammatory (II10) genes in J774 macrophages following treatment with patches loaded with PCL-THY, PCL-TYR and PCL-THY-TYR. Stimulation with LPS was carried out for 3 h and subsequently treated with patches for 12, 24, and 48 h. This assay followed the post-treatment approach. \*\* $p < 0.01$ ; \*\*\*\* $p < 0.0001$ . Error bars represent the SD of three replicas.

Among the most sensitive cytokines to LPS and the earliest to show gene expression in inflammation is II1b.<sup>300</sup> As it is shown, II1b was the only cytokine studied having the highest expression after 24 h. At two different time points, THY, TYR, and their combination were able to reduce II1b expression. THY patches present superior reduction in inflammation compared to TYR, although slight differences were found regarding PCL-THY-TYR. This demonstrates that THY is the compound that may exert the anti-inflammatory effect in combination patches. Several studies have established THY as anti-inflammatory compound through different models, i.e. by the inhibition of the expression of pro-inflammatory cytokines, such as II1b or II6.<sup>301</sup> Sheorain *et al.*<sup>302</sup> reported that THY nanoparticles presented increased anti-inflammatory

potential than free THY, suggesting the anti-inflammatory effect of THY was retained even when encapsulated within a nanoparticle.

#### IV.4.6. Cell migration towards PCL-loaded nanofibers and colonization of the patches

The role of a wound dressing is to provide the optimum conditions for wound healing while simultaneously protecting the wound from further trauma and invasion by pathogenic microorganisms. It is also important that the dressings can be removed atraumatically avoiding cell adherence and colonization so as to prevent further damage to the wound surface during dressing changes. To evaluate the patches potential as a wound dressing, we assessed their response in cell colonization. To this end, PCL-THY, PCL-TYR and PCL-THY-TYR patches were placed atop a monolayer of macrophage cells and allowed direct contact with the cells for 24 h. Following this incubation, patches were analyzed for cytotoxicity using the MTT assay and by SEM to visualize cell migration towards the patches and their colonization.

In this assessment, cells were primarily found to remain intact on the bottom wells as observed by viability testing (Figures IV.8 A and B). Similarly, this was further showcased by evaluating cell viability on the patch itself which revealed negligible values for all groups. To further validate our hypothesis, SEM was carried out on the patch to check both the fibers morphology and the potential presence of cells. SEM micrographs for all patch groups reveal no observable signs of cell colonization (Figure IV.8). These results support the feasibility of the fabricated patches as potential dressings for wound healing.

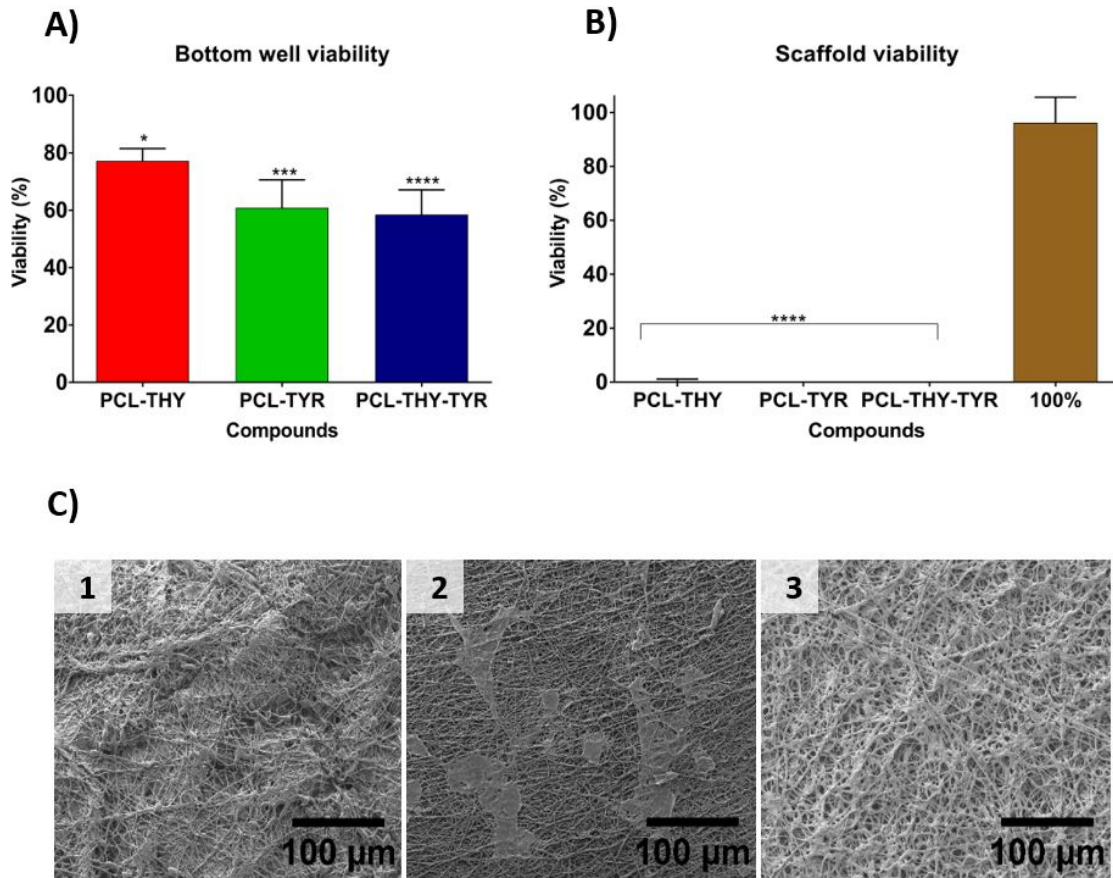


Figure IV.8: J774 migration to patch and colonization. A) Cell viability assessment using MTT was performed on seeded cells and B) Cells remaining on patch. C) SEM images of patches following 24 h exposure to cells. 1: PCL-THY; 2: PCL-TYR; 3: PCL-THY-TYR. \* $p < 0.05$ ; \*\*\* $p < 0.001$ ; \*\*\*\* $p < 0.0001$ . Error bars represent the SD of three replicas.

#### IV.4.7. Immunofluorescence assay

As PCL-THY was the most effective in anti-inflammation, it was evaluated its effect on cell morphology. To this end, both activated or non-activated macrophages were treated with PCL-THY (0.75 mg) and evaluated using confocal microscopy (Figure IV.9). Immunofluorescent images were obtained following treatment and used to assess cell size after removal of the patch. As expected, LPS-activated macrophages displayed the highest cell area when compared to untreated cells. Conversely, when cells were treated with PCL-THY, average cell area was significantly less than LPS-treated cells and only slightly higher than non-treated cells, suggesting THY may inhibit the inflammatory effects of LPS. Furthermore, PCL-THY-



treated cells showcased similar sizes as DEX-treated cells, indicating a comparable inhibition in inflammation.

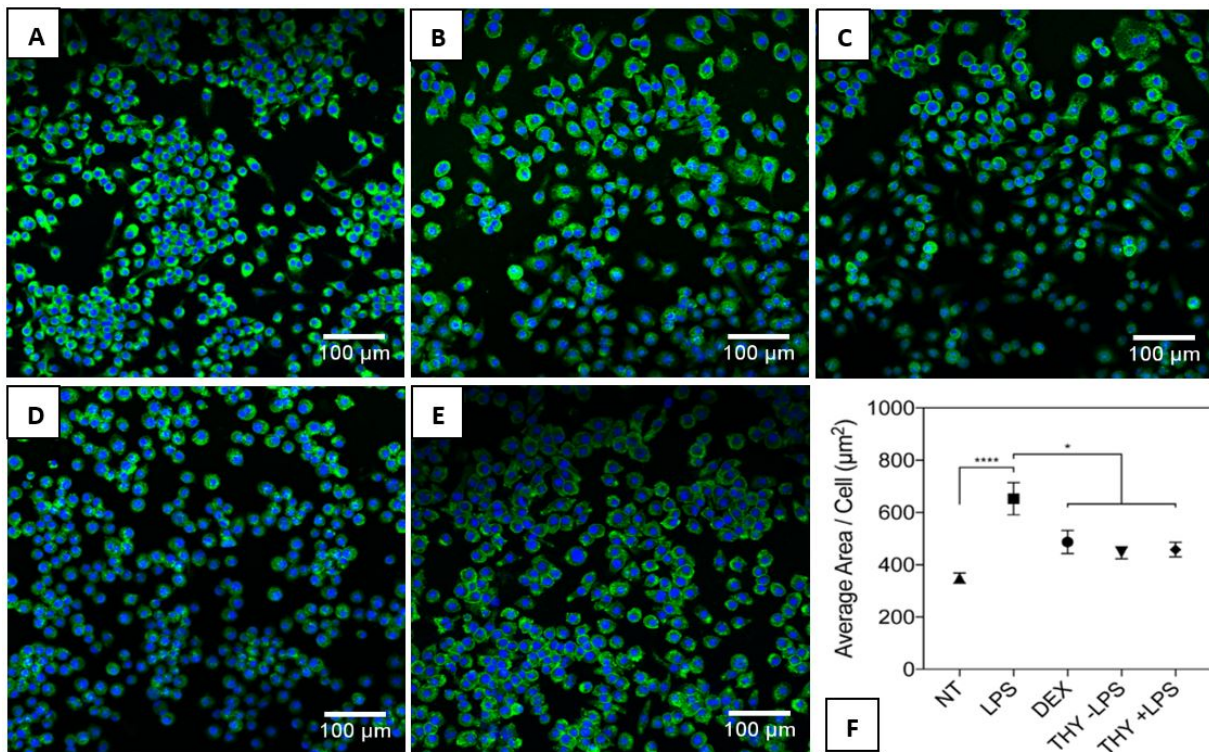


**Figure IV.9:** Confocal microscope images of J774 murine macrophages stained for cell membrane (green) and nucleus (blue). A) Non treated cells (negative control); B) LPS-treated cells (positive control); C) Cells treated with LPS- and DEX; D) Cells treated with PCL-THY; E) Cells treated with LPS- and PCL-THY; F) Average area per cell calculated from the total area obtained in cell membrane and dividing it by the total number of events counted (nuclei). NT, no treatment; DEX, dexamethasone; THY, Thymol. Error bars represent the SD of 4–8 representative field of views.

LPS can bind to many receptors on the macrophage surface resulting in activation of the NF-κB pathway and changes in cell morphology. For example, in these experiments, cells displayed an increase in size when activated with LPS (Figure IV.8). However, when they were treated with PCL THY or free DEX, the size decreased to levels comparable to untreated cells, which is in agreement with previous studies.<sup>300</sup> Specifically, LPS-stimulation of macrophage cells result in the activation of genes related to cell membrane and actin filaments.<sup>300</sup>

## IV.5. Conclusions

PCL-based electrospun patches incorporating compounds commonly present in EOs, such as THY, TYR, and SQU, and their combinations THY-TYR and THY-SQU, were able to significantly reduce inflammation in an *in vitro* model based on LPS-activated J774 murine macrophages. When encapsulated within PCL, THY demonstrated the most successful in terms of efficiency against inflammation and in inhibiting the expression of the pro-inflammatory mediators II1b and iNos. In addition, loaded patches were successful in reducing the size of inflamed cells, indicating an alleviation of the inflammatory response, with colonization assays highlighting the potential use of synthesized patches for wound healing. The work presented here demonstrates that natural compounds loaded within nanofibers hold great promise for wound healing, stemming from their unique ability to resolve two essential mechanisms in wound repair: fighting infections and mitigating inflammation. Thus, THY is proposed to be a potential therapeutic agent to be included in dressings for wound healing.

# Chapter V

## EFFICIENCY OF ANTIMICROBIAL ELECTROSPUN THYMOL-LOADED POLYCAPROLACTONE PATCHES *IN VIVO*

### Summary

In this chapter, electrospun thymol (THY)-loaded polycaprolactone (PCL) nanofibers were synthesized to be potentially used as wound dressing materials. *In vivo* studies were performed using eight to ten-week-old male SKH1 hairless mice which were subjected to an excisional wound splinting model in order to evaluate wound infection prevention. The infection progression in wounds was evaluated through a semi-quantitative method and quantitative polymerase chain reaction (qPCR). Post-mortem wounds were analyzed by histopathological and immunohistochemical studies. Results indicated that PCL-THY patches act as inhibitors of *Staphylococcus aureus* ATCC 25923 strain growth and reduce the cellular inflammatory response. Therefore, wound dressings containing natural compounds can prevent infection, promote wound healing and prompt regeneration.

The content of this chapter has been adapted from the following accepted work:

Garcia-Salinas, S.; Gamez-Herrera, E.; Asin, J.; de Miguel, R.; Andreu, V.; Sancho-Albero, M.; Mendoza, G.; Irusta, S.; Arruebo, M.

**Efficiency of Antimicrobial Electrospun Thymol-Loaded Polycaprolactone Mats *in vivo***

ACS Applied Biomaterials. Manuscript ID: mt-2020-002706.

## Table of contents

<b>V.1. Introduction</b>	<b>97</b>
<b>V.2. Objective</b>	<b>98</b>
<b>V.3. Experimental</b>	<b>99</b>
<b>V.4. Results and discussion</b>	<b>100</b>
V.4.1. Electrospun PCL nanofibers characterization	100
V.4.2. Mechanical properties of PCL-THY patches	101
V.4.3. <i>In vivo</i> bactericidal activity	101
V.4.4. Histopathological and immunohistochemical studies	103
<b>V.5. Conclusions</b>	

## V.1. Introduction

Injuries caused by burns, trauma or surgery are significant economic and social burden to healthcare providers.<sup>303</sup> Wound dressings play an important role during the healing process and they have received growing attention in recent years.<sup>304–306</sup> In general, wound dressings are required to have good biocompatibility, provide a barrier against dust and bacteria, absorb exudates and debris and facilitate blood clotting while promoting transpiration avoiding wound maceration.<sup>307</sup> It is also important for a wound dressing material to be as strong at least as human skin (tensile strength in the range 2-16 MPa) to withstand mechanical stress to support the patient daily activities.<sup>307</sup> Another expected characteristic is having adequate porosity to allow gas exchange but avoiding bacterial penetration acting as a physical barrier.<sup>303</sup>

Polymer nanofibers provide the possibility to immobilize antimicrobial compounds and their structure, similar to the extracellular matrix, has high interconnected porosity, and allows gas permeability.<sup>248</sup> Among the different fibers fabrication techniques, electrospinning is the most commonly used method because of its versatility, cost-efficiency and straightforward setup.<sup>308</sup> Synthetic (e.g., PCL, poly (L-lactic acid) (PLLA), poly(lactic-co-glycolic acid), etc.) and natural polymers (e.g., polysaccharides, proteins, polyesters, etc.) have been used to produce electrospun nanofiber patches. Among the natural polymers, collagen nanofibrous matrices have been prepared and used in preclinical models demonstrating their superior improvement of the healing process.<sup>309</sup> Microscopic examination revealed that early-stage healing in the group treated with these fibers was faster than those obtained for the control group. Also silk fibroin nanomatrices have demonstrated to accelerate re-epithelialization and wound closure in burns<sup>310</sup> and collagen/chitosan composite membranes have promoted wound healing and induced cell migration and proliferation.<sup>311</sup> In this sense, amoxicillin grafted onto regenerated bacterial cellulose sponges<sup>312</sup> and hyaluronan/silver nanocomposites<sup>313</sup> were also able to stimulate wound healing and reduce inflammation in different murine *in vivo* wound models.

However, the biodegradation rate and the relatively low mechanical strength displayed by natural polymers restrict their application as wound dressings despite of their reduced immune response and associated toxicity.<sup>314</sup> For example, edible films developed from fruit and vegetable residue flour were reported to have a maximum tensile strength as low as 0.084 MPa.<sup>315</sup> Polyvinyl acetate/chitosan/starch patches degradation in the first 7 days is reported to be in the range 15-30%.<sup>316</sup> Among the synthetic polymers, fibrous polyurethane membranes

were evaluated as wound dressings and found to show oxygen permeability, controlled water evaporation while promoting fluid drainage.<sup>317</sup> Other synthetic polymers have been used to produce electrospun wound dressings, among them poly(lactic acid-co-glycolic acid) was found to produce patches with appropriate mechanical strength (tensile modulus from  $39.23 \pm 8.15$  to  $79.21 \pm 13.71$  MPa) and porosity (38 to 60 %).<sup>318</sup> PCL, a hydrophobic polyester polymer, has been widely used to prepare electrospun wound dressings because of its biodegradability, biocompatibility, chemical and thermal stability and good mechanical properties.<sup>319</sup> Furthermore, multicoated electrospun PCL/gelatin/nanosilver membranes have been recently shown as efficient antibacterial dressings *in vivo* by protecting wounds and promoting healing.<sup>320</sup> Since bacterial infection is the most serious complication which might affect the wound healing process and can lead to impaired wound healing and increased morbidity and mortality,<sup>321</sup> it is necessary to add antimicrobial agents to the wound dressing materials. However, it is also necessary to demonstrate that those advanced dressings are more effective than simple conventional dressings in clinical settings for the treatment of infected wounds. The electrospinning process allows the production in one step of drug loaded patches with the ability of providing a sustained release in the management of wound-associated infections.

The evolution of antimicrobial resistant pathogens that are refractory to the antibiotics of last resort represents a global public health challenge.<sup>322</sup> Wound dressings containing natural products with long-term antimicrobial activity are considered as potential alternatives as cost-effective materials in combating antimicrobial resistance.<sup>323</sup> In the last years, an increased number of publications on electrospun patches loaded with essential oils has been reported.<sup>324</sup> A considerable number of these studies used pure bioactive compounds obtained from essential oils such as carvacrol and thymol (THY).<sup>325–329</sup>

Wound in mice infected with *S. aureus*, were also treated with poly(lactic-co-glycolic acid)/chitosan nanofiber wound dressings.<sup>330</sup> Dressings containing hydroxypropyltrimethyl ammonium chloride were able to reduce the wound sizes by 21.8 % after 3 days and by 100 % after 15 days. Electrospun curcumin-loaded PCL-polyethylene glycol fibers have shown an efficiency on *S. aureus* inhibition of 95 % after 12 h treatment having also anti-inflammatory effects *in vitro*.<sup>189</sup>

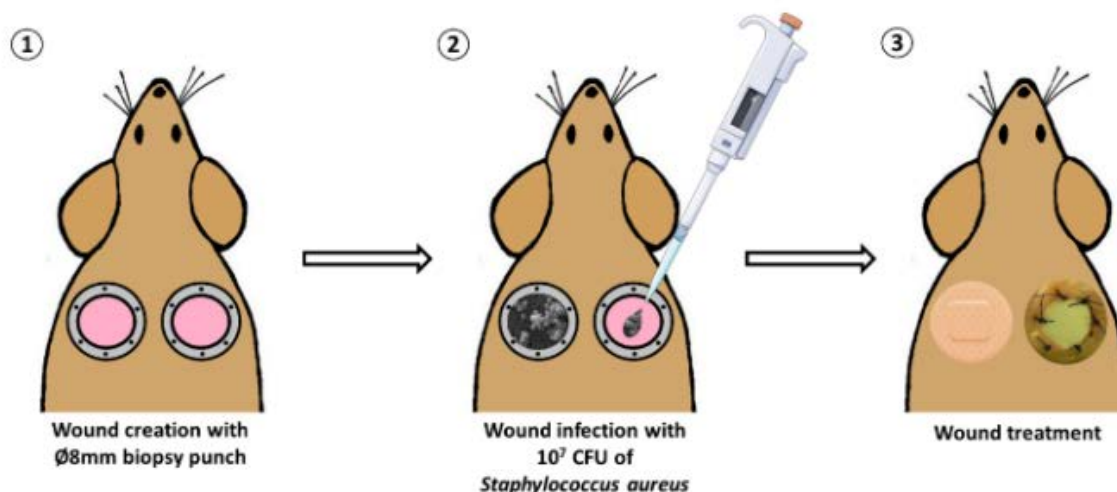
## V.2. Objective

Previous chapters demonstrated the antimicrobial and anti-inflammatory potential of THY loaded into electrospun PCL nanofibers using *in vitro* models. This chapter analyzes the *in vivo* efficacy of the THY loaded PCL nanostructured fibrous patches in a full-thickness excision wound model in eight to ten-week-old male SKH1 hairless mice. Wounds were infected using a *S. aureus* (ATCC 25923) strain and the infection progression was measured at 1,2,3 and 7 days post-infection (dpi). In addition, histopathological and immunohistochemical studies were carried out in post-mortem wounds. Herein it was evaluated the bactericidal efficiency of the prepared patches (PCL-THY group) in an *in vivo* model of infected wounds and compared to unloaded fibers (PCL group), free thymol (THY group) and free chlorhexidine (CLXD group) as disinfectant and antiseptic model widely used on the skin. Also, fibers morphology was analyzed by SEM, whereas THY loading and release from fibers were also studied to determine the appropriate amount of patches to be applied on wounds. Mechanical properties of THY loaded PCL nanofibers were studied in order to confirm the potential applicability of the material as wound dressing.

## V.3. Experimental

PCL-THY patches were synthesized by electrospinning technique and characterized by morphology, THY loading and release. Empty and THY-loaded PCL nanofibers were visualized by SEM, meanwhile drug loading and release were determined by GC-MS and UPLC liquid chromatography, respectively. To better compare with skin properties, it was studied the strength and elasticity of PCL and PCL-THY dressings.

To study the effect of PCL-THY dressings in an *in vivo* model of infected wounds, eight to ten-week-old male SKH1 hairless mice were used. The schematic procedure of the *in vivo* model is represented in Scheme V.1:



Scheme V.I: Schematic representation of the *in vivo* wound model: 1) Splinting wounds were surgically performed with a 8-mm-diameter biopsy punch and the splinting ring sutured around the wound; 2) Induction of the infection was achieved by the inoculation of *Staphylococcus aureus* ( $10^7$  colony forming units (CFU)); 3) Wound treatment was carried out by adding the different synthesized patches and covering the wounds.

The infection progression was analyzed in wounds at 1, 2, 3 and 7 dpi through a semi-quantitative analysis of microbiological cultures and quantitative polymerase chain reaction (qPCR). Euthanasia was carried out by CO<sub>2</sub> inhalation after 3 and 7 dpi. At these time points, histological samples were collected and Gram stain was carried out for bacteria determination in the tissues. Moreover, tissue sections were stained with hematoxylin and eosin (HE) for histopathological analysis and an immunohistochemical evaluation was performed by using rabbit polyclonal CD31 antibody to further assess wound angiogenesis.

The characterization techniques, and the analyses of infection, inflammation and regeneration are described in Appendix I.

## V.4. Results and discussion

### V.4.1. Electrospun PCL nanofibers characterization

The morphology of PCL and PCL-THY nanofibers was characterized by SEM (Figure V.1). The mean diameter of unloaded fibers ( $266 \pm 73$  nm) showed no significant changes when THY was incorporated to the spinning solution ( $299 \pm 71$  nm).



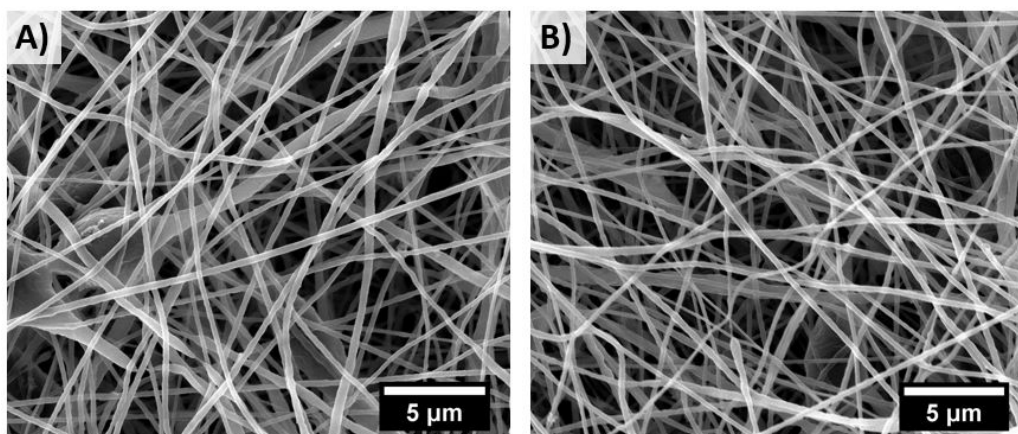


Figure V.1: SEM images of A) PCL nanofibers and B) PCL-THY nanofibers used for mice wound treatment.

Electrospun nanofibers can act as drug delivery systems that exhibit sustained drug release profiles, leading to a potential reduction in the frequency of the treatments when topical applications are envisaged. Besides, it is known that the electrospinning technique allows high loading capacities.<sup>331</sup> A THY load of  $14.92 \pm 1.31$  % w/w was achieved by incorporation of the THY to the electrospinning solution, which corresponds to an encapsulation efficiency of 74.62%, similar to previously reported papers with EOs encapsulated in PCL electrospun fibers.<sup>190,247</sup>

The *in vitro* release of THY from the PCL nanofibers shows an initial burst release observed in the first minutes. It may be related to the EO compound present on the external surface of the fibers.<sup>332</sup> This initial release was followed by a controlled release over 8 h and only 8.81 % of the loaded THY was released during this time.<sup>333</sup> Drug release from nanofibers could be caused by its desorption from the fibers surface, diffusion from the pores or matrix degradation.<sup>334</sup> The observed burst release would be attributed to the desorption from the surface.

#### V.4.2. Mechanical properties of PCL-THY patches

Since the wound dressing materials being wrapped on the wound area are likely to be subjected to pulling forces in order to adhere the patch smoothly and effectively to the skin, they are expected to have similar mechanical strength and elasticity than normal human skin. Tensile strength of human skin is in the range 2-16 MPa and its elongation-at-break in the 70-77 %

range.<sup>335</sup> One of the significant features of PCL for biomedical application is its high elongation-at-break,<sup>336</sup> in our case, the measured value of  $108.6 \pm 11.3$  % is much higher than the one of the human skin. The tensile strength retrieved of  $5.1 \pm 0.5$  MPa would be also in the required range for wound dressing applications. This value decreased to  $3.0 \pm 0.5$  MPa with the addition of THY, but it is still in the appropriate applicability range. Similar results were obtained from the elongation-at-break of THY loaded PCL fibers, the value was reduced to  $74.4 \pm 9.5$  %. It is known that the mechanical properties of pure polymers can be varied by incorporating bioactive compounds. PCL molecular chains are likely to be more uneven and disordered due to the presence of THY, resulting in reduced mechanical properties.<sup>337</sup> However, the mechanical properties of the THY loaded PCL mats here reported are mechanically appropriate for wound dressing applications.

#### V.4.3. *In vivo* bactericidal activity

Both, acute and chronic infections are severe complications worldwide that delay and complicate wound healing. If the host defense is not capable of overcoming the bacterial burden, an infection takes place, causing delayed wound healing, inflammation and tissue damage.<sup>338</sup> Since extensive abuse of antibiotics in wound care has led to new pathogens occurrence and the prevalence of multi-resistant bacteria, the use of natural components as antimicrobial and antiseptic agents is steadily growing.

*In vivo* wound infection model in SKH1 mice and treatment with the electrospun patches (PCL and PCL-THY groups), free THY and an antiseptic model CLXD was developed as Scheme V.1 indicates. Twelve mm-diameter disks were evaluated with the necessary weight to reach the minimum bactericidal concentration (MBC) value found previously by the group in *in vitro* assays on *S. aureus* (ATCC 25923) (30 mg of patch containing 4.48 mg of THY).<sup>247</sup>

None of the animals presented changes in behavior or showed any signs of physical discomfort, but a purulent secretion was observed in the PCL group as can be seen in the visual evolution photographically recorded at 7 dpi (Figure V.2.A). Microbiological swab analysis results are shown as insets in Figure V.1.A. Animals treated with unloaded fibers (PCL group) presented massive bacterial growth at any time analyzed. After one day post-surgery and infection, the application of a single dose of CLXD seemed to be the most effective treatment since no growth was observed from the collected swabs while mild bacterial growth was detected in wounds treated in PCL-THY group. On the other hand, free THY was less effective

and a moderate bacterial growth was observed. After 2 days, results were similar except for the CLXD group that showed the presence of a mild bacterial growth. In the third day a decrease in the media of colonies counted was observed for the THY group. After this time, no treatment was applied to the wounds and, as a consequence, massive bacterial growth was observed in the THY group. PCL-THY and CLXD groups showed a moderate bacterial growth; however, no massive growth was found. These high loadings, even observed for the commonly used commercially available CLXD used at the clinical concentration available, may be attributed to the enormous bacterial challenge that was used ( $4 \times 10^8$  CFU/mL).

Quantitative PCR analyses of post-mortem skin samples (Figure V.2.b) indicated that, after three days of treatment, PCL-THY and CLXD groups showed at least two log-reduction in the number of *S. aureus* (ATCC 25923) strain copies. These results would indicate that THY loaded PCL fibers act as inhibitors of this bacterial strain growth being as efficient as the model antiseptic used CLXD. However, our previous studies showed the *in vitro* detrimental effects of CLXD treatment in different human cell cultures, resulting in cell viability percentages lower than 70 % at the lowest concentration tested (4  $\mu$ g/mL) which were dramatically decreased to 20 % from 15  $\mu$ g/mL. On the other hand, THY treatment did not show cytotoxic effects (viability  $\geq$  70 %) in these cell lines up to concentrations higher than 60  $\mu$ g/mL. These results point to the more cytocompatible nature of THY compared to CLXD.

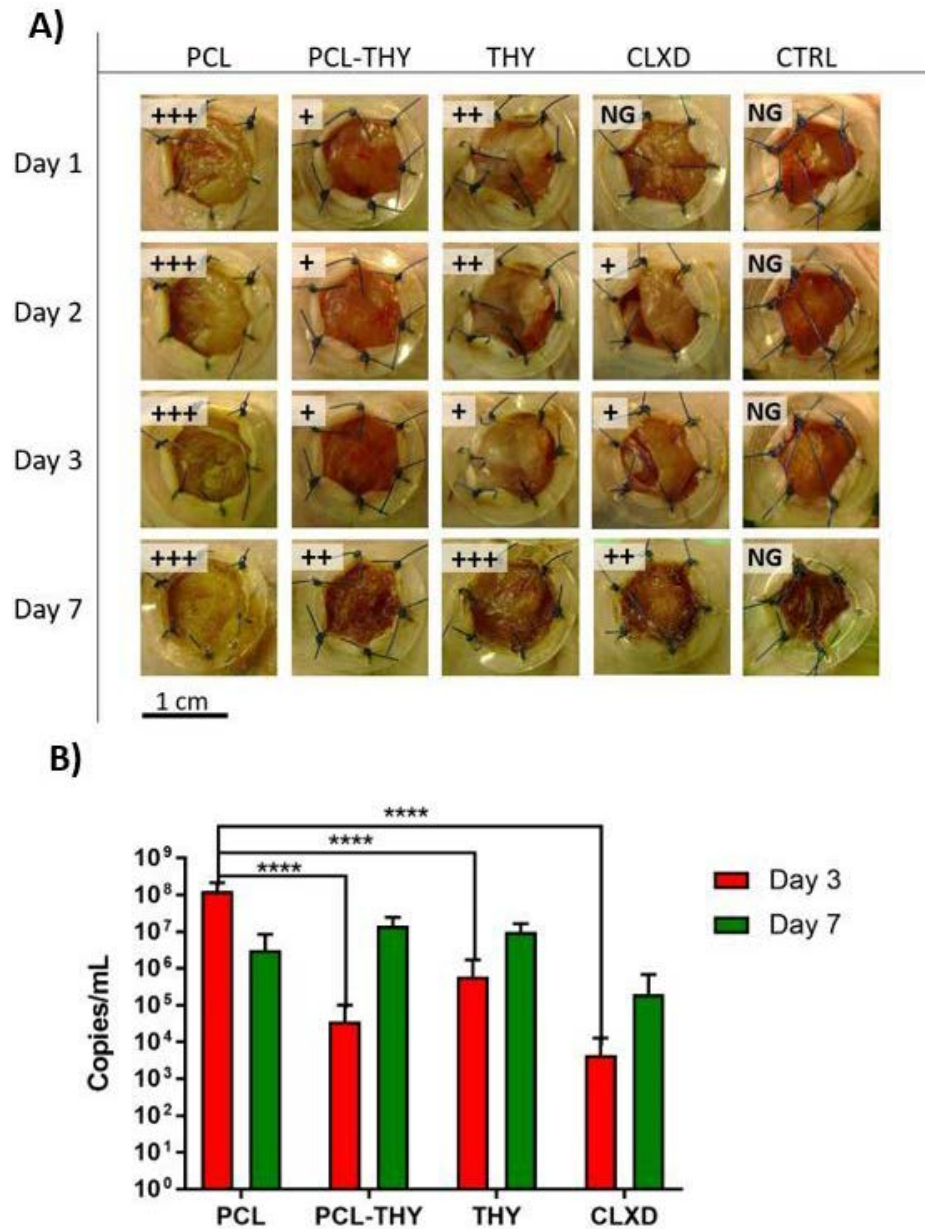


**Figure V.2:** *In vivo* wound infection model in SKH1 mice and treatment with the electrospun patches (PCL and PCL-THY groups), free THY and the model antiseptic CLXD: A) Wounds evolution at 1, 2, 3 and 7 dpi with *S. aureus* (ATCC 25923). Microbiological results in experimental and control groups are showed as insets. NG No growth; (+) Mild bacterial growth; (++) Moderate bacterial growth; (+++) Massive bacterial growth. Scale bar is the same for all wounds in the figure. B) Microbiological qPCR results in experimental and control groups. Statistics compares PCL-THY, THY and CLXD groups with PCL group. \*\*\*\* refers to p value < 0.0001.

#### V.4.4. Histopathological and immunohistochemical studies

Histopathological and immunohistochemical studies of treated wounds were carried out to evaluate the effects of PCL-THY patches related to infection, angiogenesis, and tissue regeneration (Figures V.3-5). The most important lesions were observed for the PCL group (Figure V.3.A), consisted on severe diffuse necrotizing dermatitis in the wound area that was characterized by massive infiltrations of inflammatory cells (lymphocytes and macrophages) together with severe tissue necrosis around muscle fibers. Inflammatory reaction affected all layers of the skin, reaching the adipose tissue (panniculitis). Throughout the skin layers but mostly on the surface, abundant colonies of coccoid bacteria were observed, pointed with arrows in Figure V.3.A. The PCL-THY group showed wounds that were almost free of inflammation reaction, with only a few layers of coagulative necrosis on the surface of the exposed area of the wounds (Figure V.3.B). The THY group showed a less intense, multifocal inflammatory reaction in the panniculus when compared to the inflammation caused in the PCL group (Figure V.3.C). Finally, the CLXD group also showed absence of inflammatory reaction but a much thicker layer of coagulative necrosis on the exposed surface of the wound (Figure V.3.D), which agrees with the *in vitro* detrimental findings previously reported in Chapter II.

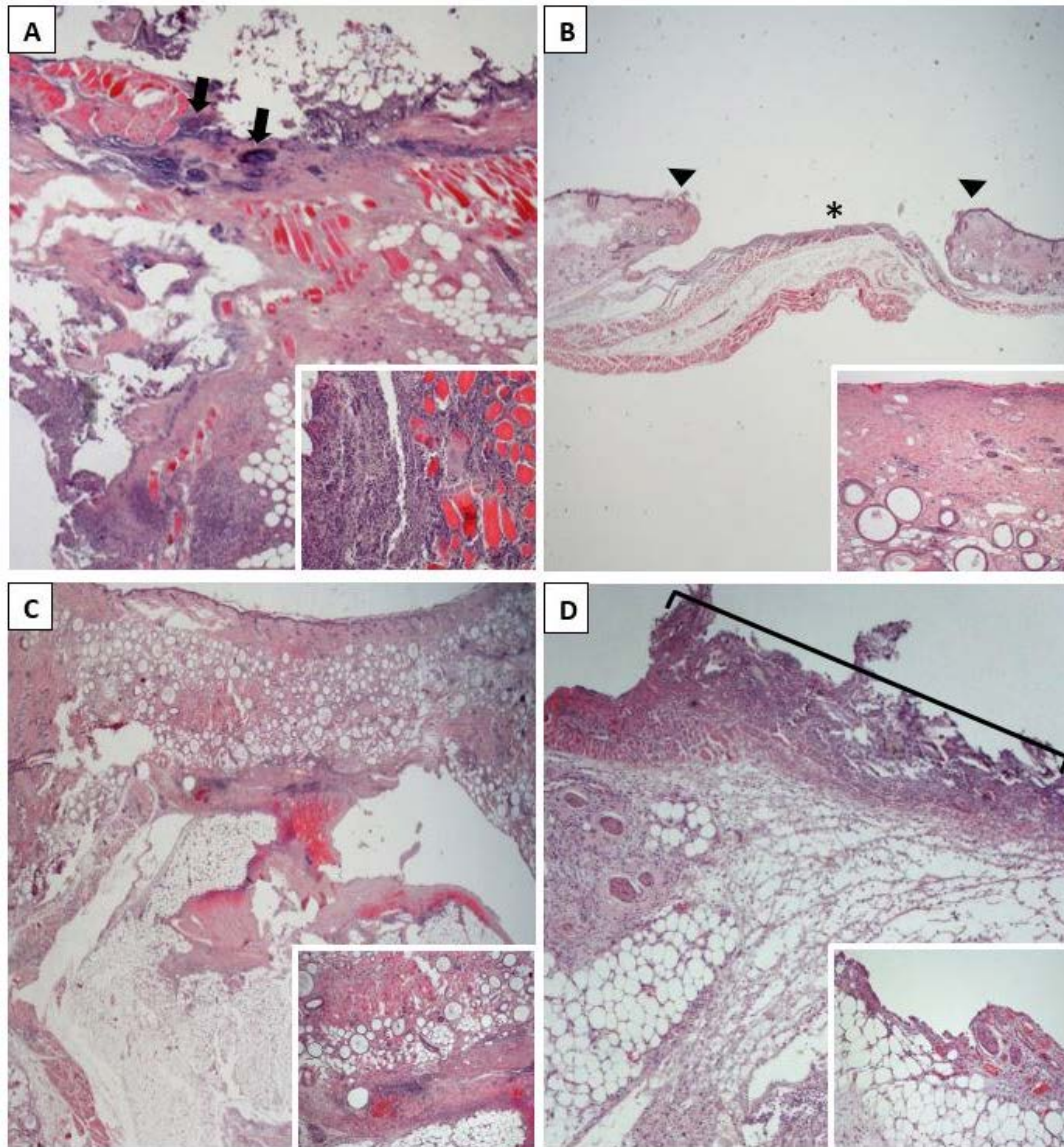


**Figure V.3:** Histological analysis of skin wounds, representative images at 3 dpi. A) PCL group. Clusters of coccoid bacteria are observed in the superficial layers (arrows). Inset: Detail of the inflammatory reaction, with numerous lymphocytes and macrophages around muscle fibers; B) PCL-THY group. Sagittal section of the wound and wound edges (arrowhead). Exposed dermis is pointed with asterisk. Inset: Absence of inflammation in another area of the dermis in the same animal; C) THY group. Focal, less severe inflammatory reaction in the panniculus. Inset: Detail of the deep inflammatory reaction; D) CLXD group. Absence of inflammation in the dermis. Exposed dermal surface presents an important superficial layer of coagulative necrosis (square bracket). Inset: Detail of another area of the same animal, showing lack of inflammation. Hematoxylin-eosin staining, 1x, insets at 20x.

Regarding bacteria presence, samples were analyzed using Gram stain. Coccoid bacteria were only observed in sections of the PCL and THY groups (Figure V.4). Figure V.4.A shows a massive growth of coccoid bacteria in clusters in superficial layers of the skin together with severe tissue necrosis in PCL samples. Figure V.4.B shows growth of coccoid bacteria within a hair follicle in THY samples. PCL-THY and CLXD groups are not represented due to the lack of bacteria.

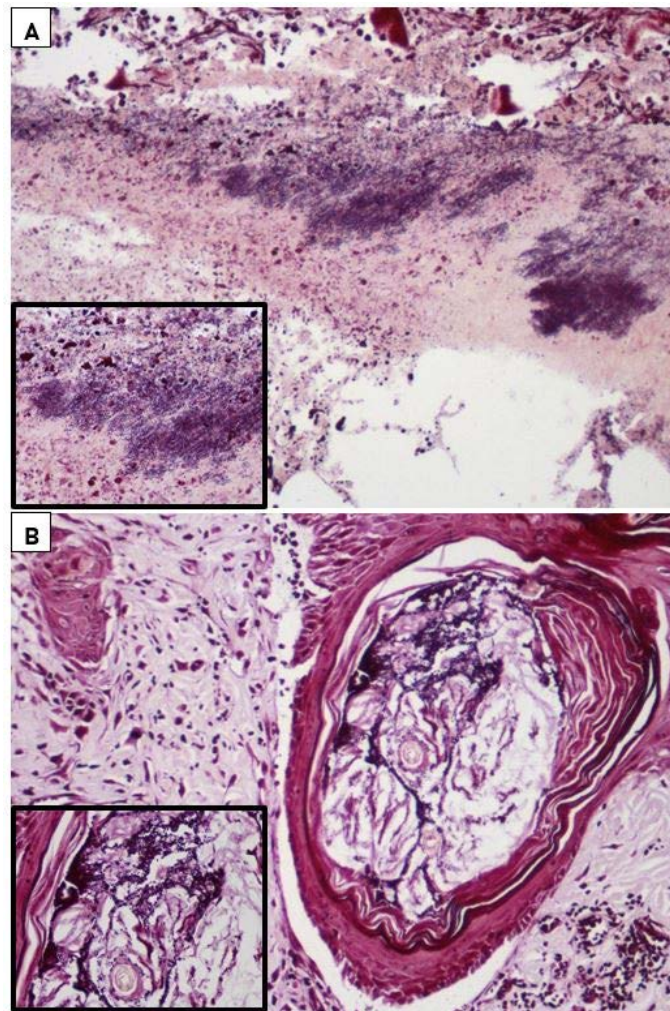


**Figure V.4:** Detection of bacteria in skin wounds. Representative images of PCL and THY groups after 3 dpi. PCL-THY and CLXD groups are not represented due to the lack of bacteria. A) PCL group. Massive growth of coccoid bacteria in clusters in superficial layers of the skin together with severe tissue necrosis. Inset: Detail of the bacteria in the same animal. B) THY group. Growth of coccoid bacteria within a hair follicle. Inset: Detail of the bacteria. Gram staining, 20x, insets at 60x.

Finally, the semi-quantitative analysis of angiogenesis performed with rabbit polyclonal CD31 antibody showed a homogeneous increase in the number of blood vessels at 7 dpi compared with samples at 3 dpi, similar for all infected groups (Figure V.5).

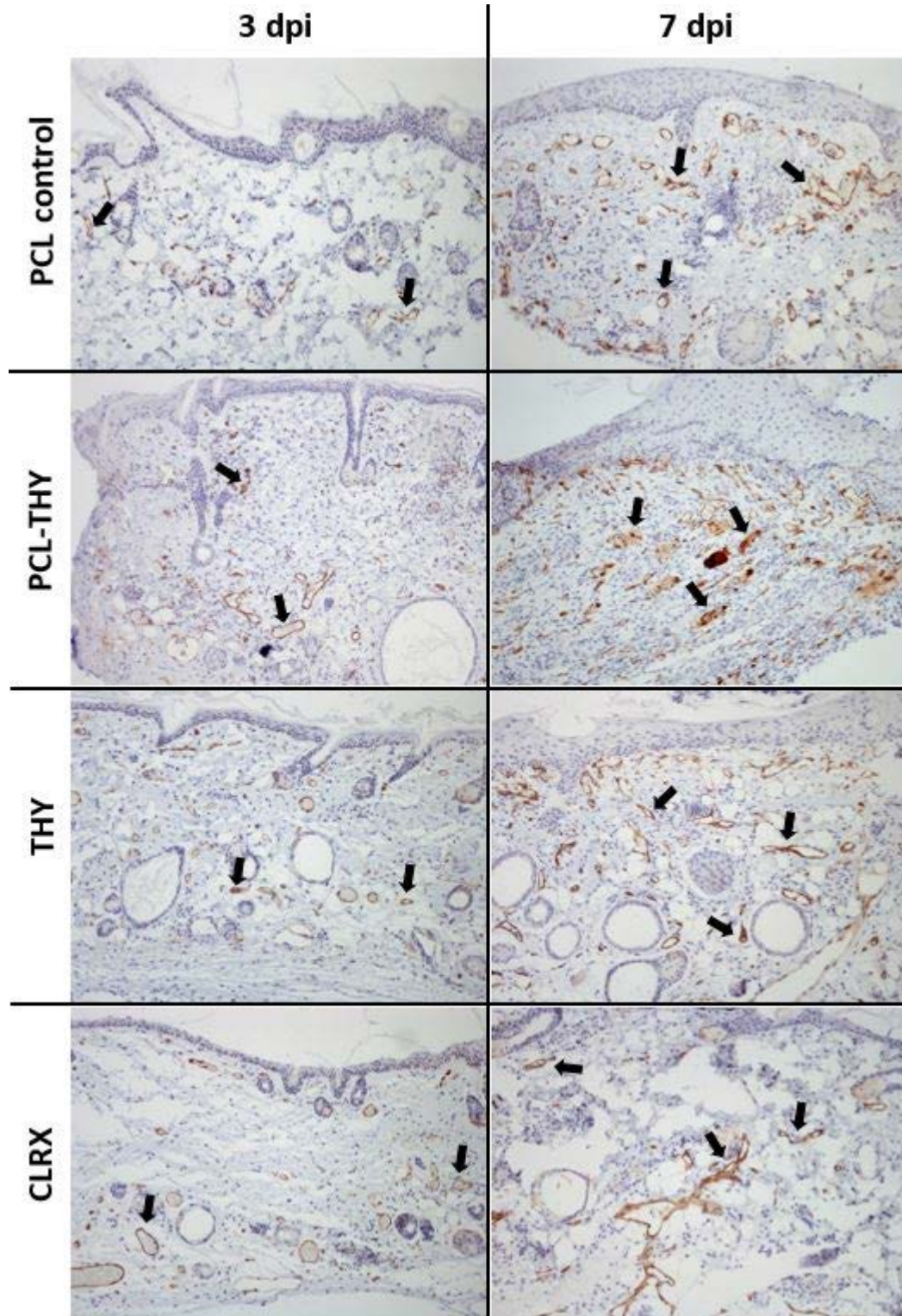




Figure V.5: Location of blood vessels in skin wound samples, representative images at 3 and 7 dpi. All groups showed an increased number of blood vessels at 7 dpi compared with samples at 3 dpi. Immunohistochemistry for CD31, 20x.

A large amount of reports and experimental evidence sustain the beneficial properties of essential oil compounds on promoting wound healing.<sup>339</sup> For example, electrospun patches based on PCL, PLA, and 50/50 hybrid composites were loaded with THY and their effects evaluated in an *in vivo* rat wound model by Karami *et al.*<sup>340</sup> Their findings pointed to a significant better performance of the PLA/PCL hybrid membranes loading THY at the end of the experiments (14 days of treatment) regarding granulation tissue formation and re-epithelialization compared to commercial dressings and gauze bandages. In this sense, THY enriched collagen hydrogels<sup>341</sup> and bacterial cellulose hydrogels<sup>102</sup> were previously reported as novel and efficient composite dressing mats in the *in vivo* healing of different rat models. Collagen-based films loading THY (1.2 mg of THY per dressing) clearly reduced inflammation and enhanced regeneration in surgical 8-mm wounds in a rat model after 7 days of treatment, highlighting the presence of mature granulation tissue due to the presence of well-formed and dilated vessels.<sup>341</sup> On the other hand, the *in vivo* effects of THY loaded bacterial cellulose hydrogels as dressings in a burn wound model also showed a decreased inflammatory reaction in the groups treated with the hydrogels loading THY compared to control groups after treatment for 15 days.<sup>102</sup> Both studies pointed to the potential stimulation of skin regeneration through the formation of granulation tissue due to the proliferative effects of THY in fibroblast and enhanced collagen deposition.

Adicionally, some studies confirm the benefits of nanostructured materials compared with commercially available wound dressings. For example, the antimicrobial peptide Tet213 immobilized onto a substrate of alginate, hyaluronic acid and collagen nanostructured composite presents a better wound closure rate when compared with commercial Aquacel Ag wound dressing after 7 days since wound infection. Also, bacterial presence in wound was lower when treated with this composite material when compared with Aquacel Ag-treated wounds after 3 days.<sup>342</sup> Another study shows the potential use of electrospun nanofibers based on honey, polyvinyl alcohol and chitosan, enriched with the aqueous extracts of *Cleome droserifolia* and *Allium sativum* as antimicrobial wound dressings. Results show a superior *in vitro* antibacterial activity against *S. aureus* of the synthesized nanofibers compared with commercial Aquacel Ag.

This study also shows a faster wound closure when using the synthesized nanofibers compared to the timing needed to reach closure with Aquacel Ag treated on infected wounds.<sup>343</sup>

### V.5. Conclusion

Tensile strength and elongation at break of PCL-THY patches make them appropriate for wound dressing applications. *In vivo* tests to evaluate the antimicrobial action of the patches showed that animals treated with unloaded fibers presented massive growth at any time analyzed. On the contrary, one day post-surgery and infection, few colonies were detected in wounds treated with THY loaded patches while a high number of colonies appeared in wounds treated with free THY, showing the importance of drug encapsulation and the need of contact between bacteria and the patch to generate a superior antimicrobial action. After treatment discontinuation, massive bacterial growth was observed in the THY group while for PCL-THY and CLXD treated wound no massive growths were found.

Histopathological and immunohistochemical studies of wounds showed severe diffuse necrotizing dermatitis in the wound area that was characterized by massive infiltrations of inflammatory cells and severe tissue necrosis in the PCL treated wounds. In addition, massive growths of coccoid bacteria were observed in these tissues. The PCL-THY treated wounds were almost free of inflammatory reaction, with only a few layers of coagulative necrosis on the surface of the exposed area of the wounds. In comparison, CLXD treated wounds showed a much thicker layer of coagulative necrosis in the exposed surface of the wound. These results show that PCL-THY mats are able to control bacterial infection as efficiently as the model antiseptic CLXD though significantly diminishing tissue damage, highlighting their potential biomedical application.

## Chapter VI

### GENERAL CONCLUSIONS

## VI. General conclusions

The main goal of the thesis was to design a bioactive dressing loading natural compounds with anti-inflammatory and antimicrobial properties for wound healing treatment. Considering this scenario, the most relevant conclusions obtained during this thesis are summarized:

- Among the natural compounds studied, CAR, CIN and THY showed the highest *in vitro* bactericidal properties against a Gram-positive model, *S. aureus* and a Gram-negative model, *E. coli*. According to SEM images, flow cytometry and confocal microscopy, plant-derived natural compounds exhibited antimicrobial activities associated with membrane disruption. In addition, THY demonstrated to be one of the most efficient compounds by the elimination of bacterial growth using low concentrations. CAR, CIN and THY also demonstrated their antimicrobial activity by inhibiting bacterial growth in preformed biofilms and during biofilm formation. When these compounds are combined, only CAR and THY showed an additive effect, while CIN had no interaction with the other compounds. Likewise, no antagonism between compounds has been found.
- Thymol and carvacrol, not only showed antimicrobial activity, but also demonstrated lower cytotoxicity (0.06 mg/mL) than chlorhexidine (< 0.004 mg/mL) in an *in vitro* metabolic assay in cell lines related to wound healing (fibroblasts, keratinocytes and macrophages). That fact provides an advantage to EOs in comparison with a compound used in the clinical practice.
- THY-loaded PCL patches demonstrated to reduce cGFP-expressing *S. aureus* growth in an *in vitro* counting assay. Moreover, confocal images demonstrated that the higher concentration of THY, the lower bacterial adhesion to surfaces and thus, the lower biofilm formation observed. PCL-THY patches showed cytotoxicity against J774 macrophages in a dose dependent manner, but at reduced doses and during short contact times, cell viability was similar to untreated controls. The antimicrobial activity of designed dressings was also observed inhibiting bacterial growth in an *in vitro* infective model of J774 macrophages with cGFP-expressing *S. aureus*. Thus, the developed patches were efficient reducing bacteria levels comparing to non-loaded PCL patches.
- Among the studied free natural compounds, CIN, B-CAR and CUR showed high cytotoxicity against J774 murine macrophages *in vitro*, meanwhile CAR, THY, SQU and TYR demonstrated higher cell viability. Among them, CAR, THY and TYR reduced the

expression of pro-inflammatory cytokines (Il-1b and iNos) to DEX control levels in an *in vitro* inflammatory model based on LPS-activated J774 murine macrophages. When these compounds were encapsulated into PCL patches, PCL-CAR demonstrated a high cytotoxicity against J774 macrophages. However, PCL-THY pointed to be the most successful inhibiting the expression of the pro-inflammatory molecules, and the combination between THY and TYR or THY and SQU did not reduce the expression of Il1b and iNos in an efficient way. By an immunofluorescence assay, PCL-THY reduced cell size to levels similar to DEX treated cells, a clinical anti-inflammatory drug, demonstrating its anti-inflammatory potential. Moreover, J774 macrophages remained attached to the well and do not migrate into PCL-patches, highlighting their potential as wound dressings.

- PCL-THY patches demonstrated to reduce bacterial growth *in vivo* in infected wounds in SKH1 mice. The results obtained in the evaluation of infection in wounds treated with PCL-THY are comparable to those obtained after chlorhexidine treatment, highlighting the antimicrobial potential of the designed patches. In addition, when PCL-THY treated wounds are compared with those treated with free THY, a lower bacteria concentration was obtained when patches are used, which demonstrates the advantage in the encapsulation of THY. When tissue samples are stained with Gram stain, bacteria can be only observed in PCL and free THY treated samples.
- Regarding histopathological studies, free chlorhexidine treated wounds showed an important superficial layer of coagulative necrosis, which it is not observed when wounds are treated with PCL-THY. Immunohistochemical analysis of tissue sections with CD31 polyclonal antibody showed an increase in the number of blood vessels at 7 dpi, that was similar for all infected groups.

The present thesis demonstrates that THY loaded PCL nanofibers hold great promise for wound healing, due to the ability to control two essential mechanisms in wound repair: fighting infections and mitigating inflammation.



## Chapter VI

### CONCLUSIONES GENERALES

## VI. Conclusiones generales

El objetivo principal de la tesis doctoral se centra en el diseño de un apósito bioactivo con capacidad de liberar compuestos naturales que poseen propiedades anti-inflamatorias y antimicrobianas esenciales para el tratamiento de heridas. Con este objetivo, se han obtenido unos resultados que nos permiten exponer las siguientes conclusiones:

- Los compuestos naturales derivados de plantas contienen propiedades antimicrobianas relacionadas con daño en la membrana celular. Entre los estudiados, CAR, CIN y THY, mostraron mayor capacidad bactericida cuando se ponen en contacto con una cepa Gram-positiva como *S. aureus* y una Gram-negativa como *E. coli*. Además, el timol demostró controlar el crecimiento bacteriano a menores concentraciones que el resto de los compuestos. CAR, CIN y THY demostraron su poder antimicrobiano inhibiendo el crecimiento bacteriano tanto en biofilms formados, como en el propio proceso de formación. Cuando estos compuestos se combinaron entre sí, solamente CAR y THY mostraron un efecto aditivo, mientras que el CIN no mostró interacción con ningún otro compuesto. Del mismo modo, no se ha encontrado antagonismo entre los diferentes compuestos.
- El THY y CAR además de mostrar actividad antimicrobiana, demostraron ser menos citotóxicos (0.06 mg/mL) que la clorhexidina (<0.004 mg/mL) en un modelo de viabilidad *in vitro* en fibroblastos, queratinocitos y macrófagos. Este hecho proporciona cierta ventaja a los aceites naturales en comparación con un producto utilizado actualmente para desinfectar heridas.
- Los apósitos de PCL-THY inhibieron el crecimiento de la cepa *S. aureus* con expresión de cGFP en un ensayo cuantitativo *in vitro*. Además, las imágenes de microscopía confocal demostraron que cuanto mayor es la concentración de THY, menor es la adhesión bacteriana a superficies y con ello, menor es la formación de biofilm. Los apósitos de PCL-THY mostraron cierta citotoxicidad en macrófagos J774 de forma dosis-dependiente. En cambio, concentraciones menores de THY en contacto con las células durante tiempos cortos, aumentaron la viabilidad celular hasta niveles del control. La actividad antimicrobiana de los apósitos diseñados fue demostrada inhibiendo el crecimiento bacteriano en un modelo de infección *in vitro* de macrófagos J774 con una cepa de *S. aureus* que expresa cGFP. Todo esto demuestra que los apósitos



de PCL-THY reducen de forma eficiente la carga bacteriana en comparación con los apósitos de PCL.

- Entre los compuestos estudiados, el CIN, B-CAR and CUR mostraron una alta citotoxicidad en macrófagos murinos J774, mientras que el CAR, THY, SQU y TYR mostraron una viabilidad celular mayor. Entre estos, CAR, THY y TYR tienen la capacidad de reducir la expresión de citoquinas pro-inflamatorias (Il1b y iNos) hasta niveles del control de DEX en un modelo inflamatorio *in vitro* basado en macrófagos J774 activados con LPS. Cuando estos compuestos son encapsulados en membranas de PCL, el apósito de PCL-CAR demostró una alta citotoxicidad en J774. En cambio, el PCL-THY fue el apósito que mejor inhibió la expresión de moléculas pro-inflamatorias, y la combinación entre el THY con SQU o TYR no redujeron la expresión de Il1b o iNos de forma eficiente. A través de un ensayo de inmunofluorescencia, el PCL-THY redujo el tamaño celular a niveles de las células tratadas con DEX, un compuesto anti-inflamatorio utilizado en la clínica. Esto demostró el potencial anti-inflamatorio de los apósitos diseñados. En un ensayo de migración los apósitos de PCL o PCL-THY no favorecen la migración celular hacia los mismos, destacando su posible aplicación como apósitos de heridas.
- Los apósitos de PCL-THY reducen el crecimiento bacteriano en un modelo *in vivo* de herida infectada en ratones SKH1 de una forma similar a la que lo hacen las heridas tratadas con clorhexidina. Además, cuando el tratamiento de PCL-THY se compara con el tratamiento con THY libre, se observa una disminución de la carga bacteriana cuando se utilizan los apósitos, remarcando la ventaja de encapsular el compuesto para conseguir una liberación sostenida en el tiempo. Cuando las muestras histológicas se tiñen con la tinción Gram, solamente se observaron bacterias en las muestras tratadas con PCL y con THY libre.
- Con relación a los estudios histopatológicos, las heridas tratadas con clorhexidina mostraron una necrosis coagulativa en capas superficiales de la herida en muestras histológicas, hecho que no se observó en las heridas tratadas con PCL-THY. Las muestras analizadas con un anticuerpo policlonal CD31 demostraron un aumento del número de vasos a los 7 dpi en comparación con 3dpi. En cambio, no hubo diferencias entre los grupos de tratamiento.

La tesis doctoral demuestra que los apósitos de PCL-THY son prometedores para el tratamiento de heridas dada su habilidad para controlar la infección bacteriana y la inflamación tisular.

# Appendix I

## MATERIALS AND METHODS

## Table of contents

<b>AI.1. Materials</b>	<b>122</b>
<b>AI.2. Synthesis of loaded PCL nanofibers</b>	<b>123</b>
AI.2.1. Solutions preparation and characterization	123
AI.2.2. Electrospinning process	124
<b>AI.3. Characterization of electrospun nanofibers</b>	<b>124</b>
AI.3.1. Morphology	124
AI.3.2. Water uptake	125
AI.3.3. Patches porosity	125
AI.3.4. Mechanical properties	125
AI.3.5. Essential oils loading and encapsulation efficiency	125
AI.3.6. Release of natural compounds	126
<b>AI.4. Antimicrobial activity</b>	<b>126</b>
AI.4.1. Bacteria culture	126
AI.4.2. Preparation of essential oils	127
AI.4.3. MIC and MBC determination	127
AI.4.4. Bacteria morphology	128
AI.4.5. Bactericidal mechanism	128
AI.4.6. Confocal microscopy	128
AI.4.7. Synergy studies	129
AI.4.8. Biofilm formation and characterization	129
AI.4.9. Antibiofilm activity measurement	130
<b>AI.5. Cell assays</b>	<b>131</b>
AI.5.1. Cytotoxicity metabolism assays	131
AI.5.2. Flow cytotoxicity for apoptosis detection	133
AI.5.3. <i>In vitro</i> model infection of J774 macrophages	133
<b>AI.6. Cell assays</b>	<b>134</b>
AI.6.1. <i>In vitro</i> inflammation	134
AI 6.2. Gene expression analysis	135
AI.6.3. Cell colonization model	135
AI.6.4. Immunofluorescence assay	136
<b>AI.7. <i>In vivo</i> experiments</b>	<b>136</b>
AI.7.1. Mouse excisional wound splinting model infection	136
AI 7.2. Evaluation of infection wounds	138
AI.7.3. Histological studies	138
<b>AI.8. Statistical analysis</b>	<b>139</b>

### AI.1. Materials

Carvacrol (CAR; food grade,  $\geq 98\%$ ), cinnamaldehyde (CIN;  $> 98\%$ ), thymol (THY;  $99\%$ ), squalene (SQU;  $\geq 98\%$ ), tyrosol (TYR;  $98\%$ ), rosmarinic acid,  $\beta$ -caryophyllene (B-CAR;  $> 98\%$ ), curcumin (CUR), Tween® 80, polycaprolactone (PCL;  $M_n = 80,000$  Da), (*S*)- (-)-limonene (food grade,  $\geq 95\%$ ), naproxen sodium salt ( $98\text{--}102\%$ ) and phosphate buffered saline (PBS) were purchased from Sigma-Aldrich (MO, USA). Eugenol (EUG) was supplied by Acros Organics (Geel, Belgium). Dichloromethane (DCM,  $> 99\%$ ) and *N,N*-dimethylformamide (DMF,  $>99\%$ ) were purchased from Fisher Scientific (Hampton, USA). Acetonitrile ( $\geq 99.9\%$ ), acetone (HPLC grade) and formic acid ( $98\text{--}100\%$ ) were purchased from VWR (Oud-Heverlee, Belgium). Dimethyl sulfoxide (DMSO) was purchased from Merck Millipore (Darmstadt, Germany).

*Escherichia coli* (*E. coli*) S17 was kindly gifted by Dr. J. A. Aínsa (Department of Microbiology, Preventive Medicine, and Public Health, University of Zaragoza, Spain). *Staphylococcus aureus* (*S. aureus*; ATCC 25923) was purchased from Ielab (Alicante, Spain), the methicillin sensitive *S. aureus* Newman strain expressing the coral green fluorescent protein (cGFP) from the vector pCN47 was kindly donated by Dr. Cristina Prat (Institut d'Investigació en Ciències de la Salut Germans Trias i Pujol, Badalona, Spain). Calcofluor White Stain, CellCrown™ inserts (24-well plate inserts), erythromycin and propidium iodide were purchased from Sigma-Aldrich (St. Louis, MO, USA), Tryptone soy broth (TSB) and agar (TSA) were obtained from Conda-Pronadisa (Madrid, Spain). Chlorhexidine gluconate 1% was purchased from Salvat (Barcelona, Spain). The Live/Dead®BacLight™ bacterial viability kit was purchased from Fisher Scientific (Hampton, USA).

Regarding cell lines, human dermal fibroblasts were purchased from Lonza (Bornem, Belgium), and THP1 human monocytes (ATCC TIB-202) from LGC Standards (Barcelona, Spain), while human keratinocytes (HaCaT) were kindly gifted by Dr Pilar Martín-Duque. J774A.1 macrophage cells (ATCC® TIB-67™) were purchased from LGC (Barcelona, Spain). Phorbol 12-myristate 13-acetate (PMA), Bovine Serum Albumin (BSA) and lipopolysaccharide (LPS) were purchased from Sigma-Aldrich (St. Louis, MO, USA). High-glucose Dulbecco's Modified Eagle's Medium (DMEM) was purchased from HyClone (South Logan, USA) and Biowest (Cedex, France), RPMI 1640 w/stable glutamine, and antibiotic-antimycotic (60 g/mL penicillin, 100 g/mL streptomycin and 0.25 g/mL amphotericin B) were supplied by Biowest

(Cedex, France). Cell culture reagents, such as fetal bovine serum (FBS), HEPES, non-essential amino acids, 2-mercaptoethanol 50 mM and sodium pyruvate 100 mM, were obtained from Gibco (Manchester, UK) and Biowest (Cedex, France), and the Blue Cell Viability assay from Abnova (Aachen, Germany). MTT (3-(4,5-dimethylthiazol-2-yl)-2,5-diphenyltetrazolium bromide), Alexa Fluor™ 488 Conjugate and TRIzol were purchased from Invitrogen (Madison, USA).

Concerning the molecular biology experiments, RNeasy mini kit was purchased from Qiagen (Cologne, Germany). iScript retrotranscription kit was purchased from BioRad Laboratories (Irvine, USA). TaqMan® Fast Advanced Master Mix and target probes were purchased from Applied Biosystems (Beverly, USA). Paraformaldehyde 3% with 0.1 M cacodylate buffer was purchased from Electron Microscopy Sciences (Hatfield, USA) and hexamethyldisilazane was supplied by Fluka Analytical (USA). Paraformaldehyde (PFA) 4% in PBS was purchased from Alfa Aesar (Karlsruhe, Germany). Saponin from Quillaja Bark pure and SDS for molecular biology were purchased from AppliChem (Darmstadt, Germany). DAPI-Mowiol and phalloidin 546 were obtained from ThermoFisher Scientific (Massachusetts, USA).

Regarding the *in vivo* experiments, eight to ten-week-old male SKH1 hairless mice were purchased from Charles River Laboratories (Barcelona, Spain). Sterile 8-mm biopsy punch was purchased from Eickemeyer Veterinary Equipment (Tuttlingen, Germany), meanwhile silicone wound splints were supplied by Grace Bio-Labs (Bend, USA). 4/0 sutures were purchased from Braun (Barcelona, Spain). Adhesive plasters and bandages were obtained from Hartman (Mataro, Spain) while the microbiological swabs were purchased from Deltalab (Barcelona, Spain).

## **AI.2. Synthesis of loaded PCL nanofibers**

### **AI.2.1. Solutions preparation and characterization**

A solution of PCL (10 w/w %) was prepared in DCM and DMF at 1:1 volume ratio. For the preparation of loaded-PCL nanofibers, THY, TYR, SQU, CAR was added to the polymeric solution at 20 w/w % (referred to PCL mass). The mixture was stirred for 30 min before the electrospinning process.

Viscosity and conductivity of PCL solutions with and without natural compounds were measured. The relative viscosity of solutions was measured at 25 °C using a Visco Basic Plus

viscometer (Visco Basic, Spain). On the other hand, the conductivity was measured with a multimeter MM41-Criston (Hach Lange, Spain).

#### AI.2.2. Electrospinning process

**Chapter III** develops the antimicrobial activity of PCL-THY patches, which were synthesized following this methodology: An Yflow 2.2 D500 electrospinner equipped with a rotating drum collector (100 rpm) was used to obtain bare and PCL-THY patches. The collection drum was covered with aluminum foil to facilitate the recovery of the electrospun nanofibers. PCL and PCL-THY solutions were electrospun through a 22-gauge needle with a syringe pump working at 1.0 mL/h flow rate. The distance from the tip of the needle to the collector was 18 cm. The voltage applied to the collector plate was -7 kV and the voltage applied to the needle was +10 kV with the aim of obtaining a stable Taylor cone. Homogeneous patches of bare and THY-loaded PCL nanofibers were obtained after 8h of electrospinning.

To develop **Chapter IV**, different types of PCL synthesis were carried out loading anti-inflammatory EOs. Patches fabrication was carried out by Mr. Enrique Gámez-Herrera and the protocol has been recently published.<sup>134</sup> Synthesis of one compound- loaded PCL patches (PCL-THY; TYR; CAR; SQU) was carried out following synthesis described in Chapter III. However, for two compounds-loaded PCL patches (PCL-THY-TYR and PCL-THY-SQU), two parallel syringes were used containing 20% w/w EO/PCL solution and a rotating drum collector to assure a homogeneous distribution. Flow rate was set at 1.0 mL/h and the distance between tips of the needles and the collector was 18 cm. Voltage applied to the collector was - 4.00 kV and needles were fixed from + 6.62 to + 10.22 with the aim of obtaining a stable Taylor cone.

In **Chapter V**, *in vivo* experiments were carried out using PCL-THY patches synthesized by Mr. Enrique Gámez-Herrera and the procedure was already published.<sup>247</sup> Synthesis follows the same methodology that those described in Chapter III and Chapter IV for PCL-THY with one difference; instead using a rotating drum collector, it was used a flat collector to achieve a higher thickness.

### AI.3. Characterization of electrospun nanofibers

#### AI.3.1. Morphology

To perform a morphological characterization of synthesized nanofibers, samples were coated with a 5 nm Au/Pd layer. Following sputter coating, images were acquired with an

Inspect F50 SEM microscope instrument equipped with an ETD (SE) detector and operating at an accelerating voltage of 10-15 keV. ImageJ software (Version 1.48f, NIG, USA) was used to measure nanofiber diameters (N=100).

#### AI.3.2. Water uptake

The water uptake ability of the prepared patches was measured after immersing the samples in purified water at room temperature for 24 h. The excess of liquid was then drained from the surface to get the final weight ( $w_t$ ). The water absorption (S) was calculated with the following equation, where  $w_i$  is the mat initial weight:

$$S (\%) = \frac{W_t - W_i}{W_i} \times 100$$

#### AI.3.3. Patches porosity

The porosity of the synthesized patches was determined by mercury intrusion porosimetry (Micromeritics' AutoPore IV 9500 Series, USA).

#### AI.3.4. Mechanical properties

The mechanical properties of the mats were tested using an Instron Microtester 5548 and a video extensometer laser without contact (Instron 2663-281). Stress-strain curves were recorded at a stretching speed of 1 mm/min. The dimensions of the tested probes were in agreement with the ISO 527-1:2012 norm (Plastics — Determination of tensile properties).

#### AI.3.5. Essential oils loading and encapsulation efficiency

Loaded compounds masses were evaluated by gas chromatography coupled with mass spectrometry (GC–MS) in a Shimadzu 2010SE GC–MS chromatograph equipped with an AOC 20i injector by using a Zebron ZB-50 capillary column (30 m × 0.25 mm, 0.25 μm thickness; Phenomenex, US).<sup>247</sup> An initial oven temperature of 50 °C was kept for 1 min and then it was raised at 10 °C/ min until reaching 160 °C, and then a second heating rate of 20 °C/min was used until reaching 200 °C. Helium was used as carrier gas at 1mL/min. The detector temperature was 250 °C and the transfer line and ion source, were set at 200 °C. One μL of each sample was injected for the chromatographic analysis.

The calibration curves were prepared using 2.5 to 30 ppm and 5 ppm of (S)-(-)-limonene as internal standard. For sample preparation, 10 mg of nanofiber patches were dissolved in DCM:acetonitrile (1:1; 10 mL). The sample was diluted, and 5 ppm of the internal standard was



added. The EO compounds' encapsulation efficiency (EE) and drug loading (DL) were calculated considering the theoretical load ( $w_t$ ), the measured load ( $w_e$ ), and the weight of the nanofibers ( $w_n$ ) using the following equations:

$$EE (\%) = \frac{w_e}{w_t} \times 100 \quad DL (\%) = \frac{w_e}{w_n} \times 100$$

#### AI.3.6. Release of natural compounds

To study THY release of PCL-THY patches in **Chapter III**, an IKA<sup>®</sup> KS 130 orbital shaker was used. Ten mg of PCL-THY patches were immersed in 4 mL of PBS and kept at 37°C under stirring (150 rpm). At different time points up to 24h, the supernatant was analyzed with in an Acquity UPLC<sup>®</sup> Waters liquid chromatography system and Waters<sup>®</sup> Empower<sup>™</sup> chromatographic software (Waters, US). An Acquity UPLC<sup>®</sup> Waters BEH C18 column (2.1 x 50 mm, 1.7  $\mu$ m particle diameter) was employed for the analysis of THY. In the determination, 25 ppm of naproxen was included as internal standard.

For **Chapters IV and V**, EOs release was evaluated by Mr. Enrique Gámez-Herrera and previously described.<sup>134</sup> It was used a Shimadzu LC-10AT VP syringe pump. Here, samples were put into the syringe and rinsed with PBS (2% w/v Tween 80) at 37 °C with a flow rate of 1 mL/ min. Samples were collected at different time intervals up to 8 h and analyzed in an Acquity UPLC<sup>®</sup> Waters liquid chromatography system and Waters<sup>®</sup> Empower<sup>™</sup> chromatographic software.<sup>247</sup> An Acquity UPLC<sup>®</sup> Waters BEH C18 column (2.1  $\times$  50 mm, 1.7  $\mu$ m particle diameter) was employed for the analysis of CAR and THY, whereas SQU, TYR, THY-SQU and THY-TYR were analyzed by a Phenomenex Kinetex EVO C18 column (2.1  $\times$  100 mm, 1.7  $\mu$ m particle diameter; Phenomenex, USA).<sup>247</sup>

### **AI.4. Antimicrobial activity**

#### AI.4.1. Bacteria culture

A Gram-negative model *E. coli* S17 strain exerting resistance to streptomycin<sup>344</sup>, a Gram-positive model as *S. aureus* ATCC 25923, well-known as not a resistant strain and used in susceptibility tests<sup>345,346</sup>, and a methicillin sensitive *S. aureus* Newman strain expressing the coral green fluorescent protein (cGFP) from the vector pCN47, exerting resistance to erythromycin, were evaluated. These strains were initially grown overnight in TSB supplemented with the corresponding selective antibiotic (streptomycin 100  $\mu$ g/mL for *E. coli*

and erythromycin 10 µg/mL) for cGFP-expressing *S. aureus*) at 37 °C under shaking (150 rpm) obtaining, in the stationary growth phase,  $10^8$ – $10^9$  colony forming units (CFU)/mL for the three strains used.

#### AI.4.2. Preparation of free EOs

The reduced solubility of plant-derived natural compounds makes necessary the introduction of an emulsifier or solvent to favour the contact between bacteria and natural oil compounds. In **Chapter II**, EO compounds were solubilized in culture medium by adding Tween® 80 (1.5–2% v/v) and mixing with vortex for 1 min prior to their dilution before the bactericidal tests. However, in **Chapter III and Chapter V**, THY was solubilized in DMSO by preparing a stock THY solution of 50 mg/mL and dissolving up to the studied concentration in culture medium.

#### AI.4.3. MIC and MBC determination

Inhibitory (MIC) and bactericidal (MBC) concentrations of active EO molecules were tested in **Chapter II**, in two bacteria strains, *E. coli* and *S. aureus*, following the broth microdilution method.<sup>216</sup> Liquid growth medium (TSB) containing an inoculum of  $10^5$  CFU/mL and concentrations of the EO compounds (0.1–4 mg/mL) were used. EOs were previously dissolved in Tween® 80 as Section AI.4.2 explains. Once bacteria suspension reached the stationary growth ( $10^8$ – $10^9$  CFU/mL), it was further diluted to  $\sim 10^5$  CFU/mL and added to solutions with different concentrations (0.1–4 mg/mL) of the antimicrobial agents. Then, samples were incubated for 24 h at 37 °C under shaking (150 rpm). After incubation, the treated bacterial suspensions were diluted in PBS and spot-plated on TSA plates to count colonies after incubation at 37 °C for 24 h. Positive control (untreated bacteria) and negative control (chlorhexidine treated bacteria) samples were also tested. Chlorhexidine was used as model antiseptic used in the clinical practice.

The same broth microdilution methodology was carried out in **Chapter III** to study the antibacterial activity of free thymol (THY; 0.01-0.15 mg/mL added to cGFP-expressing *S. aureus* cultures). However, PCL-THY patches were assayed in agar broth (TSA) according to the ASTM E-2180-18 standard test method.<sup>268</sup> A positive control (untreated bacteria) was also included in both methods.

PCL-THY patches were cut, weighted and sterilized using UV light (254 nm wavelength; 30 min each side). Warm TSA (47 °C) was inoculated with  $10^5$  CFU/mL of cGFP-expressing *S. aureus*. Nanofiber-based patches were placed in 12-well plates and 3 mL of inoculated TSA were added to each well. Samples were incubated at 37 °C for 24 h in a closed box with water to keep an adequate humidity. After incubation, each sample was collected with 7 mL of TSB, sonicated and vortexed for 1 min. Bacterial suspensions were diluted in PBS and plated on TSA to count colonies after 24 h of incubation at 37 °C.

#### AI.4.4. Bacteria morphology

In **Chapter II**, bacteria morphology before and after treatment with EO molecules was analyzed by SEM as it was previously reported.<sup>267</sup> Briefly, logarithmic growth phase *E. coli* and *S. aureus* bacteria cultures ( $\sim 10^5$  CFU/mL) were treated with the selected EO compounds at MIC and MBC values and incubated overnight at 37 °C. Following incubation, samples were spin-dried at 600 g and washed twice in PBS (0.1 M). Bacteria were fixed in 2.5% glutaraldehyde for 90 min and subsequently filtered and dehydrated in ethanol solutions series (30, 50, 70, 80, 90, and 100%; twice for 15 min). Finally, samples were air-dried at room temperature and covered with a 5 nm Pt layer. SEM micrographs were acquired in a SEM Inspect F50 equipment (FEI Co., LMA-INA, Zaragoza, Spain).

#### AI.4.5. Bactericidal mechanism

In order to study the bactericidal mechanism of the different EOs, *E. coli* and *S. aureus* bacteria samples ( $10^7$  CFU/mL) were centrifuged at 4400 g for 10 min and resuspended in the different compound solutions at MIC and MBC concentrations following the protocols previously described.<sup>227,267</sup> Control groups (not treated and chlorhexidine treated bacteria) were also analyzed. All samples were incubated overnight at 37 °C. After 25 µg/mL of propidium iodide was added, samples were analyzed by flow cytometry in Gallios equipment (Beckman Coulter Company, Cell Separation and Cytometry Unit, CIBA, IIS Aragon, Zaragoza, Spain).

#### AI.4.6. Confocal microscopy:

The Live/Dead®BacLight™ bacterial viability kit was used to detect bacteria membrane damage. The methodology is based on the double-staining by SYTO9 and propidium iodide as indicated by the manufacturer. Bacteria samples incubated at 24 h ( $10^7$  CFU/mL) and treated with the selected EO compounds at MIC, were washed in sterile saline solution and further put

in contact with the dye mixture for 15min in the dark at room temperature. Samples were then mounted on slides and visualized by confocal microscopy (Leica TCS SP2 Laser Scanning Confocal Microscope, Microscopy Unit, CIBA, IIS Aragon, Zaragoza, Spain). Control samples were also tested as described above.

#### AI.4.7. Synergy studies

The Broth Dilution Checkerboard test was used to evaluate the interaction among the three most promising bactericidal EO molecules determined by the MIC and MBC studies against *S. aureus*. In brief, a solution containing four times the MBC of each compound was prepared. By using a MW96 plate and fresh medium, compound A was diluted two-fold in vertical orientation and compound B was diluted two-fold in horizontal direction. Then, a bacterial suspension ( $10^6$  CFU/mL, 100  $\mu$ L) was added and the plate was incubated overnight at 37 °C. After incubation, bacteria growth was determined by the resazurin assay. The Fractional Inhibitory Concentration Index (FICI) of the combination of compounds A and B was calculated according to the following equation:

$$FICI = FIC_A + FIC_B$$

$$FIC_A = \frac{MIC_A \text{ in presence of } B}{MIC \text{ of } A} \quad \text{and} \quad FIC_B = \frac{MIC_B \text{ in presence of } A}{MIC \text{ of } B}$$

FICI results were classified as synergy ( $FICI < 0.5$ ), addition ( $0.5 \leq FICI \leq 1$ ), indifference ( $1 < FICI \leq 4$ ) or antagonism ( $FICI > 4$ ), as previously described.<sup>347</sup>

#### AI.4.8. Biofilm formation and characterization

*S. aureus* was grown overnight in TSB until stationary growth phase was reached. At this point, bacteria were adjusted to  $10^7$  CFU/mL and added to a MW96 microplate and incubated at 37 °C for 16 h without shaking. After incubation, culture medium was discarded, and biofilms were washed twice with PBS. In order to study the biofilm formation two methods were used:

4.8.1. Calcofluor White Stain (50 mL) was added to each well and incubated 1 min in the dark at room temperature. After incubation, the stain was removed and biofilms were washed twice with PBS. Samples were air-dried in the dark to be further visualized in an inverted fluorescence microscope (Olympus IX81).

4.8.2. To be analyzed by scanning electron microscopy (SEM): biofilms were grown on sterile glass slides by adding a *S. aureus* (ATCC 25923) planktonic suspension ( $10^7$

CFU/mL) and further incubation at 37 °C for 16 h without shaking. Then, biofilms were washed twice with PBS (0.1 M) and fixed in 2.5% glutaraldehyde for 3 h. Samples were dehydrated through a series of ethanol solutions (30, 50, 70, 80, 90 and 100%; 15 min, twice). Finally, samples were air-dried at room temperature and coated with 5nm Pt. SEM images were acquired in the energy range of 10–15 keV in a SEM Inspect™ F50 (FEI Co., Hillsboro, OR, USA).

#### AI.4.9. Antibiofilm activity measurement

In **Chapter II**, the effects of free EOs (0.25–1 mg/mL) were studied in biofilm formation and in the disruption of an already formed *S. aureus* (ATCC 25923) biofilm.

- The effects of EO molecules eradicating preformed biofilms (section AI.4.8). With a formed biofilm, EOs were added and samples were incubated for 24 h at 37 °C without shaking. After incubation, culture medium containing the EO compounds was removed and biofilms were disrupted by sonication (15 min, 200 W). Samples were then diluted and seeded onto agar plates to count the viable colonies grown after 24 h of incubation at 37 °C.
- To study the effects of the EOs on biofilm formation, compounds were added to bacterial suspensions ( $10^7$  CFU/mL) in a MW96 microplate and incubated for 16 h at 37 °C without shaking. After incubation, planktonic cells were removed by washing them twice with PBS. Biofilm samples were then sonicated as described above and serially diluted to be further plated on agar. Viable bacteria (CFU/mL) were counted after 24 h of incubation at 37 °C.

In **Chapter III**, the effects of PCL-THY patches in biofilm formation are studied using  $\mu$ -dish 35 mm ibiTreat plates and following two different methodologies:

- In the first methodology,  $10^4$  CFU/mL of bacteria were put in contact with 5 and 7 mg of PCL-THY patches and incubated for 24 h at 37 °C.
- In the second approach, bacteria in exponential phase ( $10^4$  CFU/mL) were put in contact with 10 and 12 mg of PCL-THY patches and incubated for 1 h. Later, patches were removed, and culture media was kept at 37 °C for 24 h.

After 24h incubation, both approaches were processed simultaneously; planktonic cells were removed, and wells were washed twice with PBS. Biofilm formation was analyzed by following two different methods:

- For confocal microscopy, the biofilm matrix was stained for 1 min with calcofluor white and washed with PBS. Next, 2 mL of PFA 4% in PBS were added to each plate for 30 min. After this incubation time, samples were mounted in Mowiol mounting medium and prepared for microscopical visualization. Samples were analyzed under confocal microscopy (Confocal Zeiss LSM 880 with airyscan; Microscopy Unit, CIBA, IIS Aragon, Zaragoza, Spain).
- For bacteria quantification, biofilm in PBS was sonicated for 15 min in an ultrasonic water bath to ensure its detachment from the bottom of the wells. Later, detached bacteria concentrations were tested following the conventional agar microdilution method.<sup>216</sup>

In both techniques, THY-free patches (PCL patches) were tested as control samples (not treated bacteria).

## **AI.5. Cell assays**

### AI.5.1 Cytotoxicity metabolism assays

In **Chapter II**, human dermal fibroblasts, human epidermal keratinocytes (HaCaT), and THP1 human monocytes were used to evaluate the cytotoxic effects of free EOs. Fibroblasts and HaCaT were routinely grown in high-glucose DMEM supplemented with 10% FBS and antibiotic-antimycotic in a humidified atmosphere at 37 °C and 5% CO<sub>2</sub>. Monocytes were cultured in RPMI 1640 supplemented with 10% FBS, 1% HEPES, 1% non-essential amino acids, 0.1% 2-mercaptoethanol 50 mM, 1% sodium pyruvate 100 mM, and antibiotic-antimycotic. Macrophages were obtained by the *in vitro* differentiation of monocytes by adding 1 μM PMA to the cell culture. For fibroblasts, macrophages and HaCaT cells, cytotoxicity was determined by measuring cell metabolism through the Blue Cell Viability assay. Cells were seeded on MW96 microplates and incubated with the tested molecules (0.004–0.125 mg/mL) for 24 h. Control samples (not treated and chlorhexidine treated) were also analyzed. Then, the reagent was added (10%) and cells were incubated for 4 h at 37 °C. The reduction of the dye by metabolically active cells was monitored in a microplate reader at 535/590 nm ex/em (Multimode Synergy HT Microplate Reader; Biotek, USA) Cell viability was determined by

interpolation of the emission data obtained from the treated samples and the control samples (not treated cells, 100% viability).

Cytotoxicity experiments in **Chapter III** were carried out using J774 macrophage cells (ATCC®TIB-67™). This cell type was cultured following specifications provided by the manufacturer using high-glucose DMEM supplemented with 10% fetal bovine serum (FBS, v/v) and antibiotic-antimycotic at 37 °C in a humidified atmosphere with 5% CO<sub>2</sub>. Different weights of PCL-THY patches were tested at different time points. First, cells were seeded in 6-well plates (48,000 cells/cm<sup>2</sup>), and 5 and 7 mg of PCL-THY were added to 2 mL of culture medium and incubated at 37 °C, 5% CO<sub>2</sub> for 24 h. Concurrently, 10 and 12 mg of PCL-THY were added to 2 mL of culture medium and incubated for 1 h. After incubation time, these patches were removed, and cells were further incubated at 37 °C, 5% CO<sub>2</sub> for 24h. After incubation, cells were washed twice with PBS.

After cell treatment with the loaded patches following both approaches, the MTT cytotoxicity assay for assessing cell metabolic activity was used by preparing a stock solution of the tetrazolium dye at 5 mg/mL in PBS. Cells were then incubated with 0.5 mg/mL of the MTT dye for 3 h at 37 °C. Following the incubation period, medium was removed, and the dye was solubilized with a solution containing DMSO (99.4% v/v), SDS (0.1% w/v) and acetic acid (0.6% v/v) for 15 min. The dye is reduced forming an insoluble formazan salt when the metabolism of cells is active. This salt was dissolved to obtain a purple solution which was quantified at OD of 540 nm (Multimode Synergy HT Microplate Reader; Biotek, USA). Viability percentages are calculated dividing the calculated OD of treatment samples by the calculated OD of positive control samples.

Cytotoxicity experiments in **Chapter IV** were carried out using J774A.1 macrophage cells seeded into 96-well plates and treated with free natural compounds (0.008; 0.02; 0.04; 0.06; and 0.12 mg/mL) for 24 h (37 °C and 5% CO<sub>2</sub>). Using 24-well plates, cells were treated with PCL-patches (0.75, 1 and 1.5 mg of THY, CAR, TYR, SQU patches and mixed membranes with THY-TYR and THY-SQU) in a volume of 1 mL. After treatment, MTT solution was added to the cells following the methodology used in Chapter III. Eight samples were analyzed per concentration and compound. Results were expressed as viability percentage normalized over the positive control (100% viability) and negative control (no cells) samples. Not loaded PCL patches were assigned with 100% viability.

### AI.5.2. Flow cytometry for apoptosis detection

In **Chapter IV** flow cytometry was carried out for cells treated with free compounds. J774 cells were seeded at densities of  $9 \times 10^4$  cells/well in 24-well plates and maintained at 37 °C and 5% CO<sub>2</sub> overnight. Cells were then treated with free EOs at non-lethal concentrations as determined by the MTT assay described above: 0.06 mg/mL for CAR, CIN, THY, B-CAR, and 0.12 mg/mL for TYR, CUR, SQU. After a 24 h incubation period, cells were collected and resuspended in annexin V-binding buffer (10 mM HEPES/NaOH, 140 M NaCl, 25 mM CaCl<sub>2</sub>) and treated with a solution composed of annexin V-FITC and propidium iodide. Cells were then incubated at room temperature for 15 min in the dark. Analyses were carried out using a BD FACSAria BD flow cytometer equipped with BD FACSDiva software (Cell Separation and Cytometry Unit, CIBA, IIS Aragon, Spain). Untreated control cells were used as a negative control to determine the basal status of the cells and the effect of EOs on J774 macrophages.

### AI.5.3 *In vitro* model infection of J774 macrophages

J774 macrophages were seeded in  $\mu$ -dish 35mm ibiTreat plates (130,000 cells/cm<sup>2</sup>) overnight. Prior to the infection assays, supplemented DMEM containing antibiotics was removed, cells were washed twice with PBS and DMEM renewed without adding antibiotics in order to not hamper infection. Not infected and infected cells without treatment were also run as control samples (data not shown). Equally, THY-free patches (PCL) were tested in the cultures to evaluate the treatment effect. Both methodologies described in cell cytotoxicity section were followed according to the corresponding patches weight and the results obtained in the cytotoxicity assays to elucidate the efficiency of the patches related to their weight and thus, their THY loading. Patches were added to culture cells and then infected with 10<sup>5</sup> CFU/mL of cGFP-expressing *S. aureus* in DMEM without antibiotics previously prepared. Treated cultures were incubated for 1 h (10 and 12 mg PCL-THY) or 24h (5-7 mg PCL-THY) at 37 °C and 5% CO<sub>2</sub>. After those time periods, patches were removed, cells were washed twice with PBS and fixed in PFA 4% during 30 min at room temperature.

Confocal microscopy was then used to monitor the effect of PCL-THY in the infection model of J774 macrophages mediated by cGFP-expressing *S. aureus*. After fixation, cells were first washed with PBS-BSA 1% and secondly, with saponin 0.1% in PBS-BSA solution. Straightaway, the plates were incubated in the dark with 500  $\mu$ L of phalloidin 546, (1:200 in PBS-BSA-saponin prepared solution) for 1 h at room temperature. After incubation, cells were



rinsed with PBS-BSA 1% and then with distilled water. Finally, coverslips were mounted on glass slides in DAPI-Mowiol mounting medium. Samples were analyzed under confocal microscopy (Confocal Zeiss LSM 880 with airyscan; Microscopy Unit, CIBA, IIS Aragon, Zaragoza, Spain). Z-stack orthogonal projections were used to visualize the presence of bacteria inside the cells.

## **AI.6. Anti-inflammatory studies**

These experiments were carried out in the Methodist Hospital Research Institute in Houston (Texas, US) in the group of Biomimetic Medicine headed by Professor Ennio Tasciotti.

### AI.6.1. *In vitro* inflammation

*In vitro* inflammation and treatment with EOs were developed following two different approaches, the pre-treatment approach and the post-treatment approach, which are depicted in Scheme described in Chapter IV (Scheme IV.1)

- Pre-treatment approach: In the pre-treatment approach, cells were seeded in a 12-well plate and cultured at 37 °C and 5% CO<sub>2</sub>. After 24 h, EOs were added to the cells at the subcytotoxic concentration as determined by the MTT assay. Without removing EOs, cells were activated by using 100 ng/mL of LPS for 24 h at 37 °C and 5% CO<sub>2</sub>.
- Post-treatment approach: In the post-treatment approach, cells were seeded and treated with LPS 100 ng/mL for 3 h at 37 °C and 5% CO<sub>2</sub>. Then, EOs were added to the plate without removing LPS.

This approach was also followed to study the release of the compounds present in the EOs from loaded PCL nanofibers by adding the patches to activated cells.

### AI.6.2. Gene expression analysis

J774 macrophages were treated with free EO or loaded patches for 24 h. Next, cells were collected to evaluate their gene expression by RT-PCR. For this, cells were washed with PBS and lysed with TRIZol. RNeasy mini kit was used to obtain RNA while NanoDrop ND1000 spectrophotometer (NanoDrop Technologies, USA) was used to obtain concentration. cDNA was reverse transcribed with the iScript retrotranscription kit. The amplification was carried out using TaqMan® Fast Advanced Master Mix on a StepOne Plus realtime PCR system. Gene expression was evaluated using the following target probes:

- Pro-inflammatory genes: Il1b (Mm00434228\_m1) and Nos2 (Mm00440502\_m1)

- Anti-inflammatory genes: Il10 (Mm00439614\_m1)

Gene expression was normalized to the level of actin beta (Actb, Mm00607939\_s1). The values obtained from tested genes were normalized to those obtained from control groups (non-stimulated cells).

#### AI.6.3. Cell colonization model

To study cell migration and colonization of the patches, J774 macrophages were seeded in 24-well plates (50,000 cells/well). PCL patches loaded with THY, TYR, SQU, THY-TYR or THY-SQU were added and incubated at 37 °C and 5% CO<sub>2</sub> for 24 h. Then, cell colonization was evaluated from two points of view:

- 6.3.1. Cell viability in the wells compared to that obtained from the patches: MTT assay was performed as described above to quantify cell viability and to compare viability exerted by treated cells (wells at which membranes were added) with that obtained from untreated cells (wells at which membranes were not added). At the same time, the viability assay was also carried out in the patches to evaluate cell colonization.
- 6.3.2. SEM was used to observe the patches morphology and to verify the absence of cell colonization in patches. After incubation with loaded nanofibers, cells were washed in cacodylate buffer and fixed with paraformaldehyde 3% with 0.1 M cacodylate buffer at 4 °C overnight. Then, samples were washed with cacodylate buffer and subsequently dehydrated in ethanol solutions series (50, 70, 80, 90, 100% for 5 min per concentration). Finally, samples were washed with hexamethyldisilazane, air-dried in a hood and coated with a thin 5 nm Pt layer.

#### AI. 6.4. Immunofluorescence assay

Cells were seeded at a concentration of 62,000 cells/cm<sup>2</sup> and inflamed following the post-treatment approach described above. Then, a THY patch (0.75 mg) was added to the well and maintained at 37 °C and 5% CO<sub>2</sub> for 24 h. Next, cells were washed twice in PBS and fixed in 4% paraformaldehyde for 10 min at room temperature. Following fixation, cells were stained with wheat germ agglutinin, Alexa Fluor™ 488 Conjugate for 10 min at room temperature in order to stain cell membrane. Finally, nuclei were stained with DAPI for 1 min and mounted by using SlowFade™ Diamond Antifade Mountant. Images were collected using a Nikon A1 confocal microscope with post-processing performed using NIS Elements software (Nikon Instruments Corporation, Japan).

## **AI.7. *In vivo* experiments**

### AI.7.1. Mouse excisional wound splinting model and infection

*In vivo* studies were performed under Project License 51/14 approved by the Ethic Committee for Animal Experiments of the University of Zaragoza (Spain). In these studies, eight to ten-week-old male SKH1 hairless mice were used. Mice were fed *ad libitum* and maintained under specific pathogen-free conditions accordingly with the Spanish Policy for Animal Protection RD53/2013, which meets the European Union Directive 2010/63 on the protection of animals destined to scientific purposes.

Thirty mice were experimentally divided in five groups (N = 6): a) Control group: Wounds without infection or treatment; b) PCL group: Wounds infected and treated with PCL dressings; c) PCL-THY group: Wounds infected and treated with thymol-loaded PCL dressings; d) THY group: Wounds infected and treated with free THY; e) CLXD group: Wounds infected and treated with chlorhexidine. In each group, three mice were euthanized at 3 days post-surgery and infection (dpi) and other three mice at 7 dpi.

The mouse excisional wound splinting model<sup>348</sup> with some modifications was developed to evaluate wound infection and healing while avoiding the natural murine wound closure through skin contraction with the purpose to mimic the granulation and reepithelization processes that take place during human wound healing.<sup>349</sup>

In order to evaluate potential weight loss during the experiments, the animals were daily weighted. For the surgical procedure, SKH1 hairless mice were initially anesthetized with 5 % isoflurane, and maintained with 1-2 % isoflurane (1 L/min oxygen flow). The mice were rinsed with a 70 % ethanol (v/v) swab to be sterilely prepped. Meloxicam (2.5 mg/kg body weight) was then subcutaneously administered for pain relief (daily until 48 h post-surgery). Scheme in Chapter V (Scheme V.I) shows the procedure of wound infection model, in which a sterile 8-mm punch biopsy tool was employed to pattern two full-thickness wounds in the skin of the dorsum at each side of the median line of the animal. After that, two donut-shaped silicone wound splints were sutured with six interrupted 4/0 sutures to avoid the natural murine wound closure through skin contraction. Wounds were subsequently infected by inoculation of 10<sup>7</sup> CFU (25 µL in PBS) of *S. aureus* ATCC 25923. As mentioned before, different treatments were then applied: PCL dressing patches (as control of infection), THY

loaded PCL dressing patches, free THY or free CLXD (as model antiseptic in clinical use). The dressing patches diameter was 12 mm whereas free compounds were added in a volume of 25  $\mu$ L. Free THY was also assessed to compare the effect in wound infection and healing with the encapsulated THY. Finally, wounds and dressings were covered with sterile adhesive plasters and bandages. Dressing patches were replaced every day for 3 days, then all wounds were uncovered, as recommended in the clinical practice.<sup>350,351</sup> The progression of infection as well as weight loss and potential pain were monitored daily until the end of the studies.

#### AI.7.2. Evaluation of infection in wounds

The infection progression in wounds was evaluated through a semi-quantitative analysis of microbiological cultures and quantitative polymerase chain reaction (qPCR). The microbiological results were obtained from three independent experiments run in triplicate.

Microbiological samples were harvested from wounds by means of microbiological swabs with Amies media at 1, 2, 3 and 7 dpi. The microbiological samples were cultured on blood agar and McConkey No. 3 media (Oxoid). After incubation (37 °C, 24 h), bacteria concentration in the samples was semiquantified and the microorganism identified by reseeded samples and analyzing by a MALDI-TOF system (Bruker). Concurrently, qPCR evaluation of *S. aureus* ATCC 25923 was carried out in the samples. Briefly, DNA was obtained (DNeasy Blood & Tissue Kit, Qiagen) and amplified through the EXOone *Staphylococcus aureus* one MIX qPCR kit (Exopol) and a 7500 FAST Real Time PCR System. The pre-incubation step (1 cycle, 5 min, 95 °C) was followed by an amplification stage of 42 cycles of 15 s at 95 °C and 1 min at 60 °C, to read then the plate.

#### AI.7.3. Histological studies

Euthanasia was carried out by CO<sub>2</sub> inhalation after 3 and 7 dpi. Then, wounds were totally exposed by removing splints, sutures, dressings and gauzes, and harvested together with ~ 5 mm in diameter of surrounding tissue. Samples were then fixed for 24 h in paraformaldehyde and embedded in paraffin. Five  $\mu$ m sections were stained with hematoxylin and eosin (HE), and Gram staining for histopathological and bacteria determination, respectively. In order to assess wound angiogenesis, an immunohistochemical evaluation was performed by using rabbit polyclonal CD31 antibody (ab28364, Abcam) thanks to the Histopathology Unit from CNIO (Madrid, Spain). In brief, the automated immunostaining platform Autostainer Link (Dako) was

used. The slides were dewaxed in xylene and re-hydrated in an ethanol series. Antigen retrieval was carried out by high pH buffer treatment (CC1m, Roche) and 3 % H<sub>2</sub>O<sub>2</sub> was added to block the endogenous peroxidase. Subsequently, the slides were incubated with the primary antibody (1:50 for 60 min) followed by the corresponding visualization system conjugated with horseradish peroxidase (EnVision FLEX+, Dako). The chromogen 3, 30-diaminobenzidine tetrahydrochloride (DAB) was used for the detection of the immunohistochemical reaction. Nuclei staining were carried out using Carazzi's hematoxylin. Finally, the slides were dehydrated and permanent mounted to be visualized by microscopy. The interpretation of the histological results were performed in collaboration with Dr. Lluís Luján, Dr. Marta Pérez, Dr. Javier Asín and Mr. Ricardo de Miguel (Department of Animal Pathology, University of Zaragoza, Spain).

#### **AI.8. Statistical analyses**

All results were statistically analyzed using Prism 7 software (Version 7.04, GraphPad Software Inc., USA). All values are reported as mean  $\pm$  SD. At least, three replicas for each experiment were performed. A one-way (**Chapters III and IV**) and two-way (**Chapter II and V**) analysis of variance (ANOVA) set for multiple comparisons with a Dunnett's post-test was used. Statistically significant differences were considered when  $p \leq 0.05$ .



## Appendix II

### REFERENCES

## Appendix II: References

- (1) Robson, M. C.; Steed, D. L.; Franz, M. G. Wound Healing: Biologic Features and Approaches to Maximize Healing Trajectories. *Curr. Probl. Surg.* **2001**, *38* (2), A1. <https://doi.org/10.1067/msg.2001.111167>.
- (2) Shaw, T. J.; Martin, P. Wound Repair at a Glance. *J. Cell Sci.* **2009**, *122* (18), 3209–3213. <https://doi.org/10.1242/jcs.031187>.
- (3) Alonso, J. E.; Lee, J.; Burgess, A. R.; Browner, B. D. The Management of Complex Orthopedic Injuries. *Surg. Clin. North Am.* **1996**, *76* (4), 879–903. [https://doi.org/10.1016/S0039-6109\(05\)70486-2](https://doi.org/10.1016/S0039-6109(05)70486-2).
- (4) Velnar, T.; Bailey, T.; Smrkolj, V. The Wound Healing Process: An Overview of the Cellular and Molecular Mechanisms. *J. Int. Med. Res.* **2009**, *37* (5), 1528–1542. <https://doi.org/10.1177/147323000903700531>.
- (5) Nayak, B. S.; Sandiford, S.; Maxwell, A. Evaluation of the Wound-Healing Activity of Ethanolic Extract of *Morinda Citrifolia* L. Leaf. *Evidence-based Complement. Altern. Med.* **2009**, *6* (3), 351–356. <https://doi.org/10.1093/ecam/nem127>.
- (6) Kumar, V.; Abbas, A.; Fausto, N.; Aster, J. *Patologia - Bases Patológicas Das Doenças*, 7th ed.; Elsevier: Rio de Janeiro, 2005.
- (7) Broughton, G.; Janis, J. E.; Attinger, C. E. The Basic Science of Wound Healing. *Plast. Reconstr. Surg.* **2006**, *117* (7 SUPPL.), 12–34. <https://doi.org/10.1097/01.prs.0000225430.42531.c2>.
- (8) Witte, M. B.; Barbul, A. General Principles of Wound Healing. *Surg. Clin. North Am.* **1997**, *77* (3), 509–528. [https://doi.org/10.1016/S0039-6109\(05\)70566-1](https://doi.org/10.1016/S0039-6109(05)70566-1).
- (9) Medrado, A. R. A. P.; Pugliese, L. S.; Reis, S. R. A.; Andrade, Z. A. Influence of Low Level Laser Therapy on Wound Healing and Its Biological Action upon Myofibroblasts. *Lasers Surg. Med.* **2003**, *32* (3), 239–244. <https://doi.org/10.1002/lsm.10126>.
- (10) Lamkanfi, M. Emerging Inflammasome Effector Mechanisms. *Nat. Rev. Immunol.* **2011**, *11* (3), 213–220. <https://doi.org/10.1038/nri2936>.
- (11) Hirsiger, S.; Simmen, H. P.; Werner, C. M. L.; Wanner, G. A.; Rittirsch, D. Danger Signals Activating the Immune Response after Trauma. *Mediators Inflamm.* **2012**, *2012*. <https://doi.org/10.1155/2012/315941>.
- (12) Pohlman, T. H.; Stanness, K. A.; Beatty, P. G.; Ochs, H. D.; Harlan, J. M. An Endothelial Cell Surface Factor(s) Induced in Vitro by Lipopolysaccharide, Interleukin 1, and Tumor Necrosis Factor- $\alpha$  Increases Neutrophil Adherence by a CDw18-Dependent Mechanism. *J. Immunol.* **1986**, *136* (12), 4548–4553.
- (13) Bevilacqua, M. P.; Pober, J. S.; Wheeler, M. E.; Cotran, R. S.; Gimbrone, M. A. Interleukin 1 Acts on Cultured Human Vascular Endothelium to Increase the Adhesion of Polymorphonuclear Leukocytes, Monocytes, and Related Leukocyte Cell Lines. *J. Clin. Invest.* **1985**, *76* (5), 2003–2011. <https://doi.org/10.1172/JCI112200>.
- (14) Yager, D. R.; Nwomeh, B. C. The Proteolytic Environment of Chronic Wounds. *Wound Repair*



- Regen.* **1999**, 7 (6), 433–441. <https://doi.org/10.1046/j.1524-475X.1999.00433.x>.
- (15) Goldman, R. Growth Factors and Chronic Wound Healing: Past, Present, and Future. *Adv. Skin Wound Care* **2004**, 17 (1), 24–35. <https://doi.org/10.1097/00129334-200401000-00012>.
- (16) Witte, M. B.; Barbul, A. Role of Nitric Oxide in Wound Repair. *Am. J. Surg.* **2002**, 183 (4), 406–412. [https://doi.org/10.1016/S0002-9610\(02\)00815-2](https://doi.org/10.1016/S0002-9610(02)00815-2).
- (17) Rodero, M. P.; Khosrotehrani, K. Skin Wound Healing Modulation by Macrophages. *Int. J. Clin. Exp. Pathol.* **2010**, 3 (7), 643–653.
- (18) Nathan, C. Points of Control in Inflammation. *Nature* **2002**, 420 (6917), 846–852. <https://doi.org/10.1038/nature01320>.
- (19) Li, J.; Chen, J.; Kirsner, R. Pathophysiology of Acute Wound Healing. *Clin. Dermatol.* **2007**, 25 (1), 9–18. <https://doi.org/10.1016/j.clindermatol.2006.09.007>.
- (20) Singer, A. J.; Clark, R. A. F. Epstein1999\_Woundhealing. *N. Engl. J. Med.* **1999**.
- (21) Manes, Emilia Mira, Concepcion Gome, S. Cells on the Move: A Dialogue Between Polarization and Motility. *IUBMB Life (International Union Biochem. Mol. Biol. Life)* **2000**, 49 (2), 89–96. <https://doi.org/10.1080/15216540050022386>.
- (22) Lawrence, W. T.; Diegelmann, R. F. Growth Factors in Wound Healing. *Clin. Dermatol.* **1994**, 12 (1), 157–169. [https://doi.org/10.1016/0738-081X\(94\)90266-6](https://doi.org/10.1016/0738-081X(94)90266-6).
- (23) Li, S.; Huang, N. F.; Hsu, S. Mechanotransduction in Endothelial Cell Migration. *J. Cell. Biochem.* **2005**, 96 (6), 1110–1126. <https://doi.org/10.1002/jcb.20614>.
- (24) Krizbai, I. A.; Bauer, H.; Amberger, A.; Hennig, B.; Szabó, H.; Fuchs, R.; Bauer, H. C. Growth Factor-Induced Morphological, Physiological and Molecular Characteristics in Cerebral Endothelial Cells. *Eur. J. Cell Biol.* **2000**, 79 (9), 594–600. <https://doi.org/10.1078/0171-9335-00084>.
- (25) Ruiter, D.; Schlingemann, R.; JR, W.; Denijn, M.; Rieveld, F.; De Waal, R. Angiogenesis in Wound Healing and Tumor Metastasis. *Behring Inst. Mitt.* **1993**, 92, 258–272.
- (26) Desmouliere, A.; Geinoz, A.; Gabbiani, F.; Gabbiani, G. Transforming Growth Factor-B1 Induces  $\alpha$ -Smooth Muscle Actin Expression in Granulation Tissue Myofibroblasts and in Quiescent and Growing Cultured Fibroblasts. *J. Cell Biol.* **1993**, 122 (1), 103–111. <https://doi.org/10.1083/jcb.122.1.103>.
- (27) Pierce, G. F.; Mustoe, T. A.; Altrock, B. W.; Deuel, T. F.; Thomason, A. Role of Platelet-derived Growth Factor in Wound Healing. *J. Cell. Biochem.* **1991**, 45 (4), 319–326. <https://doi.org/10.1002/jcb.240450403>.
- (28) Martin, P. Wound Healing - Aiming for Perfect Skin Regeneration. *Science (80-. )*. **1997**, 276 (5309), 75–81. <https://doi.org/10.1126/science.276.5309.75>.
- (29) Buckley, C. D. Why Does Chronic Inflammation Persist: An Unexpected Role for Fibroblasts. *Immunol. Lett.* **2011**, 138 (1), 12–14. <https://doi.org/10.1016/j.imlet.2011.02.010>.
- (30) Sampaio, S.; Rivitti, E. *Dermatologia*, 2nd ed.; Ates Médicas: Sao Paulo, 2001.

- (31) Calin, M.; Coman, T.; Calin, M. The Effect of Low Level Laser Therapy on Surgical Wound Healing. *Rom. Reports Phys.* **2010**, *62* (3), 617–627.
- (32) Clark, R. A. F. Regulation of Fibroplasia in Cutaneous Wound Repair. *Am. J. Med. Sci.* **1993**, *306* (1), 42–48. <https://doi.org/10.1097/00000441-199307000-00011>.
- (33) Pierce, G. F.; Vande Berg, J.; Rudolph, R.; Tarpley, J.; Mustoe, T. A. Platelet-Derived Growth Factor-BB and Transforming Growth Factor Beta1 Selectively Modulate Glycosaminoglycans, Collagen, and Myofibroblasts in Excisional Wounds. *Am. J. Pathol.* **1991**, *138* (3), 629–646.
- (34) Hurtado, A. J.; Crowther, D. S. Methyl Methacrylate Stent for Prevention of Postexcisional Recurrent Ear Keloid. *J. Prosthet. Dent.* **1985**, *54* (2), 245–250. [https://doi.org/10.1016/0022-3913\(85\)90298-7](https://doi.org/10.1016/0022-3913(85)90298-7).
- (35) Kivisaari, J.; Vihersaari, T.; Renvall, S.; Nunikoski, J. Energy Metabolism of Experimental Wounds at Various Oxygen Environments. *Ann. Surg.* **1975**, *181* (6), 823–828. <https://doi.org/10.1097/00000658-197506000-00011>.
- (36) Broughton, G.; Janis, J. E.; Attinger, C. E. Wound Healing: An Overview. *Plast. Reconstr. Surg.* **2006**, *117* (7 SUPPL.), 1–32. <https://doi.org/10.1097/01.prs.0000222562.60260.f9>.
- (37) Chow, L. W. C.; Loo, W. T. Y.; Yuen, K. Y.; Cheng, C. The Study of Cytokine Dynamics at the Operation Site after Mastectomy. *Wound Repair Regen.* **2003**, *11* (5), 326–330. <https://doi.org/10.1046/j.1524-475X.2003.11503.x>.
- (38) Langsdon, P. R.; Tompkins, J. J.; Goodman, R. C. Hypothyroidism as a Risk Factor for Prolonged Postoperative Edema Following Face-Lift Surgery. *JAMA Facial Plast. Surg.* **2016**, *18* (4), 315–316. <https://doi.org/10.1001/jamafacial.2016.0155>.
- (39) Van de Kerkhof, P. C.; Van Bergen, B.; Spruijt, K. Age-Related Changes in Wound Healing. *Clin. Exp. Dermatol.* **1994**, No. 19, 369–374.
- (40) Williams, D. T.; Harding, K. Healing Responses of Skin and Muscle in Critical Illness. *Crit. Care Med.* **2003**, *31* (8 Suppl). <https://doi.org/10.1097/01.ccm.0000081430.34066.1d>.
- (41) Silverstein, P. Smoking and Wound Healing. *Am. J. Med.* **1992**, *93* (1 SUPPL. 1), 22–24. [https://doi.org/10.1016/0002-9343\(92\)90623-J](https://doi.org/10.1016/0002-9343(92)90623-J).
- (42) Bowler, P. G.; Duerden, B. I.; D.G., A. Wound Microbiology and Associated Approaches to Wound Management. *Clin. Microbiol. Rev.* **2001**, *14* (2), 244–269.
- (43) Zhao, G.; Usui, M. L.; Lippman, S. I.; James, G. A.; Stewart, P. S.; Fleckman, P.; Olerud, J. E. Biofilms and Inflammation in Chronic Wounds. *Adv. Wound Care* **2013**, *2* (7), 389–399. <https://doi.org/10.1089/wound.2012.0381>.
- (44) Bendy, R. H.; Nuccio, E.; Wolfe, B.; Collins, C.; Tamburro, W.; Glass, C.M., M. Relationship of Quantitative Wound Bacterial Counts to Healing of Decubiti. Effect of Topical Gentamicin. *Antimicrob. Agents Chemother.* **1964**, *4*, 147–155.
- (45) Carbone, C.; Teixeira, M. D. C.; Sousa, M. D. C.; Martins-Gomes, C.; Silva, A. M.; Souto, E. M. B.; Musumeci, T. Clotrimazole-Loaded Mediterranean Essential Oils NLC: A Synergic Treatment of Candida Skin Infections. *Pharmaceutics* **2019**, *11* (5). <https://doi.org/10.3390/pharmaceutics11050231>.

- (46) Duerden, B. I. Virulence Factors in Anaerobes. *Clin. Infect. Dis.* **1994**, *18*, S253–S259. [https://doi.org/10.1093/clinids/18.Supplement\\_4.S253](https://doi.org/10.1093/clinids/18.Supplement_4.S253).
- (47) Mangram, A.; Horan, T.; Pearson, M.; Christine, L.; Jarvis, W. Guideline for Prevention of Surgical Site Infection. *Am. J. Infect. Control* **1999**, *27* (2), 97–134.
- (48) Tong, S. Y. C.; Davis, J. S.; Eichenberger, E.; Holland, T. L.; Fowler, V. G. Staphylococcus Aureus Infections: Epidemiology, Pathophysiology, Clinical Manifestations, and Management. *Clin. Microbiol. Rev.* **2015**, *28* (3), 603–661. <https://doi.org/10.1128/CMR.00134-14>.
- (49) Zarb, P.; Coignard, B.; Griskeviciene, J.; Muller, A.; Vankerckhoven, V.; Weist, K.; Goossens, M. M.; Vaerenberg, S.; Hopkins, S.; Catry, B.; et al. *The European Centre for Disease Prevention and Control (ECDC) Pilot Point Prevalence Survey of Healthcare-Associated Infections and Antimicrobial Use*; 2012; Vol. 17. <https://doi.org/10.2807/ese.17.46.20316-en>.
- (50) ECDC. *Surveillance of Surgical Site Infections in Europe*; 2010.
- (51) O’Keeffe, A. B.; Lawrence, T.; Bojanic, S. Oxford Craniotomy Infections Database: A Cost Analysis of Craniotomy Infection. *Br. J. Neurosurg.* **2012**, *26* (2), 265–269. <https://doi.org/10.3109/02688697.2011.626878>.
- (52) Broex, E. C. J.; van Asselt, A. D. I.; Bruggeman, C. A.; van Tiel, F. H. Surgical Site Infections: How High Are the Costs? *J. Hosp. Infect.* **2009**, *72* (3), 193–201. <https://doi.org/10.1016/j.jhin.2009.03.020>.
- (53) Gottrup, F.; Melling, A.; Hollander, D. A. An Overview of Surgical Site Infections: Aetiology, Incidence and Risk Factors. *World Wide Wounds* **2005**, *2005* (2), 11–15.
- (54) Alfonso, J. L.; Pereperez, S. B.; Canoves, J. M.; Martinez, M. M.; Martinez, I. M.; Martin-Moreno, J. M. Are We Really Seeing the Total Costs of Surgical Site Infections? A Spanish Study. *Wound Repair Regen.* **2007**, *15* (4), 474–481. <https://doi.org/10.1111/j.1524-475X.2007.00254.x>.
- (55) Anaya, D. A.; Dellinger, E. P. Necrotizing Soft-Tissue Infection : Diagnosis and Management. **2007**, *44*, 705–710. <https://doi.org/10.1086/511638>.
- (56) Abrahamian, F. M.; Goldstein, E. J. C. Microbiology of Animal Bite Wound Infections. *Clin. Microbiol. Rev.* **2011**, *24* (2), 231–246. <https://doi.org/10.1128/CMR.00041-10>.
- (57) American Burn Association. Burn Incidence and Treatment in the United States <https://ameriburn.org/who-we-are/media/burn-incidence-fact-sheet/> (accessed Feb 21, 2020).
- (58) Church, D.; Elsayed, S.; Reid, O.; Winston, B.; Lindsay, R. Burn Wound Infections. *Clin. Microbiol. Rev.* **2006**, *19* (2), 403–434. <https://doi.org/10.1128/CMR.19.2.403-434.2006>.
- (59) Dana, A. N.; Bauman, W. A. Bacteriology of Pressure Ulcers in Individuals with Spinal Cord Injury: What We Know and What We Should Know. *J. Spinal Cord Med.* **2015**, *38* (2), 147–160. <https://doi.org/10.1179/2045772314Y.0000000234>.
- (60) Li, Z.; Lin, D. F.; Thalib, P. L.; Chaboyer, P. W. Global Prevalence and Incidence of Pressure Injuries in Hospitalised Adult Patients: A Systematic Review and Meta-Analysis. *Int. J. Nurs. Stud.* **2020**, *105*, 103546. <https://doi.org/10.1016/j.ijnurstu.2020.103546>.

- (61) Hunt, T. K.; Hopf, H. W. Wound Healing and Wound Infection: What Surgeons and Anesthesiologists Can Do. *Surg. Clin. North Am.* **1997**, *77* (3), 587–606. [https://doi.org/10.1016/S0039-6109\(05\)70570-3](https://doi.org/10.1016/S0039-6109(05)70570-3).
- (62) Shortridge, D.; Flamm, R. K. Comparative in Vitro Activities of New Antibiotics for the Treatment of Skin Infections. *Clin. Infect. Dis.* **2019**, *68* (Suppl 3), S200–S205. <https://doi.org/10.1093/cid/ciz003>.
- (63) Cutting, K. F.; White, R. J. Criteria for Identifying Wound Infection--Revisited. *Ostomy. Wound Manage.* **2005**, *51* (1), 28–34.
- (64) Costerton, J. W.; Stewart, P. S.; Greenberg, E. P. Bacterial Biofilms: A Common Cause of Persistent Infections. *Science* (80-. ). **1999**, *284* (5418), 1318–1322. <https://doi.org/10.1126/science.284.5418.1318>.
- (65) Bassler, B. L.; Losick, R. Bacterially Speaking. *Cell* **2006**, *125* (2), 237–246. <https://doi.org/10.1016/j.cell.2006.04.001>.
- (66) Waters, C. M.; Bassler, B. L. QUORUM SENSING: Cell-to-Cell Communication in Bacteria. *Annu. Rev. Cell Dev. Biol.* **2005**, *21* (1), 319–346. <https://doi.org/10.1146/annurev.cellbio.21.012704.131001>.
- (67) Stewart, P. S.; Costerton, J. W. Antibiotic Resistance of Bacteria in Biofilms. *Lancet* **2001**, *358* (9276), 135–138. [https://doi.org/10.1016/S0140-6736\(01\)05321-1](https://doi.org/10.1016/S0140-6736(01)05321-1).
- (68) Grice, E.; Segre, J. Interaction of the Microbiome with the Innate Immune Response in Chronic Wounds. *Adv. Exp. Med. Biol.* **2012**, No. 946, 55–68.
- (69) Fazli, M.; Bjarnsholt, T.; Kirketerp-Møller, K.; Jørgensen, A.; Andersen, C. B.; Givskov, M.; Tolker-Nielsen, T. Quantitative Analysis of the Cellular Inflammatory Response against Biofilm Bacteria in Chronic Wounds. *Wound Repair Regen.* **2011**, *19* (3), 387–391. <https://doi.org/10.1111/j.1524-475X.2011.00681.x>.
- (70) Koller, B.; Kappler, M.; Latzin, P.; Gaggar, A.; Schreiner, M.; Takyar, S.; Kormann, M.; Kabesch, M.; Roos, D.; Griese, M.; et al. TLR Expression on Neutrophils at the Pulmonary Site of Infection: TLR1/TLR2-Mediated Up-Regulation of TLR5 Expression in Cystic Fibrosis Lung Disease. *J. Immunol.* **2008**, *181* (4), 2753–2763. <https://doi.org/10.4049/jimmunol.181.4.2753>.
- (71) Merriam-Webster <https://www.merriam-webster.com/dictionary/antibiotic> (accessed Mar 6, 2020).
- (72) World Health Organization (WHO). Ten threats to global health in 2019. <https://www.who.int/news-room/feature-stories/ten-threats-to-global-health-in-2019>.
- (73) Spellberg, B.; Bartlett, J.; Gilbert, D. The Future of Antibiotics and Resistance. *N. Engl. J. Med* **2013**, *368* (4), 299–302.
- (74) Shriram, V.; Khare, T.; Bhagwat, R.; Shukla, R.; Kumar, V. Inhibiting Bacterial Drug Efflux Pumps via Phyto-Therapeutics to Combat Threatening Antimicrobial Resistance. *Front. Microbiol.* **2018**, *9* (DEC), 1–18. <https://doi.org/10.3389/fmicb.2018.02990>.
- (75) Mulani, M. S.; Kamble, E. E.; Kumkar, S. N.; Tawre, M. S.; Pardesi, K. R. Emerging Strategies to Combat ESKAPE Pathogens in the Era of Antimicrobial Resistance: A Review. *Front.*

- Microbiol.* **2019**, *10* (APR). <https://doi.org/10.3389/fmicb.2019.00539>.
- (76) WHO. *Critically Important Antimicrobials for Human Medicine: 5th Revision*; 2017. <https://doi.org/10.1017/CBO9781107415324.004>.
- (77) Butler, M. S.; Blaskovich, M. A.; Cooper, M. A. Antibiotics in the Clinical Pipeline at the End of 2015. *J. Antibiot. (Tokyo)*. **2017**, *70* (1), 3–24. <https://doi.org/10.1038/ja.2016.72>.
- (78) O'Neill, J.; By, C.; Neill, J. I. M. O.; O'Neill, J. Securing New Drugs for Future Generations: The Pipeline of Antibiotics. *Rev. Antimicrob. Resist.* **2015**, No. May, 42.
- (79) Neill, J. O. ' . Antimicrobial Resistance: Tackling a Crisis for the Health and Wealth of Nations The Review on Antimicrobial Resistance Chaired. **2014**, No. December.
- (80) Levy, S. B.; Bonnie, M. Antibacterial Resistance Worldwide: Causes, Challenges and Responses. *Nat. Med.* **2004**, *10* (12S), S122–S129. <https://doi.org/10.1038/nm1145>.
- (81) Yap, P. S. X.; Yiap, B. C.; Ping, H. C.; Lim, S. H. E. Essential Oils, A New Horizon in Combating Bacterial Antibiotic Resistance. *Open Microbiol. J.* **2014**, *8* (1), 6–14. <https://doi.org/10.2174/1874285801408010006>.
- (82) Kojima, S.; Nikaido, H. Permeation Rates of Penicillins Indicate That Escherichia Coli Porins Function Principally as Nonspecific Channels. *Proc. Natl. Acad. Sci. U. S. A.* **2013**, *110* (28), 2629–2634. <https://doi.org/10.1073/pnas.1310333110>.
- (83) Vargiu, A. V.; Nikaido, H. Multidrug Binding Properties of the AcrB Efflux Pump Characterized by Molecular Dynamics Simulations. *Proc. Natl. Acad. Sci. U. S. A.* **2012**, *109* (50), 20637–20642. <https://doi.org/10.1073/pnas.1218348109>.
- (84) Ochs, M. M.; McCusker, M. P.; Bains, M.; Hancock, R. E. W. Negative Regulation of the Pseudomonas Aeruginosa Outer Membrane Porin OprD Selective for Imipenem and Basic Amino Acids. *Antimicrob. Agents Chemother.* **1999**, *43* (5), 1085–1090. <https://doi.org/10.1128/aac.43.5.1085>.
- (85) Wright, G. D. Bacterial Resistance to Antibiotics: Enzymatic Degradation and Modification. *Adv. Drug Deliv. Rev.* **2005**, *57* (10), 1451–1470. <https://doi.org/10.1016/j.addr.2005.04.002>.
- (86) Savage, V. J.; Chopra, I.; O'Neill, A. J. Staphylococcus Aureus Biofilms Promote Horizontal Transfer of Antibiotic Resistance. *Antimicrob. Agents Chemother.* **2013**, *57* (4), 1968–1970. <https://doi.org/10.1128/AAC.02008-12>.
- (87) Anderl, J. N.; Roe, F.; Stewart, P. S. Role of Nutrient Limitation and Stationary-Phase Existence In. *Society* **2003**, *47* (4), 1251–1256. <https://doi.org/10.1128/AAC.47.4.1251>.
- (88) Nguyen, D.; Joshi-Datar, A.; Lepine, F.; Bauerle, E.; Olakanmi, O.; Beer, K.; McKay, G.; Siehnel, R.; Schafhauser, J.; Wang, Y.; et al. Active Starvation Responses Mediate Antibiotic Tolerance in Biofilms and Nutrient-Limited Bacteria. *Science (80- )*. **2011**, *334* (6058), 982–986. <https://doi.org/10.1126/science.1211037>.
- (89) Fonder, M. A.; Lazarus, G. S.; Cowan, D. A.; Aronson-Cook, B.; Kohli, A. R.; Mamelak, A. J. Treating the Chronic Wound: A Practical Approach to the Care of Nonhealing Wounds and Wound Care Dressings. *J. Am. Acad. Dermatol.* **2008**, *58* (2), 185–206. <https://doi.org/10.1016/j.jaad.2007.08.048>.

- (90) Damour, O.; Zhi Hua, S.; Lasne, F.; Villain, M.; Rousselle, P.; Collombel, C. Cytotoxicity Evaluation of Antiseptics and Antibiotics on Cultured Human Fibroblasts and Keratinocytes. *Burns* **1992**, *18* (6), 479–485. [https://doi.org/10.1016/0305-4179\(92\)90180-3](https://doi.org/10.1016/0305-4179(92)90180-3).
- (91) Pratap Verma, U.; Gupta, A.; Kumar Yadav, R.; Tiwari, R.; Sharma, R.; Kumar Balapure, A. Cytotoxicity of Chlorhexidine and Neem Extract on Cultured Human Gingival Fibroblasts through Fluorescence-Activated Cell Sorting Analysis: An in Vitro Study. *Eur. J. Dent.* **2018**, *12* (3), 344–349. <https://doi.org/10.4103/ejd.ejd>.
- (92) Lansdown, A. B. Silver. I: Its Antibacterial Properties and Mechanism of Action. *J. Wound Care* **2002**, *11* (4), 125–130. <https://doi.org/10.12968/jowc.2002.11.4.26389>.
- (93) McDonnell, G.; Russell, D. Antiseptics and Disinfectants: Activity, Action, and Resistance. *Clin. Microbiol. Rev.* **1999**, *12* (1), 147–179.
- (94) Lam, P. K.; Chan, E. S. Y.; Ho, W. S.; Liew, C. T. In Vitro Cytotoxicity Testing of a Nanocrystalline Silver Dressing (Acticoat) on Cultured Keratinocytes. *Br. J. Biomed. Sci.* **2004**, *61* (3), 125–127. <https://doi.org/10.1080/09674845.2004.11732656>.
- (95) Bakkali, F.; Averbeck, S.; Averbeck, D.; Idaomar, M. Biological Effects of Essential Oils - A Review. *Food Chem. Toxicol.* **2008**, *46* (2), 446–475. <https://doi.org/10.1016/j.fct.2007.09.106>.
- (96) Angioni, A.; Barra, A.; Coroneo, V.; Dessi, S.; Cabras, P. Chemical Composition, Seasonal Variability, and Antifungal Activity of *Lavandula Stoechas* L. Ssp. *Stoechas* Essential Oils from Stem/Leaves and Flowers. *J. Agric. Food Chem.* **2006**, *54* (12), 4364–4370. <https://doi.org/10.1021/jf0603329>.
- (97) Perry, N. S. L.; Bollen, C.; Perry, E. K.; Ballard, C. *Salvia* for Dementia Therapy: Review of Pharmacological Activity and Pilot Tolerability Clinical Trial. *Pharmacol. Biochem. Behav.* **2003**, *75* (3), 651–659. [https://doi.org/10.1016/S0091-3057\(03\)00108-4](https://doi.org/10.1016/S0091-3057(03)00108-4).
- (98) Pichersky, E.; Noel, J. P.; Dudareva, N. Biosynthesis of Plant Volatiles: Nature's Diversity and Ingenuity. *Science (80-. )*. **2006**, *311* (5762), 808–811. <https://doi.org/10.1126/science.1118510>.
- (99) Lima de Souza, J. R.; Oliveira, P. R. de; Anholetto, L. A.; Arnosti, A.; Daemon, E.; Remedio, R. N.; Camargo-Mathias, M. I. Effects of Carvacrol on Oocyte Development in Semi-Engorged *Rhipicephalus Sanguineus* Sensu Lato Females Ticks (Acari: Ixodidae). *Micron* **2019**, *116* (September 2018), 66–72. <https://doi.org/10.1016/j.micron.2018.09.015>.
- (100) Dairi, N.; Ferfera-Harrar, H.; Ramos, M.; Garrigós, M. C. Cellulose Acetate/AgNPs-Organoclay and/or Thymol Nano-Biocomposite Films with Combined Antimicrobial/Antioxidant Properties for Active Food Packaging Use. *Int. J. Biol. Macromol.* **2019**, *121*, 508–523. <https://doi.org/10.1016/j.ijbiomac.2018.10.042>.
- (101) Mahmoodi, M.; Amiri, H.; Ayoobi, F.; Rahmani, M.; Taghipour, Z.; Ghavamabadi, R. T.; Jafarzadeh, A.; Sankian, M. Carvacrol Ameliorates Experimental Autoimmune Encephalomyelitis through Modulating Pro- and Anti-Inflammatory Cytokines. *Life Sci.* **2019**, *219* (July 2018), 257–263. <https://doi.org/10.1016/j.lfs.2018.11.051>.
- (102) Jiji, S.; Udhayakumar, S.; Rose, C.; Muralidharan, C.; Kadirvelu, K. Thymol Enriched Bacterial Cellulose Hydrogel as Effective Material for Third Degree Burn Wound Repair. *Int. J. Biol. Macromol.* **2019**, *122*, 452–460.

- (103) Vitanza, L.; Maccelli, A.; Marazzato, M.; Scazzocchio, F.; Comanducci, A.; Fornarini, S.; Crestoni, M. E.; Filippi, A.; Frascchetti, C.; Rinaldi, F.; et al. Satureja Montana L. Essential Oil and Its Antimicrobial Activity Alone or in Combination with Gentamicin. *Microb. Pathog.* **2019**, *126* (May 2018), 323–331. <https://doi.org/10.1016/j.micpath.2018.11.025>.
- (104) Pires, A. L. R.; de Azevedo Motta, L.; Dias, A. M. A.; de Sousa, H. C.; Moraes, Â. M.; Braga, M. E. M. Towards Wound Dressings with Improved Properties: Effects of Poly(Dimethylsiloxane) on Chitosan-Alginate Films Loaded with Thymol and Beta-Carotene. *Mater. Sci. Eng. C* **2018**, *93* (August), 595–605. <https://doi.org/10.1016/j.msec.2018.08.005>.
- (105) Abou El-ezz, D.; Maher, A.; Sallam, N.; El-brairy, A.; Kenawy, S. Trans-Cinnamaldehyde Modulates Hippocampal Nrf2 Factor and Inhibits Amyloid Beta Aggregation in LPS-Induced Neuroinflammation Mouse Model. *Neurochem. Res.* **2018**, *43* (12), 2333–2342. <https://doi.org/10.1007/s11064-018-2656-y>.
- (106) Murakami, Y.; Kawata, A.; Suzuki, S.; Fujisawa, S. Cytotoxicity and Pro-/Anti-Inflammatory Properties of Cinnamates, Acrylates and Methacrylates against RAW264.7 Cells. *In Vivo (Brooklyn)*. **2018**, *32* (6), 1309–1321. <https://doi.org/10.21873/invivo.11381>.
- (107) Chaieb, K.; Hajlaoui, H.; Zmantar, T.; Kahla-Nakbi, A.; Rouabhia, M.; Mahdouani, K.; Bakhrouf, A. The Chemical Composition and Biological Activity of Clove Essential Oil, *Eugenia Caryophyllata* (*Syzigium Aromaticum* L. Myrtaceae): A Short Review. *Phytoterapy Res.* **2007**, *21*, 501–506.
- (108) Fidyk, K.; Fiedorowicz, A.; Strzdała, L.; Szumny, A. B-Caryophyllene and B-Caryophyllene Oxide—Natural Compounds of Anticancer and Analgesic Properties. *Cancer Med.* **2016**, *5* (10), 3007–3017. <https://doi.org/10.1002/cam4.816>.
- (109) Petersen, M.; Simmonds, M. S. J. Rosmarinic Acid. *Phytochemistry* **2003**, *62* (2), 121–125. [https://doi.org/10.1016/S0031-9422\(02\)00513-7](https://doi.org/10.1016/S0031-9422(02)00513-7).
- (110) Moreno, S.; Scheyer, T.; Romano, C. S.; Vojnov, A. A. Antioxidant and Antimicrobial Activities of Rosemary Extracts Linked to Their Polyphenol Composition. *Free Radic. Res.* **2006**, *40* (2), 223–231. <https://doi.org/10.1080/10715760500473834>.
- (111) Lou-Bonafonte, J. M.; Martínez-Beamonte, R.; Sanclemente, T.; Surra, J. C.; Herrera-Marcos, L. V.; Sanchez-Marco, J.; Arnal, C.; Osada, J. Current Insights into the Biological Action of Squalene. *Mol. Nutr. Food Res.* **2018**, *62* (15), 1–16. <https://doi.org/10.1002/mnfr.201800136>.
- (112) Lu, X.; Ma, S.; Chen, Y.; Yangzom, D.; Jiang, H. Squalene Found in Alpine Grassland Soils under a Harsh Environment in the Tibetan Plateau, China. *Biomolecules* **2018**, *8* (4), 1–12. <https://doi.org/10.3390/biom8040154>.
- (113) Serreli, G.; Deiana, M. Biological Relevance of Extra Virgin Olive Oil Polyphenols Metabolites. *Antioxidants* **2018**, *7* (12), 11–13. <https://doi.org/10.3390/antiox7120170>.
- (114) Aree, T.; Jongrungruangchok, S. Structure–Antioxidant Activity Relationship of  $\beta$ -Cyclodextrin Inclusion Complexes with Olive Tyrosol, Hydroxytyrosol and Oleuropein: Deep Insights from X-Ray Analysis, DFT Calculation and DPPH Assay. *Carbohydr. Polym.* **2018**, *199* (July), 661–669. <https://doi.org/10.1016/j.carbpol.2018.07.019>.
- (115) Naserzadeh, P.; Hafez, A. A.; Abdorahim, M.; Abdollahifar, M. A.; Shabani, R.; Peirovi, H.; Simchi, A.; Ashtari, K. Curcumin Loading Potentiates the Neuroprotective Efficacy of Fe<sub>3</sub>O<sub>4</sub>

- Magnetic Nanoparticles in Cerebellum Cells of Schizophrenic Rats. *Biomed. Pharmacother.* **2018**, *108* (September), 1244–1252. <https://doi.org/10.1016/j.biopha.2018.09.106>.
- (116) Rakotoarisoa, M.; Angelova, A. Amphiphilic Nanocarrier Systems for Curcumin Delivery in Neurodegenerative Disorders. *Medicines* **2018**, *5* (4), 126. <https://doi.org/10.3390/medicines5040126>.
- (117) Tiwari, B. K.; Valdramidis, V. P.; O'Donnell, C. P.; Muthukumarappan, K.; Bourke, P.; Cullen, P. J. Application of Natural Antimicrobials for Food Preservation. *J. Agric. Food Chem.* **2009**, *57* (14), 5987–6000. <https://doi.org/10.1021/jf900668n>.
- (118) Dorman, H. J. D.; Deans, S. G. Antimicrobial Agents from Plants: Antibacterial Activity of Plant Volatile Oils. *J. Appl. Microbiol.* **2000**, *88* (2), 308–316. <https://doi.org/10.1046/j.1365-2672.2000.00969.x>.
- (119) Burt, S. Essential Oils: Their Antibacterial Properties and Potential Applications in Foods - A Review. *Int. J. Food Microbiol.* **2004**, *94* (3), 223–253. <https://doi.org/10.1016/j.ijfoodmicro.2004.03.022>.
- (120) Mrozik, A.; Piotrowska-Seget, Z.; Łabuzek, S. Changes in Whole Cell-Derived Fatty Acids Induced by Naphthalene in Bacteria from Genus *Pseudomonas*. *Microbiol. Res.* **2004**, *159* (1), 87–95. <https://doi.org/10.1016/j.micres.2004.02.001>.
- (121) Lambert, R. J. W.; Skandamis, P. N.; Coote, P. J.; Nychas, G. J. E. A Study of the Minimum Inhibitory Concentration and Mode of Action of Oregano Essential Oil, Thymol and Carvacrol. *J. Appl. Microbiol.* **2001**, *91* (3), 453–462. <https://doi.org/10.1046/j.1365-2672.2001.01428.x>.
- (122) Ultee, A.; Bennik, M. H. J.; Moezelaar, R. The Phenolic Hydroxyl Group of Carvacrol Is Essential for Action against the Food-Borne Pathogen *Bacillus Cereus*. *Appl. Environ. Microbiol.* **2002**, *68* (4), 1561–1568. <https://doi.org/10.1128/AEM.68.4.1561-1568.2002>.
- (123) Sikkema, J.; De Bont, J.; Poolman, B. Mechanisms of Membrane Toxicity of Hydrocarbons. *Microbiol. Rev.* **1995**, *59* (2), 201–222.
- (124) Xu, J.; Zhou, F.; Ji, B. P.; Pei, R. S.; Xu, N. The Antibacterial Mechanism of Carvacrol and Thymol against *Escherichia Coli*. *Lett. Appl. Microbiol.* **2008**, *47* (3), 174–179. <https://doi.org/10.1111/j.1472-765X.2008.02407.x>.
- (125) Nazzaro, F.; Fratianni, F.; De Martino, L.; Coppola, R.; De Feo, V. Effect of Essential Oils on Pathogenic Bacteria. *Pharmaceuticals* **2013**, *6* (12), 1451–1474. <https://doi.org/10.3390/ph6121451>.
- (126) Wendakoon, C. N.; Morihiko, S. Inhibition of Amino Acid Decarboxylase Activity of *Enterobacter Aerogenes* by Active Components in Spices. *J. Food Prot.* **1995**, *58* (3), 280–283. <https://doi.org/10.4315/0362-028X-58.3.280>.
- (127) Di Pasqua, R.; Betts, G.; Hoskins, N.; Edwards, M.; Ercolini, D.; Mauriello, G. Membrane Toxicity of Antimicrobial Compounds from Essential Oils. *J. Agric. Food Chem.* **2007**, *55* (12), 4863–4870. <https://doi.org/10.1021/jf0636465>.
- (128) Di Pasqua, R.; Hoskins, N.; Betts, G.; Mauriello, G. Changes in Membrane Fatty Acids Composition of Microbial Cells Induced by Addition of Thymol, Carvacrol, Limonene, Cinnamaldehyde, and Eugenol in the Growing Media. *J. Agric. Food Chem.* **2006**, *54* (7), 2745–



2749. <https://doi.org/10.1021/jf0527221>.
- (129) Gomes, A.; Fernandes, E.; Lima, J.; Mira, L.; Corvo, M. Molecular Mechanisms of Anti-Inflammatory Activity Mediated by Flavonoids. *Curr. Med. Chem.* **2008**, *15* (16), 1586–1605. <https://doi.org/10.2174/092986708784911579>.
- (130) González, S. B.; Houghton, P. J.; Hout, J. R. S. The Activity against Leukocyte Eicosanoid Generation of Essential Oil and Polar Fractions of *Adesmia Boronioides* Hook.F. *Phyther. Res.* **2003**, *17* (3), 290–293. <https://doi.org/10.1002/ptr.1118>.
- (131) Wei, A.; Shibamoto, T. Antioxidant/Lipoxygenase Inhibitory Activities and Chemical Compositions of Selected Essential Oils. *J. Agric. Food Chem.* **2010**, *58* (12), 7218–7225. <https://doi.org/10.1021/jf101077s>.
- (132) Dung, N. T.; Bajpai, V. K.; Yoon, J. I.; Kang, S. C. Anti-Inflammatory Effects of Essential Oil Isolated from the Buds of *Cleistocalyx Operculatus* (Roxb.) Merr and Perry. *Food Chem. Toxicol.* **2009**, *47* (2), 449–453. <https://doi.org/10.1016/j.fct.2008.11.033>.
- (133) Chao, L. K.; Hua, K. F.; Hsu, H. Y.; Cheng, S. S.; Lin, I. F.; Chen, C. J.; Chen, S. T.; Chang, S. T. Cinnamaldehyde Inhibits Pro-Inflammatory Cytokines Secretion from Monocytes/Macrophages through Suppression of Intracellular Signaling. *Food Chem. Toxicol.* **2008**, *46* (1), 220–231. <https://doi.org/10.1016/j.fct.2007.07.016>.
- (134) García-Salinas, S.; Evangelopoulos, M.; Gámez-Herrera, E.; Arruebo, M.; Irusta, S.; Taraballi, F.; Mendoza, G.; Tasciotti, E. Electrospun Anti-Inflammatory Patch Loaded with Essential Oils for Wound Healing. *Int. J. Pharm.* **2020**, *577* (January), 119067. <https://doi.org/10.1016/j.ijpharm.2020.119067>.
- (135) Yoon, W. J.; Lee, N. H.; Hyun, C. G. Limonene Suppresses Lipopolysaccharide-Induced Production of Nitric Oxide, Prostaglandin E2, and pro-Inflammatory Cytokines in RAW 264.7 Macrophages. *J. Oleo Sci.* **2010**, *59* (8), 415–421. <https://doi.org/10.5650/jos.59.415>.
- (136) Yoon, W. J.; Moon, J. Y.; Song, G.; Lee, Y. K.; Han, M. S.; Lee, J. S.; Ihm, B. S.; Lee, W. J.; Lee, N. H.; Hyun, C. G. Artemisia Fukudo Essential Oil Attenuates LPS-Induced Inflammation by Suppressing NF-KB and MAPK Activation in RAW 264.7 Macrophages. *Food Chem. Toxicol.* **2010**, *48* (5), 1222–1229. <https://doi.org/10.1016/j.fct.2010.02.014>.
- (137) Yoshimura, A. Signal Transduction of Inflammatory Cytokines and Tumor Development. *Cancer Sci.* **2006**, *97* (6), 439–447. <https://doi.org/10.1111/j.1349-7006.2006.00197.x>.
- (138) Bailey, J. D.; Diotallevi, M.; Nicol, T.; McNeill, E.; Shaw, A.; Chuaiphichai, S.; Hale, A.; Starr, A.; Nandi, M.; Stylianou, E.; et al. Nitric Oxide Modulates Metabolic Remodeling in Inflammatory Macrophages through TCA Cycle Regulation and Itaconate Accumulation. *Cell Rep.* **2019**, *28* (1), 218–230.e7. <https://doi.org/10.1016/j.celrep.2019.06.018>.
- (139) Cardeno, A.; Aparicio-Soto, M.; Montserrat-de la Paz, S.; Bermúdez, B.; Muriana, F. J. G.; Alarcón-de-la-Lastra, C. Squalene Targets Pro- and Anti-Inflammatory Mediators and Pathways to Modulate over-Activation of Neutrophils, Monocytes and Macrophages. *J. Funct. Biomater.* **2015**, *14*, 779–790.
- (140) Zhou, H.; Beevers, C. S.; Huang, S. Targets of Curcumin. *NIH Public Access* **2012**, *12* (3), 332–347.

- (141) Youn, H. S.; Lee, J. K.; Choi, Y. J.; Saitoh, S. I.; Miyake, K.; Hwang, D. H.; Lee, J. Y. Cinnamaldehyde Suppresses Toll-like Receptor 4 Activation Mediated through the Inhibition of Receptor Oligomerization. *Biochem. Pharmacol.* **2008**, *75* (2), 494–502. <https://doi.org/10.1016/j.bcp.2007.08.033>.
- (142) Aggarwal, B. B.; Van Kuiken, M. E.; Iyer, L. H.; Harikumar, K. B.; Sung, B. Molecular Targets of Nutraceuticals Derived From Dietary Spices: Potential Role on Suppression of Inflammation and Tumorigenesis. *Exp. Biol. Med.* **2011**, *234* (8), 825–849. <https://doi.org/10.1161/CIRCULATIONAHA.110.956839>.
- (143) Quintas, V.; Prada-López, I.; Donos, N.; Suárez-Quintanilla, D.; Tomás, I. Antiplatelet Effect of Essential Oils and 0.2% Chlorhexidine on an in Situ Model of Oral Biofilm Growth: A Randomised Clinical Trial. *PLoS One* **2015**, *10* (2), 1–18. <https://doi.org/10.1371/journal.pone.0117177>.
- (144) Ahmed Mohamed Abbas, A. U. Treatment of Candidal Vulvovaginitis Using Cumin Seed Extract Cream <https://clinicaltrials.gov/ct2/show/study/NCT03005353?term=essential+oils&cond=%22Infecti+on%22&draw=2&rank=3> (accessed Mar 10, 2020).
- (145) Daunton, C.; Kothari, S.; Smith, L.; Steele, D. A History of Materials and Practices for Wound Management. *Wound Pract. Res. Aust. J. Wound Manag.* **2012**, *20* (4), 174–186.
- (146) Sarabahi, S. Recent Advances in Topical Wound Care. *Indian J. Plast. Surg.* **2012**, *45* (2), 379–387. <https://doi.org/10.4103/0970-0358.101321>.
- (147) Dhivya, S.; Vijaya Padma, V.; Santhini, E. Wound Dressings - a Review. *Biomedicine* **2015**, *5* (4), 24–28. <https://doi.org/10.7603/s40681-015-0022-9>.
- (148) Boateng, J. S.; Matthews, K. H.; Stevens, H. N. E.; Eccleston, G. M. Wound Healing Dressings and Drug Delivery Systems: A Review. *J. Pharm. Sci.* **2008**, *97* (8), 2892–2923. <https://doi.org/10.1002/jps.21210>.
- (149) Rivera, A. E.; Spencer, J. M. Clinical Aspects of Full-Thickness Wound Healing. *Clin. Dermatol.* **2007**, *25* (1), 39–48. <https://doi.org/10.1016/j.clindermatol.2006.10.001>.
- (150) Strecker-McGraw, M. K.; Jones, T. R.; Baer, D. G. Soft Tissue Wounds and Principles of Healing. *Emerg. Med. Clin. North Am.* **2007**, *25* (1), 1–22. <https://doi.org/10.1016/j.emc.2006.12.002>.
- (151) Morgan, D. Wounds - What Should a Dressings Formulary Include? *Hosp. Pharm.* **2002**, *9*, 261–266.
- (152) Timothy, T. US7048966B2 - Foam Composite, 2006.
- (153) Martin, L.; Wilson, C. G.; Koosha, F.; Tetley, L.; Gray, A. I.; Senel, S.; Uchegbu, I. F. The Release of Model Macromolecules May Be Controlled by the Hydrophobicity of Palmitoyl Glycol Chitosan Hydrogels. *J. Control. Release* **2002**, *80* (1–3), 87–100. [https://doi.org/10.1016/S0168-3659\(02\)00005-6](https://doi.org/10.1016/S0168-3659(02)00005-6).
- (154) Thomas, A.; Harding, K. G.; Moore, K. Alginates from Wound Dressings Activate Human Macrophages to Secrete Tumour Necrosis Factor- $\alpha$ . *Biomaterials* **2000**, *21* (17), 1797–1802. [https://doi.org/10.1016/S0142-9612\(00\)00072-7](https://doi.org/10.1016/S0142-9612(00)00072-7).

- (155) Ishihara, M.; Nakanishi, K.; Ono, K.; Sato, M.; Kikuchi, M.; Saito, Y.; Yura, H.; Matsui, T.; Hattori, H.; Uenoyama, M.; et al. Photocrosslinkable Chitosan as a Dressing for Wound Occlusion and Accelerator in Healing Process. *Biomaterials* **2002**, *23* (3), 833–840. [https://doi.org/10.1016/S0142-9612\(01\)00189-2](https://doi.org/10.1016/S0142-9612(01)00189-2).
- (156) Xie, X.; Fu, Y.; Liu, J. Chemical Reprogramming and Transdifferentiation. *Curr. Opin. Genet. Dev.* **2017**, *46* (M), 104–113. <https://doi.org/10.1016/j.gde.2017.07.003>.
- (157) Aderibigbe, B. A.; Buyana, B. Alginate in Wound Dressings. *Pharmaceutics* **2018**, *10* (2). <https://doi.org/10.3390/pharmaceutics10020042>.
- (158) Madaghiele, M.; Sannino, A.; Ambrosio, L.; Demitri, C. Polymeric Hydrogels for Burn Wound Care: Advanced Skin Wound Dressings and Regenerative Templates. *Burn. Trauma* **2014**, *2* (4), 153. <https://doi.org/10.4103/2321-3868.143616>.
- (159) Alvarenga Botrel, D.; Vilela Borges, S.; Victória de Barros Fernandes, R.; Dantas Viana, A.; Maria Gomes da Costa, J.; Reginaldo Marques, G. Evaluation of Spray Drying Conditions on Properties of Microencapsulated Oregano Essential Oil. *Int. J. Food Sci. Technol.* **2012**, *47* (11), 2289–2296. <https://doi.org/10.1111/j.1365-2621.2012.03100.x>.
- (160) Wen, P.; Zhu, D.-H.; WU, H.; M-H, Z.; Y-R, J.; S-Y, H. Encapsulation of Cinnamon Essential Oil in Electrospun Nanofibrous Film for Active Food Packaging. *Food Control* **2016**, *59*, 366–376.
- (161) Moomand, K.; Lim, L. T. Effects of Solvent and N-3 Rich Fish Oil on Physicochemical Properties of Electrospun Zein Fibres. *Food Hydrocoll.* **2015**, *46*, 191–200. <https://doi.org/10.1016/j.foodhyd.2014.12.014>.
- (162) Donsì, F.; Annunziata, M.; Sessa, M.; Ferrari, G. Nanoencapsulation of Essential Oils to Enhance Their Antimicrobial Activity in Foods. *LWT - Food Sci. Technol.* **2011**, *44* (9), 1908–1914. <https://doi.org/10.1016/j.lwt.2011.03.003>.
- (163) Najmeh Aboutorabi, S.; Nasiriboroumand, M.; Mohammadi, P.; Sheibani, H.; Barani, H. Preparation of Antibacterial Cotton Wound Dressing by Green Synthesis Silver Nanoparticles Using Mullein Leaves Extract. *J. Renew. Mater.* **2019**, *7* (8), 787–794. <https://doi.org/10.32604/jrm.2019.06438>.
- (164) Liakos, I.; Rizzello, L.; Scurr, D. J.; Pompa, P. P.; Bayer, I. S.; Athanassiou, A. All-Natural Composite Wound Dressing Films of Essential Oils Encapsulated in Sodium Alginate with Antimicrobial Properties. *Int. J. Pharm.* **2014**, *463* (2), 137–145. <https://doi.org/10.1016/j.ijpharm.2013.10.046>.
- (165) Agarwal, S.; Wendorff, J. H.; Greiner, A. Use of Electrospinning Technique for Biomedical Applications. *Polymer (Guildf).* **2008**, *49* (26), 5603–5621. <https://doi.org/10.1016/j.polymer.2008.09.014>.
- (166) Liakos, I.; Rizzello, L.; Hajiali, H.; Brunetti, V.; Carzino, R.; Pompa, P. P.; Athanassiou, A.; Mele, E. Fibrous Wound Dressings Encapsulating Essential Oils as Natural Antimicrobial Agents. *J. Mater. Chem. B* **2015**, *3* (8), 1583–1589. <https://doi.org/10.1039/c4tb01974a>.
- (167) Cooley, J. F. Apparatus for Electrically Dispersing Fluids. US Patent 692,631. *US Pat.* 692,631 **1900**, No. 692, 1–6.

- (168) Formhals. Formhals-1934- US Patent 1975504.Pdf. 1934.
- (169) Formhals, A. Methods and Apparatus for Spinning. *Lett. Pat.* **1944**, 2,349,950.
- (170) Wang, R.; Liu, Q.; Jiao, T.; Li, J.; Rao, Y.; Su, J.; Bai, Z.; Peng, Q. Facile Preparation and Enhanced Catalytic Properties of Self-Assembled Pd Nanoparticle-Loaded Nanocomposite Films Synthesized via the Electrospun Approach. *ACS Omega* **2019**, 4 (5), 8480–8486. <https://doi.org/10.1021/acsomega.9b01085>.
- (171) Lee, K. H.; Kim, H. Y.; Khil, M. S.; Ra, Y. M.; Lee, D. R. Characterization of Nano-Structured Poly( $\epsilon$ -Caprolactone) Nonwoven Mats via Electrospinning. *Polymer (Guildf)*. **2003**, 44 (4), 1287–1294. [https://doi.org/10.1016/S0032-3861\(02\)00820-0](https://doi.org/10.1016/S0032-3861(02)00820-0).
- (172) Martin, G. E.; Cockshott, I. D. Fibrillar Lining for Prosthetic Device. U.S. Pat. 4044404, 1977.
- (173) Li, D.; Xia, Y. Electrospinning of Nanofibers: Reinventing the Wheel? *Adv. Mater.* **2004**, 16 (14), 1151–1170. <https://doi.org/10.1002/adma.200400719>.
- (174) Sun, B.; Long, Y. Z.; Zhang, H. D.; Li, M. M.; Duvail, J. L.; Jiang, X. Y.; Yin, H. L. Advances in Three-Dimensional Nanofibrous Macrostructures via Electrospinning. *Prog. Polym. Sci.* **2014**, 39 (5), 862–890. <https://doi.org/10.1016/j.progpolymsci.2013.06.002>.
- (175) Liao, Y.; Loh, C. H.; Tian, M.; Wang, R.; Fane, A. G. Progress in Electrospun Polymeric Nanofibrous Membranes for Water Treatment: Fabrication, Modification and Applications. *Prog. Polym. Sci.* **2018**, 77, 69–94. <https://doi.org/10.1016/j.progpolymsci.2017.10.003>.
- (176) Xue, J.; Wu, T.; Dai, Y.; Xia, Y. Electrospinning and Electrospun Nanofibers: Methods, Materials, and Applications. *Chem. Rev.* **2019**, 119 (8), 5298–5415. <https://doi.org/10.1021/acs.chemrev.8b00593>.
- (177) Collins, R. T.; Jones, J. J.; Harris, M. T.; Basaran, O. A. Electrohydrodynamic Tip Streaming and Emission of Charged Drops from Liquidcones. *Nat. Phys.* **2008**, 4 (2), 149–154. <https://doi.org/10.1038/nphys807>.
- (178) Reneker, D. H.; Yarin, A. L.; Fong, H.; Koombhongse, S. Bending Instability of Electrically Charged Liquid Jets of Polymer Solutions in Electrospinning. *J. Appl. Phys.* **2000**, 87 (9 I), 4531–4547. <https://doi.org/10.1063/1.373532>.
- (179) Shin, Y. M.; Hohman, M. M.; Brenner, M. P.; Rutledge, G. C. Experimental Characterization of Electrospinning: The Electrically Forced Jet and Instabilities. *Polymer (Guildf)*. **2001**, 42 (25), 09955–09967. [https://doi.org/10.1016/s0032-3861\(01\)00540-7](https://doi.org/10.1016/s0032-3861(01)00540-7).
- (180) Yarin, A. L.; Koombhongse, S.; Reneker, D. H. Bending Instability in Electrospinning of Nanofibers. *J. Appl. Phys.* **2001**, 89 (5), 3018–3026. <https://doi.org/10.1063/1.1333035>.
- (181) Junoh, H.; Jaafar, J.; Mohd Norddin, M. N. A.; Ismail, A. F.; Othman, M. H. D.; Rahman, M. A.; Yusof, N.; Wan Salleh, W. N.; Ilbeygi, H. A Review on the Fabrication of Electrospun Polymer Electrolyte Membrane for Direct Methanol Fuel Cell. *J. Nanomater.* **2015**, 2015. <https://doi.org/10.1155/2015/690965>.
- (182) Piskin, E.; Bölgen, N.; Egri, S.; Isoglu, I. A. Electrospun Matrices Made of Poly( $\alpha$ -Hydroxy Acids) for Medical Use. *Nanomedicine* **2007**, 2 (4), 441–457. <https://doi.org/10.2217/17435889.2.4.441>.

- (183) Zhang, C.; Zhang, H. *Formation and Stability of Core-Shell Nanofibers by Electrospinning of Gel-Like Corn Oil-in-Water Emulsions Stabilized by Gelatin*; 2018; Vol. 66. <https://doi.org/10.1021/acs.jafc.8b04270>.
- (184) Cui, H.; Bai, M.; Lin, L. *Plasma-Treated Poly(Ethylene Oxide) Nanofibers Containing Tea Tree Oil/Beta-Cyclodextrin Inclusion Complex for Antibacterial Packaging*; Elsevier Ltd., 2018; Vol. 179. <https://doi.org/10.1016/j.carbpol.2017.10.011>.
- (185) Rieger, K. A.; Birch, N. P.; Schiffman, J. D. Electrospinning Chitosan/Poly(Ethylene Oxide) Solutions with Essential Oils: Correlating Solution Rheology to Nanofiber Formation. *Carbohydr. Polym.* **2016**, *139*, 131–138. <https://doi.org/10.1016/j.carbpol.2015.11.073>.
- (186) Osanloo, M.; Arish, J.; Sereshti, H. Developed Methods for the Preparation of Electrospun Nanofibers Containing Plant-Derived Oil or Essential Oil: A Systematic Review. *Polym. Bull.* **2019**, No. 0123456789. <https://doi.org/10.1007/s00289-019-03042-0>.
- (187) Corona-Gomez, J.; Chen, X.; Yang, Q. Effect of Nanoparticle Incorporation and Surface Coating on Mechanical Properties of Bone Scaffolds: A Brief Review. *J. Funct. Biomater.* **2016**, *7* (3), 18. <https://doi.org/10.3390/jfb7030018>.
- (188) Moghe, A. K.; Hufenus, R.; Hudson, S. M.; Gupta, B. S. Effect of the Addition of a Fugitive Salt on Electrospinnability of Poly( $\epsilon$ -Caprolactone). *Polymer (Guildf)*. **2009**, *50* (14), 3311–3318. <https://doi.org/10.1016/j.polymer.2009.04.063>.
- (189) Bui, H. T.; Chung, O. H.; Dela Cruz, J.; Park, J. S. Fabrication and Characterization of Electrospun Curcumin-Loaded Polycaprolactone-Polyethylene Glycol Nanofibers for Enhanced Wound Healing. *Macromol. Res.* **2014**, *22* (12), 1288–1296. <https://doi.org/10.1007/s13233-014-2179-6>.
- (190) Tampau, A.; González-Martínez, C.; Chiralt, A. Release Kinetics and Antimicrobial Properties of Carvacrol Encapsulated in Electrospun Poly-( $\epsilon$ -Caprolactone) Nanofibres. Application in Starch Multilayer Films. *Food Hydrocoll.* **2018**, *79*, 158–169. <https://doi.org/10.1016/j.foodhyd.2017.12.021>.
- (191) Martínez-Abad, A.; Sánchez, G.; Fuster, V.; Lagaron, J. M.; Ocio, M. J. Antibacterial Performance of Solvent Cast Polycaprolactone (PCL) Films Containing Essential Oils. *Food Control* **2013**, *34* (1), 214–220. <https://doi.org/10.1016/j.foodcont.2013.04.025>.
- (192) Hiltunen, T.; Virta, M.; Anna-Liisa, L. Antibiotic Resistance in the Wild: An Ecoevolutionary Perspective. *Philos. Trans. R. Soc. B Biol. Sci.* **2017**, *372* (1712). <https://doi.org/10.1098/rstb.2016.0039>.
- (193) Aperce, C. C.; Amachawadi, R.; Van Bibber-Krueger, C. L.; Nagaraja, T. G.; Scott, H. M.; Vinasco-Torre, J.; Drouillard, J. S. Effects of Menthol Supplementation in Feedlot Cattle Diets on the Fecal Prevalence of Antimicrobial-Resistant Escherichia Coli. *PLoS One* **2016**, *11* (12), 1–11. <https://doi.org/10.1371/journal.pone.0168983>.
- (194) O'Neill, J. Tackling Drug-Resistant Infections Globally: Final Report and Recommendations. *Rev. Antimicrob. Resist.* **2016**, 1–40.
- (195) Chambers, H. F.; Deleo, F. R. Waves of Resistance: Staphylococcus Aureus in the Antibiotic Era. *Nat. Rev. Microbiol.* **2009**, *7* (9), 629–641. <https://doi.org/10.1038/nrmicro2200>.

- (196) Bush, K.; Courvalin, P.; Dantas, G.; Davies, J.; Eisenstein, B.; Huovinen, P.; Jacoby, G. A.; Kishony, R.; Kreiswirth, B. N.; Kutter, E.; et al. Tackling Antibiotic Resistance. *Nat. Rev. Microbiol.* **2011**, *9* (12), 894–896. <https://doi.org/10.1038/nrmicro2693>.
- (197) Scandorieiro, S.; de Camargo, L. C.; Lancheros, C. A. C.; Yamada-Ogatta, S. F.; Nakamura, C. V.; de Oliveira, A. G.; Andrade, C. G. T. J.; Duran, N.; Nakazato, G.; Kobayashi, R. K. T. Synergistic and Additive Effect of Oregano Essential Oil and Biological Silver Nanoparticles against Multidrug-Resistant Bacterial Strains. *Front. Microbiol.* **2016**, *7* (MAY), 1–14. <https://doi.org/10.3389/fmicb.2016.00760>.
- (198) Billing, J.; Sherman, P. W. Antimicrobial Functions of Spices: Why Some like It Hot. *Chicago Journals* **1998**, *73* (1), 3–49.
- (199) Langeveld, W. T.; Veldhuizen, E. J. A.; Burt, S. A. Synergy between Essential Oil Components and Antibiotics: A Review. *Crit. Rev. Microbiol.* **2014**, *40* (1), 76–94. <https://doi.org/10.3109/1040841X.2013.763219>.
- (200) Lu, Z.; Chen, Y.; Chen, W.; Liu, H.; Song, Q.; Hu, X.; Zou, Z.; Liu, Z.; Duo, L.; Yang, J.; et al. Characteristics of QacA/B-Positive Staphylococcus Aureus Isolated from Patients and a Hospital Environment in China. *J. Antimicrob. Chemother.* **2015**, *70* (3), 653–657. <https://doi.org/10.1093/jac/dku456>.
- (201) Bilia, A. R.; Guccione, C.; Isacchi, B.; Righeschi, C.; Firenzuoli, F.; Bergonzi, M. C. Essential Oils Loaded in Nanosystems: A Developing Strategy for a Successful Therapeutic Approach. *Evidence-based Complement. Altern. Med.* **2014**, *2014*. <https://doi.org/10.1155/2014/651593>.
- (202) Hui, X.; Yan, G.; Tian, F. L.; Li, H.; Gao, W. Y. Antimicrobial Mechanism of the Major Active Essential Oil Compounds and Their Structure–Activity Relationship. *Med. Chem. Res.* **2017**, *26* (2), 442–449. <https://doi.org/10.1007/s00044-016-1762-0>.
- (203) Nostro, A.; Blanco, A. R.; Cannatelli, M. A.; Enea, V.; Flamini, G.; Morelli, I.; Roccaro, A. S.; Alonzo, V. Susceptibility of Methicillin-Resistant Staphylococci to Oregano Essential Oil, Carvacrol and Thymol. *FEMS Microbiol. Lett.* **2004**, *230* (2), 191–195. [https://doi.org/10.1016/S0378-1097\(03\)00890-5](https://doi.org/10.1016/S0378-1097(03)00890-5).
- (204) Cho, Y.; Lee, H.-J. Antibacterial Effects of Carvacrol against Staphylococcus Aureus and Escherichia Coli O157:H7. *J. Biomed. Res.* **2014**, *15* (3), 117–122. <https://doi.org/10.12729/jbr.2014.15.3.117>.
- (205) Wang, L. H.; Wang, M. S.; Zeng, X. A.; Zhang, Z. H.; Gong, D. M.; Huang, Y. B. Membrane Destruction and DNA Binding of Staphylococcus Aureus Cells Induced by Carvacrol and Its Combined Effect with a Pulsed Electric Field. *J. Agric. Food Chem.* **2016**, *64* (32), 6355–6363. <https://doi.org/10.1021/acs.jafc.6b02507>.
- (206) Silva Da Luz, I.; Gomes Neto, N. J.; Tavares, A. G.; Nunes, P. C.; Magnani, M.; De Souza, E. L. Lack of Induction of Direct Protection or Cross-Protection in Staphylococcus Aureus by Sublethal Concentrations of Origanum Vulgare L. Essential Oil and Carvacrol in a Meat-Based Medium. *Arch. Microbiol.* **2013**, *195* (8), 587–593. <https://doi.org/10.1007/s00203-013-0907-5>.
- (207) Rua, J.; Fernandez, L.; Castro, C. De; Valle, P.; De Arriaga, D.; García-Armesto, M. R. Antibacterial Activity against Foodborne Staphylococcus Aureus and Antioxidant Capacity of Various Pure Phenolic Compounds. *Foodborne Pathog. Dis.* **2011**, *8* (1), 149–157.

- (208) Gavarić, N.; Mozina, S. S.; Kladar, N.; Božin, B. Chemical Profile, Antioxidant and Antibacterial Activity of Thyme and Oregano Essential Oils, Thymol and Carvacrol and Their Possible Synergism. *J. Essent. Oil-Bearing Plants* **2015**, *18* (4), 1013–1021. <https://doi.org/10.1080/0972060X.2014.971069>.
- (209) Ye, H.; Shen, S.; Xu, J.; Lin, S.; Yuan, Y.; Jones, G. S. Synergistic Interactions of Cinnamaldehyde in Combination with Carvacrol against Food-Borne Bacteria. *Food Control* **2013**, *34* (2), 619–623. <https://doi.org/10.1016/j.foodcont.2013.05.032>.
- (210) Andreu, V.; Mendoza, G.; Arruebo, M.; Irusta, S. Smart Dressings Based on Nanostructured Fibers Containing Natural Origin Antimicrobial, Anti-Inflammatory, and Regenerative Compounds. *Materials (Basel)*. **2015**, *8* (8), 5154–5193. <https://doi.org/10.3390/ma8085154>.
- (211) Fratini, F.; Mancini, S.; Turchi, B.; Friscia, E.; Pistelli, L.; Giusti, G.; Cerri, D. A Novel Interpretation of the Fractional Inhibitory Concentration Index: The Case *Origanum Vulgare* L. and *Leptospermum Scoparium* J. R. et G. Forst Essential Oils against *Staphylococcus Aureus* Strains. *Microbiol. Res.* **2017**, *195*, 11–17. <https://doi.org/10.1016/j.micres.2016.11.005>.
- (212) de Sousa, N. T. A.; Gomes, R. C.; Santos, M. F.; Brandino, H. E.; Martinez, R.; de Jesus Guirro, R. R. Red and Infrared Laser Therapy Inhibits in Vitro Growth of Major Bacterial Species That Commonly Colonize Skin Ulcers. *Lasers Med. Sci.* **2016**, *31* (3), 549–556. <https://doi.org/10.1007/s10103-016-1907-x>.
- (213) Krogsgård Nielsen, C.; Kjems, J.; Mygind, T.; Snabe, T.; Schwarz, K.; Serfert, Y.; Meyer, R. L. Antimicrobial Effect of Emulsion-Encapsulated Isoeugenol against Biofilms of Food Pathogens and Spoilage Bacteria. *Int. J. Food Microbiol.* **2017**, *242*, 7–12. <https://doi.org/10.1016/j.ijfoodmicro.2016.11.002>.
- (214) Duncan, B.; Li, X.; Landis, R. F.; Kim, S. T.; Gupta, A.; Wang, L. S.; Ramanathan, R.; Tang, R.; Boerth, J. A.; Rotello, V. M. Nanoparticle-Stabilized Capsules for the Treatment of Bacterial Biofilms. *ACS Nano* **2015**, *9* (8), 7775–7782. <https://doi.org/10.1021/acsnano.5b01696>.
- (215) Kifer, D.; Mužinić, V.; Klaric, M. Š. Antimicrobial Potency of Single and Combined Mupirocin and Monoterpenes, Thymol, Menthol and 1,8-Cineole against *Staphylococcus Aureus* Planktonic and Biofilm Growth. *J. Antibiot. (Tokyo)*. **2016**, *69* (9), 689–696. <https://doi.org/10.1038/ja.2016.10>.
- (216) Patel J.B., Cockerill R.F., Bradford A.P., Eliopoulos M.G., Hindler A.J., Jenkins G.S., Lewis S.J., Limbago B., Miller A.L., Nicolau P.D., Pwell M., Swenson M.J., Traczewski M.M., Turnidge J.D., W. P. M. Z. L. B. M07-A10: Methods for Dilution Antimicrobial Susceptibility Tests for Bacteria That Grow Aerobically; Approved Standard—Tenth Edition. *CLSI (Clinical Lab. Stand. Institute)* **2015**, *35* (2). <https://doi.org/10.1007/s00259-009-1334-3>.
- (217) Ciandrini, E.; Campana, R.; Federici, S.; Manti, A.; Battistelli, M.; Falcieri, E.; Papa, S.; Baffone, W. In Vitro Activity of Carvacrol against Titanium-Adherent Oral Biofilms and Planktonic Cultures. *Clin. Oral Investig.* **2014**, *18* (8), 2001–2013. <https://doi.org/10.1007/s00784-013-1179-9>.
- (218) Moghimi, R.; Aliahmadi, A.; Rafati, H. Ultrasonic Nanoemulsification of Food Grade Trans-Cinnamaldehyde: 1,8-Cineol and Investigation of the Mechanism of Antibacterial Activity. *Ultrason. Sonochem.* **2017**, *35*, 415–421. <https://doi.org/10.1016/j.ultsonch.2016.10.020>.
- (219) Devi, K. P.; Sakthivel, R.; Nisha, S. A.; Suganthi, N.; Pandian, S. K. Eugenol Alters the Integrity

- of Cell Membrane and Acts against the Nosocomial Pathogen *Proteus Mirabilis*. *Arch. Pharm. Res.* **2013**, *36* (3), 282–292. <https://doi.org/10.1007/s12272-013-0028-3>.
- (220) Sabulal, B.; Dan, M.; J, A. J.; Kurup, R.; Pradeep, N. S.; Valsamma, R. K.; George, V. Caryophyllene-Rich Rhizome Oil of *Zingiber Nimmonii* from South India: Chemical Characterization and Antimicrobial Activity. *Phytochemistry* **2006**, *67* (22), 2469–2473. <https://doi.org/10.1016/j.phytochem.2006.08.003>.
- (221) Slobodníková, L.; Fialová, S.; Hupková, H.; Grančai, D. Rosmarinic Acid Interaction with Planktonic and Biofilm *Staphylococcus Aureus*. *Nat. Prod. Commun.* **2013**, *8* (12), 1747–1750. <https://doi.org/10.1177/1934578x1300801223>.
- (222) Liang, Y.; Yuxia, Z.; Yabo, J.; Yajie, H.; Jianyu, W.; Zepeng, C.; Dingxin, J. ESR Study on Scavenging Effect of Squalene on Free Radicals in Mainstream Cigarette Smoke. *Appl. Magn. Reson.* **2017**, *48* (2), 201–212. <https://doi.org/10.1007/s00723-016-0856-7>.
- (223) Apolónio, J.; Faleiro, M. L.; Miguel, M. G.; Neto, L. No Induction of Antimicrobial Resistance in *Staphylococcus Aureus* and *Listeria Monocytogenes* during Continuous Exposure to Eugenol and Citral. *FEMS Microbiol. Lett.* **2014**, *354* (2), 92–101. <https://doi.org/10.1111/1574-6968.12440>.
- (224) Becerril, R.; Nerín, C.; Gómez-Lus, R. Evaluation of Bacterial Resistance to Essential Oils and Antibiotics after Exposure to Oregano and Cinnamon Essential Oils. *Foodborne Pathog. Dis.* **2012**, *9* (8), 699–705. <https://doi.org/10.1089/fpd.2011.1097>.
- (225) Magi, G.; Marini, E.; Facinelli, B. Antimicrobial Activity of Essential Oils and Carvacrol, and Synergy of Carvacrol and Erythromycin, against Clinical, Erythromycin-Resistant Group A Streptococci. *Front. Microbiol.* **2015**, *6* (MAR), 1–7. <https://doi.org/10.3389/fmicb.2015.00165>.
- (226) Kuyyakanond, T.; Quesnel, L. B. The Mechanism of Action of Chlorhexidine. *FEMS Microbiol. Lett.* **1992**, *100* (1–3), 211–215. [https://doi.org/10.1016/0378-1097\(92\)90211-6](https://doi.org/10.1016/0378-1097(92)90211-6).
- (227) Gant, V. A.; Warnes, G.; Phillips, I.; Savidge, G. F. The Application of Flow Cytometry to the Study of Bacterial Responses to Antibiotics. *J. Med. Microbiol.* **1993**, *39* (2), 147–154. <https://doi.org/10.1099/00222615-39-2-147>.
- (228) Lv, F.; Liang, H.; Yuan, Q.; Li, C. In Vitro Antimicrobial Effects and Mechanism of Action of Selected Plant Essential Oil Combinations against Four Food-Related Microorganisms. *Food Res. Int.* **2011**, *44* (9), 3057–3064. <https://doi.org/10.1016/j.foodres.2011.07.030>.
- (229) Krepker, M.; Shemesh, R.; Danin Poleg, Y.; Kashi, Y.; Vaxman, A.; Segal, E. Active Food Packaging Films with Synergistic Antimicrobial Activity. *Food Control* **2017**, *76*, 117–126. <https://doi.org/10.1016/j.foodcont.2017.01.014>.
- (230) Van den Driessche, F.; Brackman, G.; Swimberghe, R.; Rigole, P.; Coenye, T. Screening a Repurposing Library for Potentiators of Antibiotics against *Staphylococcus Aureus* Biofilms. *Int. J. Antimicrob. Agents* **2017**, *49* (3), 315–320. <https://doi.org/10.1016/j.ijantimicag.2016.11.023>.
- (231) Zhou, F.; Ji, B.; Zhang, H.; Jiang, H.; Yang, Z.; Li, J.; Li, J.; Yan, W. The Antibacterial Effect of Cinnamaldehyde, Thymol, Carvacrol and Their Combinations against the Foodborne Pathogen *Salmonella Typhimurium*. *J. Food Saf.* **2007**, *27* (2), 124–133. <https://doi.org/10.1111/j.1745-4565.2007.00064.x>.



- (232) Xiao, L.; Miwa, N. Hydrogen-Rich Water Achieves Cytoprotection from Oxidative Stress Injury in Human Gingival Fibroblasts in Culture or 3D-Tissue Equivalents, and Wound-Healing Promotion, Together with ROS-Scavenging and Relief from Glutathione Diminishment. *Hum. Cell* **2017**, *30* (2), 72–87. <https://doi.org/10.1007/s13577-016-0150-x>.
- (233) *ISO 10993-5:2009—Biological Evaluation of Medical Devices—Part 5: Tests for In Vitro Cytotoxicity*; 2009.
- (234) Melo, J. O.; Fachin, A. L.; Rizo, W. F.; Jesus, H. C. R.; Arrigoni-Blank, M. F.; Alves, P. B.; Marins, M. A.; França, S. C.; Blank, A. F. Cytotoxic Effects of Essential Oils from Three *Lippia Gracilis* Schauer Genotypes on HeLa, B16, and MCF-7 Cells and Normal Human Fibroblasts. *Genet. Mol. Res.* **2014**, *13* (2), 2691–2697. <https://doi.org/10.4238/2014.April.8.12>.
- (235) Llana-Ruiz-Cabello, M.; Gutiérrez-Praena, D.; Pichardo, S.; Moreno, F. J.; Bermúdez, J. M.; Aucejo, S.; Cameán, A. M. Cytotoxicity and Morphological Effects Induced by Carvacrol and Thymol on the Human Cell Line Caco-2. *Food Chem. Toxicol.* **2014**, *64*, 281–290. <https://doi.org/10.1016/j.fct.2013.12.005>.
- (236) Günes-Bayir, A.; Kiziltan, H. S.; Kocyigit, A.; Güler, E. M.; Karataş, E.; Toprak, A. Effects of Natural Phenolic Compound Carvacrol on the Human Gastric Adenocarcinoma (AGS) Cells in Vitro. *Anticancer. Drugs* **2017**, *28* (5), 522–530. <https://doi.org/10.1097/CAD.0000000000000491>.
- (237) Yu, C.; Liu, S. L.; Qi, M. H.; Zou, X. Cinnamaldehyde/ Chemotherapeutic Agents Interaction and Drug-Metabolizing Genes in Colorectal Cancer. *Mol. Med. Rep.* **2014**, *9* (2), 669–676. <https://doi.org/10.3892/mmr.2013.1830>.
- (238) Klein, E. Y.; Van Boeckel, T. P.; Martinez, E. M.; Pant, S.; Gandra, S.; Levin, S. A.; Goossens, H.; Laxminarayan, R. Global Increase and Geographic Convergence in Antibiotic Consumption between 2000 and 2015. *Proc. Natl. Acad. Sci. U. S. A.* **2018**, *115* (15), E3463–E3470. <https://doi.org/10.1073/pnas.1717295115>.
- (239) Deb, D. D.; Parimala, G.; Saravana Devi, S.; Chakraborty, T. Effect of Thymol on Peripheral Blood Mononuclear Cell PBMC and Acute Promyelotic Cancer Cell Line HL-60. *Chem. Biol. Interact.* **2011**, *193* (1), 97–106. <https://doi.org/10.1016/j.cbi.2011.05.009>.
- (240) García-Salinas, S.; Elizondo-Castillo, H.; Arruebo, M.; Mendoza, G.; Irusta, S. Evaluation of the Antimicrobial Activity and Cytotoxicity of Different Components of Natural Origin Present in Essential Oils. *Molecules* **2018**, *23* (6), 1–18. <https://doi.org/10.3390/molecules23061399>.
- (241) Gresham, H. D.; Lowrance, J. H.; Caver, T. E.; Wilson, B. S.; Cheung, A. L.; Lindberg, F. P. Survival of *Staphylococcus Aureus* Inside Neutrophils Contributes to Infection. *J. Immunol.* **2000**, *164* (7), 3713–3722. <https://doi.org/10.4049/jimmunol.164.7.3713>.
- (242) Froiio, F.; Ginot, L.; Paolino, D.; Lebaz, N.; Bentaher, A.; Fessi, H.; Elaissari, A. Essential Oils-Loaded Polymer Particles: Preparation, Characterization and Antimicrobial Property. *Polymers (Basel)*. **2019**, *11* (6). <https://doi.org/10.3390/polym11061017>.
- (243) Hamed Laroui, Poonam Rakhya, Bo Xiao, E. V. and D. M. Nanotechnology in Diagnostics and Therapeutics for Gastrointestinal Disorders. *Bone* **2013**, *45* (12), 995–1002. <https://doi.org/10.1038/jid.2014.371>.
- (244) Sill, T. J.; von Recum, H. A. Electrospinning: Applications in Drug Delivery and Tissue

- Engineering. *Biomaterials* **2008**, 29 (13), 1989–2006.  
<https://doi.org/10.1016/j.biomaterials.2008.01.011>.
- (245) Gilchrist, S. E.; Lange, D.; Letchford, K.; Bach, H.; Fazli, L.; Burt, H. M. Fusidic Acid and Rifampicin Co-Loaded PLGA Nanofibers for the Prevention of Orthopedic Implant Associated Infections. *J. Control. Release* **2013**, 170 (1), 64–73.  
<https://doi.org/10.1016/j.jconrel.2013.04.012>.
- (246) Manesh, K. M.; Santhosh, P.; Gopalan, A.; Lee, K. P. Electrospun Poly(Vinylidene Fluoride)/Poly(Aminophenylboronic Acid) Composite Nanofibrous Membrane as a Novel Glucose Sensor. *Anal. Biochem.* **2007**, 360 (2), 189–195.  
<https://doi.org/10.1016/j.ab.2006.09.021>.
- (247) Gámez, E.; Mendoza, G.; Salido, S.; Arruebo, M.; Irusta, S. Antimicrobial Electrospun Polycaprolactone-Based Wound Dressings: An in Vitro Study about the Importance of the Direct Contact to Elicit Bactericidal Activity. *Adv. Wound Care* **2019**, 8 (9), 438–451.  
<https://doi.org/10.1089/wound.2018.0893>.
- (248) Rasouli, R.; Barhoum, A.; Bechelany, M.; Dufresne, A. Nanofibers for Biomedical and Healthcare Applications. *Macromol. Biosci.* **2019**, 19 (2), 1–27.  
<https://doi.org/10.1002/mabi.201800256>.
- (249) Zeng, H.; Cui, J.; Cao, B.; Gibson, U.; Bando, Y.; Golberg, D. Electrochemical Deposition of ZnO Nanowire Arrays: Organization, Doping and Properties. *Sci. Adv. Mater.* **2010**, 2 (3), 336–358.
- (250) Jiang, S.; Chen, Y.; Duan, G.; Mei, C.; Greiner, A.; Agarwal, S. Electrospun Nanofiber Reinforced Composites: A Review. *Polym. Chem.* **2018**, 9 (20), 2685–2720.  
<https://doi.org/10.1039/c8py00378e>.
- (251) Jang, C. H.; Cho, Y. B.; Jang, Y. S.; Kim, M. S.; Kim, G. H. Antibacterial Effect of Electrospun Polycaprolactone/Polyethylene Oxide/Vancomycin Nanofiber Mat for Prevention of Periprosthetic Infection and Biofilm Formation. *Int. J. Pediatr. Otorhinolaryngol.* **2015**, 79 (8), 1299–1305. <https://doi.org/10.1016/j.ijporl.2015.05.037>.
- (252) Guarino, V.; Cruz-Maya, I.; Altobelli, R.; Abdul Khodir, W. K.; Ambrosio, L.; Alvarez Pèrez, M. A.; Flores, A. A. Electrospun Polycaprolactone Nanofibres Decorated by Drug Loaded Chitosan Nano-Reservoirs for Antibacterial Treatments. *Nanotechnology* **2017**, 28 (50).  
<https://doi.org/10.1088/1361-6528/aa9542>.
- (253) Adeli-sardou, M.; Torkzadeh-Mahani, M.; Yaghoobi, M. M.; Dodel, M. Antibacterial and Anti-Biofilm Investigation of Electrospun PCL/Gelatin/Lawsone Nano Fiber Scaffolds against Biofilm Producing Bacteria. *Biomacromolecular J.* **2018**, 4 (1), 46–57.
- (254) Hall-Stoodley, L.; Costerton, J. W.; Stoodley, P. Bacterial Biofilms: From the Natural Environment to Infectious Diseases. *Nat. Rev. Microbiol.* **2004**, 2 (2), 95–108.  
<https://doi.org/10.1038/nrmicro821>.
- (255) Kerekes, E. B.; Vidács, A.; Takó, M.; Petkovits, T.; Vágvölgyi, C.; Horváth, G.; Balázs, V. L.; Krisch, J. Anti-Biofilm Effect of Selected Essential Oils and Main Components on Mono- and Polymicrobial Bacterial Cultures. *Microorganisms* **2019**, 7 (9).  
<https://doi.org/10.3390/microorganisms7090345>.

- (256) Quave, C. L.; Estévez-Carmona, M.; Compadre, C. M.; Hobby, G.; Hendrickson, H.; Beenken, K. E.; Smeltzer, M. S. Ellagic Acid Derivatives from *Rubus Ulmifolius* Inhibit *Staphylococcus Aureus* Biofilm Formation and Improve Response to Antibiotics. *PLoS One* **2012**, *7* (1). <https://doi.org/10.1371/journal.pone.0028737>.
- (257) Sharifi, A.; Mohammadzadeh, A.; Zahraei Salehi, T.; Mahmoodi, P. Antibacterial, Antibiofilm and Antiquorum Sensing Effects of *Thymus Daenensis* and *Satureja Hortensis* Essential Oils against *Staphylococcus Aureus* Isolates. *J. Appl. Microbiol.* **2018**, *124* (2), 379–388. <https://doi.org/10.1111/jam.13639>.
- (258) Čabarkapa, I.; Čolović, R.; Đuragić, O.; Popović, S.; Kokić, B.; Milanov, D.; Pezo, L. Anti-Biofilm Activities of Essential Oils Rich in Carvacrol and Thymol against *Salmonella Enteritidis*. *Biofouling* **2019**, *35* (3), 361–375. <https://doi.org/10.1080/08927014.2019.1610169>.
- (259) Malone, M.; Bjarnsholt, T.; McBain, A. J.; James, G. A.; Stoodley, P.; Leaper, D.; Tachi, M.; Schultz, G.; Swanson, T.; Wolcott, R. D. The Prevalence of Biofilms in Chronic Wounds: A Systematic Review and Meta-Analysis of Published Data. *J. Wound Care* **2017**, *26* (1), 20–25. <https://doi.org/10.12968/jowc.2017.26.1.20>.
- (260) Moyano, A. J.; Mas, C. R.; Colque, C. A.; Smania, A. M. Dealing with Biofilms of *Pseudomonas Aeruginosa* and *Staphylococcus Aureus*: In Vitro Evaluation of a Novel Aerosol Formulation of Silver Sulfadiazine. *Burns* **2019**, *46* (1), 128–135. <https://doi.org/10.1016/j.burns.2019.07.027>.
- (261) Johnson, J. T.; Yu, V. L. Role of Anaerobic Bacteria in Postoperative Wound Infections Following Oncologic Surgery of the Head and Neck. *Ann. Otol. Rhinol. Laryngol.* **1991**, *100* (9 II SUPPL. 154), 46–48. <https://doi.org/10.1177/00034894911000s913>.
- (262) Martin, P.; Leibovich, S. J. Inflammatory Cells during Wound Repair: The Good, the Bad and the Ugly. *Trends Cell Biol.* **2005**, *15* (11), 599–607. <https://doi.org/10.1016/j.tcb.2005.09.002>.
- (263) Krzyszczyk, P.; Schloss, R.; Palmer, A.; Berthiaume, F. The Role of Macrophages in Acute and Chronic Wound Healing and Interventions to Promote Pro-Wound Healing Phenotypes. *Front. Physiol.* **2018**, *9* (MAY), 1–22. <https://doi.org/10.3389/fphys.2018.00419>.
- (264) Mal, P.; Dutta, K.; Bandyopadhyay, D.; Basu, A.; Khan, R.; Bishayi, B. Azithromycin in Combination with Riboflavin Decreases the Severity of *Staphylococcus Aureus* Infection Induced Septic Arthritis by Modulating the Production of Free Radicals and Endogenous Cytokines. *Inflamm. Res.* **2013**, *62* (3), 259–273. <https://doi.org/10.1007/s00011-012-0574-z>.
- (265) Miramoth, N. S.; Di Meo, C.; Zouhiri, F.; Saïd-Hassane, F.; Valetti, S.; Gorges, R.; Nicolas, V.; Poupaert, J. H.; Chollet-Martin, S.; Desmaële, D.; et al. Self-Assembled Squalenoylated Penicillin Bioconjugates: An Original Approach for the Treatment of Intracellular Infections. *ACS Nano* **2012**, *6* (5), 3820–3831. <https://doi.org/10.1021/nn204928v>.
- (266) Dey, S.; Bishayi, B. Killing of *Staphylococcus Aureus* in Murine Macrophages by Chloroquine Used Alone and in Combination with Ciprofloxacin or Azithromycin. *J. Inflamm. Res.* **2015**, *8*, 29–47. <https://doi.org/10.2147/JIR.S76045>.
- (267) Mendoza, G.; Regiel-Futyra, A.; Andreu, V.; Sebastián, V.; Kyzioł, A.; Stochel, G.; Arruebo, M. Bactericidal Effect of Gold-Chitosan Nanocomposites in Coculture Models of Pathogenic Bacteria and Human Macrophages. *ACS Appl. Mater. Interfaces* **2017**, *9* (21), 17693–17701. <https://doi.org/10.1021/acsami.6b15123>.

- (268) International, A. *ASTM E2180-18, Standard Test Method for Determining the Activity of Incorporated Antimicrobial Agent(s) In Polymeric or Hydrophobic Materials*; West Conshohocken, PA, 2018.
- (269) Sadeghianmaryan, A.; Yazdanpanah, Z.; Soltani, Y. A.; Sardroud, H. A.; Nasirtabrizi, M. H.; Chen, X. Curcumin-loaded Electrospun Polycaprolactone/Montmorillonite Nanocomposite: Wound Dressing Application with Anti-bacterial and Low Cell Toxicity Properties. *J. Biomater. Sci. Polym. Ed.* **2019**, *0* (0), 000. <https://doi.org/10.1080/09205063.2019.1680928>.
- (270) Alves, P. E.; Soares, B. G.; Lins, L. C.; Livi, S.; Santos, E. P. Controlled Delivery of Dexamethasone and Betamethasone from PLA Electrospun Fibers: A Comparative Study. *Eur. Polym. J.* **2019**, *117* (April), 1–9. <https://doi.org/10.1016/j.eurpolymj.2019.05.001>.
- (271) Alfaro De Prá, M. A.; Ribeiro-do-Valle, R. M.; Maraschin, M.; Veleirinho, B. Effect of Collector Design on the Morphological Properties of Polycaprolactone Electrospun Fibers. *Mater. Lett.* **2017**, *193*, 154–157. <https://doi.org/10.1016/j.matlet.2017.01.102>.
- (272) Aragón, J.; Costa, C.; Coelho, I.; Mendoza, G.; Aguiar-Ricardo, A.; Irusta, S. Electrospun Asymmetric Membranes for Wound Dressing Applications. *Mater. Sci. Eng. C* **2019**, *103* (April), 109822. <https://doi.org/10.1016/j.msec.2019.109822>.
- (273) Peppas, N. A.; Sahlin, J. J. A Simple Equation for the Description of Solute Release. III. Coupling of Diffusion and Relaxation. *Int. J. Pharm.* **1989**, *57* (2), 169–172. [https://doi.org/10.1016/0378-5173\(89\)90306-2](https://doi.org/10.1016/0378-5173(89)90306-2).
- (274) Badawy, M. E. I.; Marei, G. I. K.; Rabea, E. I.; Taktak, N. E. M. Antimicrobial and Antioxidant Activities of Hydrocarbon and Oxygenated Monoterpenes against Some Foodborne Pathogens through in Vitro and in Silico Studies. *Pestic. Biochem. Physiol.* **2019**, *158* (May), 185–200. <https://doi.org/10.1016/j.pestbp.2019.05.008>.
- (275) Rúa, J.; Del Valle, P.; De Arriaga, D.; Fernández-Álvarez, L.; García-Armesto, M. R. Combination of Carvacrol and Thymol: Antimicrobial Activity Against *Staphylococcus Aureus* and Antioxidant Activity. *Foodborne Pathog. Dis.* **2019**, *16* (9), 622–629. <https://doi.org/10.1089/fpd.2018.2594>.
- (276) Leaper, D. J.; Schultz, G.; Carville, K.; Fletcher, J.; Swanson, T.; Drake, R. Extending the TIME Concept: What Have We Learned in the Past 10 Years? *Int. Wound J.* **2012**, *9* (Suppl 2), 1–19.
- (277) Chung, P. Y.; Toh, Y. S. Anti-Biofilm Agents: Recent Breakthrough against Multi-Drug Resistant *Staphylococcus Aureus*. *Pathog. Dis.* **2014**, *70* (3), 231–239. <https://doi.org/10.1111/2049-632X.12141>.
- (278) Yuan, Z.; Dai, Y.; Ouyang, P.; Rehman, T.; Hussain, S.; Zhang, T.; Yin, Z.; Fu, H.; Lin, J.; He, C.; et al. Thymol Inhibits Biofilm Formation, Eliminates Pre- Existing Biofilms, and Enhances Clearance of Methicillin-resistant *Staphylococcus Aureus* (MRSA) in a Mouse Peritoneal Implant Infection Model. *Microorganisms* **2020**, *8* (1), 1–17. <https://doi.org/10.3390/microorganisms8010099>.
- (279) Joo, H. S.; Otto, M. Molecular Basis of in Vivo Biofilm Formation by Bacterial Pathogens. *Chem. Biol.* **2012**, *19* (12), 1503–1513. <https://doi.org/10.1016/j.chembiol.2012.10.022>.
- (280) Wolcott, R.; Dowd, S. The Role of Biofilms: Are We Hitting the Right Target? *Plast. Reconstr. Surg.* **2011**, *127* (SUPPL. 1 S), 28–35. <https://doi.org/10.1097/PRS.0b013e3181fca244>.

- (281) Underhill, D. M.; Goodridge, H. S. Information Processing during Phagocytosis. *Nat. Rev. Immunol.* **2012**, *12* (7), 492–502. <https://doi.org/10.1038/nri3244>.
- (282) Belato, K. K.; de Oliveira, J. R.; de Oliveira, F. S.; de Oliveira, L. D.; Camargo, S. E. A. Cytotoxicity and Genotoxicity of Thymol Verified in Murine Macrophages (RAW 264.7) after Antimicrobial Analysis in *Candida Albicans*, *Staphylococcus Aureus*, and *Streptococcus Mutans*. *J. Funct. Foods* **2018**, *40* (August 2017), 455–460. <https://doi.org/10.1016/j.jff.2017.11.035>.
- (283) Gutiérrez, L.; Batlle, R.; Sánchez, C.; Nerín, C. New Approach to Study the Mechanism of Antimicrobial Protection of an Active Packaging. *Foodborne Pathog. Dis.* **2010**, *7* (9), 1063–1069. <https://doi.org/10.1089/fpd.2009.0516>.
- (284) Satooka, H.; Kubo, I. Effects of Thymol on B16-F10 Melanoma Cells. *J. Agric. Food Chem.* **2012**, *60* (10), 2746–2752. <https://doi.org/10.1021/jf204525b>.
- (285) Oliveira, J. R. de; de Jesus Viegas, D.; Martins, A. P. R.; Carvalho, C. A. T.; Soares, C. P.; Camargo, S. E. A.; Jorge, A. O. C.; de Oliveira, L. D. Thymus Vulgaris L. Extract Has Antimicrobial and Anti-Inflammatory Effects in the Absence of Cytotoxicity and Genotoxicity. *Arch. Oral Biol.* **2017**, *82* (June), 271–279. <https://doi.org/10.1016/j.archoralbio.2017.06.031>.
- (286) Justo, O. R.; Simioni, P. U.; Gabriel, D. L.; Tamashiro, W. M. da S. C.; Rosa, P. de T. V.; Moraes, A. M. Evaluation of in Vitro Anti-Inflammatory Effects of Crude Ginger and Rosemary Extracts Obtained through Supercritical CO<sub>2</sub> Extraction on Macrophage and Tumor Cell Line: The Influence of Vehicle Type. *BMC Complement. Altern. Med.* **2015**, *15* (1), 1–15. <https://doi.org/10.1186/s12906-015-0896-9>.
- (287) Soares-Bezerra, R. J.; Calheiros, A. S.; Ferreira, N. C. da S.; Frutuoso, V. da S.; Alves, L. A. Natural Products as a Source for New Anti-Inflammatory and Analgesic Compounds through the Inhibition of Purinergic P2X Receptors. *Pharmaceuticals* **2013**, *6* (5), 650–658. <https://doi.org/10.3390/ph6050650>.
- (288) Zhang, H. L.; Gan, X. Q.; Fan, Q. F.; Yang, J. J.; Zhang, P.; Hu, H. Bin; Song, Q. S. Chemical Constituents and Anti-Inflammatory Activities of Maqian (*Zanthoxylum Myriacanthum* Var. *Pubescens*) Bark Extracts. *Sci. Rep.* **2017**, *7* (January 2016), 1–13. <https://doi.org/10.1038/srep45805>.
- (289) Liang, G.; Zhou, H.; Wang, Y.; Gurley, E. C.; Feng, B.; Chen, L.; Xiao, J.; Yang, S.; Li, X. Inhibition of LPS-Induced Production of Inflammatory Factors in the Macrophages by Mono-Carbonyl Analogues of Curcumin. *J. Cell. Mol. Med.* **2009**, *13* (9 B), 3370–3379. <https://doi.org/10.1111/j.1582-4934.2009.00711.x>.
- (290) Kawai, T.; Akira, S. The Role of Pattern-Recognition Receptors in Innate Immunity: Update on Toll-like Receptors. *Nat. Immunol.* **2010**, *11* (5), 373–384. <https://doi.org/10.1038/ni.1863>.
- (291) Jain, H.; Dhingra, N.; Narsinghani, T.; Sharma, R. Insights into the Mechanism of Natural Terpenoids as NF- $\kappa$ B Inhibitors: An Overview on Their Anticancer Potential. *Exp. Oncol.* **2016**, *38* (3), 158–168. [https://doi.org/10.31768/2312-8852.2016.38\(3\):158-168](https://doi.org/10.31768/2312-8852.2016.38(3):158-168).
- (292) Gholijani, N.; Gharagozloo, M.; Kalantar, F.; Ramezani, A.; Amirghofran, Z. Modulation of Cytokine Production and Transcription Factors Activities in Human Jurkat t Cells by Thymol and Carvacrol. *Adv. Pharm. Bull.* **2015**, *5* (Suppl 1), 653–660. <https://doi.org/10.15171/apb.2015.089>.
- (293) Povea-Cabello, S.; Oropesa-Ávila, M.; de la Cruz-Ojeda, P.; Villanueva-Paz, M.; De La Mata,

- M.; Suárez-Rivero, J. M.; Álvarez-Córdoba, M.; Villalón-García, I.; Cotán, D.; Ybot-González, P.; et al. Dynamic Reorganization of the Cytoskeleton during Apoptosis: The Two Coffins Hypothesis. *Int. J. Mol. Sci.* **2017**, *18* (11). <https://doi.org/10.3390/ijms18112393>.
- (294) Mo, Y.; Guo, R.; Zhang, Y.; Xue, W.; Cheng, B.; Zhang, Y. Controlled Dual Delivery of Angiogenin and Curcumin by Electrospun Nanofibers for Skin Regeneration. *Tissue Eng. - Part A* **2017**, *23* (13–14), 597–608. <https://doi.org/10.1089/ten.tea.2016.0268>.
- (295) Ci, X.; Zhou, J.; Lv, H.; Yu, Q.; Peng, L.; Hua, S. Betulin Exhibits Anti-Inflammatory Activity in LPS-Stimulated Macrophages and Endotoxin-Shocked Mice through an AMPK/AKT/Nrf2-Dependent Mechanism. *Cell Death Dis.* **2017**, *8* (5), e2798. <https://doi.org/10.1038/cddis.2017.39>.
- (296) Zhang, X.; Li, N.; Shao, H.; Meng, Y.; Wang, L.; Wu, Q.; Yao, Y.; Li, J.; Bian, J.; Zhang, Y.; et al. Methane Limit LPS-Induced NF- $\kappa$  B/MAPKs Signal in Macrophages and Suppress Immune Response in Mice by Enhancing PI3K/AKT/GSK-3 $\beta$ -Mediated IL-10 Expression. *Sci. Rep.* **2016**, *6* (June), 1–14. <https://doi.org/10.1038/srep29359>.
- (297) Gholijani, N.; Gharagozloo, M.; Farjadian, S.; Amirghofran, Z. Modulatory Effects of Thymol and Carvacrol on Inflammatory Transcription Factors in Lipopolysaccharide-Treated Macrophages. *J. Immunotoxicol.* **2016**, *13* (2), 157–164. <https://doi.org/10.3109/1547691X.2015.1029145>.
- (298) Yamamoto, Y.; Gaynor, R. B. Therapeutic Potential of Inhibition of the NF-KB Pathway in the Treatment of Inflammation and Cancer. *J. Clin. Invest.* **2001**, *107* (2), 135–142. <https://doi.org/10.1172/JCI11914>.
- (299) Tsao, C. J.; Pandolfi, L.; Wang, X.; Minardi, S.; Lupo, C.; Evangelopoulos, M.; Hendrickson, T.; Shi, A.; Storci, G.; Taraballi, F.; et al. *Electrospun Patch Functionalized with Nanoparticles Allows for Spatiotemporal Release of VEGF and PDGF-BB Promoting in Vivo Neovascularization*; 2018; Vol. 10. <https://doi.org/10.1021/acsami.8b19975>.
- (300) Abd-El-Basset, E.; Fedoroff, S. Effect of Bacterial Wall Lipopolysaccharide (LPS) on Morphology, Motility, and Cytoskeletal Organization of Microglia in Cultures. *J. Neurosci. Res.* **1995**, *41* (2), 222–237. <https://doi.org/10.1002/jnr.490410210>.
- (301) Rashidian, A.; Rashki, A.; Abdollahi, A.; Haddadi, N. S.; Chamanara, M.; Mumtaz, F.; Dehpour, A. R. Thymol Reduces Acetic Acid-Induced Inflammatory Response in Rat Colon Tissue through Inhibition of NF-KB Signaling Pathway. *Immunopharmacol. Immunotoxicol.* **2019**, *41* (6), 607–613. <https://doi.org/10.1080/08923973.2019.1678635>.
- (302) Sheorain, J.; Mehra, M.; Thakur, R.; Grewal, S.; Kumari, S. In Vitro Anti-Inflammatory and Antioxidant Potential of Thymol Loaded Bipolymeric (Tragacanth Gum/Chitosan) Nanocarrier. *Int. J. Biol. Macromol.* **2019**, *125*, 1069–1074. <https://doi.org/10.1016/j.ijbiomac.2018.12.095>.
- (303) Li, S.; Li, L.; Guo, C.; Qin, H.; Yu, X. A Promising Wound Dressing Material with Excellent Cytocompatibility and Proangiogenesis Action for Wound Healing: Strontium Loaded Silk Fibroin/Sodium Alginate (SF/SA) Blend Films. *Int. J. Biol. Macromol.* **2017**, *104*, 969–978. <https://doi.org/10.1016/j.ijbiomac.2017.07.020>.
- (304) Kamoun, E. A.; Kenawy, E. R. S.; Chen, X. A Review on Polymeric Hydrogel Membranes for Wound Dressing Applications: PVA-Based Hydrogel Dressings. *J. Adv. Res.* **2017**, *8* (3), 217–233. <https://doi.org/10.1016/j.jare.2017.01.005>.

- (305) Curvello, R.; Raghuwanshi, V. S.; Garnier, G. Engineering Nanocellulose Hydrogels for Biomedical Applications. *Adv. Colloid Interface Sci.* **2019**, *267*, 47–61. <https://doi.org/10.1016/j.cis.2019.03.002>.
- (306) Miguel, S. P.; Moreira, A. F.; Correia, I. J. Chitosan Based-Asymmetric Membranes for Wound Healing: A Review. *Int. J. Biol. Macromol.* **2019**, *127*, 460–475. <https://doi.org/10.1016/j.ijbiomac.2019.01.072>.
- (307) Feng, Y.; Li, X.; Zhang, Q.; Yan, S.; Guo, Y.; Li, M.; You, R. Mechanically Robust and Flexible Silk Protein/Polysaccharide Composite Sponges for Wound Dressing. *Carbohydr. Polym.* **2019**, *216* (February), 17–24. <https://doi.org/10.1016/j.carbpol.2019.04.008>.
- (308) Liao, S.; Li, B.; Ma, Z.; Wei, H.; Chan, C.; Ramakrishna, S. Biomimetic Electrospun Nanofibers for Tissue Regeneration. *Biomed. Mater.* **2006**, *1* (3). <https://doi.org/10.1088/1748-6041/1/3/R01>.
- (309) Rho, K. S.; Jeong, L.; Lee, G.; Seo, B. M.; Park, Y. J.; Hong, S. D.; Roh, S.; Cho, J. J.; Park, W. H.; Min, B. M. Electrospinning of Collagen Nanofibers: Effects on the Behavior of Normal Human Keratinocytes and Early-Stage Wound Healing. *Biomaterials* **2006**, *27* (8), 1452–1461. <https://doi.org/10.1016/j.biomaterials.2005.08.004>.
- (310) Ju, H. W.; Lee, O. J.; Lee, J. M.; Moon, B. M.; Park, H. J.; Park, Y. R.; Lee, M. C.; Kim, S. H.; Chao, J. R.; Ki, C. S.; et al. Wound Healing Effect of Electrospun Silk Fibroin Nanomatrix in Burn-Model. *Int. J. Biol. Macromol.* **2016**, *85*, 29–39. <https://doi.org/10.1016/j.ijbiomac.2015.12.055>.
- (311) Chen, J. P.; Chang, G. Y.; Chen, J. K. Electrospun Collagen/Chitosan Nanofibrous Membrane as Wound Dressing. *Colloids Surfaces A Physicochem. Eng. Asp.* **2008**, *313–314*, 183–188. <https://doi.org/10.1016/j.colsurfa.2007.04.129>.
- (312) Ye, S.; Jiang, L.; Wu, J.; Su, C.; Huang, C.; Liu, X.; Shao, W. Flexible Amoxicillin-Grafted Bacterial Cellulose Sponges for Wound Dressing: In Vitro and in Vivo Evaluation. *ACS Appl. Mater. Interfaces* **2018**, *10* (6), 5862–5870. <https://doi.org/10.1021/acsami.7b16680>.
- (313) Abdel-Mohsen, A. M.; Jancar, J.; Abdel-Rahman, R. M.; Vojtek, L.; Hyršl, P.; Dušková, M.; Nejezchlebová, H. A Novel in Situ Silver/Hyaluronan Bio-Nanocomposite Fabrics for Wound and Chronic Ulcer Dressing: In Vitro and in Vivo Evaluations. *Int. J. Pharm.* **2017**, *520* (1–2), 241–253. <https://doi.org/10.1016/j.ijpharm.2017.02.003>.
- (314) Miguel, S. P.; Figueira, D. R.; Simões, D.; Ribeiro, M. P.; Coutinho, P.; Ferreira, P.; Correia, I. J. Electrospun Polymeric Nanofibres as Wound Dressings: A Review. *Colloids Surfaces B Biointerfaces* **2018**, *169*, 60–71. <https://doi.org/10.1016/j.colsurfb.2018.05.011>.
- (315) Wu, H.; Xiao, D.; Lu, J.; Jiao, C.; Li, S.; Lei, Y.; Liu, D.; Wang, J.; Zhang, Z.; Liu, Y.; et al. Effect of High-Pressure Homogenization on Microstructure and Properties of Pomelo Peel Flour Film-Forming Dispersions and Their Resultant Films. *Food Hydrocoll.* **2020**, *102*, 105628. <https://doi.org/10.1016/j.foodhyd.2019.105628>.
- (316) Adeli, H.; Khorasani, M. T.; Parvazinia, M. Wound Dressing Based on Electrospun PVA/Chitosan/Starch Nanofibrous Mats: Fabrication, Antibacterial and Cytocompatibility Evaluation and in Vitro Healing Assay. *Int. J. Biol. Macromol.* **2019**, *122*, 238–254. <https://doi.org/10.1016/j.ijbiomac.2018.10.115>.

- (317) Khil, M. S.; Cha, D. I.; Kim, H. Y.; Kim, I. S.; Bhattarai, N. Electrospun Nanofibrous Polyurethane Membrane as Wound Dressing. *J. Biomed. Mater. Res. - Part B Appl. Biomater.* **2003**, *67* (2), 675–679. <https://doi.org/10.1002/jbmb.10058>.
- (318) Kumbar, S.; Nukavarapu, S.; James, R.; Nair, L.; Laurencin, C. Electrospun Poly(Lactic Acid-Co-Glycolic Acid) Scaffolds for Skin Tissue Engineering. *Biomaterials* **2008**, *29* (30), 4100–4107. <https://doi.org/10.1038/jid.2014.371>.
- (319) Suwantong, O. Biomedical Applications of Electrospun Polycaprolactone Fiber Mats. *Polym. Adv. Technol.* **2016**, *27* (10), 1264–1273. <https://doi.org/10.1002/pat.3876>.
- (320) Tra Thanh, N.; Ho Hieu, M.; Tran Minh Phuong, N.; Do Bui Thuan, T.; Nguyen Thi Thu, H.; Thai, V. P.; Do Minh, T.; Nguyen Dai, H.; Vo, V. T.; Nguyen Thi, H. Optimization and Characterization of Electrospun Polycaprolactone Coated with Gelatin-Silver Nanoparticles for Wound Healing Application. *Mater. Sci. Eng. C* **2018**, *91* (2017), 318–329. <https://doi.org/10.1016/j.msec.2018.05.039>.
- (321) Aljghami, M. E.; Saboor, S.; Amini-Nik, S. Emerging Innovative Wound Dressings. *Ann. Biomed. Eng.* **2019**, *47* (3), 659–675. <https://doi.org/10.1007/s10439-018-02186-w>.
- (322) Furfaro, L. L.; Payne, M. S.; Chang, B. J. Bacteriophage Therapy: Clinical Trials and Regulatory Hurdles. *Front. Cell. Infect. Microbiol.* **2018**, *8* (October), 376. <https://doi.org/10.3389/fcimb.2018.00376>.
- (323) Ramalingam, R.; Dhand, C.; Leung, C. M.; Ong, S. T.; Annamalai, S. K.; Kamruddin, M.; Verma, N. K.; Ramakrishna, S.; Lakshminarayanan, R.; Arunachalam, K. D. Antimicrobial Properties and Biocompatibility of Electrospun Poly- $\epsilon$ -Caprolactone Fibrous Mats Containing Gymnema Sylvestre Leaf Extract. *Mater. Sci. Eng. C* **2019**, *98* (January), 503–514. <https://doi.org/10.1016/j.msec.2018.12.135>.
- (324) Zhang, W.; Ronca, S.; Mele, E. Electrospun Nanofibres Containing Antimicrobial Plant Extracts. *Nanomaterials* **2017**, *7* (2), 1–17. <https://doi.org/10.3390/nano7020042>.
- (325) Scaffaro, R.; Lopresti, F. Processing, Structure, Property Relationships and Release Kinetics of Electrospun PLA/Carvacrol Membranes. *Eur. Polym. J.* **2018**, *100* (December 2017), 165–171. <https://doi.org/10.1016/j.eurpolymj.2018.01.035>.
- (326) Figueroa-Lopez, K. J.; Vicente, A. A.; Reis, M. A. M.; Torres-Giner, S.; Lagaron, J. M. Antimicrobial and Antioxidant Performance of Various Essential Oils and Natural Extracts and Their Incorporation into Biowaste Derived Poly(3-Hydroxybutyrate-Co-3-Hydroxyvalerate) Layers Made from Electrospun Ultrathin Fibers. *Nanomaterials* **2019**, *9* (2), 1–22. <https://doi.org/10.3390/nano9020144>.
- (327) Yildiz, Z. I.; Celebioglu, A.; Kilic, M. E.; Durgun, E.; Uyar, T. Fast-Dissolving Carvacrol/Cyclodextrin Inclusion Complex Electrospun Fibers with Enhanced Thermal Stability, Water Solubility, and Antioxidant Activity. *J. Mater. Sci.* **2018**, *53* (23), 15837–15849. <https://doi.org/10.1007/s10853-018-2750-1>.
- (328) Scaffaro, R.; Lopresti, F.; D'Arrigo, M.; Marino, A.; Nostro, A. Efficacy of Poly(Lactic Acid)/Carvacrol Electrospun Membranes against Staphylococcus Aureus and Candida Albicans in Single and Mixed Cultures. *Appl. Microbiol. Biotechnol.* **2018**, *102* (9), 4171–4181. <https://doi.org/10.1007/s00253-018-8879-7>.



- (329) Celebioglu, A.; Yildiz, Z. I.; Uyar, T. Thymol/Cyclodextrin Inclusion Complex Nanofibrous Webs: Enhanced Water Solubility, High Thermal Stability and Antioxidant Property of Thymol. *Food Res. Int.* **2018**, *106*, 280–290. <https://doi.org/10.1016/j.foodres.2017.12.062>.
- (330) Yang, S.; Han, X.; Jia, Y.; Zhang, H.; Tang, T. Hydroxypropyltrimethyl Ammonium Chloride Chitosan Functionalized-PLGA Electrospun Fibrous Membranes as Antibacterial wound Dressing: In Vitro and in Vivo Evaluation. *Polymers (Basel)*. **2017**, *9* (12), 1–19. <https://doi.org/10.3390/polym9120697>.
- (331) Miguel, S. P.; Sequeira, R. S.; Moreira, A. F.; Cabral, C. S. D. An Overview of Electrospun Membranes Loaded with Bioactive Molecules for Improving the Wound Healing Process. *Eur. J. Pharm. Biopharm.* **2019**, *139* (January), 1–22. <https://doi.org/10.1016/j.ejpb.2019.03.010>.
- (332) Manjula Sheeja Rajiv, R. In Vitro Release of Fragrant L-Carvone from Electrospun Poly ( $\epsilon$ -Caprolactone)/Wheat Cellulose Scaffold. *Carbohydr. Polym.* **2015**, *133*, 328–336. <https://doi.org/10.1016/j.carbpol.2015.07.015>.
- (333) Bose, S.; Vu, A.; Emshadi, K.; Bandyopadhyay, A. Effects of Polycaprolactone on Alendronate Drug Release from Mg-Doped Hydroxyapatite Coating on Titanium. *Mater. Sci. Eng. C* **2018**, *88*, 166–171. <https://doi.org/10.1016/j.msec.2018.02.019>.
- (334) Goonoo, N.; Bhaw-luximon, A.; Jhurry, D. Drug Loading and Release from Electrospun. *J. Biomed. Nanotechnol.* **2014**, *10* (9), 2173–2199. <https://doi.org/10.1166/jbn.2014.1885>.
- (335) Trinca, R. B.; Westin, C. B.; da Silva, J. A. F.; Moraes, Â. M. Electrospun Multilayer Chitosan Scaffolds as Potential Wound Dressings for Skin Lesions. *Eur. Polym. J.* **2017**, *88*, 161–170. <https://doi.org/10.1016/j.eurpolymj.2017.01.021>.
- (336) Mishra, R. K.; Mishra, P.; Verma, K.; Mondal, A.; Chaudhary, R. G.; Abolhasani, M. M.; Loganathan, S. *Electrospinning Production of Nanofibrous Membranes*; Springer International Publishing, 2019; Vol. 17. <https://doi.org/10.1007/s10311-018-00838-w>.
- (337) Wang, B.; Zheng, H.; Chang, M. W.; Ahmad, Z.; Li, J. S. Hollow Polycaprolactone Composite Fibers for Controlled Magnetic Responsive Antifungal Drug Release. *Colloids Surfaces B Biointerfaces* **2016**, *145*, 757–767. <https://doi.org/10.1016/j.colsurfb.2016.05.092>.
- (338) Quartinello, F.; Tallian, C.; Auer, J.; Schön, H.; Vielnascher, R.; Weinberger, S.; Wieland, K.; Weihs, A. M.; Herrero-Rollett, A.; Lendl, B.; et al. Smart Textiles in Wound Care: Functionalization of Cotton/PET Blends with Antimicrobial Nanocapsules. *J. Mater. Chem. B* **2019**, *7* (42), 6592–6603. <https://doi.org/10.1039/c9tb01474h>.
- (339) Pérez-Recalde, M.; Ruiz Arias, I. E.; Hermida, É. B. Could Essential Oils Enhance Biopolymers Performance for Wound Healing? A Systematic Review. *Phytomedicine* **2018**, *38*, 57–65. <https://doi.org/10.1016/j.phymed.2017.09.024>.
- (340) Karami, Z.; Rezaeian, I.; Zahedi, P.; Abdollahi, M. Preparation and Performance Evaluations of Electrospun Poly( $\epsilon$ -Caprolactone), Poly(Lactic Acid), and Their Hybrid (50/50) Nanofibrous Mats Containing Thymol as an Herbal Drug for Effective Wound Healing. *J. Appl. Polym. Sci.* **2013**, *129* (2), 756–766. <https://doi.org/10.1002/app.38683>.
- (341) Riella, K. R.; Marinho, R. R.; Santos, J. S.; Pereira-Filho, R. N.; Cardoso, J. C.; Albuquerque-Junior, R. L. C.; Thomazzi, S. M. Anti-Inflammatory and Cicatrizing Activities of Thymol, a Monoterpene of the Essential Oil from *Lippia Gracilis*, in Rodents. *J. Ethnopharmacol.* **2012**,

143 (2), 656–663. <https://doi.org/10.1016/j.jep.2012.07.028>.

- (342) Lin, Z.; Wu, T.; Wang, W.; Li, B.; Wang, M.; Chen, L.; Xia, H.; Zhang, T. Biofunctions of Antimicrobial Peptide-Conjugated Alginate/Hyaluronic Acid/Collagen Wound Dressings Promote Wound Healing of a Mixed-Bacteria-Infected Wound. *Int. J. Biol. Macromol.* **2019**, *140*, 330–342. <https://doi.org/10.1016/j.ijbiomac.2019.08.087>.
- (343) Sarhan, W. A.; Azzazy, H. M. E.; El-Sherbiny, I. M. Honey/Chitosan Nanofiber Wound Dressing Enriched with *Allium Sativum* and *Cleome Droserifolia*: Enhanced Antimicrobial and Wound Healing Activity. *ACS Appl. Mater. Interfaces* **2016**, *8* (10), 6379–6390. <https://doi.org/10.1021/acsami.6b00739>.
- (344) Strand, T. A.; Lale, R.; Degnes, K. F.; Lando, M.; Valla, S. A New and Improved Host-Independent Plasmid System for RK2-Based Conjugal Transfer. *PLoS One* **2014**, *9* (3), 1–6. <https://doi.org/10.1371/journal.pone.0090372>.
- (345) Ribeiro, J.; Vieira, F. D.; King, T.; D’Arezzo, J. B.; Boyce, J. M. Misclassification of Susceptible Strains of *Staphylococcus Aureus* as Methicillin-Resistant *S. Aureus* by a Rapid Automated Susceptibility Testing System. *J. Clin. Microbiol.* **1999**, *37* (5), 1619–1620. <https://doi.org/10.1128/jcm.37.5.1619-1620.1999>.
- (346) Treangen, T. J.; Maybank, R. A.; Enke, S.; Friss, M. B.; Diviak, L. F.; David, D. K.; Koren, S.; Ondov, B.; Phillippy, A. M.; Bergman, N. H.; et al. Complete Genome Sequence of the Quality Control Strain *Staphylococcus Aureus* Subsp. *Aureus* ATCC 25923. *Genome Announc.* **2014**, *2* (6), 25923. <https://doi.org/10.1128/genomeA.01110-14>.
- (347) Gutierrez, J.; Barry-Ryan, C.; Bourke, P. The Antimicrobial Efficacy of Plant Essential Oil Combinations and Interactions with Food Ingredients. *Int. J. Food Microbiol.* **2008**, *124* (1), 91–97. <https://doi.org/10.1016/j.ijfoodmicro.2008.02.028>.
- (348) Wang, X.; Ge, J.; Tredget, E. E.; Wu, Y. The Mouse Excisional Wound Splinting Model , Including Applications for Stem Cell Transplantation. *Nat. Protoc.* **2013**. <https://doi.org/10.1038/nprot.2013.002>.
- (349) Galiano, R. D.; Michaels, J.; Dobryansky, M.; Levine, J. P.; Gurtner, G. C. Technical Article Quantitative and Reproducible Murine Model of Excisional Wound Healing. **2004**, 485–492.
- (350) Chapter 10: Medical and minor surgical procedures <https://medicalguidelines.msf.org/viewport/CG/english/dressings-18482377.html#> (accessed Mar 16, 2020).
- (351) Santalla, A.; López-Criado, M. S.; Ruiz, M. D.; Fernández-Parra, J.; Gallo, J. L.; Montoya, F. *Surgical Site Infection. Prevention and Treatment*; 2007; Vol. 34. [https://doi.org/10.1016/S0210-573X\(07\)74505-7](https://doi.org/10.1016/S0210-573X(07)74505-7).





## Appendix III

PUBLISHED SCIENTIFIC PAPERS & PARTICIPATION IN  
CONFERENCES

Appendix III: Published scientific papers

- III.1. **García-Salinas, S.<sup>‡</sup>**; Elizondo-Castillo, H.<sup>‡</sup>; Arruebo, M.; Mendoza, G.; Irusta, S.  
(<sup>‡</sup> *These authors contributed equally to this work*)

**Evaluation of the Antimicrobial Activity and Cytotoxicity of Different Components of Natural Origin Present in Essential Oils.**

*Molecules* **2018**, *23* (6), 1–18. <https://doi.org/10.3390/molecules23061399>.

- III.2. **Garcia-Salinas, S.**; Himawan, E.; Mendoza, G.; Arruebo, M.; Sebastian, V.

**Rapid On-Chip Assembly of Niosomes: Batch versus Continuous Flow Reactors.**

*ACS Appl. Mater. Interfaces* **2018**, *10* (22), 19197–19207.  
<https://doi.org/10.1021/acsami.8b02994>.

- III.3. Mendoza, G.; De Solorzano, I. O.; Pintre, I.; **Garcia-Salinas, S.**; Sebastian, V.; Andreu, V.; Gimeno, M.; Arruebo, M.

**Near Infrared Dye-Labelled Polymeric Micro- and Nanomaterials: In Vivo Imaging and Evaluation of Their Local Persistence.**

*Nanoscale* **2018**, *10* (6), 2970–2982. <https://doi.org/10.1039/c7nr07345c>.

- III.4. **García-Salinas, S.\***; Evangelopoulos, M.; Gámez-Herrera, E.; Arruebo, M.; Irusta, S.; Taraballi, F.; Mendoza, G.; Tasciotti, E.

(\* *Corresponding author*)

**Electrospun Anti-Inflammatory Patch Loaded with Essential Oils for Wound Healing.**

*Int. J. Pharm.* **2020**, *577* (January), 119067.  
<https://doi.org/10.1016/j.ijpharm.2020.119067>.

- III.5. Gámez-Herrera, E.; Elizondo-Castillo, H.; Tascon, J.; **Garcia-Salinas, S.**; Navascués, N.; Mendoza, G.; Arruebo, M.; Irusta, S.

**Antibacterial Effect of Thymol Loaded SBA-15 Nanorods Incorporated in PCL Electrospun Fibers.**

*Nanomaterials* **2020**, *10* (616). <https://doi.org/10.3390/nano10040616>

- III.6. **Garcia-Salinas, S.\***; Gamez-Herrera, E.; Landa, G.; Arruebo, M.; Irusta, S.; Mendoza, G.  
(\* *Corresponding author*)

**Antimicrobial Wound Dressings Against Fluorescent and Methicillin-Sensitive Intracellular Pathogenic Bacteria.**

Submitted for publication: ACS Applied Materials & Interfaces Manuscript ID: am-2020-05668q.

- III.7. **Garcia-Salinas, S.**; Gamez-Herrera, E.; Asin, J.; de Miguel, R.; Andreu, V.; Sancho-Albero, M.; Mendoza, G.; Irusta, S.; Arruebo, M.

**Efficiency of Antimicrobial Electrospun Thymol-Loaded Polycaprolactone Mats *in vivo***

Accepted for publication: ACS Applied Biomaterials. Manuscript ID: mt-2020-002706.

- III.8. Gamez-Herrera, E.; **Garcia-Salinas, S.**; Salido, S.; Sancho-Albero, M.; Andreu, V.; Perez, M.; Lujan, L.; Irusta, S.; Arruebo, M.; Mendoza, G

**Drug Eluting Wound Dressing Having Sustained Release of Antimicrobial Compounds**

Submitted for publication: European Journal of Pharmaceutics and Biopharmaceutics Manuscript ID: EJPB-D-19-00133

### Participation in conferences

- III.9. Title: Niosomes nanoparticle loaded with essential oils for wound dressing applications

Authors: **Garcia-Salinas, S**; Elizondo, H; Sebastian, V; Arruebo, M; Irusta, S; Mendoza, G.

Contribution: Poster

Event: International conference on Nanomedicine and Nanobiotechnology (ICONAN). Paris, France; September 28<sup>th</sup>-20<sup>th</sup> 2016

Scope: International

- III.10. Title: *In vivo* imaging and local persistence of polymeric micro- and nanomaterials labelled with the near-infrared dye IR820.

Authors: Ortiz de Solorzano, I; Mendoza, G; Pintre I; **Garcia-Salinas, S**; Sebastian, V; Andreu, V; Gimeno, M; Arruebo, M.

Contribution: Poster

Event: International conference on Nanomedicine and Nanobiotechnology (ICONAN).

Paris, France; September 25<sup>th</sup>-27<sup>th</sup> 2017

Scope: International

III.11. Title: Capacidad bactericida y anti-inflamatoria de aceites esenciales encapsulados en nanofibras de policaprolactona

Authors: **Garcia-Salinas, S**; Gamez-Herrera, E; Arruebo, M; Mendoza, G; Irusta, S.

Contribution: Poster

Event: 36 Jornadas Nacionales de Ingeniería Química (XXXVI JNIQ). Zaragoza, Spain; September 4<sup>th</sup>-6<sup>th</sup> 2019

Scope: National

III.12. Title: Electrospun nanostructured wound dressings for the sustained release of natural antimicrobial compounds

Authors: Mendoza, G; Gamez-Herrera, E; **Garcia-Salinas, S**; Salido, S; Irusta, S; Arruebo, M.

Contribution: Poster

Event: XII<sup>th</sup> Spanish-Portuguese Conference on Controlled Drug Delivery. Santiago de Compostela, Spain; January 22<sup>nd</sup>-24<sup>th</sup> 2020

Scope: International